

Novel strategies for DNA detection and assay.

BOURIN, S.

1998

The author of this thesis retains the right to be identified as such on any occasion in which content from this thesis is referenced or re-used. The licence under which this thesis is distributed applies to the text and any original images only – re-use of any third-party content must still be cleared with the original copyright holder.

NOVEL STRATEGIES FOR DNA DETECTION AND ASSAY

A thesis submitted to the Robert Gordon University as partial fulfilment for the degree of Doctor of Philosophy in the School of Applied Science. 1998

Stephanie Bourin, DUT, BSc(Hns)

THE ROBERT GORDON UNIVERSITY



0004470575 ABERDEEN

NOVEL STRATEGIES FOR DNA DETECTION AND ASSAY

TABLE OF CONTENTS	PAGE
Acknowledgements	i
Abstract	ii
Table of figures	iv
CHAPTER 1: INTRODUCTION	
1.1. The importance of DNA analysis	1
1.2. Nucleic acids structure and chemistry	3
1.3. DNA Sequencing	11
<i>1.3.1. DNA sequencing chemistries</i>	11
1.3.1.1. Maxam and Gilbert sequencing	11
1.3.1.2. Sanger sequencing	13
<i>1.3.2. Analytical techniques for the sizing of DNA sequencing fragments</i>	15
1.3.2.1. Slab gel electrophoresis	15
1.3.2.2. Capillary electrophoresis	17
1.3.2.3. Use of MALDI mass spectrometry for DNA sequencing applications	19
<i>1.3.3. Other sequencing strategies</i>	21
1.4. Hybridization assays /use of DNA probes	23

1.5. Labeling of nucleic acids	27
<i>1.5.1. General strategies for nucleic acids labeling</i>	27
<i>1.5.2. Labeling for DNA sequencing</i>	35
1.6. Optical DNA detection techniques	40
<i>1.6.1. Fluorescence detection techniques</i>	40
1.6.1.1. Fluorescence detection methods	42
1.6.1.2. Signal processing for improved sensitivity	42
<i>1.6.2. Non linear optical methods</i>	44
1.7. Conclusions and strategy of present work	52

CHAPTER 2: DEVELOPMENT OF A LABELLING STRATEGY FOR DNA SEQUENCING USING LANTHANIDE CHELATES

2.1. Introduction	53
2.2. Synthesis of a triphosphate 5' amino thymidine analogue	56
2.3. Synthesis of BCPDA and DTPAA -pAs	61
2.4. Spectroscopic study of the chelates/ lanthanide complexes	66
<i>2.4.1. Methods</i>	66
<i>2.4.2. Spectroscopic study of BCPDA and lanthanide ions complexes</i>	66
<i>2.4.3. Spectroscopic study of DTPAA-As and lanthanide ions complexes</i>	70

2.5. Incorporation of the lanthanide chelate chemistry	73
into an enzymatic chain extension reaction	
<i>2.5.1. Aims of the experiment and principle</i>	73
<i>of Polymerase chain reaction (PCR)</i>	
<i>2.5.2. PCR protocol</i>	74
<i>2.5.3. Results</i>	75
2.6. Summary of results and conclusion	79

CHAPTER 3: SPECTROSCOPIC STUDY OF THE INTERACTION BETWEEN LANTHANIDES IONS AND DNA

3.1. Introduction	81
3.2. Determination of the melting temperature of a DNA duplex by UV	85
spectrometry	
<i>3.2.1. UV spectrometry, thermal analysis of a DNA duplex formation</i>	85
<i>3.2.2. Determination of the influence of pH on the T_m</i>	87
<i>3.2.3. Study of the interaction of $TbCl_3$ with DNA</i>	89
<i>3.2.4. Study of the interaction of Eu^{3+} chlorides with DNA</i>	92
3.3. HPLC study of DNA /lanthanide ion complexes	93
3.4. Study of the interaction of lanthanide ions with DNA using NMR	99
spectroscopy	
<i>3.4.1. Aims</i>	99

3.4.2. Phosphorus NMR study of the interaction of Eu^{3+} ions with DNA	100
3.4.3. Study of the interaction of Tb^{3+} and Eu^{3+} ions with DNA using Proton NMR with presaturation water suppression technique	102
3.5. Fluorescent study of the interaction of Tb^{3+} ions with DNA	108
3.6. Study of the action of Tb^{3+} on the tertiary structure of natural DNA	111
3.7. Summary of results and conclusions	113
 CHAPTER 4: STOICHIOMETRIC CHARACTERISATION OF LANTHANIDE ION/ DNA INTERACTION BY MALDI MASS SPECTROMETRY	
4.1. Introduction	114
4.2. Experimental set up	116
4.3. Results	119
4.3.1. Study of the interaction of a 20 mer polydT oligonucleotide with lanthanide ions	119
4.3.2. Analysis of lanthanide adducts of a 12 mer dA_6T_6 oligonucleotide	126
4.3.3. Improvement of the reproducibility of the MALDI MS analysis using internal standards	128
4.4. Discussion and conclusions	137

CHAPTER 5: THE APPLICATION OF SURFACE SECOND HARMONIC GENERATION TO THE DETECTION OF NUCLEIC ACIDS ON SURFACES

5.1. Introduction	139
5.2. Experimental set up	140
<i>5.2.1. SSHG system</i>	140
<i>5.2.2. Sample preparation</i>	142
5.3. Results	148
<i>5.3.1. Variation of second harmonic signal with laser power</i>	148
<i>5.3.2. Variation of second harmonic signal with surface DNA density</i>	149
<i>5.3.3. Variation of second harmonic signal with the size of the oligonucleotide</i>	151
<i>5.3.4. Effect of increased salt concentration on the SSHG signal</i>	152
<i>5.3.5. Variation of SSHG signal with the incident angle of the laser</i>	153
<i>5.3.6. Measurements using a detection system with reference</i>	154
5.4. Discussion and conclusion	159

CHAPTER 6: DISCUSSION AND CONCLUSIONS

6.1. New labelling methods for DNA sequencing	160
6.2. The interaction of lanthanide ions with DNA: the basis of a novel DNA hybridisation bioassay?	161
6.3. Applying SSHG detection to DNA hybridisation bioassays.	162

6.4. Overall conclusions	163
---------------------------------	------------

CHAPTER 7: FURTHER WORK.

7.1. Lanthanide chelates and DNA sequencing.	165
7.2. A novel hybridisation labelling format using lanthanide ions	167
7.3. A novel hybridisation labelling format using SSHG	170
7.4. Conclusions	178

REFERENCES	179
-------------------	------------

Acknowledgements:

I wish to thank the many people that played a part in helping me to complete this work. Firstly, I wish to give special thanks to my supervisors, Danny McStay, my Director of Studies, Paul Kong, my second supervisor and Liam Martin, for guiding me through the project and supporting me while writing this thesis.

Other people in the Robert Gordon University helped me greatly:

Thanks to Ala Albaidi who built the second harmonic systems used for this work.

Thanks to Eric Brechet who let me use his fluorescence scanning microscope, as well as Ian Campbell, both of them lent me a helping and encouraging hand many times.

Thanks to Rachel Wakefield who has been the most supportive friend and who could understand what “multidisciplinary” work means, being herself a biologist working with a group of physicists.

Thanks to Peter Quinn for allowing me to use the NMR facilities in King’s college London, and to Garry Duncan for being of great help while using the MALDI MS instrument at the Rowett institute.

My new work place, where most of the writing up was carried out, Amersham Pharmacia Biotech, provided me with very good equipment to write and print this work, as well as the right scientific environment to help write an altogether better thesis.

Many thanks go to Terek Schwartz and Mike Reeve from Amersham Pharmacia Biotech, who gave me the confidence to finish writing up by proof reading the manuscript and providing very helpful comments as well as much needed support.

My final thanks go to my parents, who helped me financially during all these years of study and always believed in my success.

ABSTRACT

The work carried out during this project was aimed at developing new strategies for DNA bioassays, using alternative detection techniques and new labelling methods.

Firstly, a new labelling technique for DNA sequencing was developed using lanthanide chelates. These compounds were identified as likely candidates to replace traditional dyes in four colour sequencing strategies because of their advantageous spectroscopic properties. Several chelates were synthesised and their fluorescent properties tested in presence of various lanthanide ions. None of the chelates tested was fluorescent in presence of the four ions (Tb^{3+} , Eu^{3+} , Sm^{3+} , Dy^{3+}). A triphosphate amino- thymidine derivative was synthesised. The triphosphate was covalently bound to a linear chelate, and was tested for incorporation in the PCR reaction as this reaction uses a polymerase similar to that of Sanger's sequencing reaction. There was no detectable incorporation of the compound. Studies of the toxicity of those derivatives, of the chelates and of the free lanthanide ions on the same polymerase enzyme were carried out. They showed a high sensitivity of the enzyme to unbound metal ions and to the chelates themselves in a smaller proportion.

These effects were studied in more detail, and the hypothesis that lanthanide ions might prevent polymerisation by acting on the DNA itself was raised. Thermal stability of synthetic DNA duplexes was studied in the presence of lanthanide ions. NMR spectrometry was used to further improve the knowledge on the interaction, and this work was done in collaboration with King's college London. The results obtained showed that about 1 lanthanide ion binds to 4 nucleotide bases. They bind first to the phosphate back bone, increasing the stability of the double chain. Once these sites are saturated, the lanthanide ions bind on the bases, and their bulkiness causes distortions that prevent proper Watson and Crick hydrogen bonding, thus decreasing the T_m . It

was also found, using MALDI mass spectrometry, that lanthanide ions did not all bind to DNA with the same stoichiometry, which may be due to a difference in affinity between the metal ion and the nucleic acid. As well as confirming that this interaction with DNA is certainly the cause of the inhibition of polymerisation (PCR), this study was used as a preliminary study for the development of a DNA hybridisation assay, using lanthanides as fluorescent labels.

Finally, work was carried out on the characterisation of DNA coated surfaces by second harmonic generation. This work was done to assess the feasibility of a non labelling DNA hybridisation assay using surface second harmonic generation (SSHG) detection techniques. It was found that the density of DNA monolayers deposited on the surface affected strongly the second harmonic signal and that the structure and size of the nucleic acid also affected the intensity of the signal. A detection limit of 10^{-13} mol nucleic acids/mm² was achieved. It was therefore concluded that SSHG was a suitable method for solid surface hybridisation assays, although it would probably be necessary to improve further its sensitivity to make it a commercially viable diagnostic tool.

TABLE OF FIGURES:	PAGE
Figure 1.1a. Pyrimidine bases	3
Figure 1.1b. Purine bases	4
Figure 1.2a. Ribose (left) and 2'deoxyribose (right)	4
Figure 1.2b. Phosphate group	4
Figure 1.3. 4 mer oligonucleotide showing the association of bases, sugars and phosphate groups to form an “orientated “ linear chain.	5
Figure 1.4. Part of a hypothetical polynucleotide chain in DNA	7
Figure 1.5. Watson and Crick base pairing, showing hydrogen bonding	8
Figure1.6. 3 forms of the DNA helix: B and A are right handed with 10 and 11 phosphates per helical turn. Z is left handed with 12 phosphates per turn.	9
Figure 1.7. Sequencing by the Maxam and Gilbert chemical degradation method	12
Figure 1. 8. Sanger’s sequencing technique	14
Figure 1.9. Schematic representation of DNA migration during electrophoresis	16
Figure 1.10. Photograph of a typical electrophoretic separation in a polyacrylamide gel	17
Figure 1.11. Schematic representation of capillary electrophoresis apparatus	18
Figure 1.12. Schematic representation of MALDI TOF apparatus.	21
Fig 1.13. Schematic representation of the solid phase hybridisation assay technique	24
Figure 1.14. Schematic representation of 2 possible models for solid phase hybridization	25
Figure 1.15. β diketone complexes emission spectra	30
Figure 1.16. Assay designs in DNA hybridisation using lanthanide chelates	31
figure 1.17. Chemical structures of different lanthanide chelates	32
figure 1.18. Energy transfer mechanism	34

Figure 1.19. Emission spectra and structures of the four ABI dyes	36
Figure 1.20. Chemical structure of DOTA-benzyl-NCS and its attachment to oligonucleotides	37
Figure 1.21. Representation of the processes involved in fluorescence emission of a fluorophore	40
Figure 1.22. Principles of time resolved fluorometry	43
Figure 1.23. Second - harmonic generation from an interface between media.	47
Figure 1.24. Illustration of the wavelength difference between SHG signal, laser light and fluorescence.	50
Figure 1.27. Schematic diagram of a typical experimental arrangement for surface second harmonic generation	50
Figure 2.1. Preparation of 2,3- anhydrothymidine-5-benzoate	57
Figure 2.2. Preparation of 3'-azido-2' deoxythymidine	58
Figure 2.3. Synthesis of AZT triphosphate	59
Figure 2.4. Presumed structure of the product formed from the reaction between DTTAA-pAS and a nucleoside. The amide linkage is formed with an exocyclic amine present on the nucleoside	61
Figure 2.5. Schematic representation of the chemical structure of BCPDA bound to a nucleoside (or DNA)	62
Figure 2.6. Schematic representation of the synthesis of BCPDA	65
Figure 2.7. Measured fluorescence spectrum of DMSO	67
Figure 2.8. Measured fluorescence spectrum of BCPDA (1 mM) in DMSO	67
Figure 2.9. Measured fluorescence spectrum of BCPDA complexed with Eu^{3+}	69
Figure 2.10. Measured fluorescence spectrum of BCPDA complexed with Tb^{3+}	69
Figure 2.11. Measured fluorescence spectrum of Phosphate buffer	70
Figure 2.12. Fluorescence spectrum of DTPAA-pAS in phosphate buffer	71
Figure 2.13. Fluorescence spectrum of DPTAA-pAS complexed with Tb^{3+}	71

Figure 2.14. Fluorescence spectrum of Tb^{3+} in ethanol.	72
Figure 2.15. Fluorescence spectrum of DTPAA-pAs complexed with Sm^{3+} in phosphate buffer	72
Figure 2.16. Schematic representation of the agarose gel used to analyse PCR mixtures in presence of Eu^{3+}	75
Figure 2.17. Schematic representation of the electrophoretic gel produced for the analysis of the PCR mixtures in presence of amino dideoxyribothymine triphosphate	77
Figure 3.1: highly electronegative atoms (*) susceptible to react with metal ions in CG base pairs.	83
Figure 3.2. Probable binding sites for metal ions on DNA molecules.	83
Figure 3.3. Typical melting curve of a DNA duplex	85
Figure 3.4. Scheme describing processes involved in DNA double helix de and renaturation.	87
Figure 3.5. Influence of the pH on the T_m values of a self complementary 12 mer AT oligonucleotide in 6xSSC buffer.	88
Figure 3.6. Influence of Tb^{3+} concentration on T_m of a 12 mer AT oligonucleotide at pH 5.	89
Figure 3.7. Influence of Tb^{3+} concentration on T_m of a 12 mer AT oligonucleotide at pH 7	90
Figure 3.8. Influence of Tb^{3+} concentration on T_m of a 12 mer AT oligonucleotide at pH 9	90
Figure 3.9. Study of the influence of $EuCl_3$ concentration on T_m of a 12 mer AT oligonucleotide in SSC buffer pH 7	92
figure 3.10. HPLC plot of the analysis of oligonucleotide sequence 5'-ACTTGGCCACCATTG-3'	94
figure 3.11. HPLC plot for the analysis of oligonucleotide 5'-CAAAATGGTGGCCAAGT-3'	95
Figure 3.12. HPLC plot for the analysis of a mixture of oligonucleotides ACTTGGCCACCATTG-3' and 5'-CAAAATGGTGGCCAAGT-3'.	96

Figure 3.13. HPLC plot for the analysis of a mixture of oligonucleotides ACTTGCCACCATTTTG-3' and 5'-CAAAATGGTGGCCAAGT-3' with denaturing amounts of Er^{3+} chloride.	97
Figure 3.14. HPLC plot for the analysis of a mixture of oligonucleotides ACTTGCCACCATTTTG-3' and 5'-CAAAATGGTGGCCAAGT-3' with denaturing amounts of Eu^{3+} .	97
Figure 3.15. ^{31}P spectra of 12 mer oligonucleotide in the presence of EuCl_3 .	101
Figure 3.16. Presaturated ^1H NMR spectrum of 12 mer oligonucleotide in 10% H_2O /90% H_2O	103
Figure 3.17. Presaturated ^1H NMR spectrum of 12 mer oligonucleotide 5' AAAAAATTTTTT 3' in 10% H_2O /90% H_2O , 0.285 M NaCl.	103
Figure 3.18. Schematic representation of "Watson and Crick" hydrogen bonding between adenine and thymine	104
Figure 3.19. 2 possible adenine -thymine wobble base pairing schemes	104
Figure 3.20: ^1H NMR of 12 mer oligonucleotide in SSC buffer (no presaturation)	105
Figure 3.21. ^1H NMR spectrum of 12 mer oligonucleotide in SSC buffer/0.015M Eu (15 μl)	106
Figure 3.22. Phosphorus NMR of 12 mer oligonucleotide in SSC buffer/0.03M Eu^{3+}	107
Figure 3.23. Fluorescence of a double stranded oligonucleotide/ Tb^{3+} complex, showing 2 peaks at 488nm and 545 nm (characteristic of Tb^{3+})	109
Figure 3.24. Fluorescence of a single stranded oligonucleotide/ Tb^{3+} chloride complex	109
figure 3.25. Comparative study of the fluorescence of single strand and double stranded DNA complexes of Tb^{3+} chloride.	110
figure 3.26. Schematic representation of the agarose gel obtained for the plasmid/ Tb^{3+} complexes.	112
Figure 4.1. Spectrum of the analysis of 70pmol of 12 mer AT oligonucleotide using hydroxy picolinic acid	117
Figure 4.2. Analysis of 70 pmol of 12 mer oligonucleotide using HAP	118

Figure 4. 3. Analysis of 350 pmol 20 mer polydT oligo in HAP	120
Figure 4.4. Analysis of 350pmol of 20 mer polydT oligo +30 nmol TbCl ₃ using HAP	121
Figure 4.5. Analysis of 350pmol of 20 mer polydT oligo +60 nmol TbCl ₃ using HAP	122
Figure 4.6. Analysis of 350pmol of 20 mer polydT oligo +90 nmol TbCl ₃ using HAP	123
Figure 4.7. Analysis of 350pmol of 20 mer polydT oligo +120 nmol TbCl ₃ using HAP	123
Figure 4.8. Analysis of 350pmol of 20 mer polydT oligo +150 nmol TbCl ₃ using HAP	124
Figure 4.9. Analysis of 12 mer AT oligonucleotide in HAP	127
Figure 4.10. Above (a): spectrum obtained for insulin in HAP below (b): spectrum of the analysis of insulin/Eu ³⁺ in HAP.	130
Figure 4.11. Spectrum of insulin and AT 12 mer in Hydroxyacetophenone	131
Figure 4.12. Spectrum of the 12 mer in the presence of Eu ³⁺	132
Figure 4.13. Spectrum of insulin chain B and 20 mer polyT in Hydroxyacetophenone	135
Figure 4. 14. Spectrum of insulin B chain and 20 mer polyT in Hydroxyacetophenone	135
Figure 5.1. Diagram of the experimental set-up for surface second-harmonic generation studies of DNA. [(a)filter to cut the visible light, (b) half wave , (c) polarizer, (d) iris, (e) sample, (f) filter to cut the 1064 nm].	141
figure 5.2. Photograph of the SSHG system no 1.	141
figure 5.3. Typical PMT output on the second harmonic system. (a). Single pulse. (b)average of 10 pulses.	142
Figure 5.4. Schematic representation of the scanning fluorescence microscope used to monitor the coating of surfaces.	143

Figure 5.5. Photograph of the scanning fluorescence microscope used to monitor the coating of surfaces.	144
figure 5.6. Fluorescence scan of silanised slides	145
Figure 5.7. Fluorescent scan of plastic wells containing fluorescein labelled oligonucleotide	147
Figure 5.8. The surface second harmonic generated from a 12 mer oligonucleotide coated glass surface (a) at different incident laser energies and (b) plotted against the square of the laser power.	148
figure 5.9. SSHG signal of glass cover slips covered with DNA layers of different densities (data point at density=0 corresponds to the SSHG signal of a control surface without DNA)	149
figure 5.10. SSHG signal of multiwell plate plastic wells covered with DNA layers of different densities	150
figure 5.11. SSHG signal for different sizes of AT containing oligonucleotides	152
Figure 5.12. Influence of salt concentration on SSHG on a DNA sample of a fixed concentration.	153
figure 5.13. Angle dependence of SSHG signal when using an incident laser beam	154
figure 5.14. Schematic representation of the surface second harmonic system with reference.	155
figure 5.15. Second harmonic signal variation with density of DNA coating on Maxisorb™ wells.	157
figure 7.1. Schematic representation of a surface based DNA bioassay using lanthanide ions as labels	169
figure 7.2. Schematical representation of solid phase hybridisation.	171
figure 7.3. Schematic diagram illustrating the procedure for straightening and optical mapping of single DNA molecules	172
figure 7.4. DNA incubated at the appropriate pH binds by one or 2 extremities onto a treated surface. As the interface moves, the DNA is stretched perpendicular to the receding meniscus. It is left linearised and dry behind the meniscus	173

CHAPTER 1: INTRODUCTION

1.1. The importance of DNA analysis

Deoxyribonucleic acid (DNA) carries the genetic information of all living cells. Its structure was first described by Watson and Crick in 1953. Since then, research has been intensively carried out to further the knowledge of its biological functions and chemistry. These studies have given rise to many applications such as gene therapy, medicine, the food industry and forensic science. DNA analysis looks set to progressively replace many existing biological and microbiological assays as the techniques involved are both rapid and reliable. Numerous methods of DNA analysis exist. Amongst these are the techniques of sequencing, which determines the precise base order in a DNA fragment, and mapping which relates various marker regions in the genome. A world wide project has been set up with the aim of sequencing and mapping the whole human genome (containing 3×10^9 bases). This “human genome project” will require an immense amount of sequencing and has created a high demand for new technologies and strategies to achieve this huge task. The method of sequencing most widely used is the Sanger method. This is used together with electrophoretic separation as the sequencing reaction produces a highly complex mixture of DNA fragments that have to be separated and sized.

Another field of great current interest is DNA hybridization bioassays. These techniques aim at recognizing the presence of a specific sequence of bases in a given sample, using oligonucleotide (short synthetic nucleic acid) probes of complementary sequence to the region of interest. Such assays can be used for numerous applications

to replace costly and lengthy biochemical and immunological techniques in routine clinical and microbiological testing and screening.

Both types of assays, sequencing and hybridisation, are widespread and sophisticated instrumentation and labelling strategies have been designed to suit a large number of applications. However, a lot of research is still required to further improve the sensitivity, speed and sample throughput of the techniques.

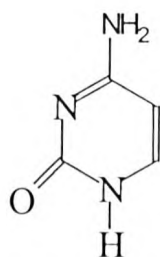
This chapter will introduce the principal chemical features of DNA; DNA hybridisation and sequencing techniques will be described and existing labelling and detection strategies will be critically reviewed. Finally, the project plan which forms the basis of this work will be presented.

1.2. Nucleic acids structure and chemistry

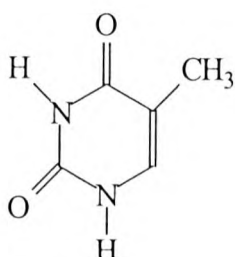
Nucleic acids are linear polymers whose monomeric units are referred to as nucleotides. Their molecular weight varies from around 25000 Daltons for transfer RNA, to 10^{12} Daltons for chromosomes. The primary structure of the molecule is as follows:

Each monomer, the nucleotide, is composed of

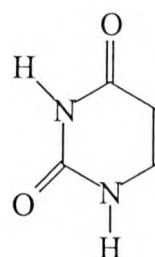
- a base, either a pyrimidine (cytosine C, thymine T and uracil U) (figure 1.1a), or a purine (adenine A and guanine G) (figure 1.1b)
- a sugar, ribose for RNA, 2' deoxyribose for DNA (figure 1.2a).
- a phosphate (1.2b)



Cytosine



Thymine



Uracil

Figure 1.1a. Pyrimidine bases

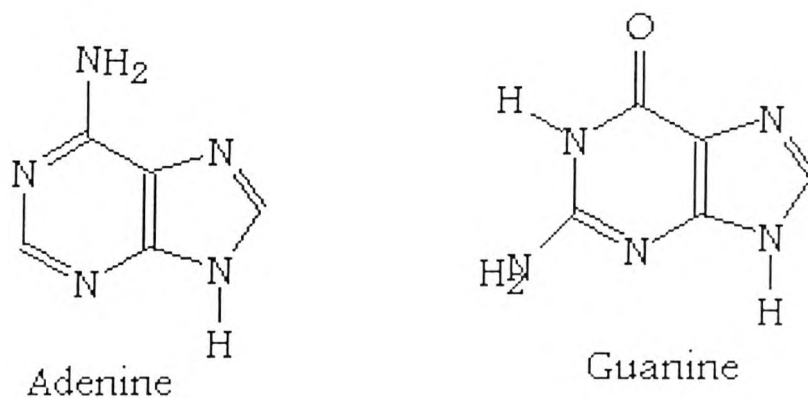


Figure 1.1b. Purine bases

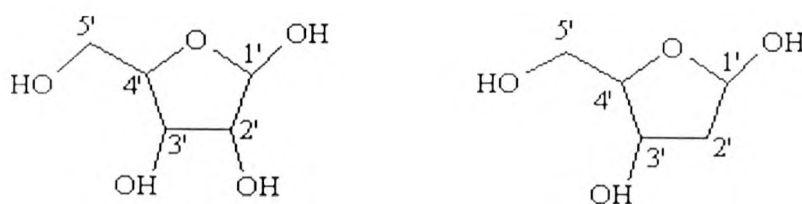


Figure 1.2a. Ribose (left) and 2'deoxyribose (right)

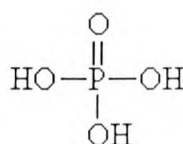


Figure 1.2b. Phosphate

The phosphate group serves as a bond between the 3' carbon on a sugar and the 5' carbon of the next sugar on the chain. This linkage is often referred to as the sugar-

phosphate backbone, where the bases are attached on the 1' carbon of the sugar. The association of the 3 units forms a linear chain (figure 1.3).

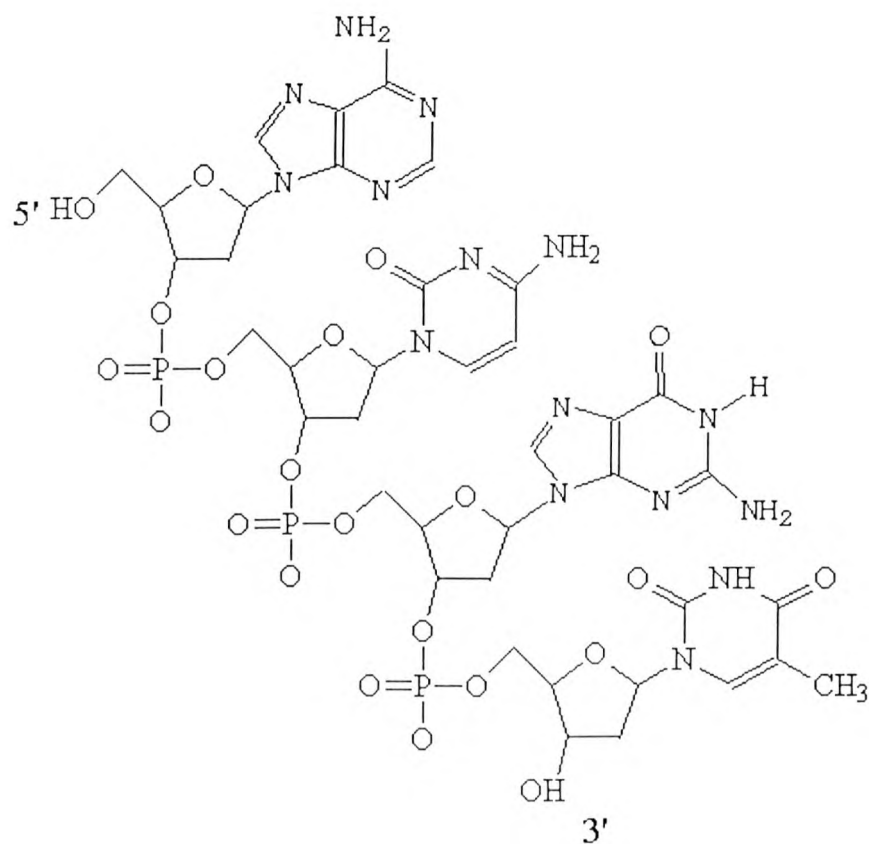


Figure 1.3. 4 mer oligonucleotide showing the association of bases, sugars and phosphate groups to form an “orientated” linear chain.

The discovery of the secondary structure of DNA was the result of numerous research works. The “puzzle” was eventually solved by Watson and Crick (1953). Essential preliminary findings leading to this first model of DNA were:

- Furberg in 1951 published data describing the structure of cytidine, using X ray crystallography. The structures of the other nucleotides present in DNA, Adenine, Thymidine and Guanine were established shortly after.
- Todd (Dekker *et al* 1953) established that nucleotides are linked via 3'5' phosphodiester bonds, to produce a linear polymer, DNA.

- Chargaff and coworkers (Zamenhof *et al* 1952) found that in DNA's of varying compositions, A/T and G/C ratios are always one.
- Base stacking was discovered by Astbury (1947), using X ray photography.
- Gulland (1947) found that bases were linked by hydrogen bonding, using electrotitrimetric techniques.

The model proposed by Watson and Crick was the following:

DNA is often present as a duplex, composed of 2 linear chains, of complementary sequence. This is due to the specific complementarity properties that allow adenine to bind to thymine only, and cytosine to bind to guanine.

The 2 chains are of opposite polarity, i.e. one strand goes from 3' to 5', and the other one goes in the other direction. This model is schematically represented in figure 1.4.

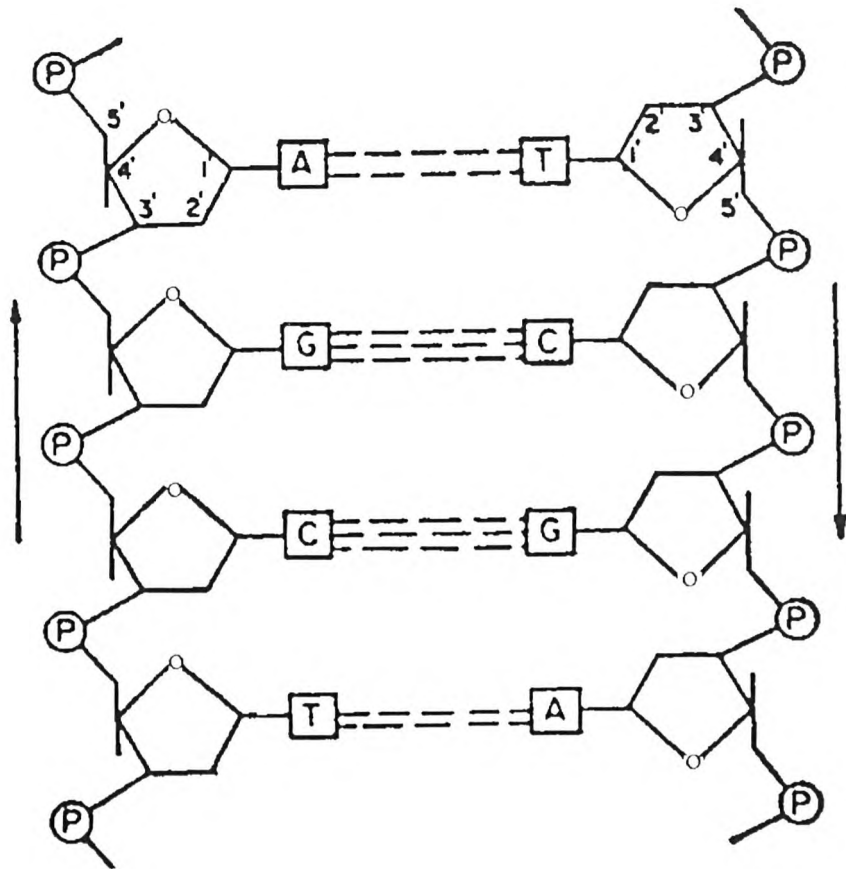


Figure 1.4. Part of a hypothetical polynucleotide chain in DNA

The 2 strands are held together by a number of chemical forces:

- Hydrogen bonding, between the bases. There are 2 bonds between A and T, and there are 3 bonds between C and G (see figure 1.5). This means that CG pairs are more stable than AT pairs.

- Base stacking

- Electrostatic forces: the presence of counterions on the phosphate backbone stabilizes the double helix as it balances the negative charges

present on the phosphate group that are repulsive and would otherwise push the 2 chains apart.

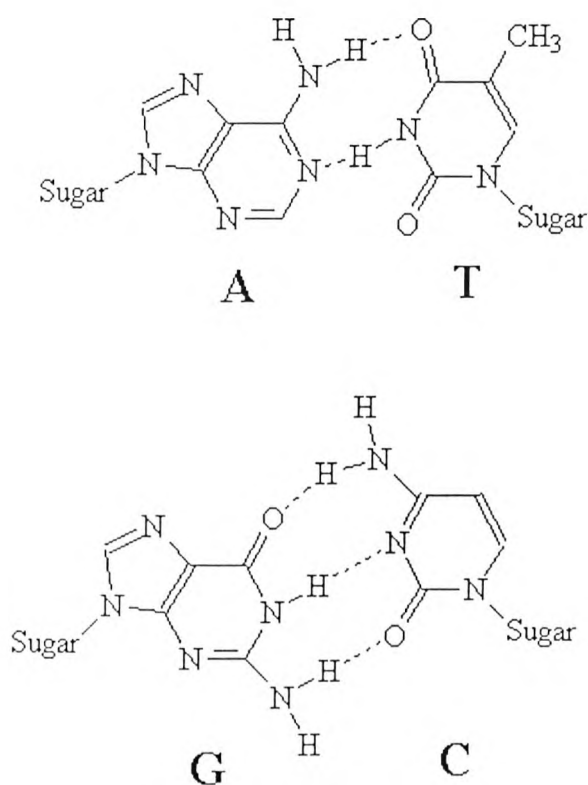


Figure 1.5. Watson and Crick base pairing, showing hydrogen bonding (represented by dotted lines)

Base stacking is stabilized by entropic contributions. Hydrophobic bonding occurs when non polar molecules are dissolved in water (nucleic acid bases are insoluble in water). They tend to aggregate to reduce the contacts between solvent-solute, and therefore contribute to the stabilization of secondary structure. 2 theories have been described to explain the phenomenon; the first is the so-called iceberg water (F. Francks 1975) and the second deals with water cavities (O. Sinanoglu 1968).

Dipolar and London dispersion forces (Hanlon 1966) are also of importance in stacking stabilization, that explains the specificity of stacking, i.e. purines stack better than pyrimidines.

Double stranded nucleic acid forms naturally a helix, that can be found in 3 main forms: A, B and Z. the A form contains 11 phosphate groups per turn, B form 10 and the Z form 12. Figure 1.6 shows a schematic representation of these conformations.

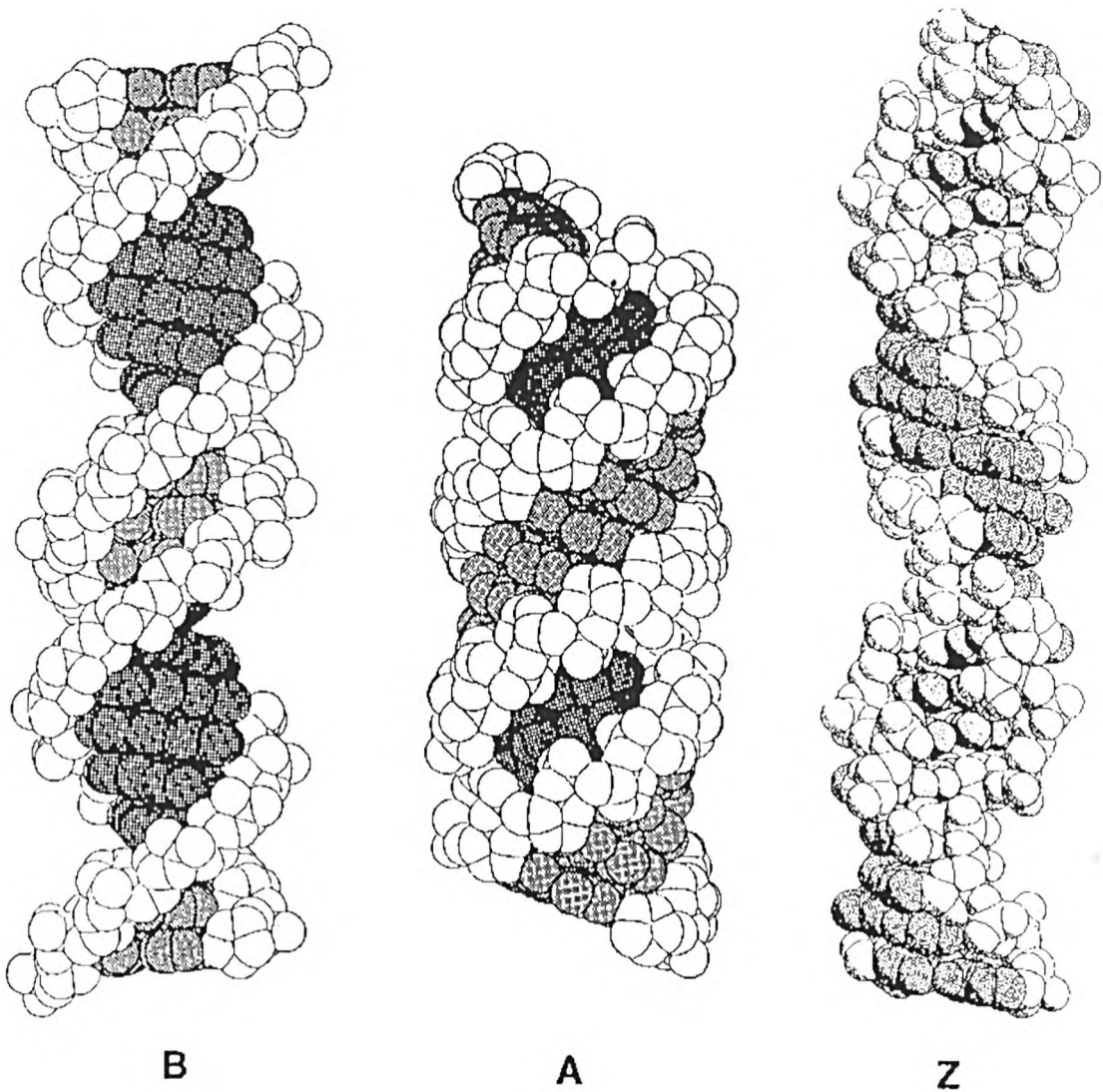


Figure1.6. 3 forms of the DNA helix: B and A are right handed with 10 and 11 phosphates per helical turn. Z is left handed with 12 phosphates per turn (reproduced from Calladine and Drew 1992).

Complex models have been described to explain why DNA forms a helix, why several types of helices can be found and what their biological functions are. These are discussed elsewhere (Saenger 1984).

It is from studying the essential properties of DNA structure and functions that bioassays were developed. For example, DNA hybridization is based on the fact that a short oligonucleotide will possess a strong affinity to another DNA single chain (denatured DNA sample) whose sequence is complementary to the oligonucleotide. If the sequence of the sample is not complementary, no binding will occur. The Sanger Sequencing technique also uses essential biochemical processes occurring naturally in cells, as it utilizes enzymes called polymerases. Similar types of enzymes are found in cells, and they are involved in DNA replication, before cell division.

1.3. DNA Sequencing

Sequencing aims to determine the primary structure of DNA, (i.e the order in which the four bases A, T, C and G appear in a DNA chain). This is important because the order of the bases determines the nature and order of amino acids in the protein for which the DNA codes. There are essentially two types of sequencing: (i) *de novo* sequencing, where the sequence of the nucleic acid is initially completely unknown, (ii) confirmatory sequencing, used for example in mutation detection on known regions of DNA.

Sequencing DNA generally relies upon the generation of nested sets of 5'coterminial sequences, followed by analysis of the resulting product using a variety of analytical tools.

Sanger's sequencing technique coupled with laser induced fluorescence (LIF) detection capillary electrophoresis (CE) is rapidly becoming a preferred option for researchers carrying out high throughput sequencing. There are numerous efforts being carried out on other sequencing strategies. This section will review these briefly and detail the more commercially viable option of CE and LIF.

1.3.1. DNA sequencing chemistries

1.3.1.1. Maxam and Gilbert sequencing

When the Maxam and Gilbert and Sanger sequencing techniques were developed in the 1970's (Maxam and Gilbert 1977, Sanger 1977), the first method was the preferred option because it was more reproducible and more accessible to workers. However, primer synthesis has since been automated and reliable enzymes are now available, thus Sanger's method is now preferred, due to its speed. Maxam and

Gilbert sequencing is however still useful for the sequencing of synthetic oligonucleotides and chemically modified nucleic acids. Briefly, this sequencing technique involves two stages, the first one being a base-specific chemical modification of the radioactively end labeled DNA and the second being a cleavage of the DNA strand at the 5',3' phosphodiester bonds of the modified base. This is carried out in 4 different reaction mixtures, involving modification and cleavage at G, A+G, C+T and C. The resulting mixtures are run in parallel on a sequencing gel and the sequence can be deduced from the order of bands on an autoradiogram. The method is summarized in figure 1.7, where the G specific reaction is shown as an example.

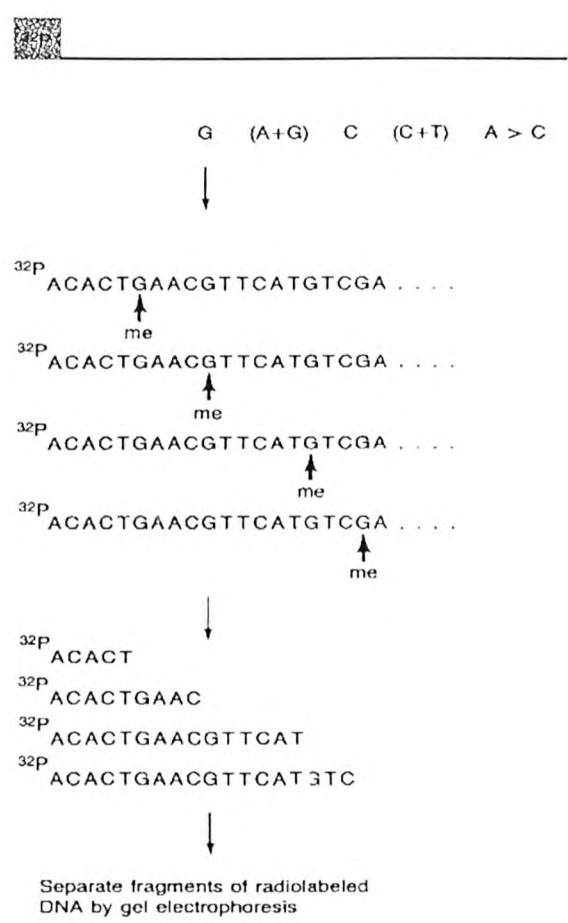


Figure 1.7. Sequencing by the Maxam and Gilbert chemical degradation method (Sambrook *et al* 1989)

1.3.1.2. Sanger sequencing

In the Sanger's sequencing technique (Sanger 1977), dideoxynucleoside analogues that act as chain terminators are incorporated during the replication of a DNA template by a DNA polymerase enzyme. When 2',3' dideoxythymidine triphosphate (ddTTP) is incorporated in a growing chain reaction with DNA polymerase, the chain cannot grow any further because ddTTP does not contain a 3' hydroxyl group. Hence the termination occurs specifically at positions where dTTP should be incorporated. If a radioactively labeled primer and template are incubated with a DNA polymerase in the presence of a mixture of ddTTP and dTTP in addition to the other 3 deoxyribonucleosides, a mixture of fragments all having the same 5' end and with ddTTP residues at the 3' end is obtained. When this mixture is separated by electrophoresis on polyacrylamide gel, the pattern of bands shows the distribution of ddTTP in the newly synthesised DNA. By using analogous terminators for the other nucleosides in separate incubations and running the samples in parallel on the same gel, a pattern of bands is obtained from which the sequence can be read off. Gel electrophoresis analysis is however gradually being replaced by capillary electrophoresis, which has greater sensitivity (see below).

See figure 1.8 for a schematic description of the Sanger sequencing technique.

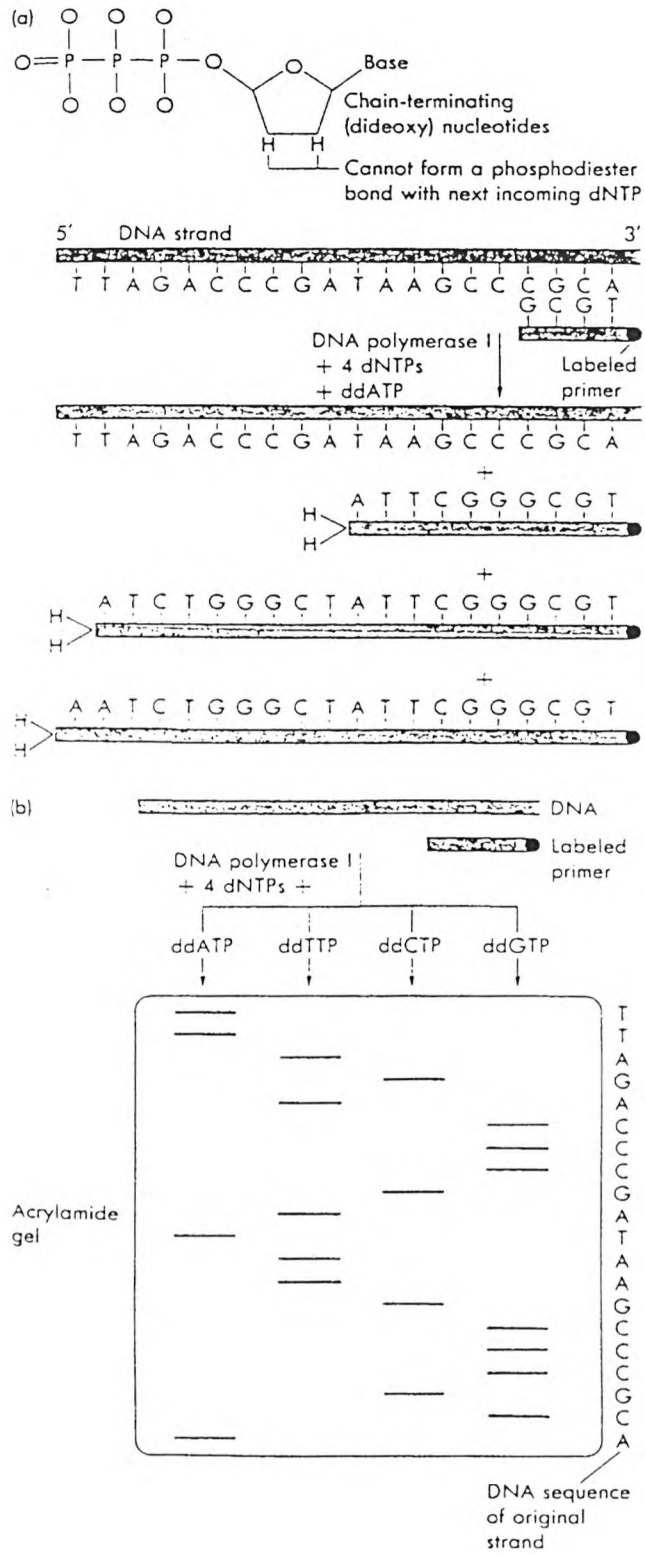


Figure 1. 8. Sanger's sequencing technique

1.3.2. Analytical techniques for the sizing of DNA sequencing fragments

Below are described analytical techniques that permit direct sizing of DNA fragments. They are necessary for the analysis of the complex mixtures resulting from the sequencing reactions described above, but are also used for a variety of routine DNA analyses (size of PCR products, etc..)

1.3.2.1. Slab gel electrophoresis

As described in section 1.2 (page 3), nucleic acids are formed from linear chains containing a phosphate/sugar backbone. Because of the negative charge on the phosphate group under the conditions employed, a DNA molecule, when placed in an electric field, is attracted to the positive electrode. Electrophoresis is based on this principle which is illustrated in figure 1.9. A mixture of DNA fragments is injected at one end of a gel (usually agarose or polyacrylamide) and a high voltage is applied. DNA molecules migrate at rates that are inversely proportional to the \log_{10} of the number of bases (Helling *et al* 1974). This will result in the formation of “bands that contain all molecules of similar molecular weight, large molecules migrating more slowly than smaller ones.

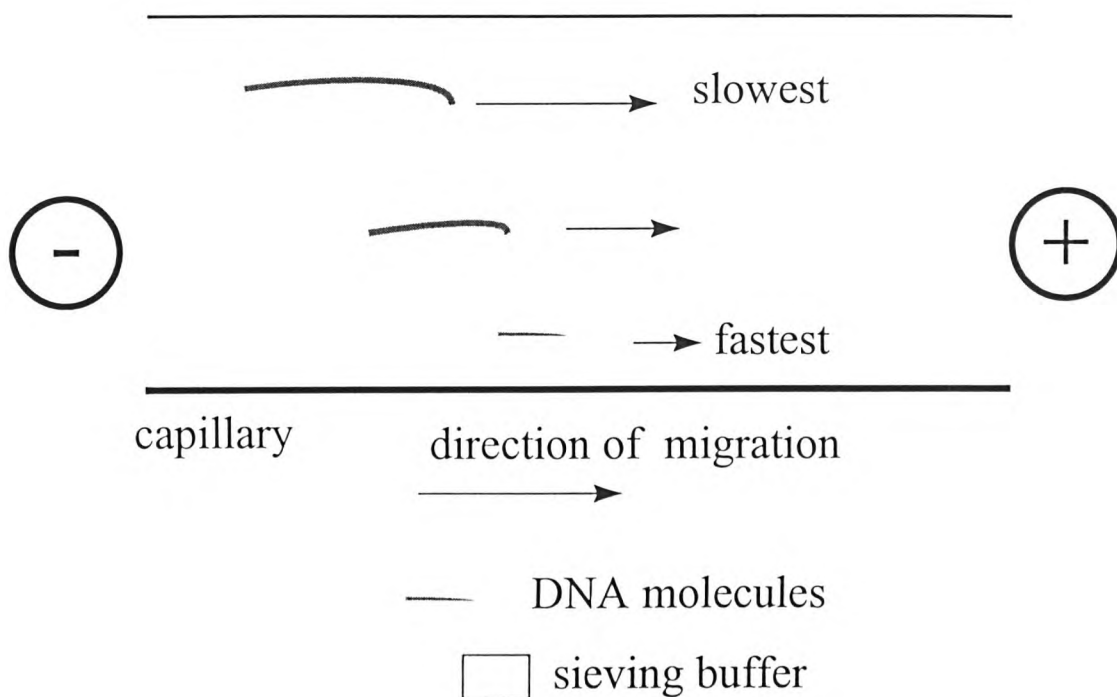


Figure 1.9. Schematic representation of DNA migration during electrophoresis

The bands are usually detected using ^{32}P labelling or ethidium bromide staining. The use of a “ladder”, composed of restriction fragments of known molecular weight, run in parallel with the samples, will allow an approximate determination of the size of the fragments present in the sample. Figure 1.10 represents a photograph of a typical electrophoretic separation in a polyacrylamide gel. Although slab gel electrophoresis is still used by the majority of molecular biologists because of its simplicity and its low cost, capillary electrophoresis is considered to be far superior in terms of sensitivity, speed and potential for automation. These considerations become very important strategically when a task as huge as the sequencing of the human genome is undertaken. More emphasis will therefore be given to CE here. Additional details on electrophoresis are available in the literature (Sambrook *et al* 1989).

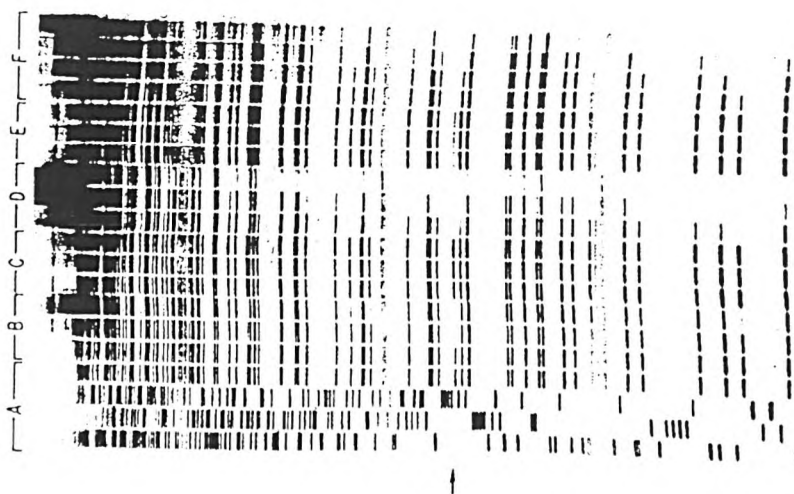


Figure 1.10. Photograph of a typical electrophoretic separation in a polyacrylamide gel (Tabor and Richardson 1990).

1.3.2.2. Capillary electrophoresis

Capillary electrophoresis aims to overcome the problems encountered with the slab gel techniques that are used for DNA analysis. In essence, the capillary format increases the rate of heat dissipation resulting from Joule heating. As this is responsible for band broadening, CE facilitates higher throughput by permitting the use of a higher electrical field. This technique is readily automatable and is in theory able to provide a higher resolution than with slab gels. Sequencing of more than 600 bases in a single run has been reported (Swerdlow *et al* 1991, Gesteland 1990).

Principle: A sample is introduced into a capillary that has been equilibrated with a continuous buffer. Both ends of the capillary and electrodes are placed into buffer solutions and up to 30kV are applied to the system. As electrophoretic separation occurs, molecules pass through a detector where the information is collected and

stored by an appropriate data acquisition system. Fig 1.11 represents the schematic representation of a CE system.

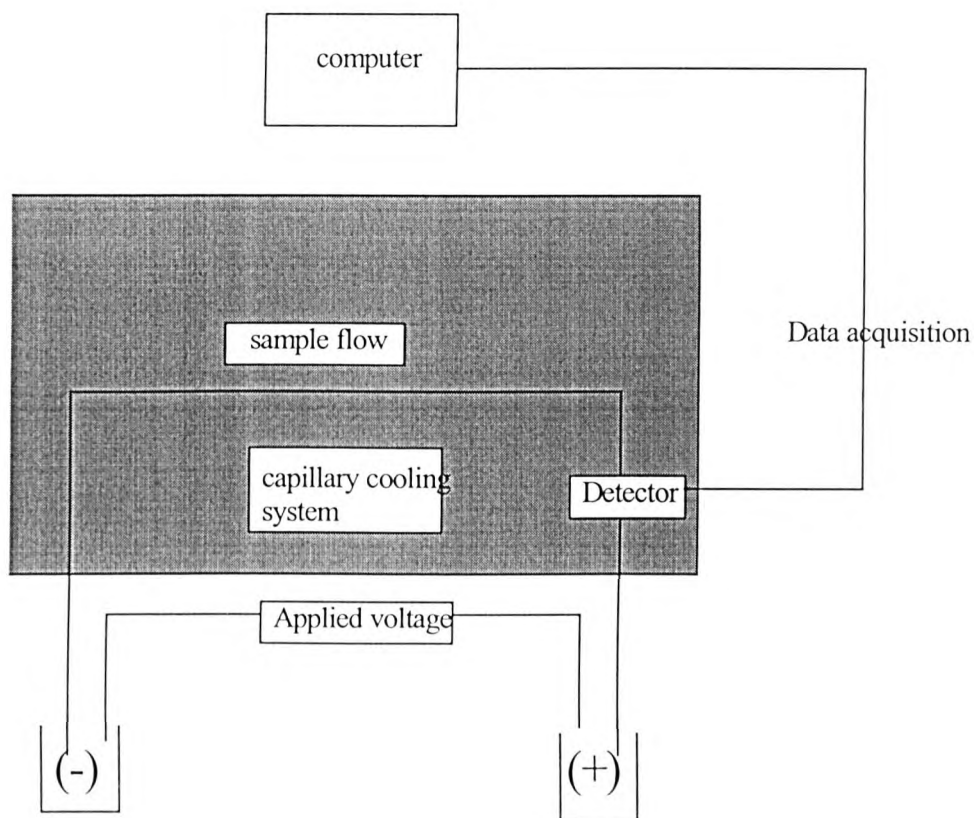


Figure 1.11. Schematic representation of capillary electrophoresis apparatus.

The use of a capillary as the separation environment is ideal for electrophoresis. The high surface to volume ratio allows for very efficient dissipation of Joule heating caused by the applied electric field (Slater *et al* 1995). Consequently the voltage applied for separation can be very high without overheating (which causes broadening of bands) and a faster separation is obtained with better resolution than for slab gels.

Nucleic acids have a constant negative charge per unit length so that the mobility of the molecules is independent of molecular weight in free solution. Therefore sieving

buffers are required and some systems use prefilled polyacrylamide capillaries. This poses problems because the gel cannot be pumped out and the capillary has to be changed very often. Entangled polymer solutions are therefore preferred, as they can be pumped in and out after each run.

As the charge on DNA molecules is negative due to the phosphate ions present in the chain, the poles of the CE have to be inverted so the sample is injected at the cathode pole and the molecules are attracted by the anode. The electroosmotic flow is then inverted and goes from the anode to the cathode, inhibiting DNA molecules migration, in the case of liquid buffers. The capillary must therefore be coated with a neutral layer to reduce the zeta potential. Coating also prevents any unwanted DNA adsorption onto the capillary walls.

1.3.2.3. Use of MALDI mass spectrometry for DNA sequencing applications

Matrix Assisted Laser Desorption Ionisation mass spectrometry, or MALDI mass spectrometry can be used for the mass determination step with nested sets generated using Sanger sequencing chemistry (Pieles 1993, Fitzgerald 1993, Chen *et al* 1995). The technique provides the advantage of not requiring radioactive or fluorescent labeling over more conventional electrophoresis analysis. MALDI also shortens the overall sequencing process (lengthy because of the long electrophoretic separation step). Furthermore, this technique can be automated, which is a requirement for high throughput sequencing. Although the technique is well established for sequencing

short polynucleotides (Schuette *et al* 1995), MALDI does not allow easy analysis of large nucleic acids (due to the instability of gas phase DNA ions) and therefore routine sequencing of DNA is not yet possible (Fitzerald *et al* 1995). Because it has so much potential, the use of MALDI -MS has triggered a lot of research in the development of matrices. Furthermore, new strategies for stabilising the sugar phosphate backbone of the larger DNA molecules are currently being developed (Kirpekar *et al* 1995), thereby rendering DNA sequencing by MALDI possible.

Principles of MALDI MS

Mass spectrometry is based on producing, differentiating and detecting ions in the gas phase. The production of ions from a sample of interest has traditionally been performed using thermal vaporization. This is, however, of little use for the analysis of thermolabile biopolymers and non volatile compounds. The recent development of Matrix Assisted Laser Desorption Ionization sources has opened up many possibilities for the routine mass determination analysis of large biomolecules such as proteins, peptides, carbohydrates and nucleic acids.

In the MALDI technique, a high intensity pulsed (usually UV) laser beam is used to desorb and ionize a sample embedded in a matrix on a metal surface. Intact gas phase ions of the sample are generated and directed electrostatically into a mass analyzer (Siuzdak 1994), which is typically a time-of-flight (TOF) mass analyzer. Figure 1.12 shows a schematic representation of the MALDI apparatus used in the present work. The choice of a suitable matrix in MALDI MS analysis of oligonucleotides is crucial. Despite the large number of matrices that have been studied for various applications (Fitzerald and Smith 1995, Fitzgerald, Parr, Smith

1993), research to find better matrices is still an ongoing activity. Useful matrices reported to date are usually aromatic compounds containing carboxylic acid moieties. The requirement for aromatic compounds is due to their absorption band which is close to the emission wavelength of the lasers commonly used in MALDI (Fitzerald, , Parr, Smith 1993).

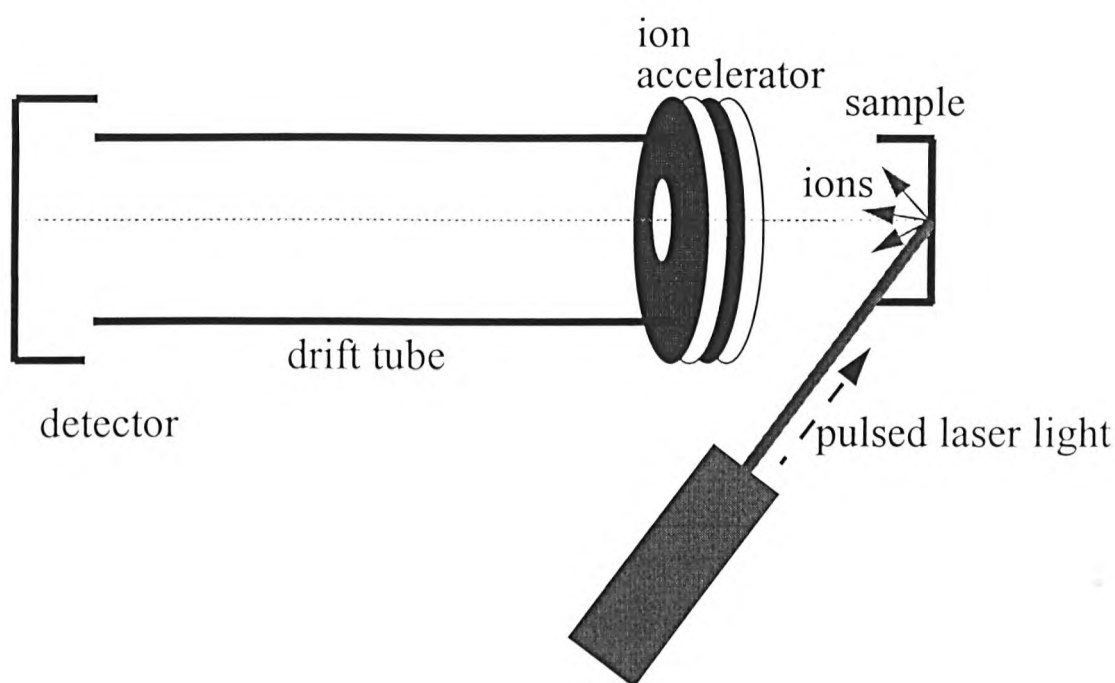


Figure 1.12. Schematic representation of MALDI TOF apparatus.

1.3.3. Other sequencing strategies

A range of alternative techniques for sequencing DNA have also been investigated by numerous researchers. For example, Hettich and Buchanan (1991) have reported the

ability to completely sequence oligomers as long as 25 bases in length using Fourier transform mass spectrometry, while others have reported the use of electrospray mass spectrometry sequencing for sequence verification of modified oligonucleotides (Barry *et al* 1995). This technique seems to be useful when the Sanger sequencing technique fails because the enzyme does not usually recognize modified bases in DNA sequence. Fragmentation occurs across the oligonucleotide and the pattern of the spectrum allows verification of the sequence. However, as with MALDI MS, electrospray mass spectrometry is currently used effectively only for short oligonucleotides.

Other techniques, such as a flow based continuous DNA sequencing technique using single molecule detection of enzymatically cleaved fluorescent nucleotides have been reported (Schecker *et al* 1995). Even though its feasibility has been demonstrated, its main advantage over simpler and cheaper CE techniques remains unclear.

While all the techniques described so far are used for *de novo* sequencing, confirmatory sequencing utilises a completely different set of instrumentation tools and is actually often performed using oligonucleotide hybridisation methods. This will therefore be discussed in more detail in the hybridisation section of this chapter.

1.4. Hybridisation assays/use of DNA probes

DNA hybridisation is a phenomenon that occurs when complementary nucleic acids bind together because of base pairing. It can be done either in solution, or one of the strands involved in the process can be attached to a solid surface. Solid phase hybridisation, despite having relatively poor kinetics as compared to solution hybridisation, is the basic technique chosen for many routinely used assays such as dot blot (Kafatos *et al* 1979) and Southern blot (Southern 1975).

Solid phase hybridisation assays generally involve a **bound target**, which is a known nucleic acid, either PCR product representing a gene, or an oligonucleotide of known sequence. To this target are hybridised **labelled probes**, that are of unknown composition. These probes are produced either by direct labelling of the sample nucleic acids or by reamplification of the sample involving incorporation of labels in the same process. However, other schemes involve the binding of the sample to a surface and the labelled nucleic acid is of known sequence. After hybridisation has occurred, the unbound probe is washed away using stringency washes. This washing step also aims at removing any loosely bound material that does not match the target perfectly. Once this is done, detection of the labelled bound occurs if the complementary sequence of the target nucleic acid was present in the probe. The solid phase hybridisation assay technique is schematically represented in figure 1.13.

Sequences of nucleotides can also be identified within sample cells or tissues, by using “in situ” hybridization techniques (Bauman *et al* 1984). Biological tissue is fixed to a microscope slide and hybridized to a labeled nucleic acid probe. The results are recorded microscopically.

This technique is sufficiently sensitive to detect single base mutations on a single copy gene in total genomic DNA . It therefore allows the observation of alterations of the DNA of patients suffering from genetic diseases. It also allows determination of nucleic acid homologies (Kafatos *et al* 1979), that can be used for example for paternity testing. It can also form the basis for microbiological tests such as the detection of organisms that are not readily cultured or biochemically identified, or organisms that do not possess diagnostic antigens, the differentiation of pathogenic from non virulent strains, the identification of antibiotic resistant genes, epidemiological studies/typing schemes and rapid culture confirmation (Nicholls and Malcom 1989, Heller and Morrisson 1985).

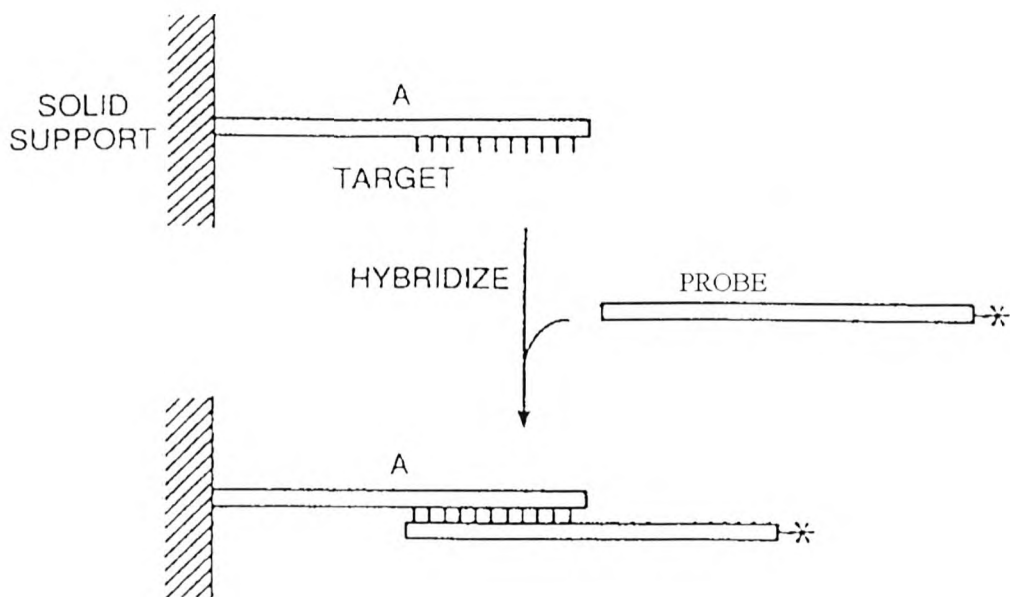


Fig 1.13. Schematic representation of the solid phase hybridisation assay technique (from Nicholls and Malcom 1989).

Although very simple in principle, solid phase hybridisation involves complex physico chemical mechanisms during which the capture of the complementary probe by the bound target can be described as a limited irreversible reaction-diffusion (Chan *et al* 1995). Existing mathematical models are based on two different models, one assuming that the probe interacts with the target through direct three dimensional interaction, and the other involving non specific adsorption of the probe to the surface, followed by a two dimensional diffusion to the target. These two model are schematically represented on figure 1.14.

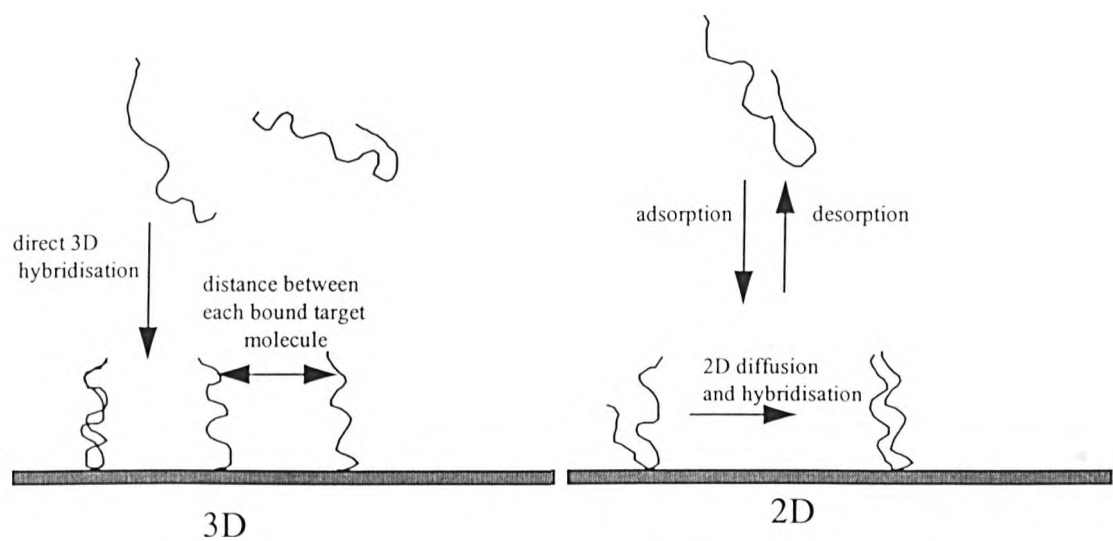


Figure 1.14. Schematic representation of 2 possible models for solid phase hybridization

In the reactions illustrated above, the speed of hybridization is highly dependent on the concentration of free DNA, the distance between each bound DNA target and the rate of adsorption/desorption of the probe in the case of the 2D mechanism. It was also found that the density of the bound material possessed an optimum value. When the density of target is too high, the signal obtained from hybridization decreases, probably due to steric hindrance (Shchepinov *et al* 1997). Southern blot and dot blots are usually conducted on nitrocellulose or nylon membranes. These pose the problem

of requiring large amounts of probe (which can be the limiting factor when they are prepared from small samples such as biopsies) and require long hybridisation times.

More recent techniques can solve these problems. Arrays of many different target DNA in the form of microscopic spots are immobilised on a surface such as glass. The probe is then hybridised as above. These arrays offer the advantage of analysis of a very large number of possible interactions (up to 200,000 for Affymetrix's genechips) for each sample in a reduced volume and incubation time. The preparation of such arrays relies upon automation technologies such as by depositing presynthesised PCR products or oligonucleotides using robotic arms, in-situ synthesis of oligonucleotides by photoactivated chemistry (McGall *et al* 1996) or ink jet deposition. The types of surfaces used in such technology range from glass microscope slides to silicon chips.

Sequencing by hybridization is one of the major applications where microarrays have been successfully developed. High density arrays of oligonucleotide probes are generated using combined solid phase chemistry, photolabile protecting groups and photolithography to produce DNA chips of densities approaching 10^6 sequences/cm² (McGall *et al* 1996). Those chips are then hybridized to the sample DNA, directly yielding sequence information. These chips are limited to confirmatory sequencing, but allow extensive sample throughput when the region or gene of interest is already known.

1.5. Labeling of nucleic acids

It is possible to use the UV absorption properties of DNA molecules to detect and quantify them without labeling but the sensitivity of this approach is not always sufficiently high. Thus in most DNA analysis techniques, DNA molecules have to be labeled to enhance detection.

Radioisotopes were predominantly used until recently, because of the great sensitivity of detection they provide, with Phosphorus 32 (Southern 1975), Sulfur 35 (Collins and Hunsaker 1985), Tritium and Iodine 125 (Edelstein 1986) being the main radioisotopes used. Radioisotopes are, however, being progressively replaced by non-isotopic methods of labeling because of the associated problems of safety, stability and radioactive waste disposal. Non-isotopic analyses of biomolecules have generated great interest in recent years and several extensive reviews have been published (Viale and Dell'Orto 1992, Kessler 1994). The replacement labels for radionucleides include fluorescence chromophores and chemiluminescent labels. The type of labeling is often chosen according to the particular application. General nucleic acid labeling strategies will be described below. Particular emphasis will be given afterwards to labeling for DNA sequencing since the approach used is rather specific to this application.

1.5.1. General strategies for nucleic acids labeling

An ideal label for a DNA probe used in hybridisation assays would be readily attached to DNA, be detectable at very low concentration using simple instrumentation and would produce a signal that is modulated when the labeled DNA probe is hybridised to its complementary sequence (thus facilitating non separation DNA probe assays).

Two main types of labelling strategies have evolved:

The first one is direct labelling, in which a label is attached directly via a covalent bond to DNA. The second one is indirect labeling, in which either a hapten (usually biotin) is attached to the DNA and detected by using a label binding with specificity to the hapten, or a hybrid formation is detected by using a binding protein with specificity for double stranded DNA.

A DNA molecule has few chemical groups suitable for the covalent attachment of a label. Most labeling procedures target the amino group substituent on the purine and the pyrimidine rings. When this type of labelling is used for DNA hybridisation assays, removal of the unbound probe is required. Non covalent labelling is also possible and generally involves the formation of intercalation complexes with fluorescent organic molecules. The fluorescence intensity of these compounds increases only upon binding to double stranded DNA (Glazer and Rye 1992), and the removal of the unbound DNA probes during hybridisation assays is not necessary. Compounds such as ethidium bromide (LePecq and Paoletti 1971), YOYO (dimer of benzoxazolium-4 quinolinium dyes, Srinivasan *et al* 1993) and TOTO (dimer of benzothiazolium-4 quinolinium dyes) offer such properties, and have been used, mainly for the labeling of PCR products separated by CE.

The overall sensitivity of nucleic acid quantitative assays can be increased by improving the quantum yield of chromophores, improving detection systems and lowering the background noise. Another approach is to increase the number of reporter groups on each molecule. This can be achieved, for example, by using branched oligonucleotides (Horn *et al* 1997). A range of other types of labeling strategies can be found in the literature. For example, Sloop *et al* (1994) have developed strategies to use metallo-organic labels for DNA sequencing and

mapping, such as ferrocene labels and triethylstannylpropanoic acid labels. These labeling strategies exploit the longer fluorescence life times of metal complexes compared to conventional fluorescent dyes, and therefore allow the use of different detection approaches, such as time resolved emission analysis. This detection technique allows background fluorescence rejection, leading to a higher sensitivity of detection. Complexes of organic molecules with lanthanide ions such as Eu^{3+} , Tb^{3+} , Sm^{3+} and Dy^{3+} also possess suitable characteristics to use this detection technique: these complexes have exceptional Stoke's shifts and narrow emission bands and their absorptions correspond to readily available laser bands. In addition they offer the potential for very high sensitivities of detection and their long life time fluorescence allow the use of time-resolved fluorometry. This type of signal processing permits the filtering out of shorter lived background fluorescence signals, as discussed below (see page 44) .

In figure 1.15, the spectra of 4 different lanthanide ions complexed with a chelate is shown. When compared with the conventional fluorescent dyes described later (p35), the spectra are seen to be much narrower and non overlapping, which is a considerable advantage for the design of a multicolour fluorescence detector.

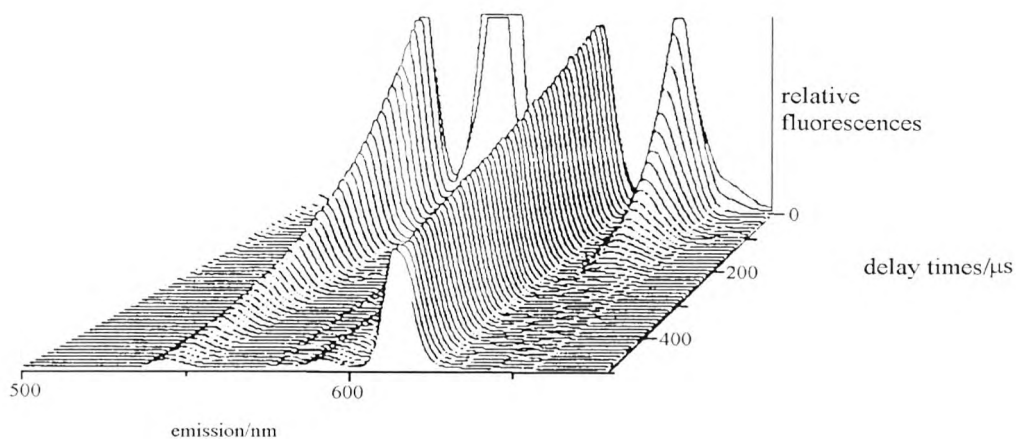


Figure 1.15. β diketone complexes emission spectra

The fluorescence of inorganic salts of the lanthanides is weak because the absorption of the ion itself is very low. This can be dramatically enhanced when the ion M^{3+} is bound to appropriate organic ligands and it was shown that the excitation light is absorbed by the organic part of the complex and emitted as the line spectrum of the lanthanide ion following an energy transfer process (described below page 34). All these features make lanthanide chelates very attractive candidates for ultrasensitive bioassays (Dickson *et al* 1995).

Applications of lanthanide chelate chemistry in nucleic acids labeling

Lanthanide chelate technology, using a wide range of chelates and lanthanide metals (Xu *et al* 1992), is already well established for immunoassays. The technique is available commercially for immunoassays, with DELFIA systems (Wallac Inc.) routinely being used in laboratories (Soini and Lövgren 1987, Dickson *et al* 1995).

More recently, the application of lanthanide chelates to nucleic acids detection and analysis has generated a lot of interest. For example, Eu^{3+} chelates have been used successfully to detect PCR products fixed on a solid support (Lopez *et al*, 1993), in solution (Nørgaard-Pedersen *et al* 1993) or in agarose gels (Chan *et al* 1993). Eu^{3+}

chelates linked to antihapten antibodies or streptavidin have also been used to detect hapten or biotin labelled probes in DNA hybridisation assays (Dahlen 1993, Syvanen 1986). More simply, the PCR amplified targets (DNA containing the gene or sequence of interest), can be hybridised to allele specific lanthanide chelate labelled probes (Huoponen *et al* 1994). Figure 1.16 shows the different formats available when designing a DNA hybridisation reaction using lanthanide chelates.

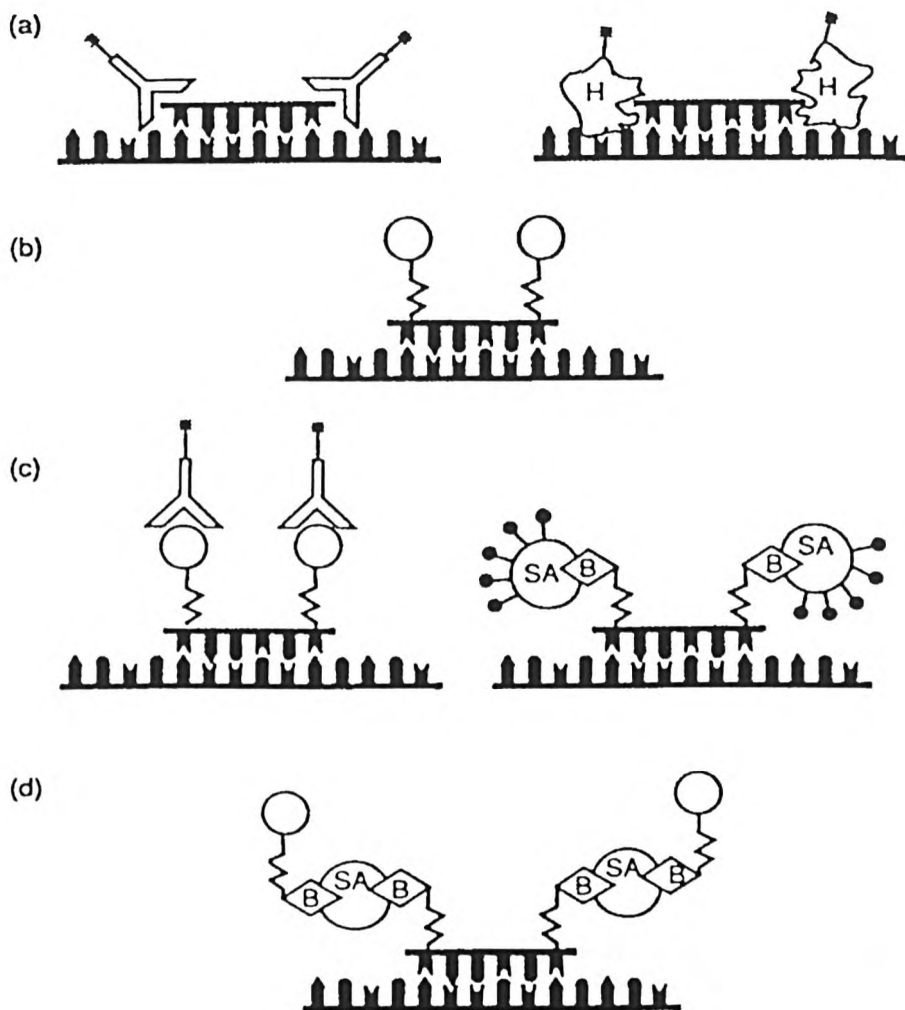


Figure 1.16. Assay designs in DNA hybridisation using lanthanide chelates (reproduced from Diamantis and Christopoulos 1990). (a) The DNA probe is used unlabelled and the hybrid is detected using either labelled antibodies or histones. (b) The DNA probe is directly labelled with a reporter molecule (c) the DNA molecule is conjugated to a hapten molecule and antihapten labelled antibodies are used to detect the hybrid. The probe can also be biotinylated and labelled streptavidin is used as the detection reagent or (d) unlabelled Streptavidin is used to bridge a biotinylated probe with a biotinylated reporter molecule

The detection of DNA in polyacrylamide gel electrophoresis separations using DTAA-pAS /Tb³⁺ chelates has also been reported (Saavedra and Picozza 1989). Most of the DNA detection research performed using time resolved fluorometry (described lower on page 44) is carried using a single label, usually Eu³⁺ or Tb³⁺, although Sm³⁺ and Dy³⁺ chelates have also been described (Freeman and Crosby 1963). It has been found that chelators can be lanthanide specific, such as 5-fluorosalicylic acid which is specific to Tb³⁺ (figure 1.17), but that they can also form fluorescent complexes with several metal ions, such as 4-hydroxy-7-trifluoromethyl-3-quinolinecarboxylic acid or 4-hydroxy-7-methyl-1,8-naphthyridine-3-carboxylic acid which can both form fluorescent complexes with Eu³⁺ and Tb³⁺ (Diamantis 1992).

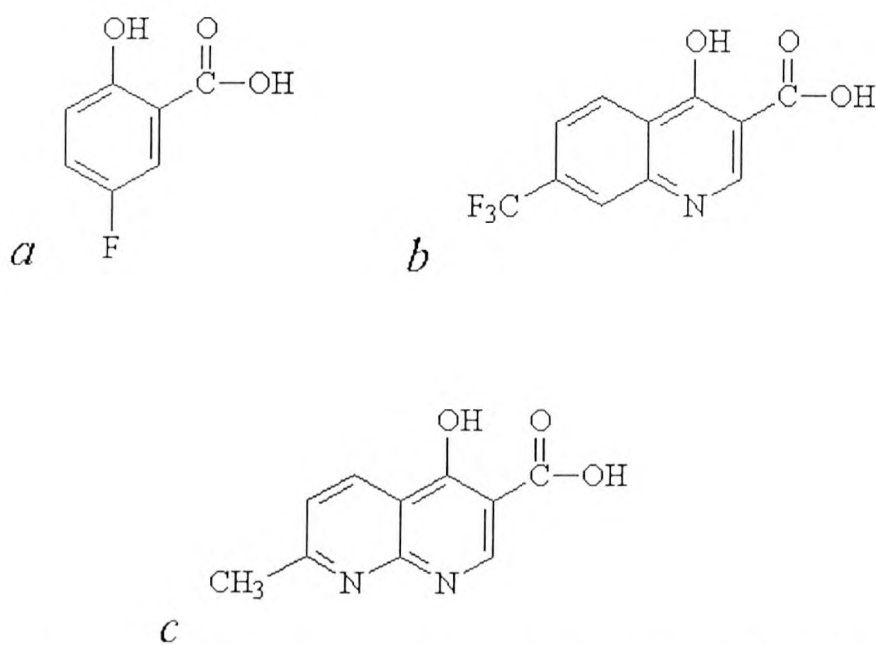


figure 1.17. Chemical structures of different lanthanide chelates (from Diamantis 1992): a: 5-fluorosalicylic acid, b: 4-hydroxy-7-trifluoromethyl-3-quinolinecarboxylic acid, c: 4-hydroxy-7-methyl-1,8-naphthyridine-3-carboxylic acid.

The most recent development for hybridisation applications used as many as 7 colours, by incorporating chelating agents into oligonucleotide probes and labeling them using combinations of Tb³⁺, Eu³⁺ and Sm³⁺ (Samiotaki *et al* 1997). Importantly, studies have shown that once complexed, lanthanide chelates remained stable with

negligible signs of exchange of ions between co-incubated labeled oligonucleotides (Kwiatkowski *et al* 1994).

In some bioassays, the chelates are attached to the “binding molecule”, either the antibody, or the DNA probe, and the fluorescence is revealed after separation of the unbound material by the use of enhancement solutions. These contain chelates of stronger affinity for the metal than the chelate initially bound (Xu *et al* 1992) which results in fluorescence enhancement.

In other cases, the chelate attached to the binding molecule does not require enhancement, because it is directly detectable. More recent developments include FRET or Fluorescence Resonance Energy Transfer. This is a strongly distance dependent excited state interaction in which the emission of one fluorophore is coupled to the excitation of another. The mechanism that permits the metal to absorb the excitation radiation and to emit fluorescence in return is mainly energy transfer. It was described for the first time by Weissman (Weissman 1942).

Theory of fluorescence energy transfer mechanisms:

Energy transfer from a ligand based state to the emitting state of a lanthanide ion has been demonstrated to occur with high efficiency. The phenomenon is illustrated on figure 1.18. The organic ligand absorbs energy and is raised from its singlet ground state S_0 to any one of the vibrational multiplets of the first singlet excited state, S_1 where it rapidly loses its excess vibrational energy and falls to the lowest S_1 level. From there, the molecule can either deactivate by a radiative transition (ligand fluorescence) or go over to one of the triplet states T_1 or T_2 . Deactivation then occurs via molecular phosphorescence ($T \rightarrow S_0$) or the excitation is transferred to the metal

ion. If the ion comes to resonance upon receiving this excitation, it undergoes a radiative transition resulting in a characteristic emission line (ion fluorescence) .

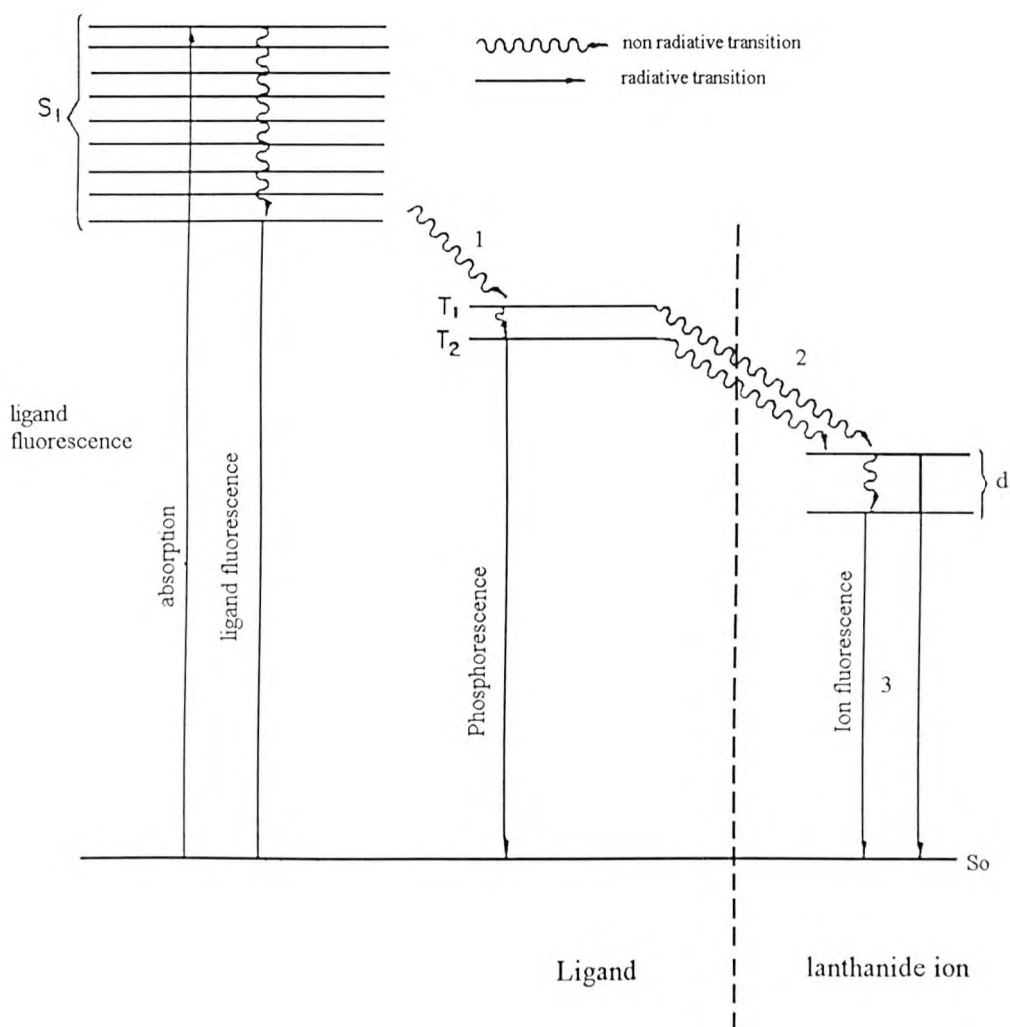


figure 1.18. Energy transfer mechanism

All these features make lanthanide chelates a labelling strategy with many advantages. It might be possible to adapt the existing chemistry to new applications that would benefit from such characteristics, such as DNA sequencing.

1.5.2. Labelling for DNA sequencing

Although it is possible to use only one type of label for the four reactions corresponding to each base of the sequence (radioactive or fluorescent label) and then run them down four parallel electrophoretic lanes, the trend to use multicolor labelling schemes has become predominant in the 1990's. This allows the user to run simultaneously the four reaction mixtures generated from the Sanger sequencing reaction from a given template in the same electrophoretic lane or capillary and hence increases the sample output of any sequencing machine by a factor of four.

This approach, pioneered and developed by Smith *et al* in 1986, together with the Applied Biosystems slab gel four color sequencers, now is routinely used by most sequencing laboratories. Furthermore, they developed a chemistry for the synthesis of fluorescent oligonucleotide primers. A derivative of thymidine was synthesised, which contained a phosphoramidite moiety at the 3' end and a protected amino group at the 5' carbon. This molecule is used in the final addition cycle of oligonucleotide synthesis by the phosphoramidite method (Atkinson and Smith 1984). This material may readily be conjugated to many of the various commercially available amino reactive fluorescent dyes to yield a corresponding fluorescent oligonucleotide derivative. The dyes employed by Smith *et al* were chosen with absorption and emission maxima in the visible region. Their emission spectra were well resolved from one another and they were highly fluorescent the dyes were also chosen such that they did not impair significantly the hybridisation of the oligonucleotide primer. The electrophoretic mobility should ideally not be distorted by the presence of the dyes, but the chosen dyes (NBD, fluorescein, tetramethylrhodamine, texas red) do, in fact, affect the electrophoretic mobility, such that a mobility correction to the

sequence data is necessary. The dyes structure and fluorescence spectra are shown in figure 1.19.

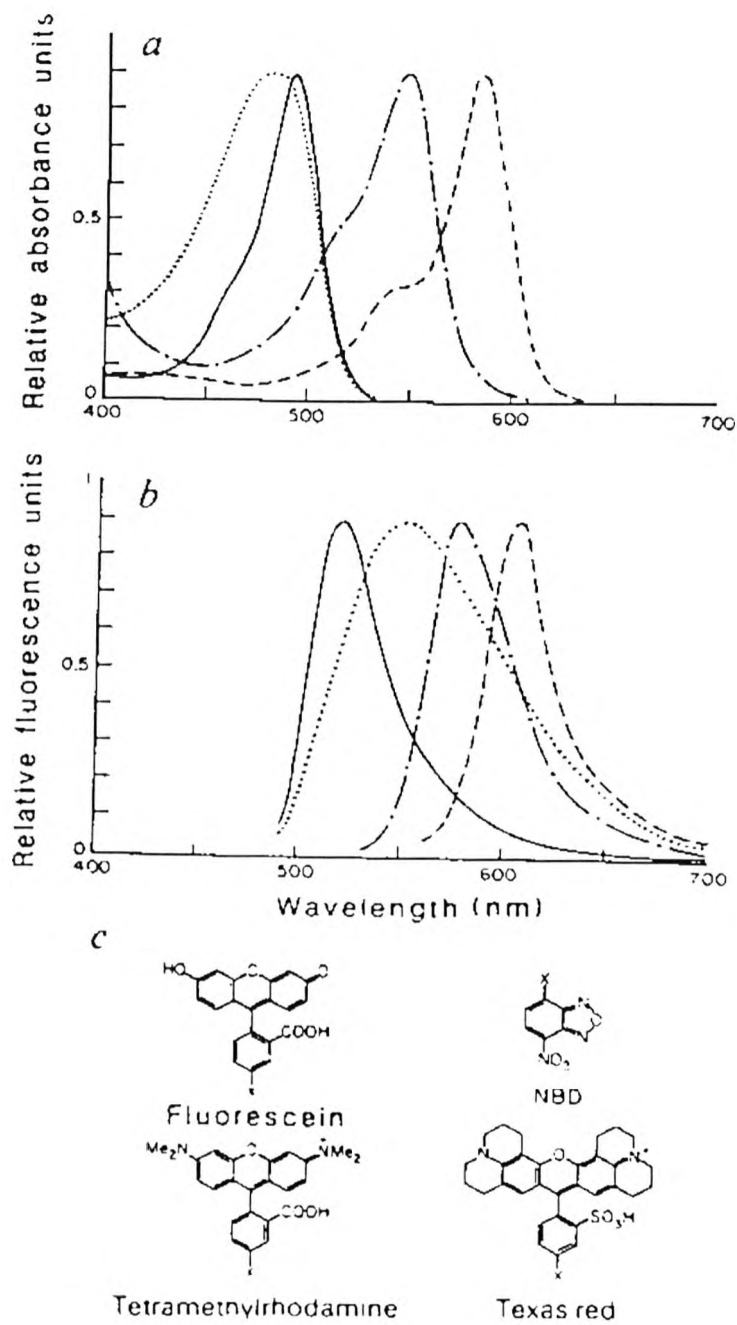


Figure 1.19. Emission spectra and structures of the four ABI dyes. Legend:— fluorescein, NBD, —.—.— tetramethylrhodamine,----Texas red. Adapted from Smith *et al* (1986).

Lanthanide chelates were also identified as suitable candidates for DNA sequencing, because of their superior spectroscopic properties, that can be highlighted by comparing figure 1.15 and figure 1.19. A sequencing technique using Sm^{3+} , Eu^{3+} , Tb^{3+} , and Dy^{3+} chelates was described in 1994 (Sloop *et al* 1994). In this technique, a tailor made chelate, a naphthalene derivative of DOTA (1,4,7,10-tetraazacyclodecane-1,4,7,10-tetraacetic acid, figure 1.20) was used. That chelate was designed to provide a higher absorption coefficient than DOTA itself. This chelate was attached to primers, which were suitable for use in sequencing reactions.

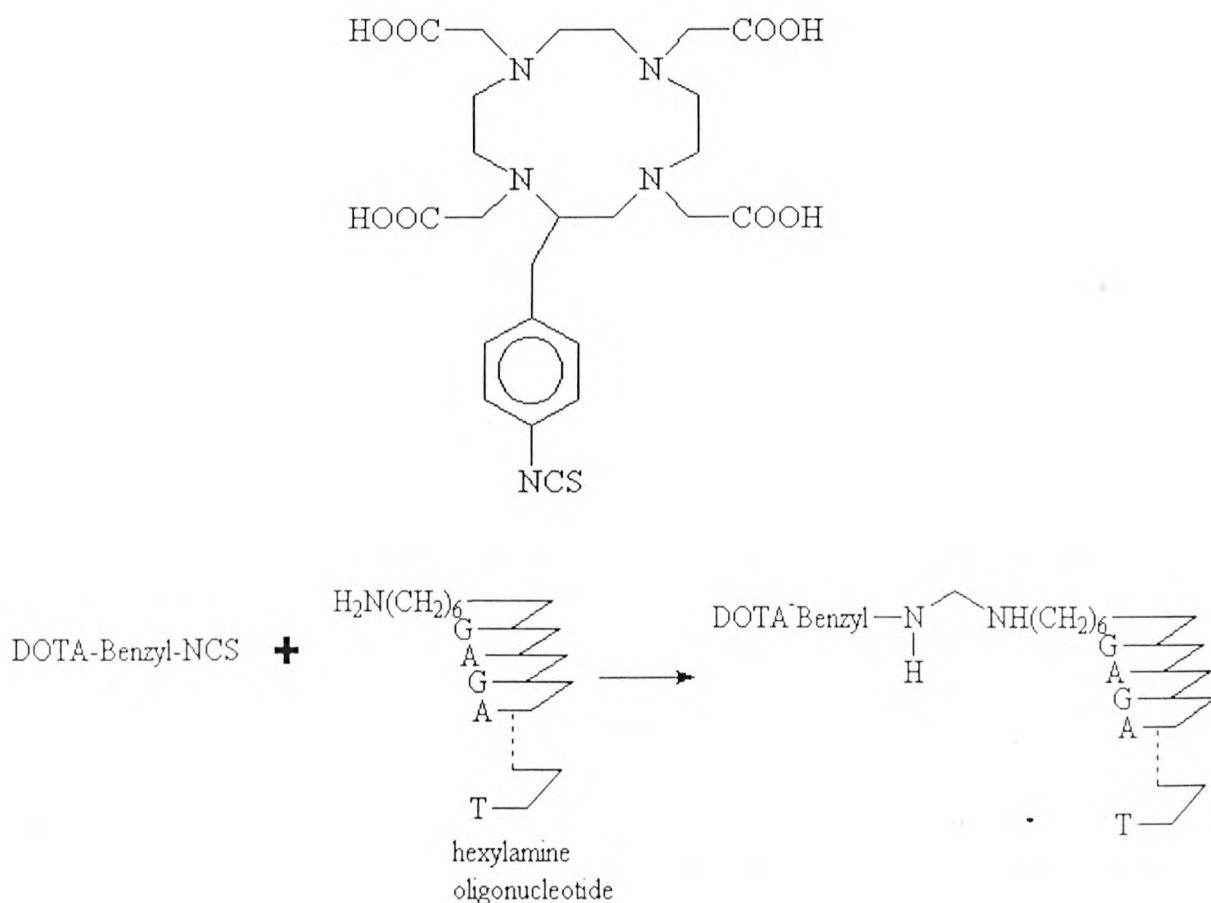


Figure 1.20. Chemical structure of DOTA-benzyl-NCS and its attachment to oligonucleotides (from Sloop *et al* 1994)

The location of the labels during DNA sequencing is an important factor that can determine the quality of the results. End labeling of sequencing primers can create ambiguous sequencing gels, because of the natural tendency of the polymerase to dissociate from the template during replication. This creates fragments that are not terminated due to incorporation of dideoxynucleotides and that are therefore not representative of the sequence. This means that the sequencing technique using lanthanide chelates attached to the sequencing primers, described page 38 is not ideal. A solution to this problem is to label the ddNTPs directly. This can be achieved by attaching the fluorophores onto the chain terminators, that can subsequently be incorporated during the sequencing reaction. This, however, demanded huge efforts in terms of optimisation of the chemical structure of the nucleotide-dye complexes because of difficulties of incorporation of the modified nucleotides by the enzyme (Parker *et al* 1995). Other labelling methods are also being developed to overcome the problems encountered with the conventional dyes described above. One example is the use of 4 coupled pairs of dyes offering fluorescence energy transfer properties (Mathies *et al* 1995). These are all excitable at 488 nm and give a large Stoke's shift. Their emission spectra do not overlap and they show a stronger fluorescence intensity than commercially available dyes. Near IR fluorescent dyes (Soper *et al* 1995) which contain a unique intramolecular heavy atom and possess the required lifetime differences to permit base identification during CE separation have recently been developed. Near IR dyes such as polymethine cyanines offer the advantage of being excitable using semiconductor laser lines (Chen *et al* 1993, Williams *et al* 1993). These lasers allow easier automation and miniaturisation of the process and are relatively cheap compared to conventional lasers.

1.6. Optical DNA detection techniques

For any labeling strategy to be successful, i.e. sensitive and representative of the sample measured, it has to be coupled with a suitable detection method. As the focus of this thesis is fluorescent labeling, other types of labeling such as radioactive labels and their associated detection methods will not be discussed here.

1.6.1. Fluorescence detection techniques

Fluorescence techniques are predominant in DNA analysis, because of the advantages they provide. Potential sensitivity is very great, as some techniques allow single molecule detection (Nguyen and Keller 1987). A wide dynamic range is achievable, rendering small populations of molecules detectable simultaneously with large populations.

Theory of fluorescence

Fluorescence is a form of luminescence in which light is emitted from molecules for a short period of time, after an initial absorption of light. The emitted light is termed fluorescence if the delay between absorption and emission is of the order of 10^{-8} s or less (Ploem 1992). Compounds exhibiting fluorescence are called fluorophores or fluorochromes. The three stages of the fluorescence process are schematically represented in figure 1.21. Stage 1 is referred to as the excitation, whereby a photon of energy $h\nu_{\text{EX}}$ is supplied by an external source and absorbed by the fluorophore, creating an excited singlet state (S_1'). This process distinguishes fluorescence from chemiluminescence, in which the excited state is created by a chemical reaction. Stage 2 is called the excited state lifetime. The excited state lasts for a finite period of time, which is very short (typically $1-10 \times 10^{-9}$ s). The energy of S_1' is partially dissipated yielding a relaxed singlet state S_1 from which fluorescence originates. Not all the

molecules excited in stage 1 will return to S_0 by fluorescence emission. Other processes such as collisional quenching or energy transfer (described page 34) can also depopulate S_1 . The quantum efficiency of the process, ϕ , is defined as the ratio of the energy of the photons emitted by fluorescence to the energy of the total photons absorbed and is a relative measure of the extent to which these processes occur. Stage 3 is the final stage where fluorescence emission occurs. A photon of energy $h\nu_{EM}$ is emitted, returning the fluorophore to its ground state S_0 . Due to energy dissipation, the energy of this photon is lower than the excitation one, and therefore of longer wavelength. This is the principle of Stoke's law, which states that the wavelength of emission is usually longer than the wavelength of excitation.

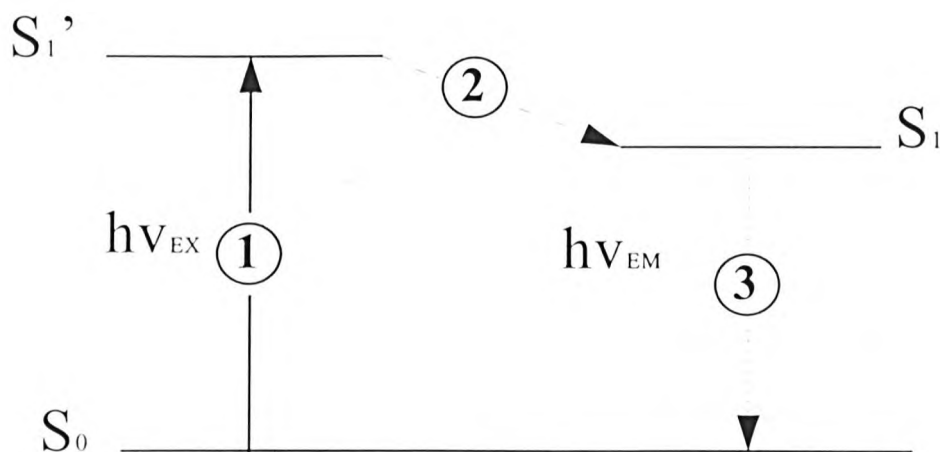


Figure 1.21. Representation of the processes involved in fluorescence emission of a fluorophore. The labelled stages 1,2 and 3 are referred to in the text.

The intensity of the emitted light depends on the intensity of the excitation light, the quantum efficiency (which may be as high as 0.9) and the concentration of the

fluorophore. The intensity of the emitted light after the excitation source is being turned off for time t is given by

$$I(t) = I_0 e^{-t/\tau} \quad (1)$$

where τ is the fluorescence lifetime. I_0 is the intensity of emitted light at $t=0$. The decay time is given by

$$\tau = 1.5/f\nu^2 \quad (2)$$

where f is the oscillator strength for the absorption.

Other important phenomena include quenching (Chen 1988), which occurs when the quantum yield is decreased, but the emission spectrum is unchanged. It can result from collisional quenching or from formation of non fluorescent excited state species. Self quenching is the quenching caused by one fluorophore acting on another and occurs when high loading concentrations or labeling densities are used. Therefore, although the intensity of the fluorescence signal can be increased to increase sensitivity, excessive quantities of fluorophores can reduce this sensitivity.

Photobleaching is another phenomenon that should be taken into account when designing a labelling/detection system. Bleaching is the destruction of the fluorophore under ultra high intensity illumination conditions. Therefore sensitivity of detection should be optimised to allow reduction of the intensity of the excitation light.

1.6.1.1. Fluorescence detection methods

In fluorescence detection systems, the sample is usually excited by radiation from a high power xenon arc or mercury lamp, or a laser whose line is absorbed by the sample. The emitted radiation is then detected (usually at right angles to the incident beam) through a wavelength selector (interference filter or monochromator). A detector (Photodiode, photomultiplier tube or charge coupled device) is used to collect the fluorescence photons. This is in turn connected to a read out device (chart recorder or computer).

1.6.1.2. Signal processing for improved sensitivity

Due to the extremely low levels of fluorescence detection required in some application, such as capillary electrophoresis where the capillaries used are extremely small (typically 100 μ M internal diameter), precise alignment and sensitive light detectors do not always suffice to achieve suitable sensitivity. In such cases, it may be necessary to employ complex signal processing of the output of a given detector, to improve signal/noise ratios or to extract supplementary information on the fluorophore such as fluorescence life times.

Phase sensitive detection:

In this technique, the light is modulated, often using a rotating wheel, creating a sinusoidal signal of known frequency (usually around 100 Hz). The resulting fluorescence will be emitted at the same frequency. The output of the detector (a PMT or photodiode for example) is then processed by a “lock in amplifier” (Horowitz and Hill 1989). This lock in amplifier is linked to a reference which is the frequency of the chopper and the lock in after adjustment, will amplify the signal

detected at this frequency only, thus eliminating all other sources of interference that might occur at different frequencies, resulting in a much better signal/noise ratio.

Time resolved fluorescence:

This technique is of interest when using labelling that possesses long lifetime fluorescence emission characteristics. The principles of this technique are summarised in figure 1.22. it represents a typical fluorescence decay curve, where short lived fluorescent components (mostly background noise) decrease rapidly, whereas longer lived fluorescence remains measurable for a longer period of time. Measurement is therefore delayed after excitation until short lived fluorescence has decayed, thereby improving the signal to noise ratio.

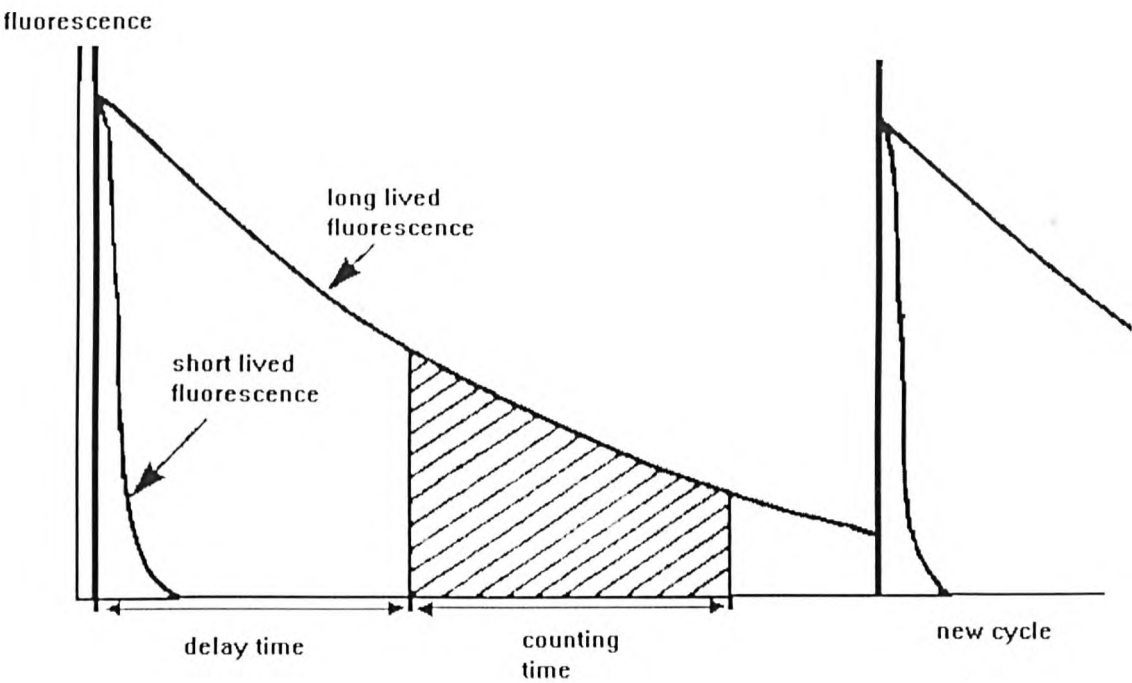


Figure 1.22. Principles of time resolved fluorometry
(reproduced from Soini and Lövgren 1987)

Although time resolved detection was not reported as a detection strategy for CE, it was assessed on dyes used in DNA sequencing (Chang and Forcé 1993). This was done to overcome the problem posed by the overlap of the emission peaks found in the 4 colour labeling technique described above. Generally the lifetime of unspecific background signal is less than 10ns. For an interference free measurement of a specific signal, labels are required whose life time is at least ten times the decay time of the background.

Suitable organic fluorophores with a life time superior to 50ns are very rare. Emission lifetimes can be measured using several techniques, two of which are phase modulation and single photon counting techniques (Straughan and Walker 1976). The phase modulation technique consists of modulating the excitation beam at high frequency. By using an electronic circuit capable of comparing the phase of the fluorescence to that of the excitation beam, p the phase difference can be determined. τ is given by:

$$\omega\tau = \tan p \quad (3)$$

where ω is the modulation frequency.

1.6.2. Non linear optical methods

Most DNA hybridisation assays are now realised on solid surfaces. Linear optical techniques such as fluorescence detection as described above are well established, but are prone to difficulties, such as light scattering and self fluorescence of the bulk

material. Linear optical detection techniques also require the use of labels to improve their sensitivity. Although labelling techniques are extensively and routinely used, they are time consuming, often requiring incubation, purification and characterisation steps. Few techniques offer the possibility to analyse DNA without such a labelling step. There are however a small number of non labelling-surface based detection techniques. An example which has been able to successfully monitor biomolecular interactions is Surface Plasmon Resonance (SPR) (Goddard *et al* 1994, Nilsson *et al* 1997). This technique has been the subject of extensive investigation in recent years. The sensors are constructed from a thin layer of metal (gold or silver) deposited on a dielectric prism or grating. Measurements are made by exciting surface plasmon resonance at the boundary between the metal and the sensing layer, which results in the absorption of the incident radiation and a subsequent reduction in the reflected light intensity. The condition for exciting resonance (i.e. the angle of incidence of the exciting radiation), is extremely sensitive to any changes in the refractive index of the sensing layer at the metal film boundary, and therefore sensing reaction can be followed by monitoring the angular position of the reduction in reflectivity. The resolution and hence the sensitivity, is limited by the resonance width, which is itself determined by the absorption in the metal layer. This limits the choice of the metal layer to highly conductive metals such as gold and silver. The performance of SPR sensors is ultimately determined by the physical properties of the metal layer and can therefore not easily be improved. A biomolecular analysis device is commercially available (BIAcore) and is currently being used widely (Wood 1993). However, as said before, it involves the production of highly homogeneously metal coated slides, onto which the sample is applied and the difficulty to prepare slides with

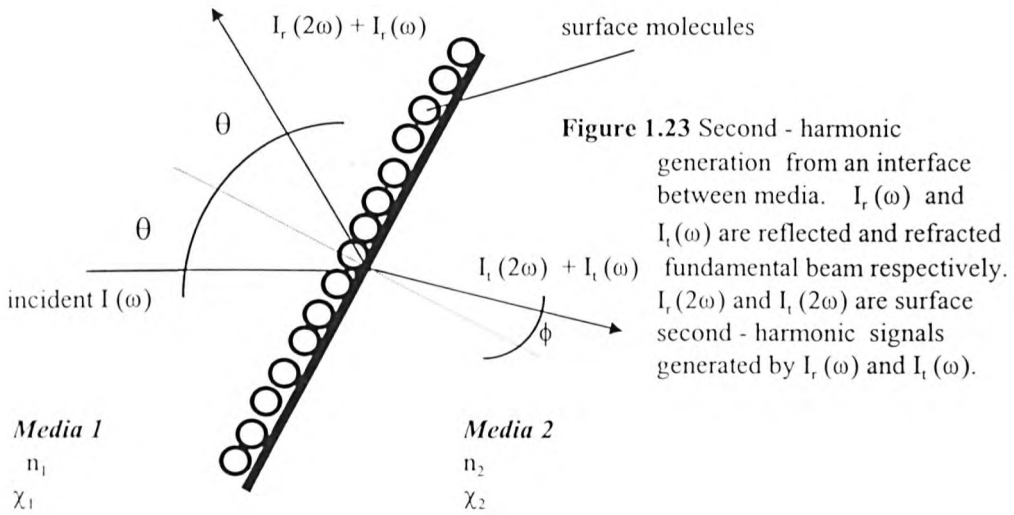
reproducible quality. This has made the technique rather difficult to apply and expensive, hence its relatively poor commercial success.

Non linear as well as linear optical techniques can be used to probe surfaces. Perhaps the simplest one to apply is Surface Second Harmonic Generation (SSHG). This has been extensively used in the study of molecular adsorption on metal surfaces (Tom 1984), adsorption of molecules or atoms onto semiconductor surfaces (Malvezzi *et al* 1984). Other works describe the use of SHG to study monolayer films of organic molecules deposited on a substrate (Mizrahi and Stegeman 1989). The technique has been shown to be sufficiently sensitive to detect sub-monolayer levels on a solid substrate and can be used to probe surfaces in a more physiological environment. A significant feature of the technique is that this submonolayer sensitivity can be achieved on non-metal surfaces. It has the advantage over fluorescence that the signal is surface specific and has angular dependence. Sub picosecond laser pulses can be used for probing, giving the technique the potential for subpicosecond time resolution, thus making it useful for *in situ*, real time, probing of fast surface dynamics and reactions (such as DNA hybridisation). It is also capable of *in situ* mapping of molecular arrangement and composition of a surface monolayer, because of the good spatial and spectral resolutions that lasers can bring (Shen 1989). It is therefore of interest to study in more details the surface second harmonic generation phenomenon and its theory, and by doing so, identifying how it may be possible to apply the technique to bioassay applications.

Theory of surface second harmonic generation

The SHG phenomenon involves a second-order non-linear optical process, which converts two incident photons of frequency ω into a single emission photon of frequency 2ω .

The second-order non-linear optical process of second harmonic generation, in the electric dipole approximation, occurs only in a medium of noncentrosymmetry, or where centrosymmetry or inverse-symmetry is broken. At surfaces and interfaces of media, the latter condition is naturally satisfied. Therefore, the second harmonic generation phenomenon will occur at such places when light energy is incident upon them. Figure 1.23 shows a schematic representation of second-harmonic generation at the interface of two media.



If the optical wave impinging on the medium probed has a frequency ω , dipole oscillation will be induced for each molecule in the medium. Oscillating dipoles emit electromagnetic radiation, and because the molecules behave like anharmonic

oscillators, output radiations at ω , 2ω , 3ω and so on, should be expected. In the second harmonic technique, one focuses attention on the frequency 2ω .

The induced second order polarisation per unit volume $P^{(2)}(2\omega)$ can be written as

$$P^{(2)}(2\omega) = \chi^{(2)} E(\omega) E(\omega) \quad (1.4)$$

where $\chi^{(2)}$ is known as the non linear susceptibility and is characteristic for a given medium.

$E(\omega)$ is the incoming electric field of strength E at frequency ω .

Solutions of equation 1.4 yield a second harmonic output $I(2\omega)$ in the reflected direction given by

$$I(2\omega) = (32 \pi^3 \omega^2 \sec^2 \theta_{2\omega} 2E(2\omega) \cdot \chi^{(2)} \cdot E(\omega) E(\omega) 2^2 I^2(\omega) / c^3) \quad (1.5)$$

where θ is the angle from the surface normal at which SHG occurs

$E(\omega)$ and $E(2\omega)$ are vectors describing the fundamental and second harmonic fields at the surface

c is the speed of light.

$\chi^{(2)}$ can be calculated using the following equation:

$$\chi^{(2)} = -\zeta N_e \cdot e^3 / (2m^2 (\omega_0^2 - \omega^2)^2 (\omega_0^2 - 4\omega^2)) \quad (1.6)$$

where ζ is a constant of anharmonicity, N_e is the number of electrons in the system and e and m are the charges and mass of an electron respectively, ω_0 is the resonance frequency.

Equation (1.6) indicates that the value of $\chi^{(2)}$ is proportional to the number of electrons in the system. This means that $\chi^{(2)}$ is proportional to the surface molecular concentration and thus $P^{(2)}(2\omega)$ will also depend linearly on the surface concentration of molecules. $I(2\omega)$ in turn will be affected by the concentration since its value is a

solution of the equation that defines $P^{(2)}(2\omega)$ (equation 1.4). Xiao and Shen (1993) have identified three different components that affect $\chi^{(2)}(\sigma)$ where σ is the surface coverage of the surface. According to them, the second harmonic signal comes from the bare substrate, the adsorbates and the interaction between the substrate and the adsorbate. The second order susceptibility can be defined as

$$\chi^{(2)}s(\sigma) = \chi^{(2)}_{ss} + \chi^{(2)}_m(\sigma) + \chi^{(2)}_i(\sigma) \quad (1.7)$$

With atoms or small molecules as the adsorbate, $\chi^{(2)}_m(\sigma)$, the adsorbate contribution is usually negligible, as is the substrate contribution $\chi^{(2)}_{ss}(\sigma)$. The coverage dependence $\chi^{(2)}s(\sigma)$ is mainly from the interaction part, $\chi^{(2)}_i(\sigma)$.

These characteristics of second harmonic generation therefore make the technique very suited for surface based bioassays such as DNA hybridisation where quantitative determination of surface concentration is an essential part of the assay.

Advantages of SSHG over other detection methods:

The second harmonic generation technique has a number of advantages over conventional fluorescence detection techniques. Firstly, in fluorescence detection systems, scattering and fluorescence of the bulk material is often a source for background noise. Because the SH signal is highly directional, spatial filtering of stray light or fluorescence is easily achieved. This is eased further because the second harmonic signal is upshifted compared to the laser wavelength. For example, a surface excited by a Nd:YAG laser at 1064nm will give a SSHG signal at 532nm. This allows easy spectral filtering of fluorescence, with none of the difficulties encountered when detecting fluorescence (need for a large Stoke's shift, difficulty to remove all scattered

light using spectral filters etc.), as illustrated in figure 1.24. Another feature of second harmonic generation which makes detection easier is the fact that the temporal profile of SH signal is unaffected by changes in surface properties and is always matched exactly with the excitation pulse. This is not the case for fluorescence which has a lifetime depending on the fluorescent molecule and its environment, which can make time gating to suppress background signals difficult. It is easy to use time gating methods with second harmonic generation, and this further reduces problems of non specific signal. A typical SHG system is represented on figure 1.25.

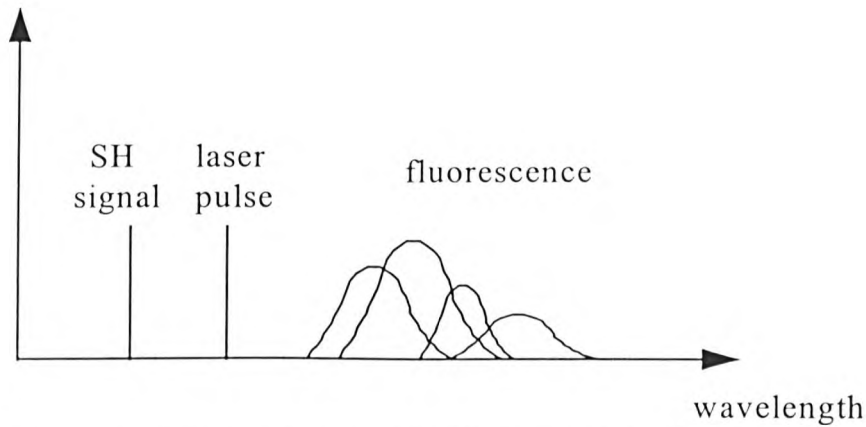


Figure 1.24. Illustration of the wavelength difference between SHG signal, laser light and fluorescence.

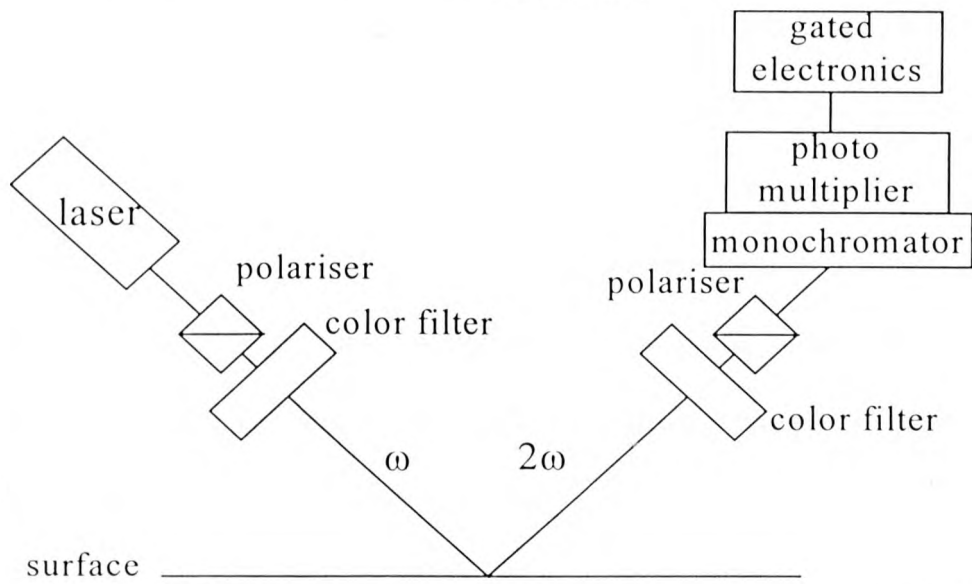


Figure 1.25. Schematic diagram of a typical experimental arrangement for surface second harmonic generation

The surface second harmonic phenomena has been applied to study a range of surfaces (Shen 1989) and has recently been applied to the study of immunological reactions (Yang *et al* 1998). Non linear optical studies were performed on wet spun DNA films, including second harmonic generation for the first time in 1993 (Williamson *et al* 1993). Suggestions have been made that DNA exhibits non linear optical properties because of possible nonlinearities in the polarisabilities of the oxygen atoms in the phosphate groups (Bilz *et al* 1987). Other sources on non linearity in DNA are possible in the hydrogen bonds between the 2 bases of a base pair (Techera *et al* 1989) the ribose pucker (Krumhansi *et al* 1985) and the interaction between adjacent base pairs (Muto *et al* 1989).

In other reports, solutions of double stranded DNA were studied using electric field induced second harmonic generation (Large *et al* 1996). These studies all aimed at better understanding the structural and conformational features of DNA, as well as its interactions with ions such as sodium (Williamson *et al* 1993).

It would be a very advantageous technique if it could be implemented in place of existing scanning systems for the detection of DNA hybrids, as the restrictions due to autofluorescence of the substrate and stability of fluorophores would not apply, the bioassay would have the sensitivity to detect monolayers of molecules on any surfaces commonly employed in biology laboratories and it would use simple, reliable and sturdy optical instruments. No previous studies to this one have approached the possibility of using SSHG of DNA monolayers on surfaces as a basis for a hybridisation assay detection scheme.

1.7. Conclusions and strategy of present work

It is clear that the field of DNA analysis is a very large and promising one, as illustrated by the huge number of journals, research groups and industries that are active in the field. It is also an area where major economic issues are raised and the intellectual property is very important.

The above review has highlighted the need for improved labelling strategies in the DNA sequencing field. The four colour sequencing strategies are now well established, but still possess problems such as overlapping emission bands, which makes base calling difficult, or the need for 2 lasers to excite the 4 different dyes. These spectral properties and the associated problems are intrinsic to the dye molecules used to label the DNA. There is therefore a need to develop new labeling schemes that can be used together with well spectrally adapted detection systems, giving an overall improved sensitivity.

Other areas such as non linear optical detection methods have been well studied for DNA conformation studies on surfaces, but there are obvious opportunities to be gained by applying this knowledge to solid phase DNA hybridisation assays, with the potential advantage of requiring no labeling and being able to perform real time measurements.

It is therefore proposed to assess both alternative labelling and detection schemes for their suitability to produce improved DNA assay systems. In particular, it is proposed to explore the possibility to use lanthanide chelates chemistry in a improved labelling scheme for DNA sequencing. It is also proposed to investigate the use of second harmonic generation for a new application, DNA hybridisation.

CHAPTER 2: DEVELOPMENT OF A LABELLING STRATEGY FOR DNA SEQUENCING USING LANTHANIDE CHELATES

2.1. Introduction

The review on DNA sequencing labelling strategies in chapter 1 highlighted the need for a better set of labelling molecules. Indeed, it seems obvious that the dyes used in the four colour method (see page 36) do not possess the ideal spectroscopic features for this application, such as well separated narrow band emission spectra. This results in the instrumentation used in this high throughput technology being complex and expensive. The development of new labels for DNA sequencing, which could provide improved sensitivity as well as features that would allow easier detection is desirable. Section 1.5.1 (p 27) of the introductory chapter introduced a class of reporter molecules called lanthanide chelates. These complexes offer lifetimes that are specific to the metal used and this permits the detection of several probes at the same time using time resolved fluorescence. In addition, they possess broad excitation spectra and narrow emission bands, as well as a large Stoke's shift. The use of one chelate which could support several metals offers the added advantage of a common excitation wavelength. It is thus now proposed to assess the feasibility of applying the well established chemistry and spectroscopy of lanthanide chelates to a new labelling strategy for DNA sequencing. The spectroscopic features of lanthanide chelates highlighted above could be used in an improved four colour sequencing reaction. This could be done by using a labelled chain terminating nucleotide chemistry, as opposed to a primer labelled sequencing chemistry.

In the proposed strategy, chelates with 4 different lanthanide metals could be attached to functionalised chain terminating nucleosides, thereby allowing incorporation into the DNA fragments resulting from a sequencing reaction (see chapter 1 where Sanger sequencing chemistry is described on page 13). The reaction mixture could be separated by electrophoresis. For a template containing n bases, one would obtain n bands, each corresponding to partial copies of the template DNA. An end terminated fragment for each possible location on the template would be present in the reaction mixture. These fragments would be end labelled, due to the presence of a lanthanide chelate on the modified nucleotide that caused the chain to be terminated. This label would therefore be specific for the base that was present on the template DNA. After detection of the bands in an electrophoretic gel, one could deduce the sequence of the original sample.

Ideally, one chelate would be chosen together with 4 different metals, one metal being the representative of each of the bases A,C,T or G and by using a single laser and a single gel lane or capillary electrophoresis, one would be able to simultaneously detect the four labels present in the sample mixture. This would allow to analyse more samples in each gel and ease the detection, because of the well defined emission bands. An other distinctive advantage over the current dye chemistry currently used is that the chelates would all have very similar molecular weight, so that the electrophoretic migration of the samples would not be affected by the difference from one label to the other.

The work was carried out as follows:

Firstly, an analogue of dideoxytriphosphate thymidine was synthesised, to serve as a chain terminator during the Sanger sequencing reaction, onto the 2' end of this terminator was attached the chelate. The second task was to choose a chelate that once complexed with a suitable lanthanide ion would have the required spectroscopic features. Ideally, this would be a chelate that would accept 4 lanthanide ions with distinctive emission spectra to ease detection and possess only 1 excitation line (reducing greatly costs and bulk when lasers are used). As described in the literature review above (page 29), it is possible to use several metals to complex some chelates. The chelate of choice would also have to withstand electrophoretic separations and incorporation into a sequencing reaction, without loss of fluorescence. Finally, the chelate should not require the use of enhancement solutions which are impractical when using electrophoretic separations. The last step of this study was to examine the feasibility of incorporating this new chain terminator with an enzymatic chain extension reaction. Inhibitory effects of the presence of lanthanides or free chelates in solution also had to be tested for.

2.2. Synthesis of a triphosphate-5' amino thymidine analogue

A functionalised analogue of thymidine, to be used as a chain terminating nucleotide in a DNA sequencing reaction was synthesised. An amino group on the 3' end allowed the attachment of the chosen chelate. This analogue was also triphosphorylated to allow its incorporation by a polymerase enzyme in a chain extension reaction. It was prepared as follows:

Preparation of 2,3- anhydrothymidine-5-benzoate:

Thymidine (1.28g, 5.284 mmol) was dissolved in DMF (dimethylsulfoxide, 34ml). Benzoic acid (2.078g, 7.926mmol), triphenyl phosphine (2.078g, 7.926mmol) and DEAD (diethyl azodicarboxylate, 1.248ml, 7.926mmol) were added to the solution. After 15 min, the same amount of triphenylphosphine and DEAD were added in DMF (3ml) to the reaction mixture. After 2 hours stirring, the solution was poured into ether cooled in dry ice. The white precipitate was filtered off and dried. TLC (thin layer chromatography) analysis showed a single spot. A yield of 80% was obtained and this product was used without further purification. ^1H NMR spectroscopy confirmed the structure of the product 2,3- anhydrothymidine-5-benzoate (δ 1.88, 2.5, 2.71, 4.44, 4.5, 4.6, 5.45, 5.9, 7.3-7.9).

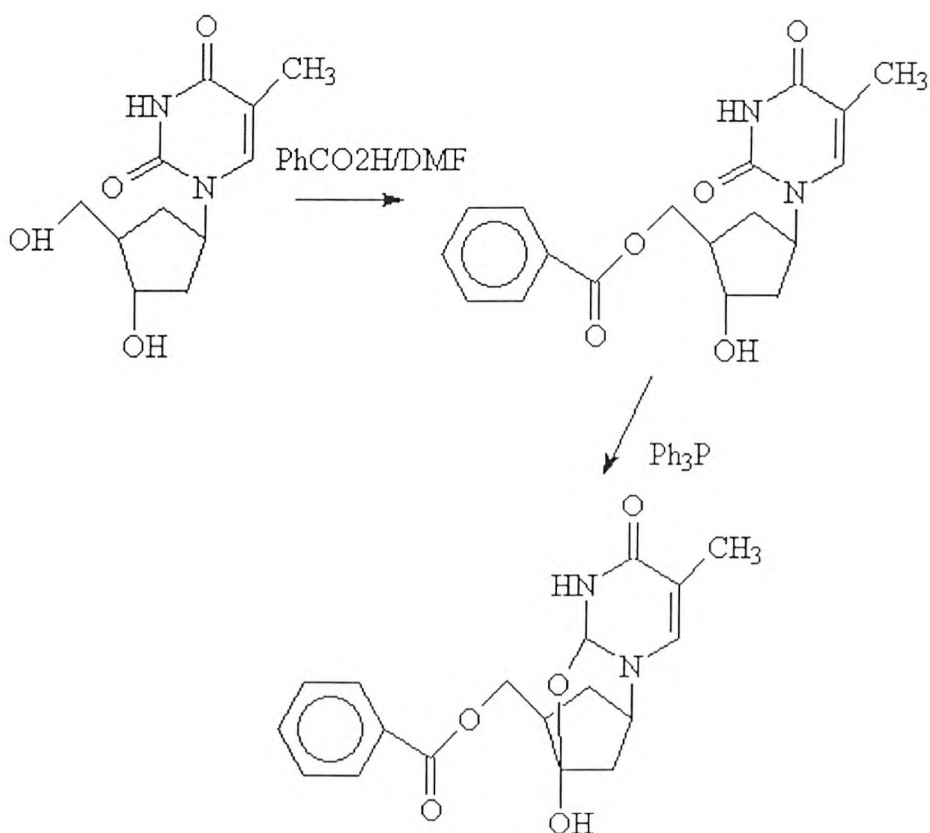


Figure 2.1. Preparation of 2,3- anhydrothymidine-5-benzoate

Preparation of 3'-azido-2' deoxythymidine (AZT):

2,3- anhydrothymidine-5-benzoate (1g, 3.05 mmol) was dissolved in dry DMF (25ml). Sodium azide (0.4g, 6.02 mmol) was added and the solution stirred for 20 hours at 123°C. The solvent was evaporated under vacuum. The yellow residue was dissolved in CH₂Cl₂ (100 ml) and washed twice with saturated solution of NaHCO₃, twice with saturated NH₄Cl and once with brine. The organic layer was evaporated under vacuum. The product was purified using silica column chromatography. Structural confirmation of the pure product (0.7 g, 62%) was obtained using ¹H NMR spectroscopy: δ 1.75, 2.4, 4.1-4.9, 6.2, 7.2-8.2, 8.9.

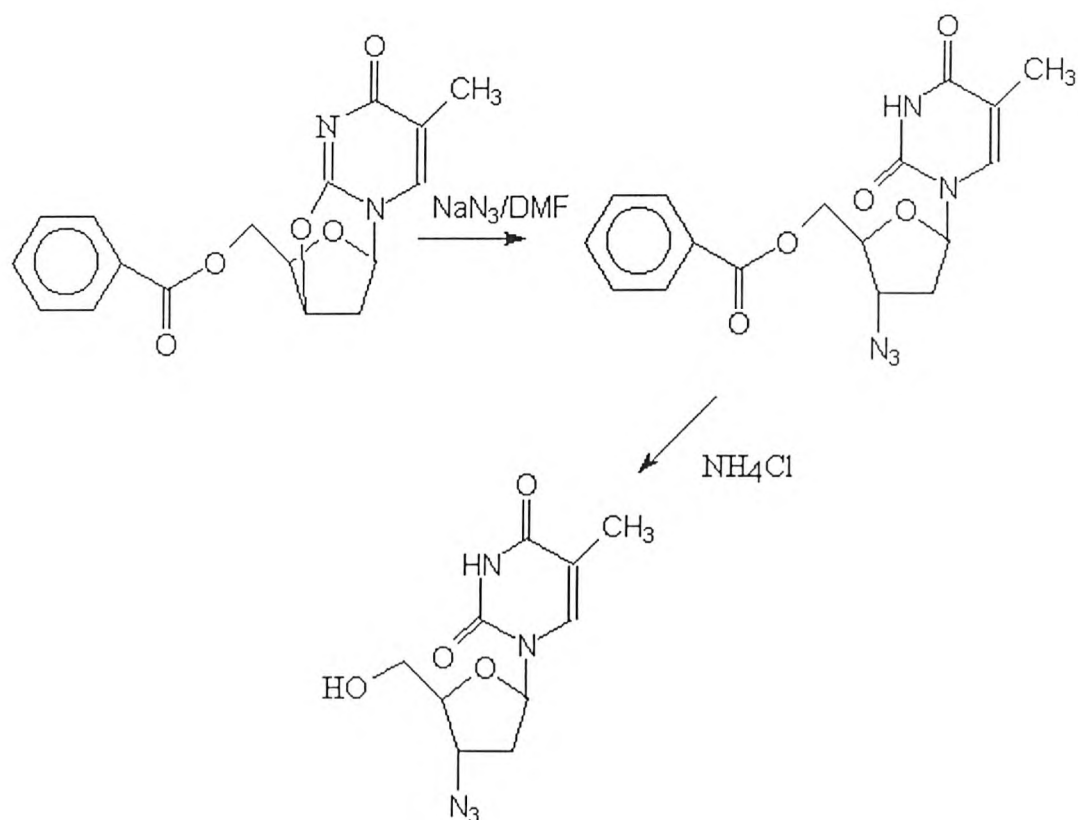


Figure 2.2. Preparation of 3'-azido-2' deoxythymidine

Phosphorylation of AZT:

AZT (48mg, 0.2 mmol) were added to anhydrous pyridine (200 μl) and anhydrous dioxane (600 μl). The mixture was stirred and kept under a low pressure. Through the septum was added $\text{PO}(\text{OMe})_3$ (200 μl). 12 μl of POCl_3 were added and the reaction mixture was flash cooled in an ice bath, then mixed for 1.5h. Tributylammonium pyrophosphate (0.145 g) dissolved in anhydrous DMF (600 μl) and B_3N (200 μl) were injected quickly. TEAB (triethylamine ammonium bicarbonate, 0.5 M) was prepared by mixing of Et_3N (59ml) and distilled water (931 ml). The pH of the solution was adjusted from 10 to 7 by addition of solid CO_2 (dry ice). TEAB (5ml) were added and

the reaction was stirred for 3 h at 25°C. Finally, TEAB was removed by evaporation.

The reaction procedure is summarised in figure 2.3.

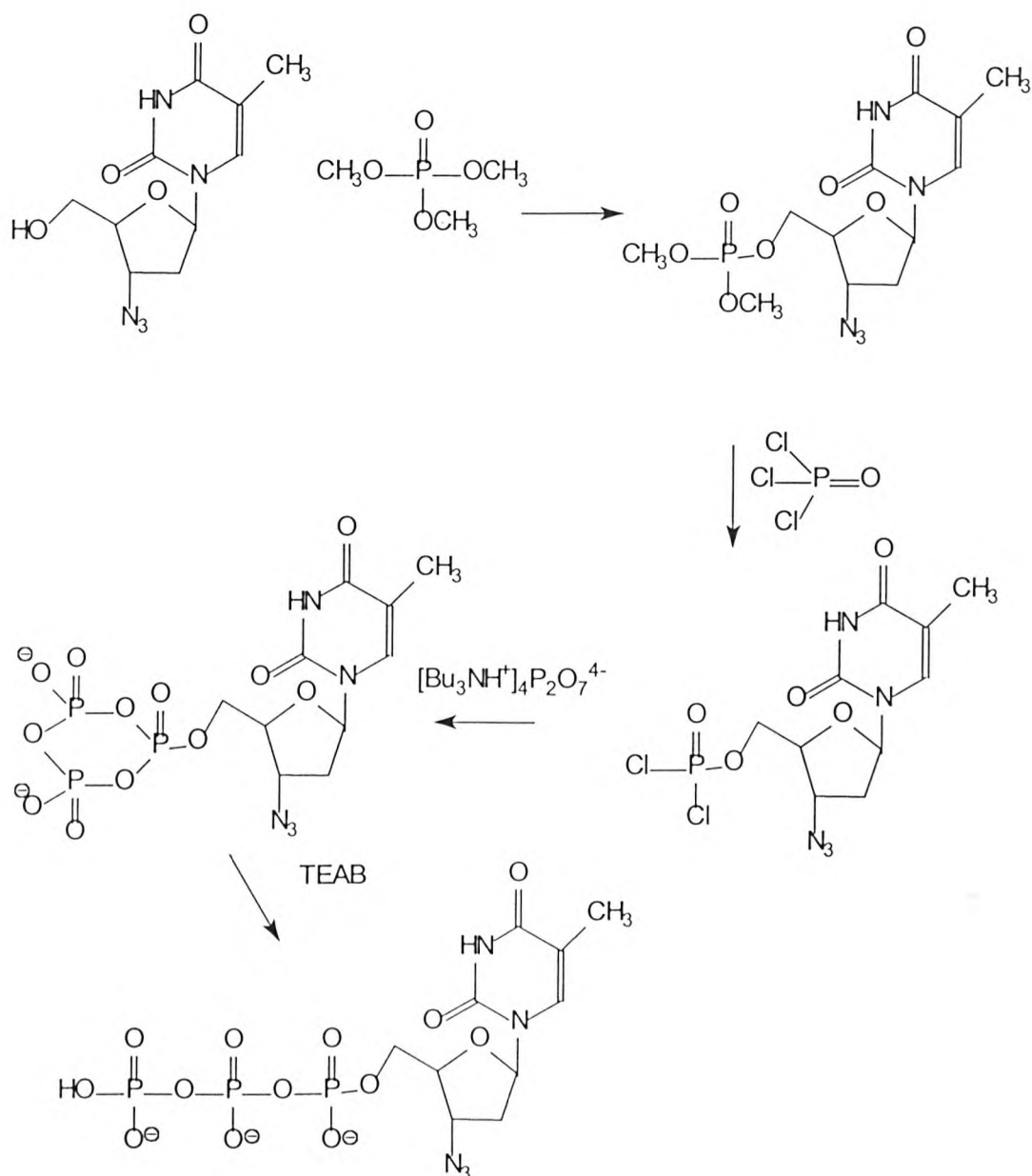


Figure 2.3. Synthesis of AZT triphosphate

The final product was found to be a mixture of mono, di and triphosphate of AZT.

This mixture was purified using ion exchange chromatography (Cohn and Bollum 1961). Triphosphate (17mg) was dissolved in pyridine (420 μl).

Triphenylphosphine was added and the reaction mixture was stirred for 5 hours. Then 5% aqueous solution of NH_3 (500 μl) was added. The mixture was stirred for another 2 hours to give the 3'-amino triphosphate thymidine product.

2.3. Synthesis of BCPDA and DTPAA -pAs

Among the numerous chelates described in the literature, two were selected for study. These were BCPDA and DTPAA- pAs: These 2 chelates were chosen as the test chelates in this study because they have both been used to label DNA and are suitable for electrophoresis. These two chelates were reported not to require the use of enhancing solutions, whose use is not practical during gel electrophoresis or capillary electrophoresis. Their differences in structure also allowed for comparisons in terms of accepting several metals and incorporation in the chain extension process during PCR.

Diethylenetriaminepentaacetic acid dianhydride- p-aminosalicylate (DTPAA-pAS) is a linear chelate that has been used as a label in fluorescent immunoassays (Bailey *et al* 1984) and more recently for the detection of DNA in polyacrylamide gel electrophoresis separations (Saavedra and Picozza 1989). Its structure is represented in figure 2.4.

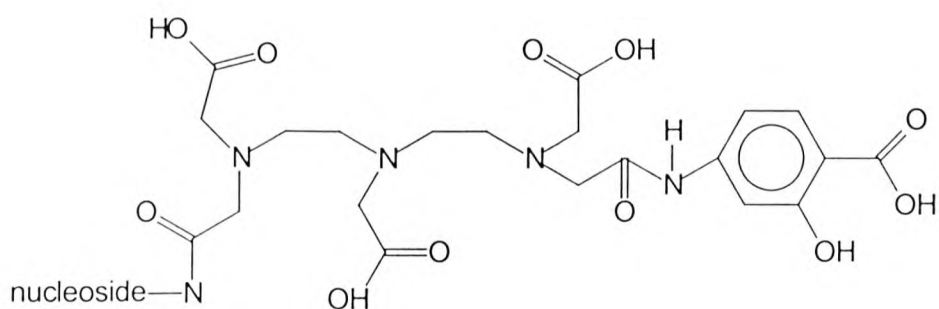


Figure 2.4. Presumed structure of the product formed from the reaction between DTPAA-pAS and a nucleoside. The amide linkage is formed with an exocyclic amine present on the nucleoside (Saavedra and Picozza 1989)

DTPAA-pAS has been used as a Tb³⁺ chelate and it has been shown by Saavedra and Picozza that the resulting complexes are stable under high electrical fields and

that they remain fluorescent under the conditions usually encountered during acrylamide gel electrophoresis.

4,7-bis (chlorosulphonyl)-1,10-phenanthroline -2,9- dicarboxylic acid (BCPDA) is a molecule containing numerous aromatic rings, and has been reported to form fluorescent complexes with Eu^{3+} (Evangelista *et al* 1988). It was also tested in electrophoretic separations, this time in agarose (Chan *et al* 1993) Its structure is represented in figure 2.5.

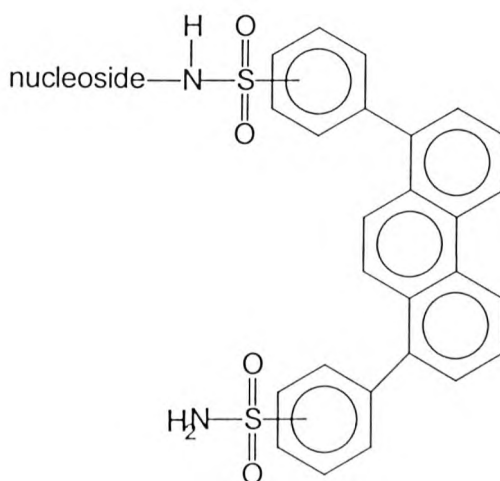


Figure 2.5. Schematic representation of the chemical structure of BCPDA bound to a nucleoside (or DNA)

Preparation of DTPAA-pAS:

This chelate was synthesised according to Saavedra *et al* (1989), and prepared as follows:

sodium *p* aminosalicylate (pAS) was dried overnight at 110°C. Diethylenetriaminepentaacetic (DTPAA) and pAS were made into 0.1M solutions in dry dimethyl sulphoxide (DMSO). Equimolar triethylamine (TEA) were added to the DTAA solution to facilitate dissolution. An equal volume of the pAS solution was added dropwise to the DTPAA solution followed by stirring for 60 min.

Preparation of BCPDA:

The BCPDA chelate was synthesised according to Evangelista *et al* (1988), and was prepared in the following manner:

2,9-Bis (trichloromethyl)-4,7-diphenyl-1,10- phenanthroline (product II, see figure 2.6):

Bathocuproine(I) (4 g) was mixed with benzoyl peroxide (0.011g) and N Chlorosuccinimide (9.8g) in carbon tetrachloride (100 ml) and were refluxed with stirring for 6h. The cooled reaction mixture was filtered to remove succinimide. The solvent was removed from the filtrate by vacuum evaporation. The residue was dissolved in chloroform (100ml). The organic layer was washed once with saturated aqueous Na_2CO_3 (100ml) and dried over anhydrous MgSO_4 . The product was obtained with a 95% yield after removal of solvent by vacuum evaporation.

^1H NMR was performed to confirm the structure of the compound in CDCl_3 : δ 7.56 (m, 10H), 7.98 (s, 2H), 8.27 (s, 2H).

I. 4,7-Diphenyl-1,10- Phenanthroline-2,9- dicarboxylic acid (product III, see figure 2.6)

2,9 -bis(trichloromethyl)-4,7- Diphenyl-1,10-Phenanthroline (0.56g, 0.97 mmols) and concentrated sulphuric acid (2.4 ml) were mixed and heated at 80°C for 2 hours. The mixture was then cooled in an ice bath and water (1.2 ml) was added. The mixture was further heated for an hour at 80°C . Ice water (37 ml) were added, and the yellow solid was collected by vacuum filtration. The product (37 mg) was collected, giving

a yield of 90.7%. ^1H NMR of the compound was performed in deuteriated dimethylsulfoxide (CD_3) $_2\text{SO}$: δ 7.63 (m, 10H), 7.99 (s, 2H), 8.25 (s, 2H).

4,7-Bis (Chlorosulphophenyl)-1,10-Phenanthroline-2,9-dicarboxylic acid (BCPDA)
(product IV, see figure 2.6):

Compound III (0.42g) was added in small portions to continuously stirred cold chlorosulfonic acid (2.1 ml). The mixture was then stirred for 4 hours in a 80° oil bath. After cooling to room temperature, the mixture was added to stirred ice water (80 ml) that was cooled externally by a large ice bath. The light yellow product precipitated immediately. The product was quickly collected on a sintered glass funnel by vacuum filtration, washed with cold distilled water and dried in vacuum for 12 hours. ^1H NMR in (CD_3) $_2\text{SO}$ gave δ 7.61 to 7.67 (m, 4H), 7.83 to 7.87 (m, 4H), 8.02 to 8.13 (m, 2H), 8.30 to 8.33 (m, 2H).

The structure of intermediate compounds produced during this synthesis can be seen on figure 2.6.

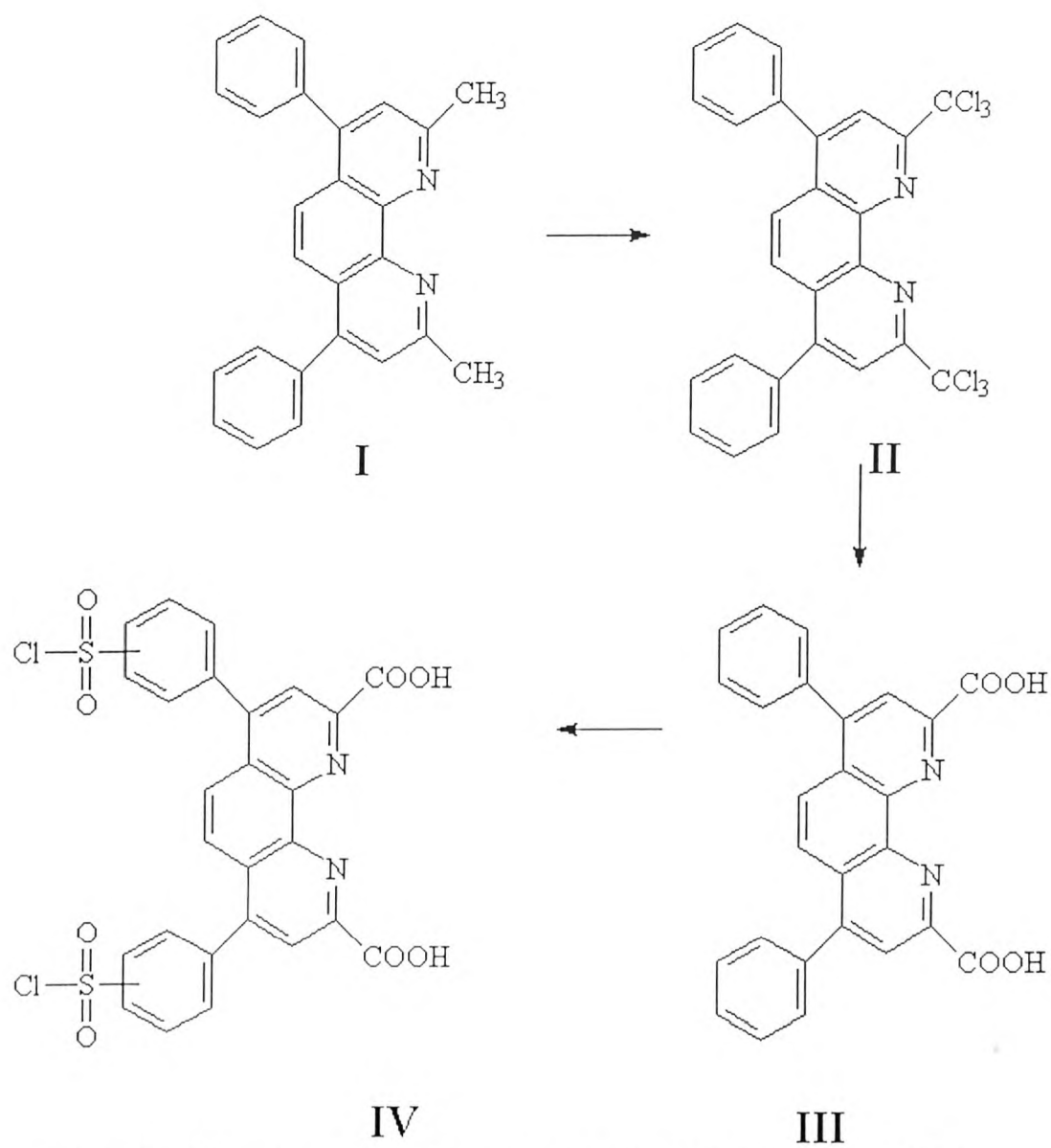


Figure 2.6. Schematic representation of the synthesis of BCPDA (compound IV) from bathocuproine (Evangelista *et al* 1988)

2.4. Spectroscopic study of the chelates/ lanthanide complexes

2.4.1. Methods

This series of tests were designed to assess the background fluorescence of the chelates and their solvents and to determine the fluorescent spectra of the chelates complexed with 4 different metals. All measurements in this set of experiments were performed using a MPF-3Perkin Elmer fluorimeter, and the samples were contained in 4ml 4 polished sides quartz cuvettes. Excitation and emission slits were set at 10nm, excitation wavelengths were measured in steps of 10 nm and emission wavelengths were recorded in steps of 5 nm. The sensitivity was adjusted to obtain best signal for each sample. However, all graphs shown are to the same scale (that of the most intense spectrum, being 700 relative fluorescence intensity units for BCPDA and 1000 units for DTPAA-pAs) so that overall spectral characteristics are directly comparable.

2.4.2. Spectroscopic study of BCPDA and lanthanide ions complexes

BCPDA is a Eu^{3+} chelate (Evangelista *et al* 1988). This was dissolved in DMSO and a background fluorescence spectrum of DMSO and of the chelate in DMSO were performed (figure 2.7 and 2.8). The measurements were performed from 250nm to 570 nm for the excitation and 270nm to 620nm for the emission.

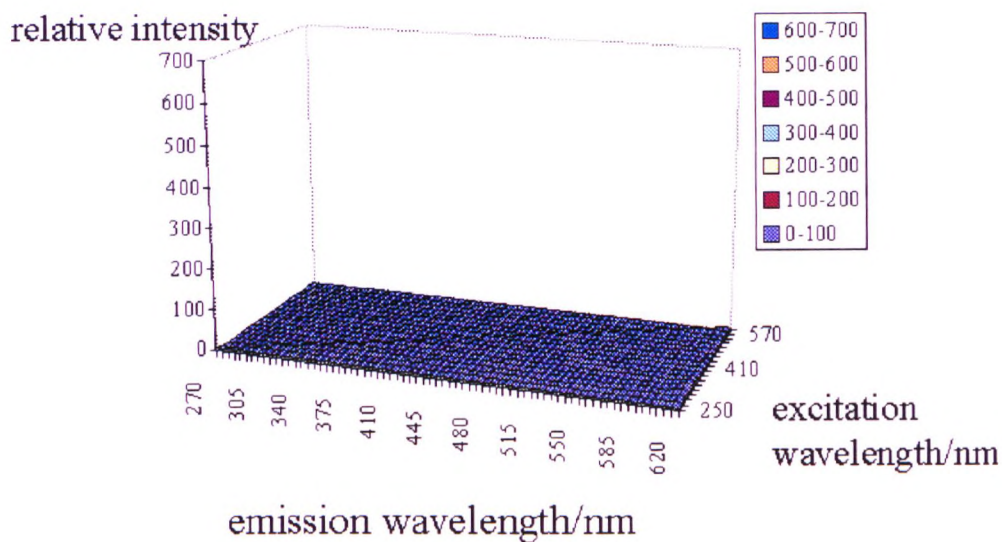


Figure 2.7. Measured fluorescence spectrum of DMSO

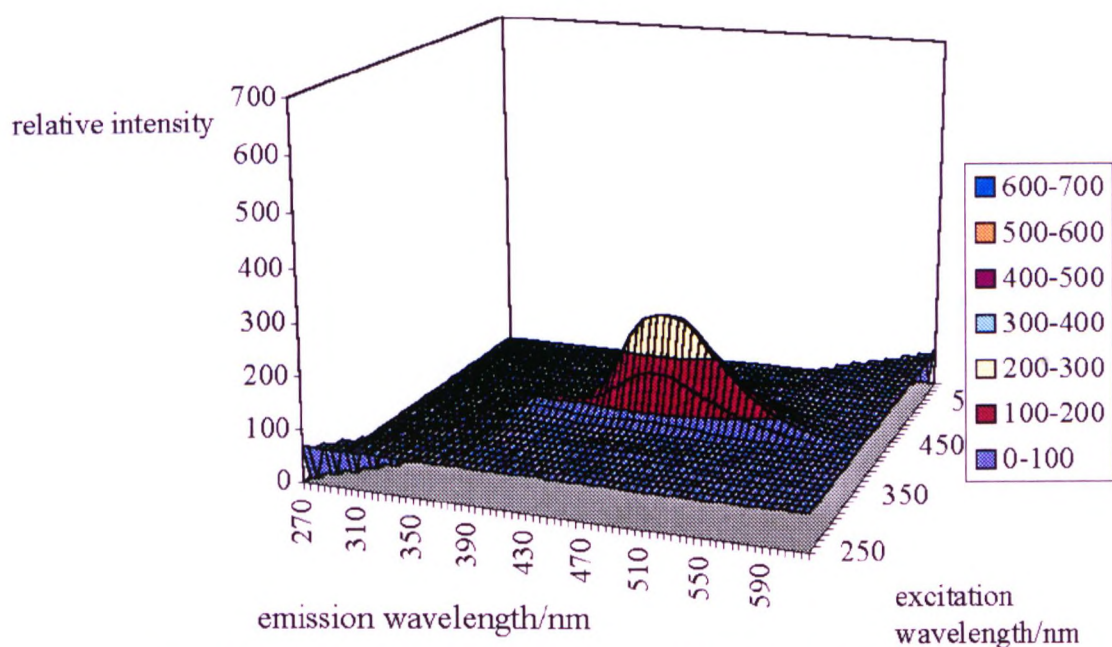


Figure 2.8. Measured fluorescence spectrum of BCPDA (1 mM) in DMSO

As can be seen from figure 2.7, DMSO has no significant fluorescence in the range scanned and BCPDA (figure 2.8) shows maximum fluorescence at 400nm excitation, 490 nm emission.

A Eu^{3+} /BCPDA complex was prepared: BCPDA (0.048 mmol) in ethanol was added to Eu^{3+} Chloride III (0.044 mmol) in ethanol and 3 drops of water were added. The mixture was stirred and solvent was removed. The remaining compound was redissolved in ether, filtered and finally dried. The resulting complex (3.8 mg) was dissolved in DMSO (5 ml) to a final concentration of 1mM. Figure 2.9 shows the fluorescence spectrum measured for this solution. Two peaks are observed at 560nm and 600nm, showing that BCPDA had interacted with the Eu^{3+} ions and fluorescence enhancement had occurred (Eu^{3+} in DMSO shows a flat fluorescence spectrum at this sensitivity of measurement, data not shown).

A Tb^{3+} /BCPDA complex was prepared in the same proportion as the Eu^{3+} complex (1mmol in 5 ml DMSO) and the spectrum in figure 2.10 was obtained. The spectral characteristics of the chelate BCPDA were obtained, without any additional peaks due to Tb^{3+} interaction with the chelate. One can conclude that no fluorescence enhancement occurred between BCPDA and Tb^{3+} and possibly no interaction between the metal and the chelate occurred. Other complexes were prepared in the same manner using Er^{3+} , Sm^{3+} , Yt^{3+} and Tb^{3+} similar results were obtained, showing no fluorescence enhancement.

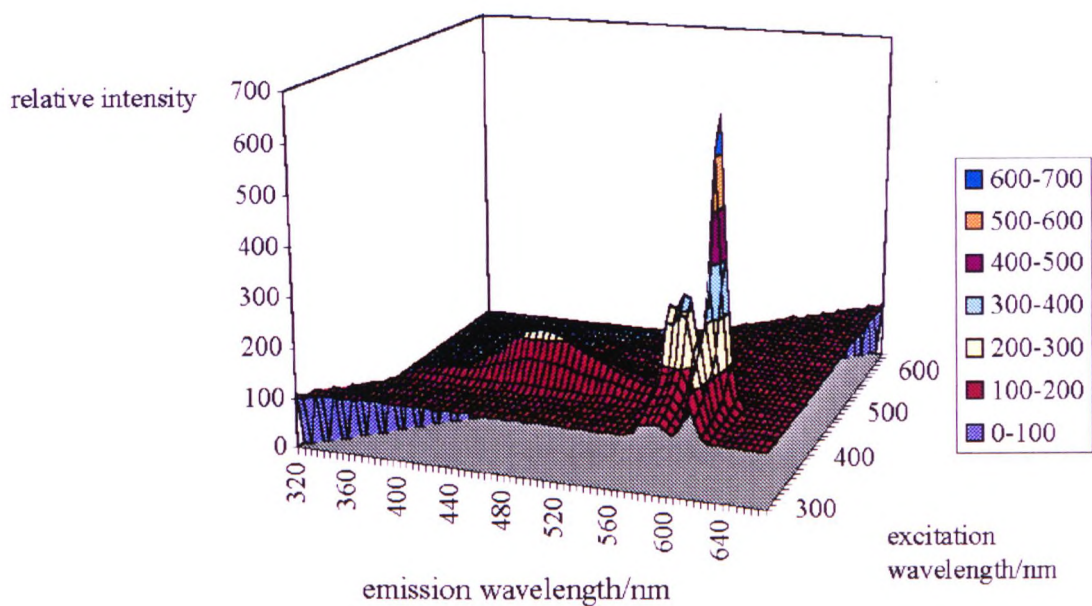


Figure 2.9. Measured fluorescence spectrum of BCPDA complexed with Eu^{3+}

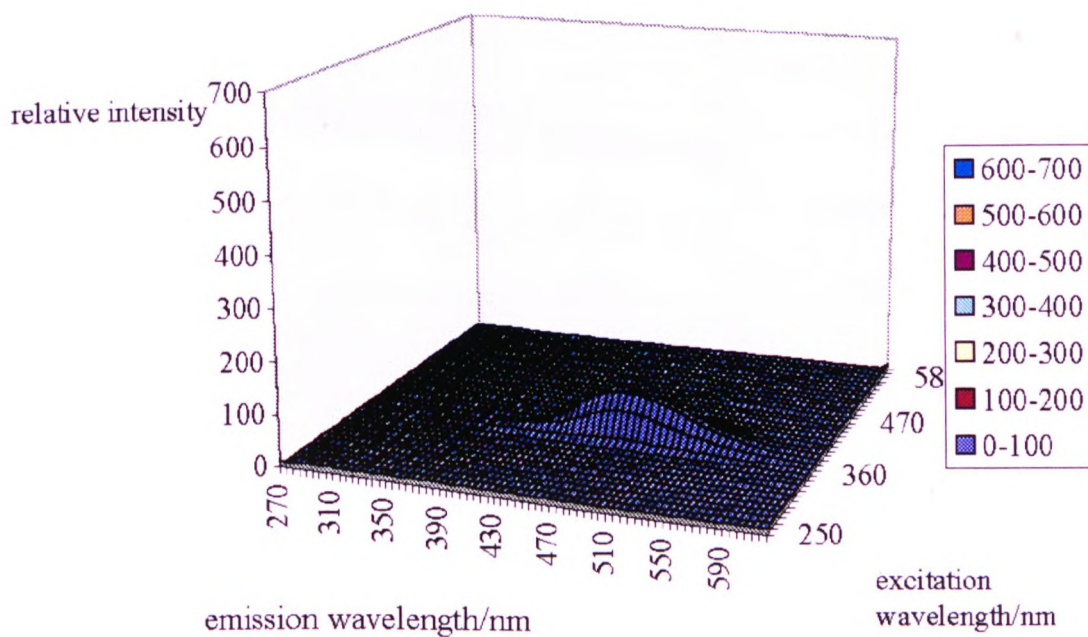


Figure 2.10. Measured fluorescence spectrum of BCPDA complexed with Tb^{3+}

2.4.3. Spectroscopic study of DTPAA-As and lanthanide ions complexes

The same methodology was used as with BCPDA and this time the measurements were performed from 300nm to 370nm for the excitation and 320nm to 700nm for the emission. pAs (0.42 mmol) was dissolved in DMSO (2.1 ml). DTPAA (0.42 mmol) and TEA (0.42 mmol) were dissolved in DMSO (2.1 ml). The pAs solution was added to the DTPAA solution and stirred for 60 minutes. Phosphate buffer (5 ml 0.1M potassium phosphate pH 7.2) and solution of Tb³⁺ chloride (0.8 ml 0.56 M) were added. Fluorescence spectra of the buffer and the chelate in buffer were measured (figure 2.11 and 2.12). Negligible levels of fluorescence were observed for the phosphate buffer.

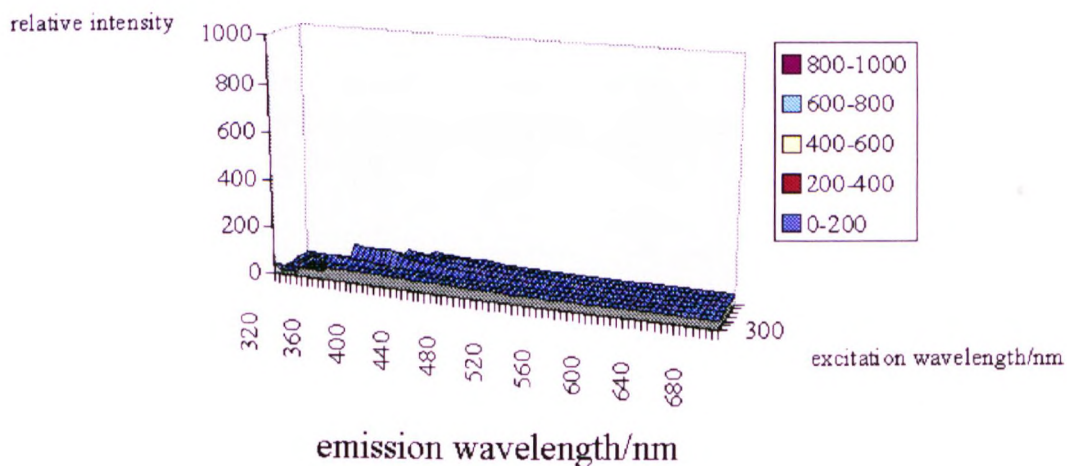


Figure 2.11. Measured fluorescence spectrum of Phosphate buffer

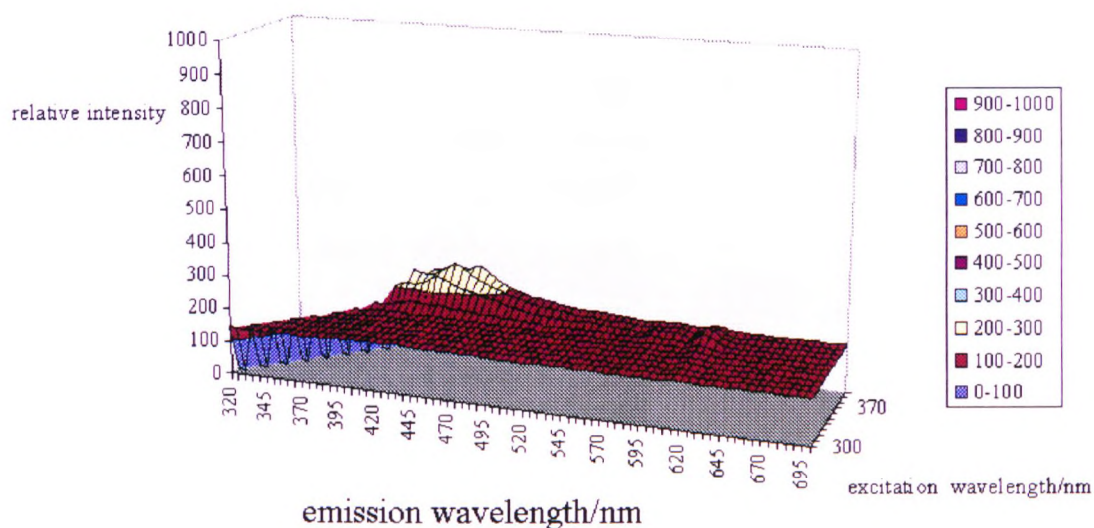


Figure 2.12. Fluorescence spectrum of DTPAA-pAS in phosphate buffer

A complex of pAs-DTpAA with Tb^{3+} was prepared. The measured fluorescence spectrum is shown in figure 2.14. Peaks at 495nm and 530nm, characteristic of Tb^{3+} , show that binding has occurred between Tb^{3+} and pAs-DTPAA. This enhances the fluorescence of Tb^{3+} , whose fluorescence would not normally be detectable at such a sensitivity of measurement.

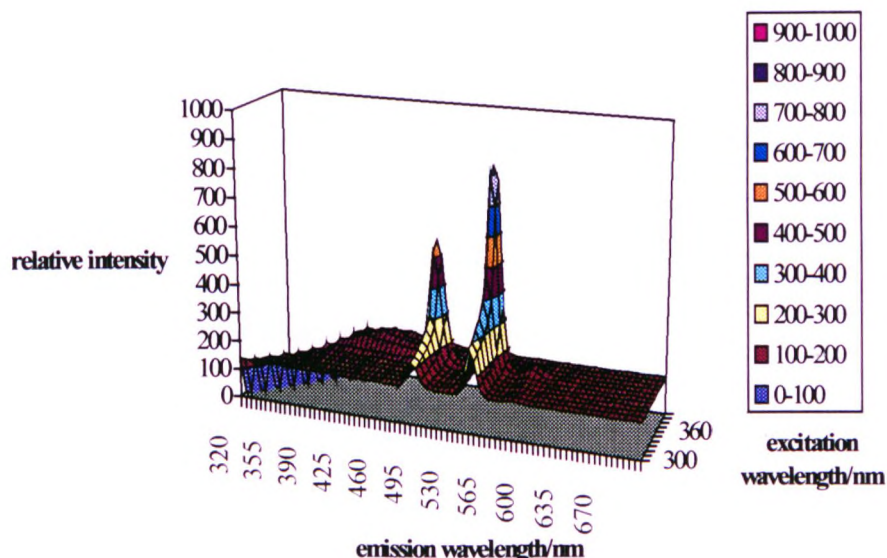


Figure 2.13. Fluorescence spectrum of DPTAA-pAS complexed with Tb^{3+}

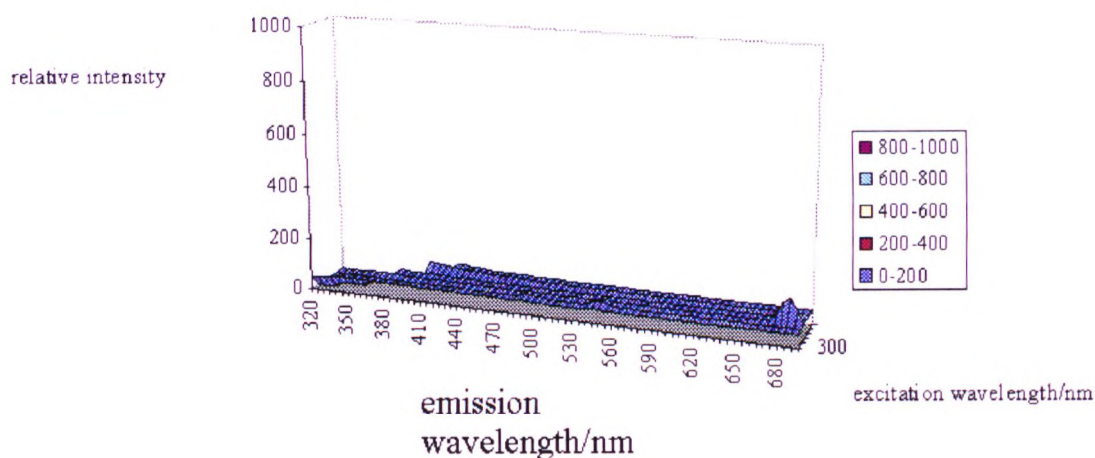


Figure 2.14. Fluorescence spectrum of Tb^{3+} in ethanol.

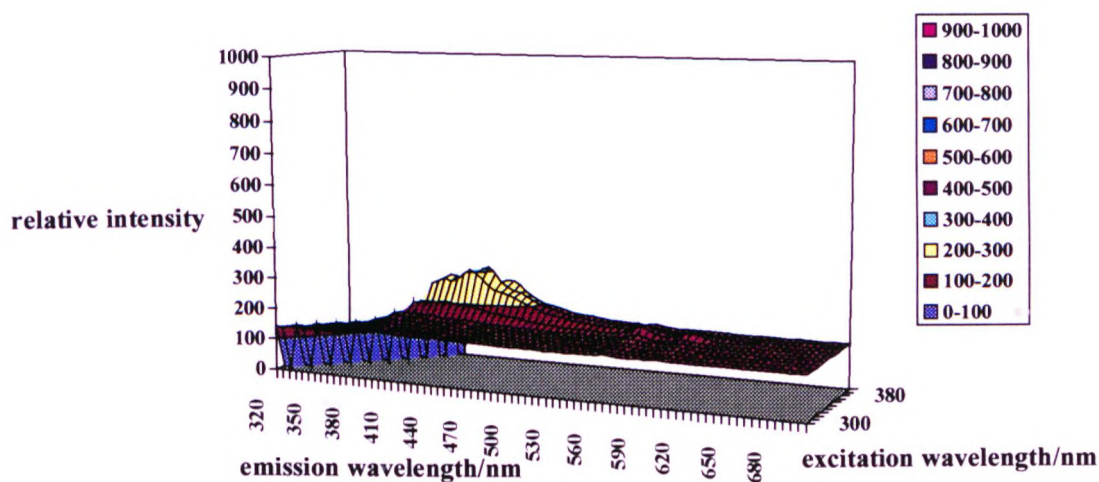


Figure 2.15. Fluorescence spectrum of DTPAA-pAs complexed with Sm^{3+} in phosphate buffer

Complexes of other metals such as Sm^{3+} (figure 2.15) were prepared and no visible interaction or fluorescence enhancement was observed.

These results obtained mean that both chelates studied are lanthanide specific and it would not be possible to use one of them to serve in a four color sequencing scheme.

2.5. Incorporation of the lanthanide chelate chemistry into an enzymatic chain extension reaction

2.5.1. Aims of the experiment and principle of Polymerase Chain Reaction (PCR)

In addition to finding a suitable chelate, it is important to study the incorporation of the modified thymidine triphosphate in an enzyme mediated chain extension process (similar to the one used for Sanger sequencing), as well as the tolerance of polymerases to the presence of free chelates and lanthanide metal ions in the reaction mixture. Polymerase chain reaction (PCR) was the chain extension process chosen for this study. It is a reaction that is used to amplify segments of DNA that lie between 2 regions of known sequence. In the reaction, two synthetic oligonucleotides are used as primers of enzymatic polymerisation reactions. They typically have different sequences, complementary to portions of the template on opposite strands and flank the region that is to be amplified. The template DNA is denatured using heat in presence of the primers and free triphosphate nucleotides. The reaction mixture is then cooled to a temperature suitable for the primers to anneal to their complementary region on the template DNA. These annealed primers are extended by the enzyme polymerase. The resulting double strand is then denatured as before, to permit further amplification of the template. The cycle of denaturing, reannealing and synthesis is repeated many times. Because each newly synthesised strand is used as a template in the following cycle, the amount of DNA doubles at each cycle. Original protocols (Saiki et al 1985) used the Klenow fragment of E.Coli DNA polymerase I, but this enzyme was denatured by the high temperatures of the denaturation step of PCR, so that addition of more enzyme was necessary at every

step. The problem was solved by the introduction of a thermostable polymerase purified from the thermophilic bacterium *Thermus aquaticus*, Taq polymerase (Chien *et al* 1976), which can survive extended incubation at 90°C.

2.5.2. PCR protocol

Into a 0.5ml microcentrifuge tube was added

- 2µl template DNA solution
- 40 µl deoxyribonucleoside triphosphates (1.25mM): A, C, T and G
- 6µl primer 1
- 6 µl primer 2
- 10 µl reaction buffer
- 10 µl *Taq* polymerase
- 25 µl sterile water

the solution was overlaid with 100µl mineral oil to prevent water loss by evaporation during the amplification process. The tubes were placed in a thermal cycler, programmed in the following manner:

Cycle number	Denaturation	reaction phase/annealing	synthesis
1	5 min at 94 ⁰ C	1 min at 50 ⁰ C	1 min at 72 ⁰ C
2-24	1 min at 94 ⁰ C	1 min at 50 ⁰ C	1 min at 72 ⁰ C
25	1 min at 94 ⁰ C	1 min at 50 ⁰ C	3 min at 72 ⁰ C

Table 2.1: thermal cycles used for the PCR

The amplified DNA was then separated by electrophoresis in a 1% agarose gel in TBE buffer. 10 µl of the amplification reaction was transferred to a sterile tube and 5µl loading dye as well as 5µl of sterile distilled water were added. 15 µl of this mixture was deposited in a well of the gel. A standard was used and 2 µl of Hind III digest

digest were mixed with 5µl sterile water and 5µl of loading dye. The gel was then placed under a current of 50mA until the loading dye bands are visible at the other end of the gel. The gel is then placed in a solution of Ethidium Bromide for 45 min and the bands are viewed under UV light.

3.5.3. Results

A. Toxicity of free Eu^{3+} ions

Several PCR reactions were performed in the manner described above, and part of the water added was replaced with various amounts of Eu^{3+} Chloride solution.

The gel obtained from the resulting PCR products is schematically represented on figure 2.16.

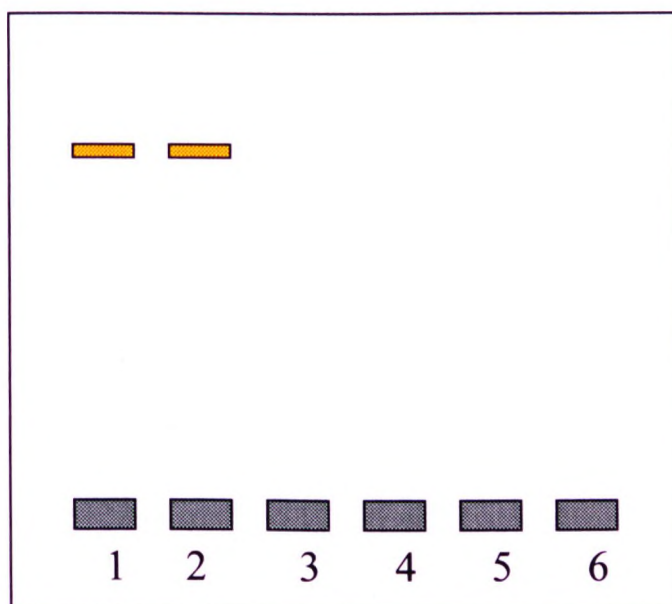


Figure 2.16. Schematic representation of the agarose gel used to analyse PCR mixtures in presence of Eu^{3+} . Samples in wells are as follows.

- | | |
|----------|--|
| 1 | control PCR product |
| 2 | 1 µl EuCl_3 in addition to all other components |
| 3 | 3 µl EuCl_3 in addition to all other components |
| 4 | 5 µl EuCl_3 in addition to all other components |
| 5 | 8 µl EuCl_3 in addition to all other components |
| 6 | blank (no template DNA) |

Results show that when more than 1 nmol of EuCl_3 is added, the PCR reaction is inhibited. This means that if free ions are present in the reaction mixture, the normal

chain extension process is prevented, or the annealing/ denaturation process that should occur between each PCR cycle is disturbed. This inhibitory effect of Eu^{3+} could also be explained by a competition between magnesium ions present on the PCR buffer and the free lanthanide ions. Free ions presence could occur if EuCl_3 is added in molar excess of the chelate. Therefore, purification will have to be performed to remove all the unbound ion before addition of the nucleoside labelled with the chelate/metal complex to the reaction mixture.

B. Study of the toxicity of BCPDA in solution.

The experiment was repeated using various amounts of BCPDA 1mM solution as a replacement for part of the water of the PCR reaction mix. 1 μl to 8 μl of this solution were added. After thermocycling, the electrophoretic gel revealed that none of the mixtures containing free BCPDA had undergone polymerase chain reaction. As little as 1nmol was enough to inhibit the PCR reaction. Therefore, any unbound chelate will also have to be removed from the nucleoside/ chelate complex before addition to the reaction mixture.

C. Incorporation of the 3' amino 2'thymidine triphosphate into a chain extension reaction.

This experiment was performed using the same PCR reaction parameters as described in paragraph 2.5.2. To this reaction for which the volume of water was modified accordingly, various amounts of 1.25 mM amino dideoxythymidine triphosphate were added (from 2 to 10 μl), as well as 10 μl of 1.25 mM triphosphate deoxyribo thymidine. The electrophoretic gel showed (figure 2.18) that no effect was observed

when adding up to 5 μ l of the amino derivative. However, when adding 10 μ l, the intensity of the band obtained is decreased. This means that above a certain concentration, the amino derivative starts to compete with the normal nucleotide, therefore reducing the number of PCR products having all the maximum fragment size.

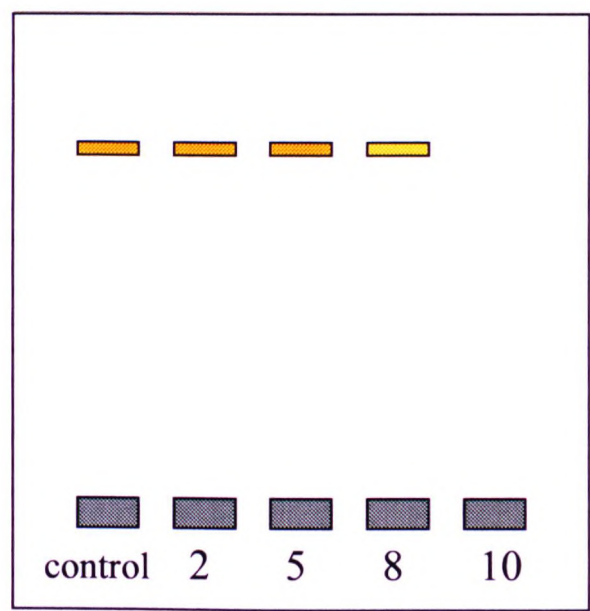


Figure 2.17. Schematic representation of the electrophoretic gel produced for the analysis of the PCR mixtures in presence of amino dideoxyribothymine triphosphate (values under the wells correspond to the volume of 1.25mM nucleotide solution added instead of water to the PCR mix). The band on well 8 is represented in lighter orange colour to illustrate the lower intensity of the fluorescence.

Two explanations are possible: the first one could be a simple inhibitory effect, where the amino nucleotide affects the activity of the polymerase enzyme. The other possibility is that the amino thymine is incorporated in the place of the deoxy. This should produce a mixture of fragments of many different sizes, corresponding to the chain termination when the enzyme has incorporated the chain terminating agent (the amino nucleotide). In this case, many bands should appear on the gel, which is not the case. Either the agarose gel does not possess a sufficient band separation power, or not enough specimens of each size were produced to be detected using this technique.

The last possibility is that no intermediate size fragments were present, which means that no incorporation of the amine was obtained. Further work would be useful, using a higher number of thermal cycles, to increase the potential number of specimens of each size, or change the separation technique to a more sensitive one (for example Capillary electrophoresis).

D. Other tests

Since the incorporation of amino modified thymidine was not observed (it either failed or was not detected), it was not expected that the chelate-nucleoside complex would be incorporated either, adding the difficulty of the bulk effect of the chelate, rendering the recognition of the nucleoside by the active site of the enzyme difficult. One would have to consider the synthesis of a linker arm to reduce this steric hinderence effect to a tolerable level for the enzyme.

2.6. Summary of results and conclusion

The results obtained in this part of the work were the following: 2 different chelates were identified as candidates for this labelling strategy. They were synthesised and complexed to various lanthanide metals. The fluorescence spectra of these complexes were measured and it was found that only the metal for which each chelate had been reported previously was successfully fluorescently enhanced (Eu^{3+} for BCPDA and Tb^{3+} for DTPAA-pAs). Trials to incorporate amino modified thymidine nucleotide in a polymerase mediated chain extension reaction were unsuccessful and free ions or chelates in the reaction were found to inhibit it. In conclusion, it can be said that a chelate suitable for all lanthanide metal ions, at least for the 4 metal ions of interest, was not identified. However, the 2 chelates studied in this work could still be used, together with 2 other chelates for Dy^{3+} and Er^{3+} . Several laser lines would have to be used, or a light source with a wider emission spectrum than lasers, covering the suitable range for the different chelates. The narrow features of the lanthanide emission bands would still be exploitable, although a more complex base calling software would have to be implemented due to the molecular weight difference between each chelate. This difference would affect the electrophoretic bands, changing their migration properties. This effect would however be relatively low, because the difference in molecular weight between each chelate is very small when compared to the overall molecular weight of the amplified DNA chain.

The PCR studies showed that the Taq enzyme is extremely sensitive to the presence of free lanthanide ions in solution, as well as free chelates.

This problem could be addressed by purifying all nucleoside solutions using column chromatography before they are mixed into the sequencing reaction.

It is apparent that the incorporation of chain terminating lanthanide chelate labelled nucleotide will be a problem during chain extension reaction. This could be overcome either by labelling the fragments after the DNA has been sequenced using unlabelled dideoxynucleotides (Sanger's chemistry) or by using 5' labelled primers that have been shown to be incorporated without any problem (Sloop *et al* 1994). The last strategy may however cause some problems with partial copies of the DNA template being due to spontaneous "drop off" of the enzyme from the template DNA during replication. This would result in partial copies, not representative of the sequence. If one, however chose to follow this strategy, it would be possible to increase the relative sensitivity of the technique by using multilabelled primers. It is indeed possible to synthesise phosphoramidites labelled with protected chelates, that can be used in the automated synthesis of oligonucleotides. The chelates are subsequently deprotected and complexed with lanthanide ions (Kwiatkowski *et al* 1994). However, for all types of DNA sequencing, labelled chain terminating nucleotides is the preferred option.

CHAPTER 3: SPECTROSCOPIC STUDY OF THE INTERACTION BETWEEN LANTHANIDES IONS AND DNA

3.1. Introduction

Eu^{3+} ions were observed to inhibit the polymerase chain reaction (PCR) when performed in the presence of *Taq* polymerase enzymes as described in chapter 2. It was suggested that this inhibition may be due either to an interaction of the metal ion Eu^{3+} with the enzyme, resulting in its degradation or changes in its conformation. The inhibition can also be due to the Eu^{3+} ions competing with Mg^{2+} ions that are necessary for the functioning of the enzyme. Finally, the inhibition could be due to binding of the ions to the DNA, which would perturb normal chemical interaction within double stranded DNA and hence prevent polymerisation.

Elements in the lanthanide group have no known physiological function, but have been of particular interest due to their fluorescence properties and hence their increasing use in a number of DNA assays, sequencing procedures and as fluorescent probes for the study of DNA structure (Klakamp and Horrocks 1992, article 1 and 2, Topal and Fresco 1980, Yonuschot *et al* 1978, Hörer *et al* 1977). It is therefore of interest to investigate further the interaction between DNA and lanthanide ions in solution.

The interaction of metals with nucleic acids has for a long time generated a lot of interest since metals are involved in many biological functions, such as DNA replication, transcription and translation (Pieles *et al*, 1993, Fitzgerald 1993, Wang *et al* 1994). Magnesium ion for example, is a cofactor for the enzyme DNA polymerase and also interacts directly with nucleic acids by increasing the stability of

their tertiary structure (Clement *et al* 1973). Copper, zinc and lead ions are known to decrease the stability of the DNA helical structure and also act as catalysts in the cleavage of the phosphodiester backbone of DNA (Richard 1973), while Platinum II compounds are known for their anticancer properties (Roberts and Thomson 1979). Extensive literature is available on the subject of DNA/ metals interactions, with mainly alkaline, alkaline earth and transition metal complexes of DNA (Pezzano and Podo 1980, Sissoëff *et al* 1976).

Sissoëff has classified metals into 3 main groups according to their mode of binding to DNA. The first group consists of metals that bind to the phosphate groups of the DNA only. The second group of metals binds to phosphates and bases, and the third group contains metals that bind to the bases only. One could classify lanthanides as group 2 metals because it was shown that phosphate linkages were a binding site for Tb^{3+} , and that a direct coordination of Tb^{3+} ions with electron donor groups on the nucleoside bases also exists (Gross and Simpkins 1981). It is also common to classify metals according to their effect on DNA structure. The double helix can be stabilised when K^+ , Na^+ and Cs^{2+} interact with it or destabilised with Cu^{2+} , Ag^+ and Hg^{2+} . One has to observe DNA at the molecular level in order to understand how metals interact with it. Figure 3.1 shows the highly electronegative atoms susceptible to react with metal ions in CG base pairs.

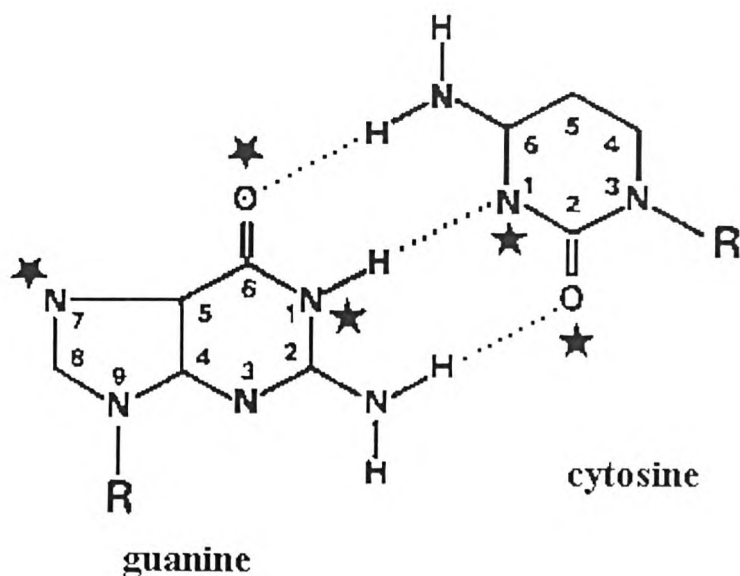


Figure 3.1: highly electronegative atoms (*) susceptible to react with metal ions in CG base pairs. Conventional numbering of atoms is indicated, R: desoxyribose moiety of the DNA backbone (Sissoëff *et al* 1976)

There are many ways by which metal ions can bind to DNA. Figure 3.2 illustrates all the possible modes.

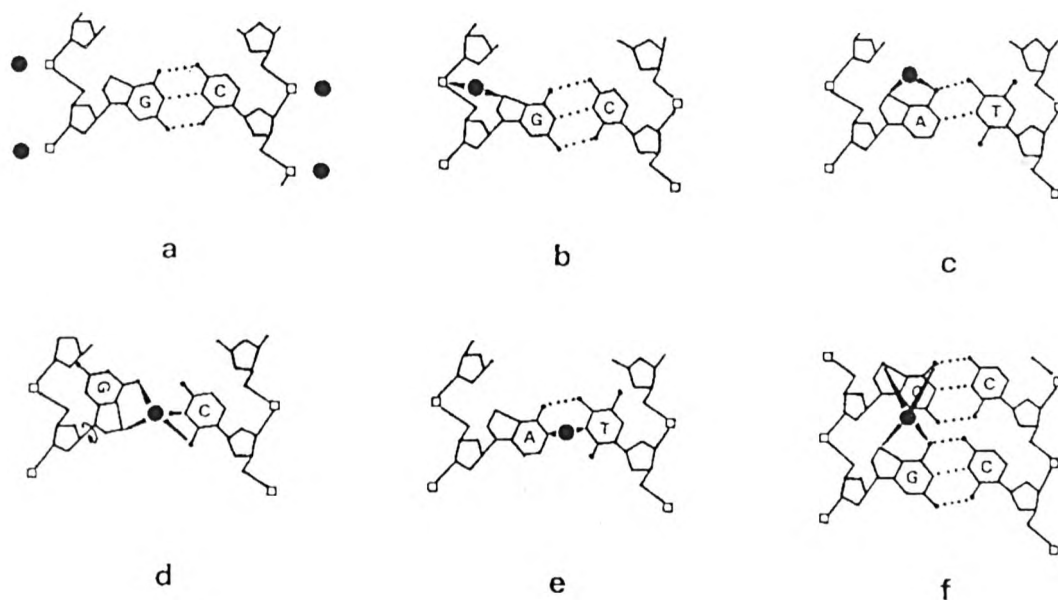


Figure 3.2. Probable binding sites for metal ions on DNA molecules. (a) Electrostatic binding to negatively charged phosphate groups. (b) Mixed chelate between N7 of purine base and phosphate group of the same strand. (c) Internal chelate between N7 and O6 of the same purine base. (d) Interstrand complex between reoriented guanine base and its corresponding cytosine base. (e) Interstrand cross link between N1 of purine base on one strand and N1 of pyrimidine base on the opposite strand. (f) Charge transfer complex between 2 successive guanine bases located on the same strand involving N7 and O6. (Sissoëff *et al* 1976).

pH, temperature, ionic strength and base composition are also considered to influence the actual mode and binding strength of the metal ion to DNA. For example, the formation of Ca^{2+} or Mg^{2+} complexes with DNA requires high concentration of cation at acidic pH and the ions bind stoichiometrically to 2 phosphate groups. At basic pH, only 1 phosphate group of the DNA binds to each metal ion (Mathieson and Olayemi 1975).

The structure of metal ion complexes of DNA has been investigated by many methods, such as Infra Red spectroscopy (Heidar-Ali *et al* 1993, article 2), NMR spectroscopy (Steinkopf *et al* 1995, Gross *et al* 1982), Raman spectroscopy (Stangret and Savoie 1993, Duguid *et al* 1993) X Ray crystallography (Holbrook *et al* 1977), equilibrium dialysis (Gross and Simpkins 1981), electrophoresis, hydrogen ion titration and thermal stability studies (Sissoëff *et al* 1976).

In this chapter, *in vitro* studies were carried out in order to observe the effect of lanthanide ions on the secondary structure of nucleic acids. The techniques used included (i) UV spectrophotometry, (ii) thermal stability studies, (iii) NMR spectroscopy and (iv) relaxation studies of supercoiled DNA. The studies were performed with known oligonucleotides sequences in the presence of a number of lanthanide salts. The aims of this study involving lanthanide ions interactions with nucleic acids were to confirm previous observations in the literature and to try and understand why the presence of lanthanides had an inhibitory effect on *Taq* polymerase enzymes as shown in chapter 2.

3.2. Determination of the melting temperature of a DNA duplex by UV spectrometry

3.2.1. UV spectrometry, thermal analysis of duplex formation

The melting point or T_m of a double stranded DNA is the temperature at which 50% of the bases of this DNA duplex are unpaired. Base stacking in the DNA molecule is usually accompanied by reduction in UV absorption at 260 nm (Saenger 1984), therefore UV spectrometry is a convenient technique to monitor formation and breakdown of the helical structure of DNA. A solution containing double stranded DNA of interest is slowly heated and the UV absorption suddenly increases when the 2 strands separate. The midpoint of the transition is called the “melting temperature” or T_m , and is determined at the maximum of the derivative of the melting curve (inflexion point of the curve). A typical melting curve can be seen in figure 3.3.

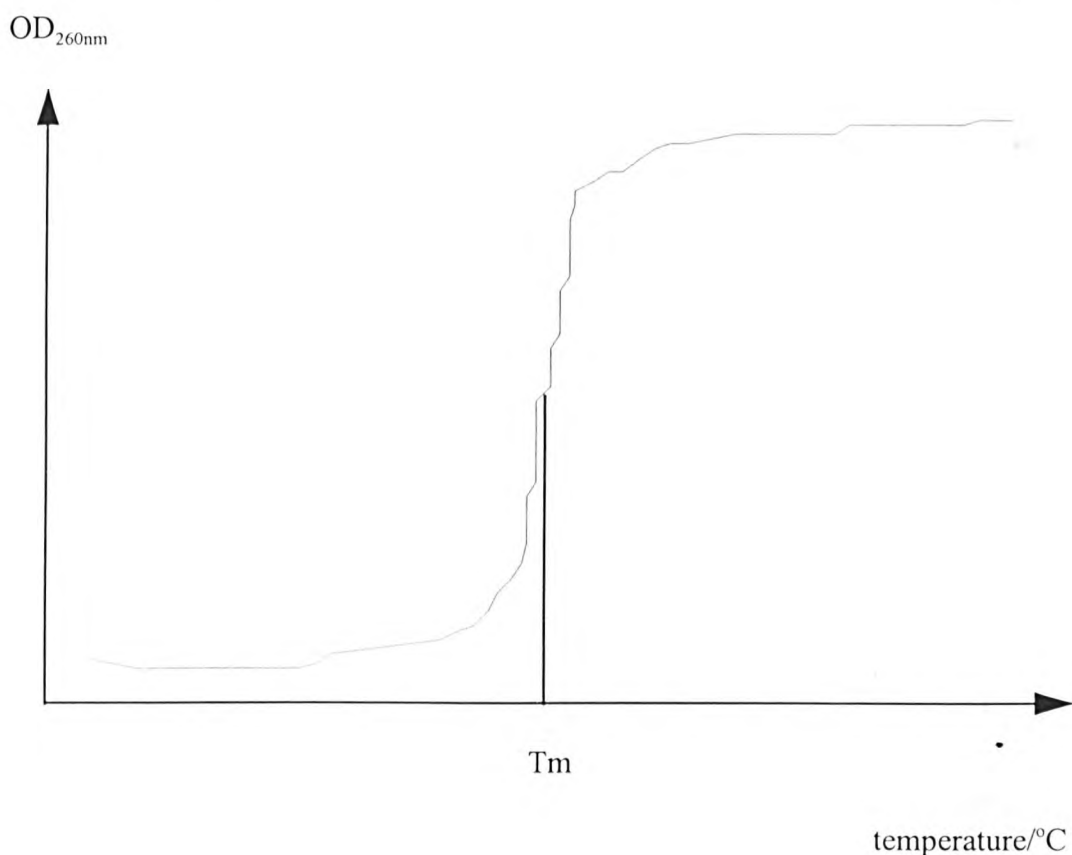


Figure 3.3. Typical melting curve of a DNA duplex

The T_m value is representative of the stability of the double helix. DNA is an ordered structure where melting and duplex formation are cooperative. Resistance of the structure to thermal disruption is proportional to the stability of the helix. Changes in the melting temperature therefore gives an indication of conformational change in the DNA molecule (Luck and Zimmer 1972). The double helical structure of DNA is maintained by mainly three contributing factors:

- (i) The tendency for the hydrophobic bases within a single strand to stack above one another with the plane of their ring parallel (Herskovits, 1962).
- (ii) The hydrogen bonds between the strands, that form between complementary bases, called “Watson and Crick” bonds.
- (iii) The electrostatic forces created by the electronegativity of the oxygens on the phosphates. The phosphates of one strand repel the phosphates on the other strand, thereby destabilising the helix. These negative charges can be neutralised by the presence of counterions, usually sodium ions, that thereby stabilise the structure and increase the T_m value.

Denaturation of double stranded DNA occurs during a phenomenon known as Helix-coil transition. It is a cooperative process, that can be described as follows:

When a specific temperature is reached, bombardment of the molecule by solvent molecules tends to break the hydrogen bonds between complementary bases. This happens preferentially at AT rich regions, because only 2 hydrogen bonds are involved in the base pairing of A and T bases and at the ends of a DNA molecule, because the terminal base pair is stabilised only by one pair of stacked bases (figure 3.4). This breakage destabilises the next pair and denaturation progresses inwards.

Hydrogen bond breakage and base destacking are synergic, rendering the whole process of denaturation/ renaturation cooperative.

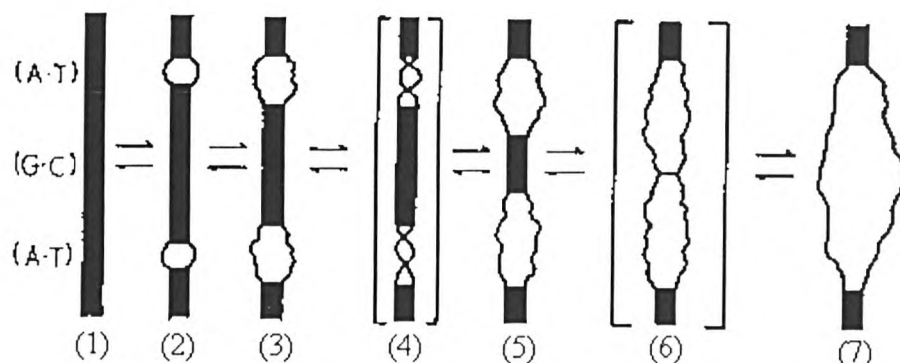


Figure 3.4. Scheme describing processes involved in DNA double helix de and renaturation. AT regions melt first, giving rise to states (2) and (3). In (4), additional base pairs are opened and the twist is taken up in coil regions. (Saenger 1984).

To monitor the effect of the presence of metal ions in solution on the thermal stability of synthetic double stranded DNA, a series of T_m measurement experiments was performed. All experiments were performed using a Perkin Elmer $\lambda 2$ UV spectrometer fitted with a PTP-1 Peltier block. A stoppered 1 cm path quartz cell (0.5 ml sample) was used. And the cells were heated from 25°C to 75°C at a rate of 1°C/min.

3.2.2. Determination of the influence of pH on the T_m .

The influence of pH on the T_m values of an oligonucleotide duplex was investigated. A self complementary 12 mer AAAAAATTTTTT oligonucleotide (0.5 OD) was dissolved in 6SSC buffer (0.5ml 0.95M NaCl and 0.01 M sodium citrate) at pH 3, 5, 7, 9 and 11. The T_m value of each of these samples was determined and plotted as shown in figure 3.5.

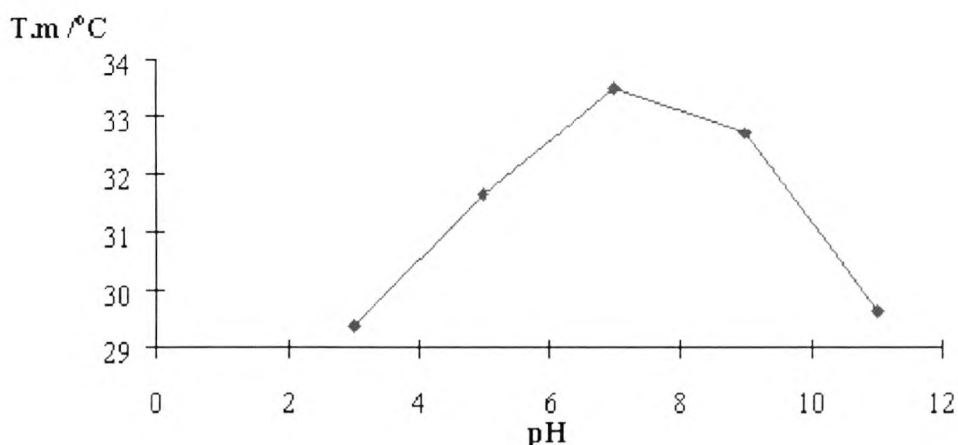


Figure 3.5 : Influence of the pH on the T_m values of a self complementary 12 mer AT oligonucleotide in 6xSSC buffer.

On the graph (figure 3.5), it can be seen that the pH has a strong influence on T_m values of the AT oligonucleotide. An increase in pH from 3 to 7 tends to stabilise the DNA duplex by showing an increase in T_m values from 29.8 to 33.5°C. However, a pH higher than 7 shows a destabilising effect. This can be explained as follows: Under basic conditions (pH>7), the hydrogens at N-3 on thymine and N-1 on guanine are released whereas under acidic conditions (pH<7), N-1 of Adenine and N-3 of cytosine are protonated as well as N-7 of Guanine and Adenine. The phosphate group is also affected by pH variation because at pH below 2, all oxygen atoms in the DNA backbone bearing negative charges are neutralised by protons hence reducing electrostatic interactions. When the pH is increased and is close to the Pka values of the phosphate groups, then protons are removed, thereby increasing electrostatic interactions. It is therefore obvious that the T_m value is affected by these protonation changes and the experimental values obtained here are consistent with theory.

3.2.3. Study of the interaction of $TbCl_3$ with DNA

It is suggested that the way by which a given metal will affect the stability of a DNA double helix will be different depending on the pH of the solution. To verify this, the effect on the T_m values when adding $TbCl_3$ to a solution of DNA was observed in 6xSSC buffer at different pHs. A 12 mer AT oligonucleotide was used (0.5 OD) and prepared in 3 different SSC buffer solutions (pH 5, 7, 9) in a volume of 0.5ml for each sample. A $TbCl_3$ solution (0.5M) was prepared in SSC buffer and aliquots of this solution were added to the DNA samples to reach concentrations in metal ions up to 80 mM.

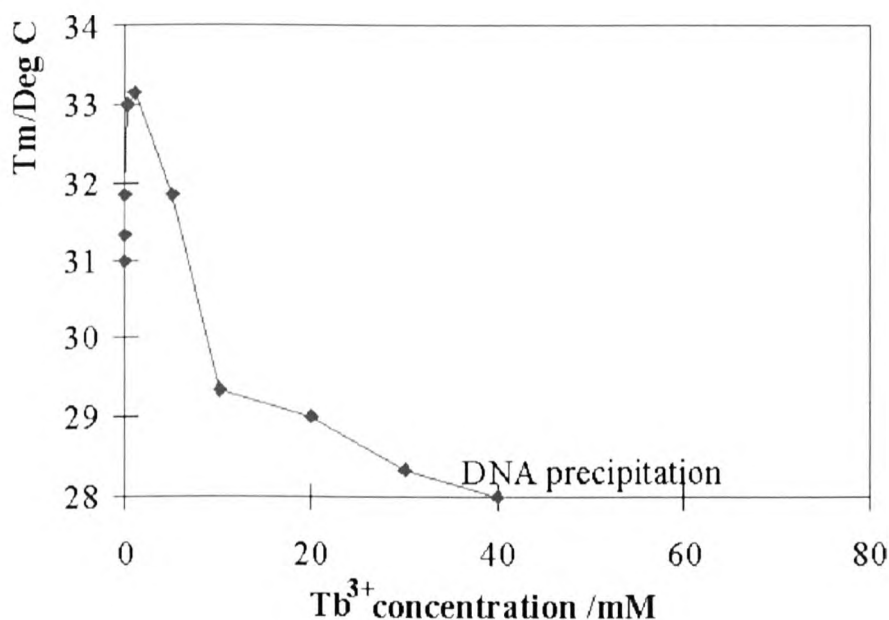


Figure 3.6. Influence of Tb^{3+} concentration on T_m of a 12 mer AT oligonucleotide at pH 5. Metal ions were added until no melting transition was observed on the UV spectrum (marked as DNA precipitation).

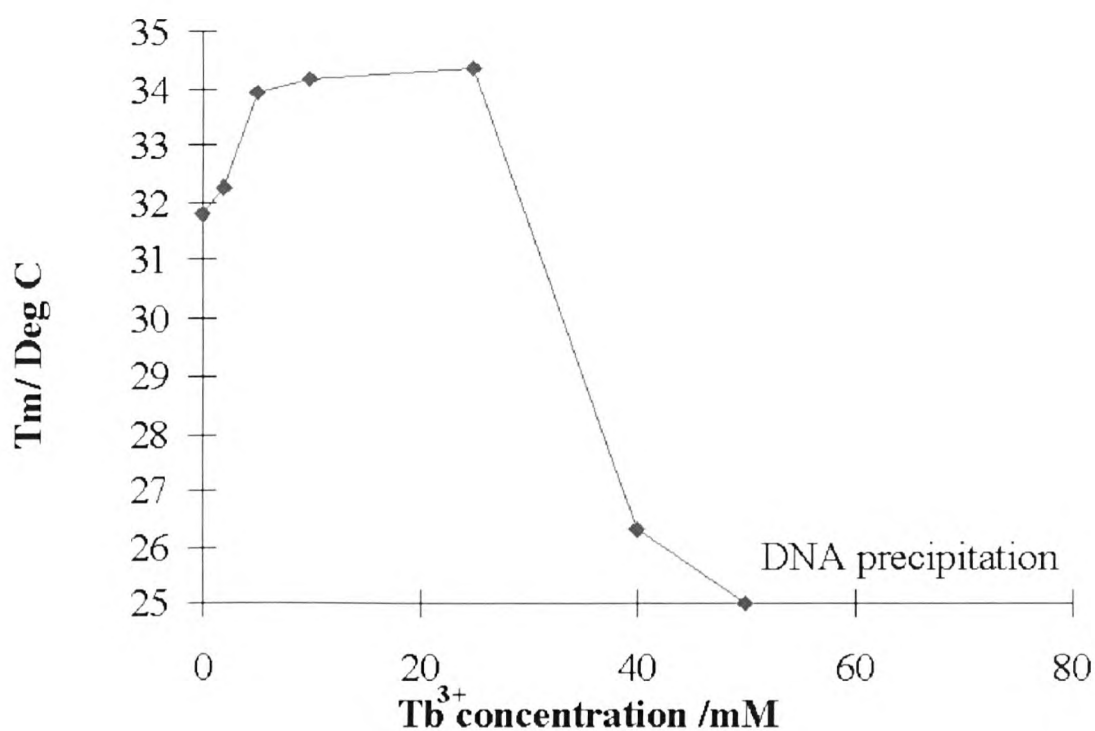


Figure 3.7. Influence of Tb³⁺ concentration on T_m of a 12 mer AT oligonucleotide at pH 7

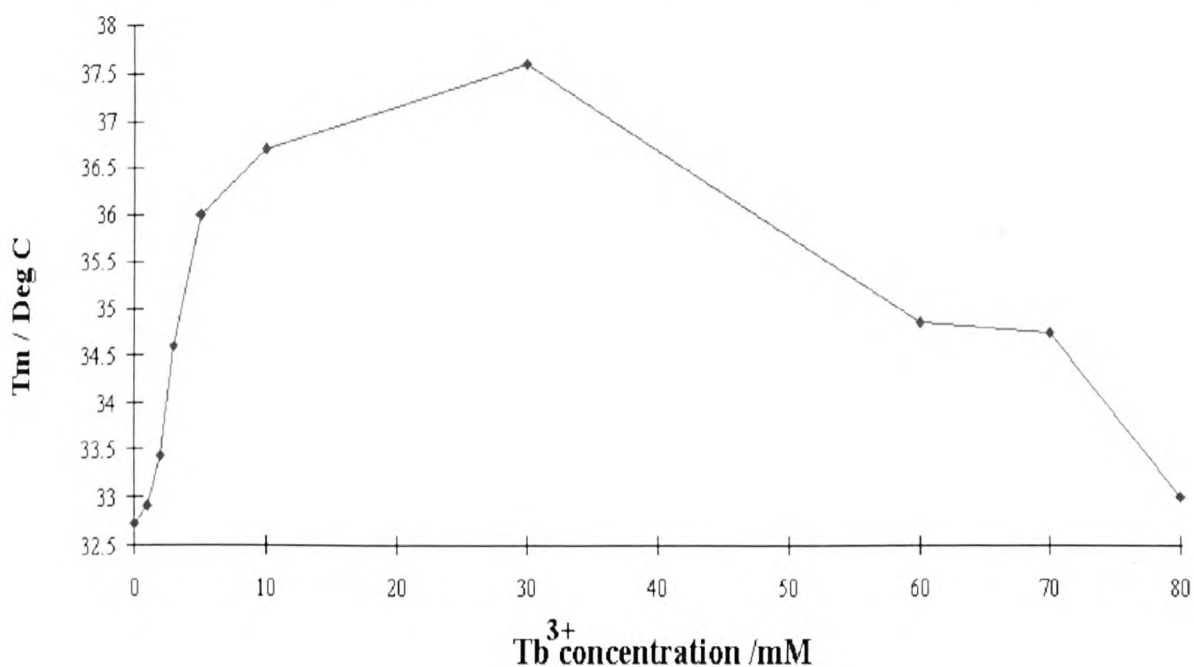


Figure 3.8. Influence of Tb³⁺ concentration on T_m of a 12 mer AT oligonucleotide at pH 9

The graphs in figures 3.6, 3.7 and 3.8 show the effect on T_m values of solutions of AT oligonucleotide at different pHs when aliquots of Tb³⁺ were added to them. In

general, those graphs exhibited two characteristic regions. The first one corresponds to an increase of when Tb^{3+} was added. The second region marks a decrease of T_m with higher Tb^{3+} concentrations. The above observations could be explained as follows: at low metal ion concentrations (0-5mM), the interaction of the metal ion with DNA is essentially concentrated on the phosphate groups. An ionic interaction occurs, thereby neutralising the negative charges and stabilising the duplex, hence the increase in T_m values. At higher ion concentrations, when all phosphates have been neutralised, the ions start to interact with the bases which affects base pairing, resulting in the decrease of T_m values.

One can also observe that the concentration at which T_m values start to decrease is different for each buffer of different pH tried. The decrease in T_m values occurs at 2mM $TbCl_3$ at pH 5, at 20mM $TbCl_3$ at pH 7 and 30mM $TbCl_3$ at pH 9. At low pH, the oxygens of the phosphate groups along the DNA backbone are protonated, making only a few negative groups available for the positively charged Tb^{3+} ions to bind. These therefore interact with the bases instead, disrupting the Watson and Crick base pairing in the DNA. This is why for the experiment at pH 5 (see figure 3.6), T_m values of the oligonucleotide decreases at low ions concentration. When pH is increased, the oxygens of the phosphate backbone are deprotonated and more sites are available for the metal ions to bind and stabilise the duplex, so it takes more metal ions to saturate all the sites of the phosphate backbone before binding to the bases. These observations confirm the hypothesis as previously reported (Gross and Simpkins 1981) that Tb^{3+} ions bind to the phosphate groups as well as the bases.

3.2.3. Study of the interaction of Eu^{3+} chloride with DNA

Study of Eu^{3+} interaction with the 12 mer 5' AAAAAATTTTTT 3' was attempted under the same conditions as in the previous paragraph, (i.e using a buffer based on citrate). However, although similar concentrations of Eu^{3+} ions were used as with Tb^{3+} , no major changes of T_m values were observed (figure 3.9), up to the value of concentration of metal ion that caused precipitation of the sample (120 mM).

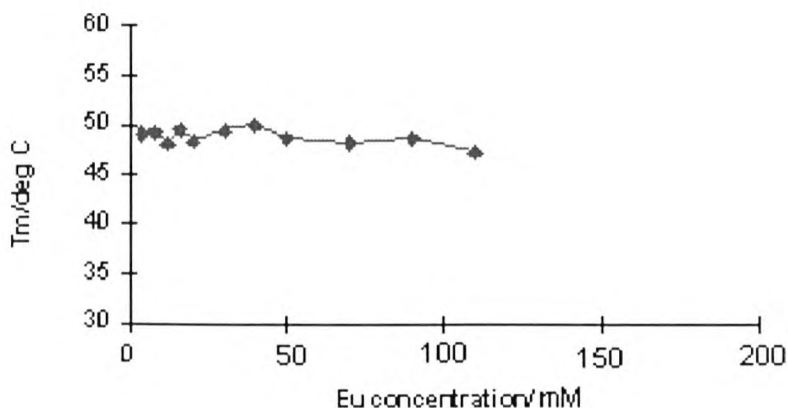


Figure 3.9 : Study of the influence of EuCl_3 concentration on T_m of a 12 mer AT oligonucleotide in SSC buffer pH 7

It can be suggested that the affinity of Eu^{3+} for citrate is higher than for the oligonucleotide. This observation was confirmed by NMR spectroscopy as discussed in section 3.4. Although Tb^{3+} was also shown by NMR spectroscopy to interact with the citrate of the buffer, it remains unexplained why the T_m values of the oligonucleotide were affected in the experiments involving Tb^{3+} , and not in the one involving Eu^{3+} .

3.3. HPLC study of destabilised DNA duplexes/lanthanide complexes

From the previous set of experiments, it was found that:

- (a) T_m is strongly affected by the presence of lanthanide metals
- (b) beyond a critical concentration of lanthanide, which varies with the pH of the solution, melting no longer occurs.

T_m determination provides information on the secondary structure of DNA. It would however be useful to understand more about the nature of the “precipitate” obtained when melting is no longer observable. Indeed, it is not yet known at this point of the investigation whether the absence of transition at high metal ion concentration during a melting experiment is due to break down of the oligonucleotide chain, or to the two strands being prevented from binding to each other via hydrogen bonding. Reverse phase HPLC (high pressure liquid chromatography) was used during this investigation to clarify which of the two possible explanations is the correct one.

HPLC is an analytical tool commonly for the purification and characterisation of oligonucleotides. Chromatography involves the partition of a solute between a mobile phase and a stationary phase. An oligonucleotide dissolved in the mobile phase and introduced into the inlet of a column containing the stationary phase will migrate through at a rate dependent on its interaction between these two phases. Reverse phase columns are usually chosen to analyse or purify oligonucleotides. This is performed using a non polar stationary phase such as silica and a polar mobile phase. The hydrophobic interactions determine the velocity of migration along the stationary phase. Polar solutes are eluted relatively early from the column. Elution of a particular compound is effected by reducing the polarity of the aqueous mobile phase by the addition of organic solvents. Gradients of solvents are used for the

progressive elution of materials. Because of the high resolution achieved by HPLC systems, it is possible to differentiate between oligonucleotides of different size and composition.

Two complementary oligonucleotides of sequence 5'-ACTTGGCCACCATTTTG-3' (oligonucleotide named 111) and 5'-CAAAATGGTGGCCAAGT-3' (oligonucleotide named 117) were used in this series of experiments.

Reverse phase HPLC was performed using the following conditions:

Time/min	% buffer A	%buffer B	flow ml/min
5	100	0	1
25	70	30	1
30	60	40	1
40	100	0	1

Table 3.1. Program for the gradient used in the RP-HPLC analysis of lanthanide-oligonucleotides complexes. Buffer A: 15.42g ammonium acetate,2000 ml distilled water
Buffer B: 200ml of buffer A, 640 ml HPLC grade acetonitrile, 160 ml distilled water

Samples of the pure oligonucleotides were first analysed of comparison purposes (figure 3.10 and 3.11).

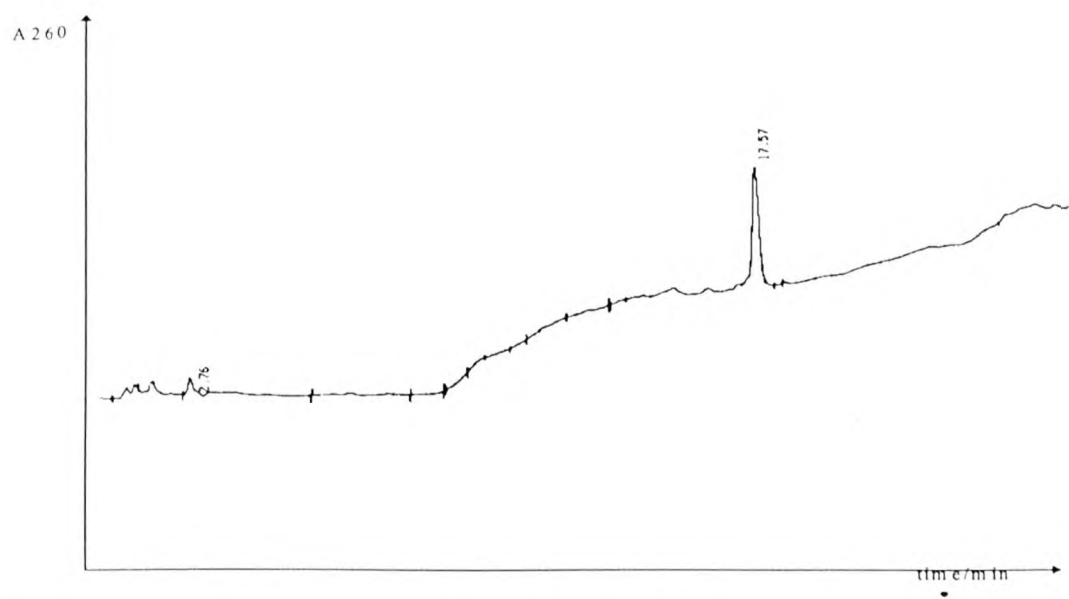


figure 3.10: HPLC plot of the analysis of oligonucleotide sequence 5'-ACTTGGCCACCATTTTG-3'Buffer A: 15.42g ammonium acetate,2000 ml distilled water
Buffer B: 200ml of buffer A, 640 ml HPLC grade acetonitrile, 160 ml distilled water
Reverse phase column: Hichrom, Hypersil H5ODS (25cm x 8mm). The samples (10 µl) were injected at time 0.

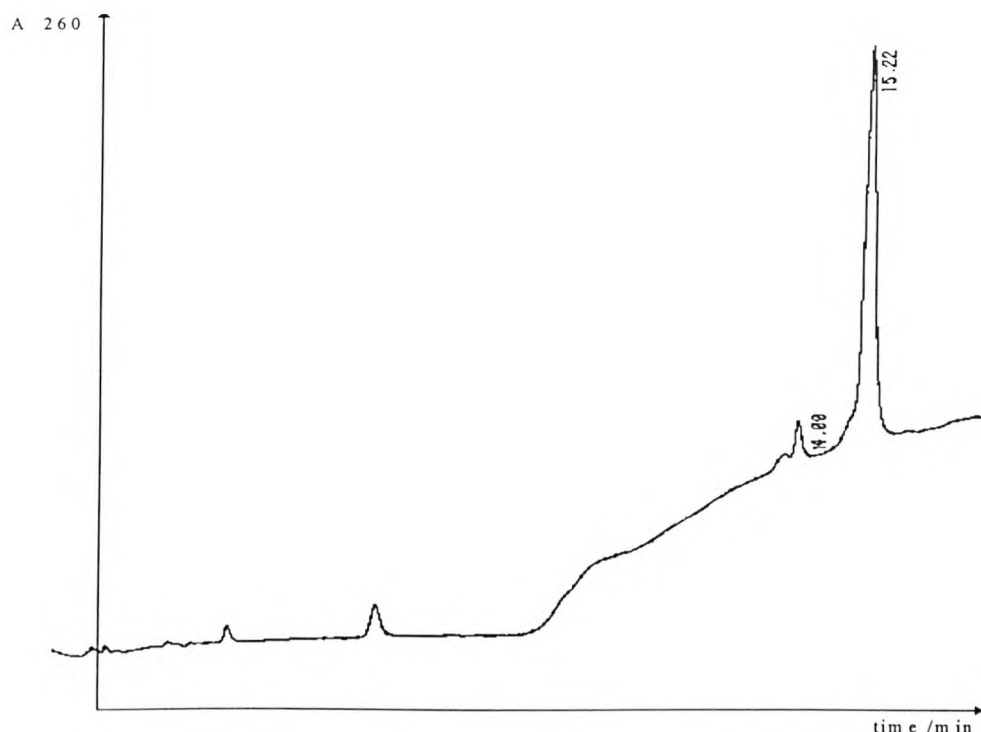


figure 3.11: HPLC plot for the analysis of oligonucleotide 5'-CAAAATGGTGGCCAAGT-3'

Buffer A: 15.42g ammonium acetate, 2000 ml distilled water

Buffer B: 200ml of buffer A, 640 ml HPLC grade acetonitrile, 160 ml distilled water

Reverse phase column: Hichrom, Hypersil H5ODS (25cm x 8mm). The samples (10 μ l) were injected at time 0.

Oligonucleotides ACTTGGCCACCATTTTG-3' (111) and 5'-CAAAATGGTGGCCAAGT-3' (117) gave retention times of 17.57 and 15.22 minutes respectively (figure 3.10 and 3.11). When a mixture of the 2 oligonucleotides was then analysed, it gave a single peak at 15.44 minutes (figure 3.12), which means that the two complementary oligonucleotides had formed a duplex in the current experimental conditions.

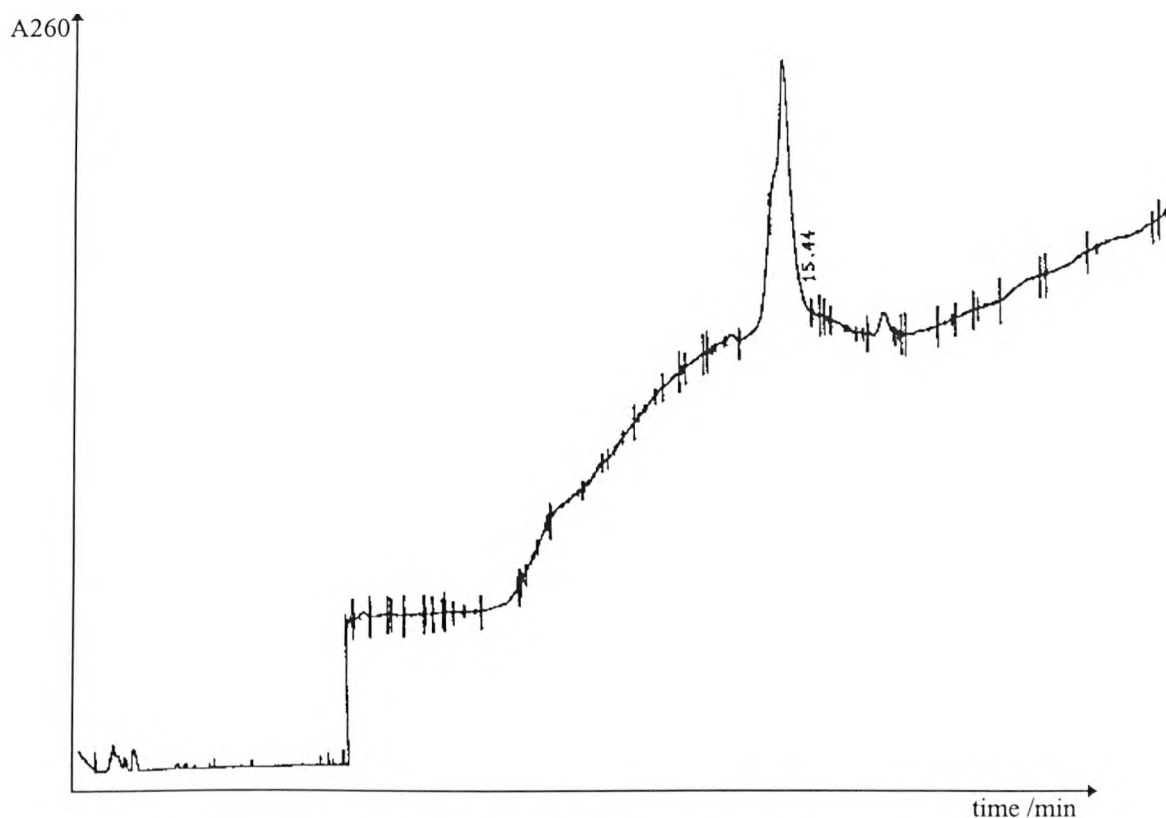


Figure 3.12. HPLC plot for the analysis of a mixture of oligonucleotides ACTTGGCCACCATTG-3' and 5'-CAAAATGGTGGCCAAGT-3'. Buffer A: 15.42g ammonium acetate, 2000 ml distilled water. Buffer B: 200ml of buffer A, 640 ml HPLC grade acetonitrile, 160 ml distilled water. Reverse phase column: Hichrom, Hypersil H5ODS (25cm x 8mm). The samples (10 μ l) were injected at time 0.

A sample was prepared with the two complementary oligonucleotides and denaturing amounts of Er^{3+} chloride were added (no melting was observed upon heating, using the UV spectrophotometer and Peltier block as described in section 3.2). This sample was analysed and 2 peaks were obtained (figure 3.13), with same retention times as the 2 separate oligonucleotides (figure 3.10 and 3.11). This means that the two oligonucleotides were eluted separately as two compounds and had not been hydrolysed by the metal ions. The experiment was repeated using other lanthanide ions, such as Eu^{3+} , Tb^{3+} , Yb^{3+} and Sm^{3+} .

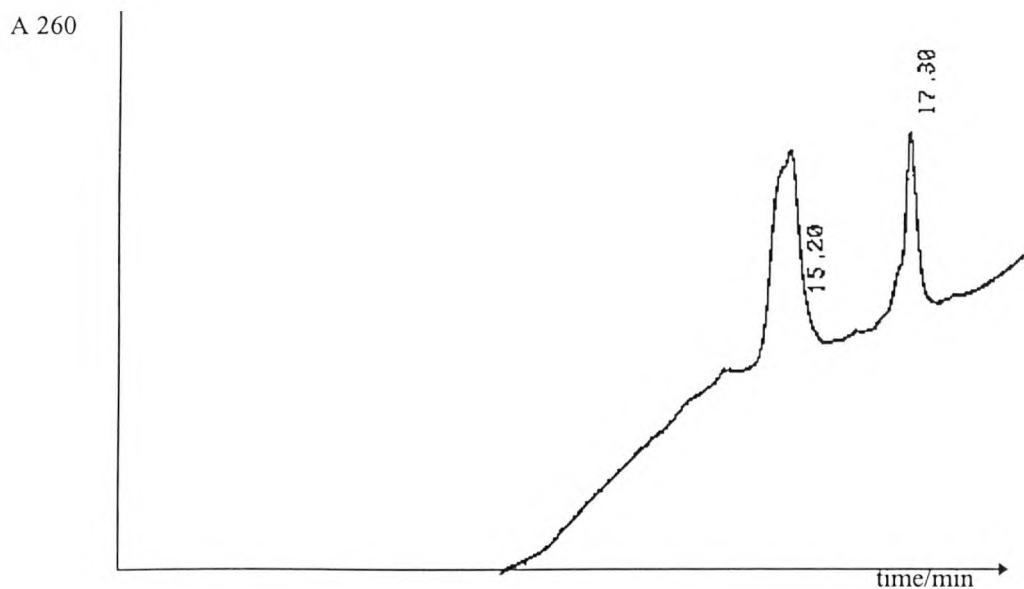


Figure 3.13. HPLC plot for the analysis of a mixture of oligonucleotides ACTTGCCACCATTG-3' and 5'-CAAAATGGTGGCCAAGT-3' with denaturing amounts of Er^{3+} chloride. Buffer A: 15.42g ammonium acetate, 2000 ml distilled water. Buffer B: 200ml of buffer A, 640 ml HPLC grade acetonitrile, 160 ml distilled water
Reverse phase column: Hichrom, Hypersil H5ODS (25cm x 8mm). The samples (10 μl) were injected at time 0.

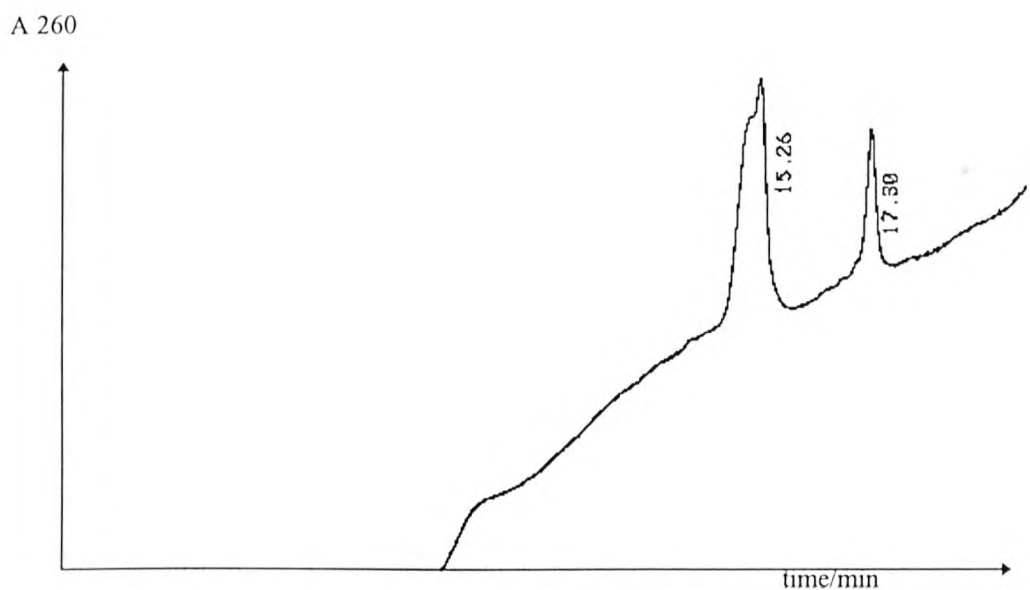


Figure 3.14. HPLC plot for the analysis of a mixture of oligonucleotides ACTTGCCACCATTG-3' and 5'-CAAAATGGTGGCCAAGT-3' with denaturing amounts of Eu^{3+} . Buffer A: 15.42g ammonium acetate, 2000 ml distilled water. Buffer B: 200ml of buffer A, 640 ml HPLC grade acetonitrile, 160 ml distilled water. Reverse phase column: Hichrom, Hypersil H5ODS (25cm x 8mm). The samples (10 μl) were injected at time 0.

Similar results were obtained for Eu^{3+} (figure 3.14) and for all other metals (data not shown). The experiments described above clearly show that cleavage of oligonucleotides do not occur when lanthanide ions are present but they bind to the oligo in such a manner that they prevent a double helix from forming, probably by binding to the phosphate backbone as well as to the bases, as suggested by previous experiments.

3.4. Study of the interaction of lanthanides with DNA using NMR spectroscopy

3.4.1. Aims

Previous experiments in this chapter strongly suggest that lanthanide ions bind to phosphate groups as well as the bases on DNA. Direct study of the atoms involved in these interactions is possible using Nuclear magnetic resonance (NMR). ^{31}P NMR can be used to investigate binding of the metal ions to the phosphate groups at low concentration of metal ions. For higher concentrations of metal ions, binding onto the bases can be studied by observing hydrogen bonding that occurs during Watson and Crick base pairing and this can be done using proton NMR. Because the protons that participate in Watson Crick hydrogen bonding exchange rapidly, they cannot be seen in standard NMR techniques using D_2O . However, in non aqueous solvents, for example DMSO-d_6 (Shoup *et al* 1966), it is possible to detect these protons. It is also possible to observe these protons in D_2O using water suppression techniques. Imino proton spectra can be recorded using the 1-3'-3-1' water suppression pulse sequence $(11.25^\circ)_x - \tau - (33.5^\circ)_x - \tau - (33.75^\circ)_x - \tau - (11.25^\circ)_x$ acquire. Presaturation techniques (Le Guerneve and Seigneuret 1996) can also be used to suppress water and this was the technique chosen for this set of experiments. It is well established that imino protons involved in H bonds with ring nitrogen atoms (in C-G and T-A Watson and Crick base pairs) show large down field shifts, appearing in the 12 to 14 ppm chemical shift range (Le Guerneve and Seigneuret 1996).

Oligonucleotides are a preferred choice over large DNA molecules for NMR studies of nucleic acids because NMR analysis of high molecular weight rigid molecules usually poses the problem of serious line broadening. Moreover, in high molecular

weight chains, the situation is complicated by the fact that nucleic acids are predominantly composed of four nucleotide units, each of which is represented many times in the sequence. Consequently, in the NMR spectrum, a given area of absorption will represent a superposition of the absorption of a particular kind of base from various parts of the structure. The NMR spectra of oligonucleotides are much easier to analyse than that of polynucleotides for three reasons:

- (i) The number of bands is smaller, facilitating both detection and spectral assignment.
- (ii) The molecular weight is small, enabling studies at high concentration.
- (iii) Any ordered structures should be small enough so that tumbling is fast enough to average out dipolar broadening, thereby enabling the observation of sharp resonances.

It is most convenient to study the shortest oligonucleotides that will form a given structure of interest, otherwise, the observed conformational free energy is a sum over many different interactions, and a whole series of analogous complexes must be examined before individual contributions can be factored out.

The NMR spectrometer used for these experiments was a Bruker B-ACS60 400MHz, run using a UXNMR software for data collection and analysis, located in the Chemistry Department at King's College London.

3.4.2. Phosphorus NMR study of the interaction of Eu^{3+} with DNA

^{31}P NMR was performed using the 12 mer AT oligonucleotide in the presence of EuCl_3 . Aliquots (200 μl) of a saturated solution of EuCl_3 was added to 0.5 ml of

0.5 M solution of oligonucleotide. Figure 3.15 shows the ^{31}P spectra obtained with increasing Eu^{3+} concentrations. The peaks obtained were found to be shifted and broadened with the addition of the metal ions. With higher amounts of metal ions being added, several peaks appeared in addition to the original unique peak found for the pure oligonucleotide. This observation strongly suggests that the Eu^{3+} ions interacts with the phosphate groups of the oligonucleotide.

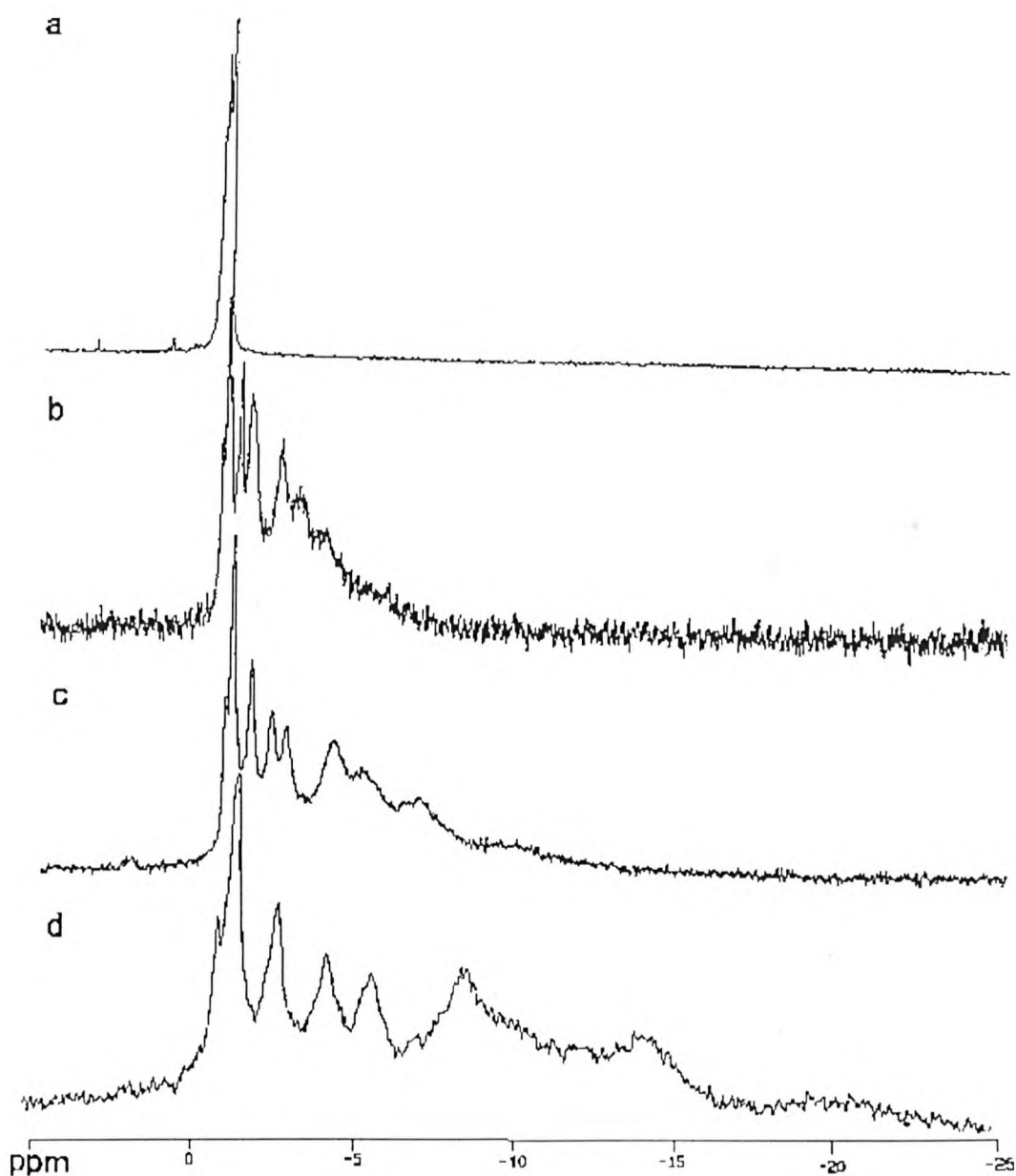


Figure 3.15: ^{31}P spectra of 12 mer oligonucleotide in the presence of EuCl_3 . Volume of saturated solution added per 0.5ml of 0.5M: (a):0, (b): 200 μl , (c): 400 μl , (d): 600 μl .

It can also be observed on the spectra in figure 3.15 that as soon as EuCl_3 was added, 7 distinct peaks appeared, corresponding each to a phosphorus atom in a different environment. When adding increasing amounts of EuCl_3 , the number of peaks remains constant but the chemical shift and band broadening is increased, proportionally to the amount added. This could possibly allow to determine from a given sample the concentration of ions present by measuring the chemical shift using phosphorus NMR.

3.4.3. Study of the interaction of Tb^{3+} and Eu^{3+} with DNA using Proton NMR with presaturation water suppression technique

As previously mentioned (section 3.4.1. page 99), the hydrogens involved in Watson and Crick bonding can be observed using water suppression techniques. The 12 mer AT oligonucleotide NMR sample was diluted in 0.5 ml 10% H_2O / 90% H_2O , and NMR data was accumulated on 128 scans. The data was then processed using a presaturation programme. The resulting spectrum can be seen in figure 3.16. It is well known that protons taking part in hydrogen bonding in Watson and Crick base pairing exhibit resonances in the region of 12-14 ppm (Nedderman *et al* 1993). However in our experiment, no resonance peaks were observed in that region, suggesting the absence of any hydrogen bonds between the bases. This could be due to the absence of salt in the sample, that would not allow the formation of a detectable duplex. When 200 μl of 1M NaCl were added to give a total concentration of sodium ions of 0.285 M, the spectrum as shown in figure 3.17 was obtained (160 scans).

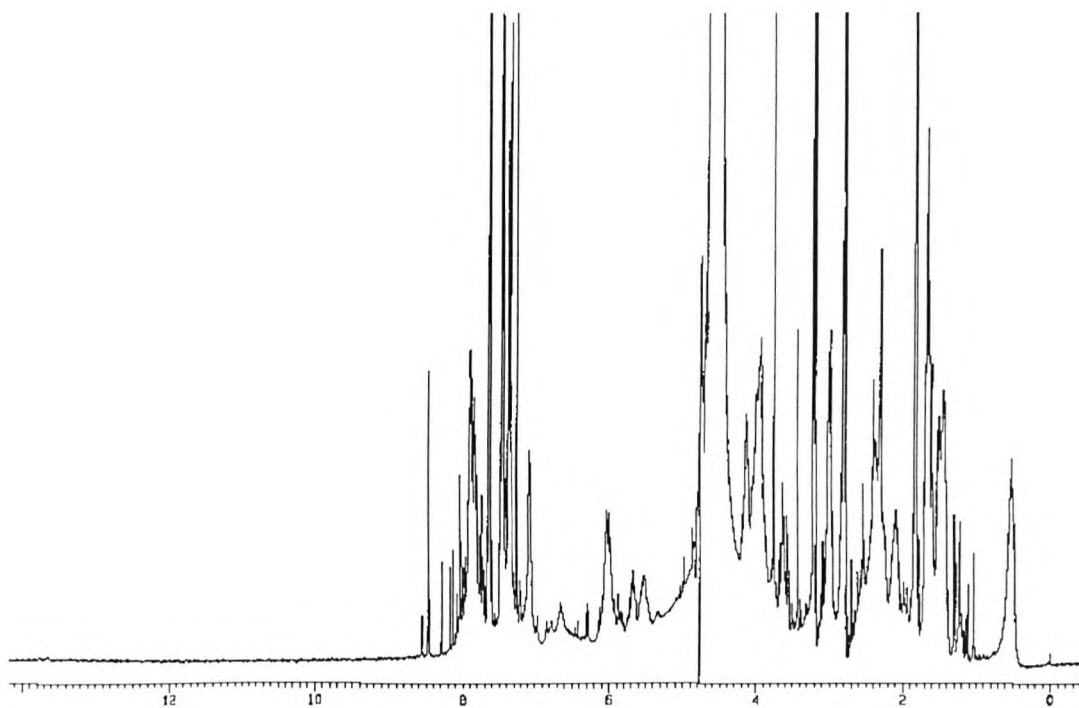


Figure 3.16. Presaturated ^1H NMR spectrum of 12 mer oligonucleotide in 10% H_2O /90% H_2O

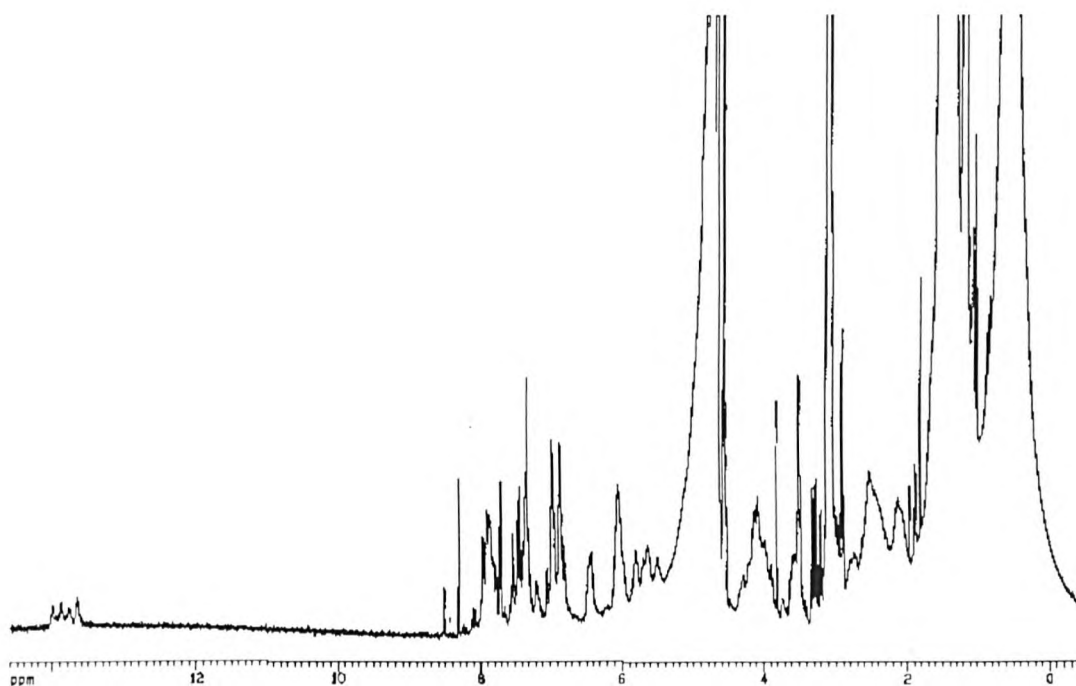


Figure 3.17. Presaturated ^1H NMR spectrum of 12 mer oligonucleotide 5' AAAAAATTTTTT 3' in 10% H_2O /90% H_2O , 0.285 M NaCl. Peaks in the 13.5-14ppm region can be attributed to hydrogens involved in base pairing.

Spectrum in figure 3.17 showed 4 peaks in the region of 13.5-14 ppm, which could be attributed to Watson and Crick bonding. If all the bases in the sample form A-T

base pairs, only 2 types of hydrogen bonds should be seen. The observation of 4 peaks in the NMR spectrum indicated the presence of 4 hydrogen bonds in different environments. Two of those peaks could be attributed to the normal Watson and Crick base pairing as seen in figure 3.18 and the other 2 peaks could be due to the presence of non Watson and Crick base pairing, for example wooble pairs and this could occur when one of the bases has moved either up or down to generate 1 hydrogen bond only (wooble base pairs are represented figure 3.19).

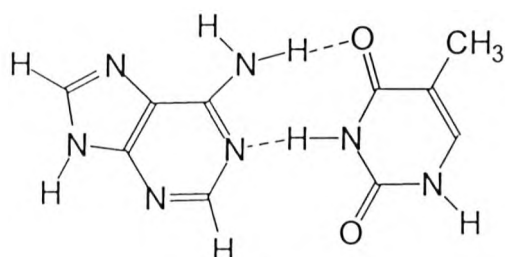


Figure 3.18. Schematic representation of “Watson and Crick” hydrogen bonding between adenine and thymine

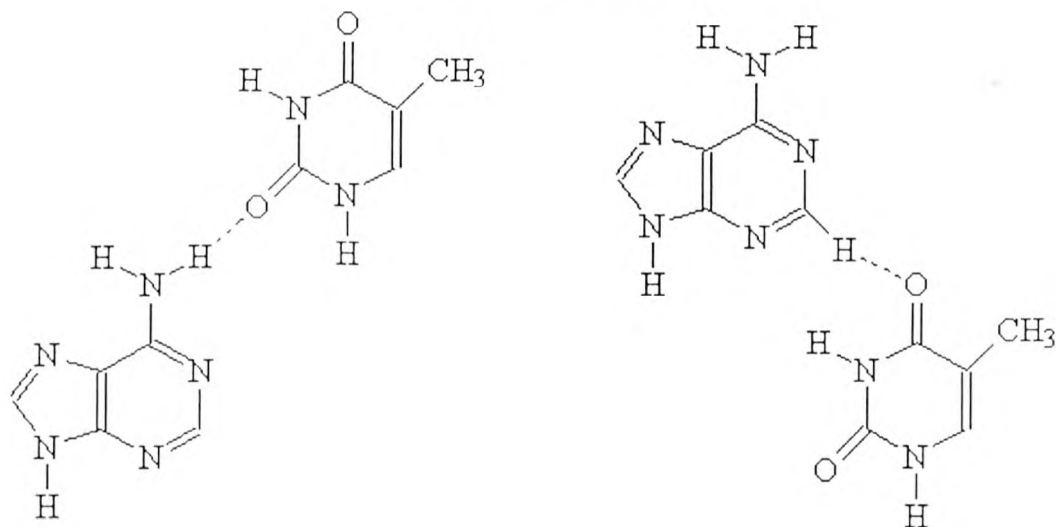


Figure 3.19. 2 possible adenine -thymine wooble base pairing schemes

To verify our observations in section 3.2.3 page 92, where the addition of EuCl_3 to an oligonucleotide 5'AAAAAATTTTTT3' in 6SSC buffer did not appear to alter the T_m of the oligonucleotide, Eu^{3+} was added to an dA_6dT_6 oligonucleotide NMR sample

prepared with 6xSSC buffer. SSC buffer (1M NaCl, 0.15 M sodium citrate) contains sodium citrate and the hydrogens of the citrate appeared in the spectrum in the 2-3 ppm region, which did not interfere with the area of interest. A 0.5M solution of the oligonucleotide was prepared in SSC buffer and the spectrum as shown in figure 3.20 was obtained (no presaturation, 64 scans, figure3.20).

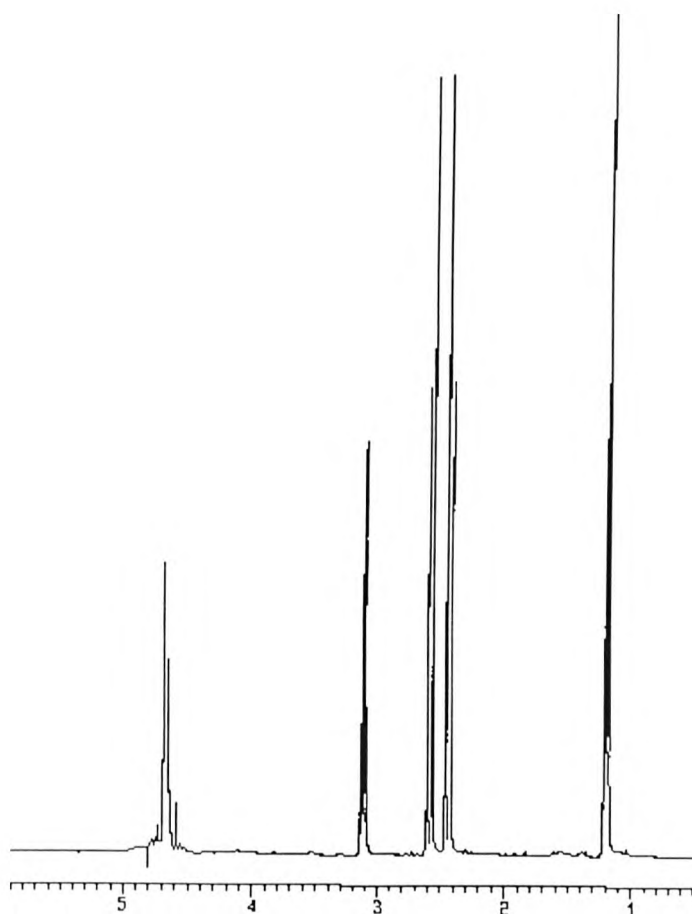


Figure 3.20: ^1H NMR of 12 mer oligonucleotide in SSC buffer (no presaturation)

When $5\mu\text{l}$ of 0.5M EuCl_3 were added, as the peaks obtained between 2 and 3 ppm were up-shifted and broadened, which meant that the metal interacted with the citrate's hydrogens (figure3.21).

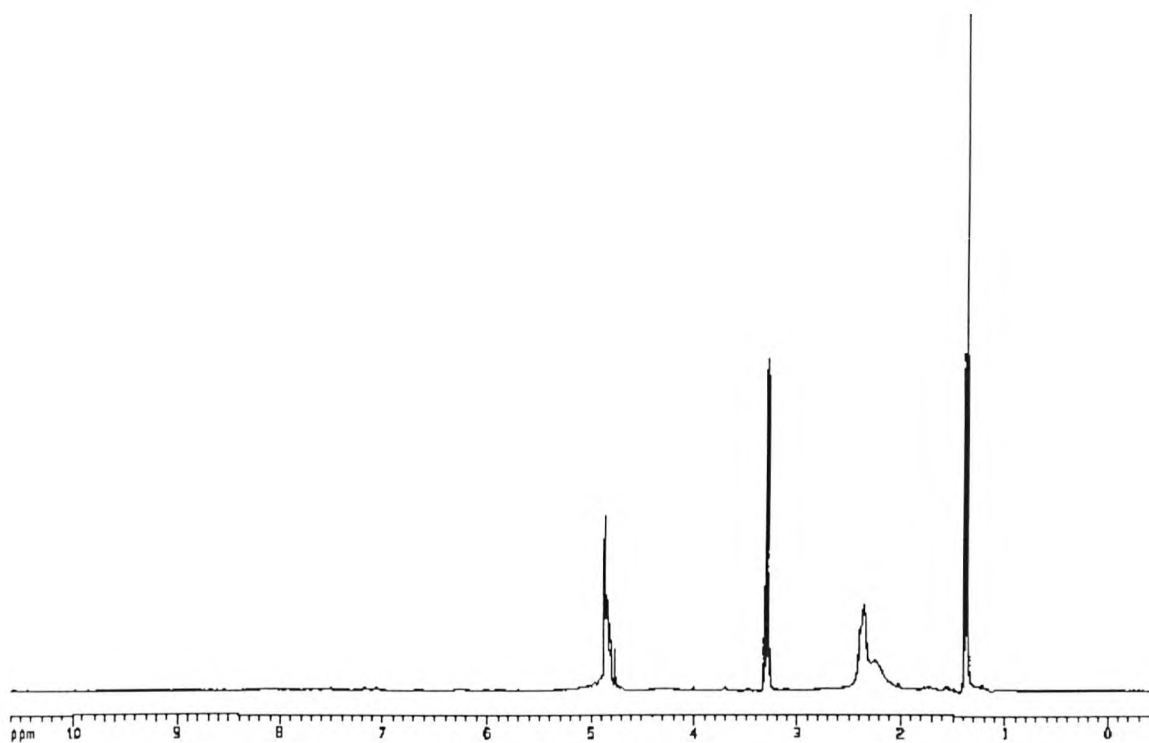


Figure 3.21. ^1H NMR spectrum of 12 mer oligonucleotide in SSC buffer/0.015M $\text{Eu}(15\mu\text{l})$

The presaturation data of the same sample showed no interaction with the Watson and Crick hydrogen bonds at this stage. Increasing amounts of Eu^{3+} were added up to precipitation concentration and no change in the base pairing was observed. A ^{31}P NMR spectrum was measured and used to verify any eventual interaction of the metal with the phosphates. The spectrum shown figure 3.22 was obtained. No interaction with the phosphate group was observed.

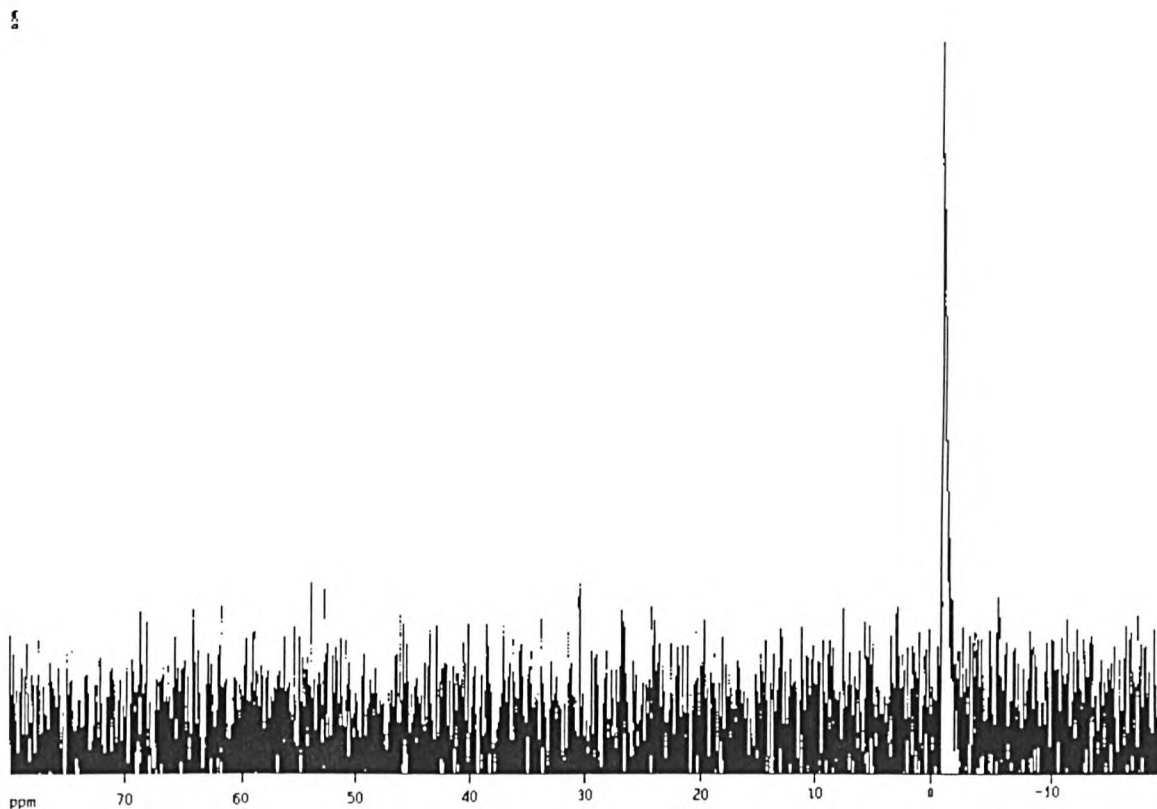


figure 3.22. Phosphorus NMR of 12 mer oligonucleotide in SSC buffer/0.03M Eu^{3+}

This data means that the metal ion added to the original sample interacted totally with the citrate in solution and not with the nucleic acid, which confirmed the observation of UV spectrometry, where no major changes in T_m values were observed up to precipitating concentrations of metal ions. This however does not explain why Tb^{3+} ions affected the T_m in section 3.2.2.

3.5. Fluorescent study of the interaction of Tb^{3+} with DNA

The fluorescence properties of some complexes of metals with DNA have led to some insight on the structure of the DNA. For example, Tb^{3+} can be used as a probe for single stranded DNA (Topal and Fresco 1980). In this work, it was shown that single stranded DNA/ Tb complexes are fluorescent whereas double stranded DNA fragment complexes of the same metal are not. Using the same phenomenon, Tb^{3+} has been used as a probe to assess the single stranded content of DNA (Ringer *et al* 1980). The mechanism by which Tb^{3+} becomes fluorescent upon binding of DNA is similar to that of lanthanide chelates, i.e. energy transfer (see page 34). Fluorescence spectroscopy is therefore a useful tool to study the interaction between nucleic acids and metals. Other spectroscopic methods such as infra red (Heidar Ali *et al* 1993, article 2) and Raman spectroscopy (Duguid *et al* 1993) have also been used to study these interactions.

The fluorescent properties of lanthanide ions are greatly increased in intensity when bound to DNA. Fluorescence studies of the DNA/lanthanides interaction were performed using a computer driven Perkin Elmer fluorometer model LS-5B and 4 sides polished quartz cells. The excitation was fixed at 325nm and the emission signal was measured from 345 to 600nm. A single stranded oligonucleotide (20 mer polydT) and a double stranded 12 mer AT oligonucleotide were dissolved in a NaCl solution (1M) to obtain 4 ml solutions of 0.5 OD.

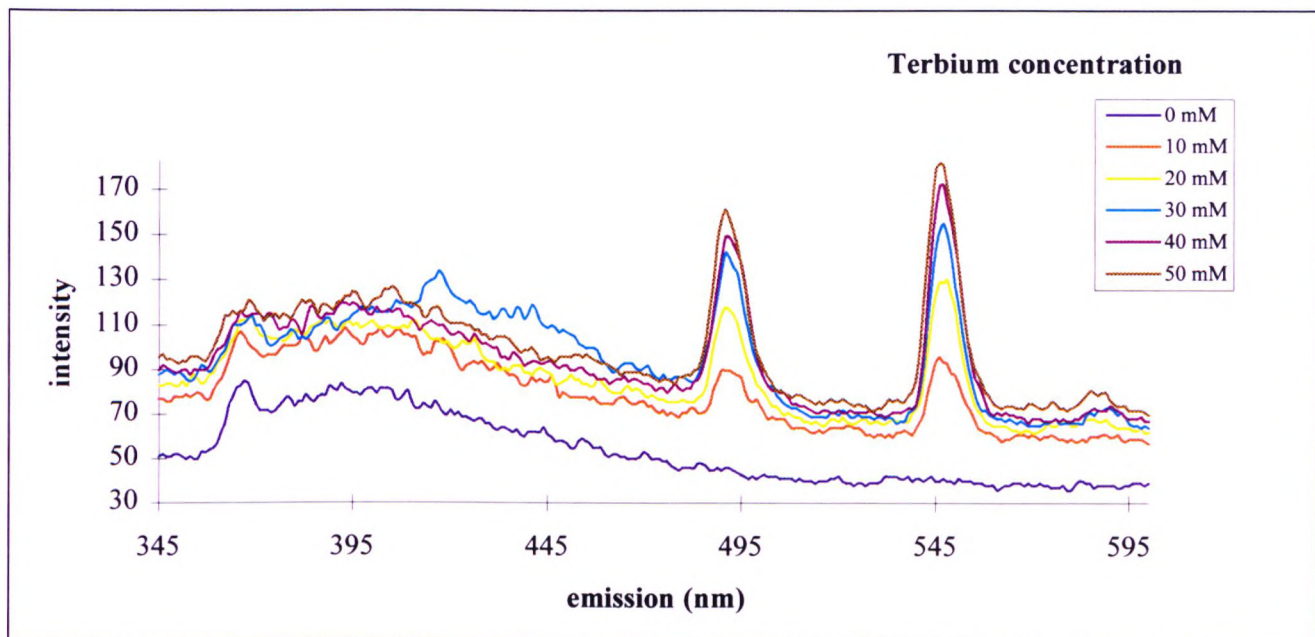


figure 3.23. Fluorescence of a double stranded oligonucleotide/ Tb^{3+} complex, showing 2 peaks at 488nm and 545 nm (characteristic of Tb^{3+})

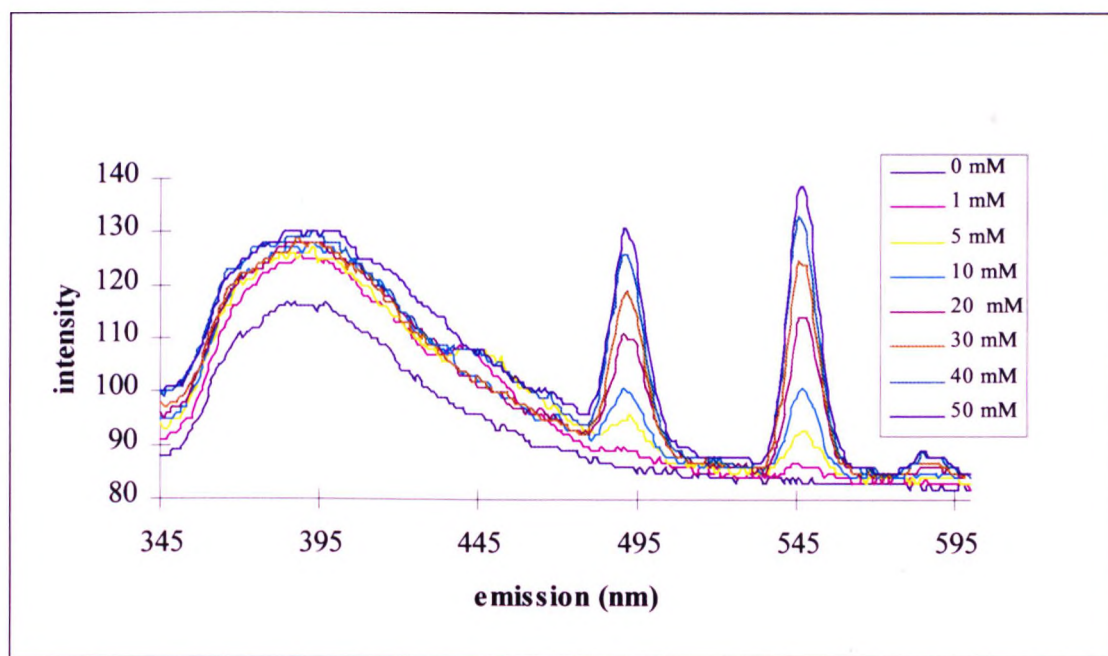


figure 3.24. Fluorescence of a single stranded oligonucleotide/ Tb^{3+} chloride complex

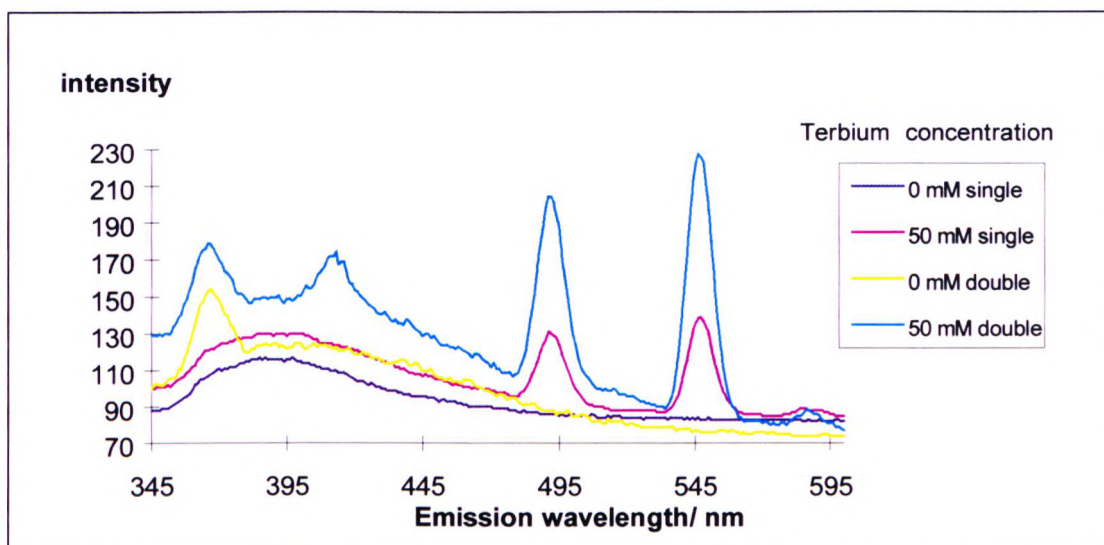


figure 3.25. Comparative study of the fluorescence of single strand and double stranded DNA complexes of Tb^{3+} chloride.

The first graph, on figure 3.23, shows that a solution containing the double stranded oligo on its own possesses a fluorescent background that is very low and flat between 445 and 600 nm. When Tb^{3+} is added, two peaks that are characteristic for Tb^{3+} appear at 495 and 545 nm, showing that the ion interacts with the DNA, getting a strong fluorescence enhancement by doing so. The single stranded oligo behaved in the same manner when Tb^{3+} was added to it, i.e. fluorescent peaks were measured at 495 nm and 545nm. When the two curves obtained for the oligos with 50mM Tb^{3+} were superimposed to compare them (figure3.25), it showed that the double stranded DNA complex possessed more fluorescence.

The experiment shows that double stranded DNA is more fluorescent than single stranded DNA when complexed with Tb^{3+} ions. This is in contradiction to the previous research work mentioned in the beginning of this section (Topal and Fresco 1980).

3.6. Study of the tertiary structure of natural DNA in the presence of Tb^{3+} .

The effect on the addition of Tb^{3+} and Eu^{3+} on oligonucleotides has been studied throughout this chapter. It is also interesting to observe the interaction of these metal ions on larger nucleic acids, such as plasmids, that exhibit supercoiled conformations. In the following experiment, the Plasmid PBR 322 was used. It has molecular weight of 2.83×10^6 Daltons and it is supercoiled. During electrophoresis, supercoiled plasmids migrate faster than plasmids of same molecular weight in a relaxed state. (The supercoiled state gives a smaller volume for the molecule, which can therefore pass through the network of gel easier).

A 1% agarose gel in TBE buffer was prepared (TBE: 0.045 M Tris-Borate, 0.001M EDTA). Plasmid DNA samples were prepared in 6SSC buffer at pH7 and the gel was stained with Ethidium Bromide and the gel was viewed under UV illumination. The Tb^{3+} concentration in the sample was increased from 0 to 0.5M. After migration on the agarose gel, one could observe that all the samples with a concentration in Tb^{3+} under 0.03M were unaffected, as they migrated in the same manner as the control (sample with no metal ions). Above 0.03M of $TbCl_3$, the plasmids were found to have migrated only half way through the gel, which implies that alteration of the supercoiled state has occurred. Above 0.1M of $TbCl_3$, the rate of migration of the plasmid decreases even more, implying that the Tb^{3+} ions at that concentration are affecting the tertiary structure of the plasmid. Above 0.5M of $TbCl_3$, the sample is precipitated and no migration is visible. The gel obtained is schematically represented in figure 3.26.

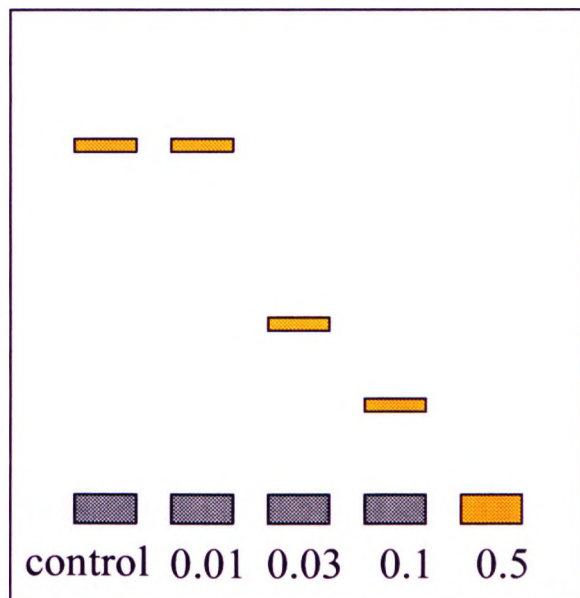


figure 3.26. Schematic representation of the agarose gel obtained for the plasmid/ Tb^{3+} complexes. Under each well, concentration of Tb^{3+} salt is stated in mol/l.

This experiment shows that Tb^{3+} affects the tertiary structure of nucleic acids, by destroying the supercoiled nature of a DNA plasmid.

3.7. Summary of results and conclusion

In this chapter, a number of techniques were used to study the interaction of lanthanide ions with oligonucleotides and plasmid DNA. The lanthanide ions used throughout this study comprise Eu^{3+} , Tb^{3+} , Sm^{3+} , Er^{3+} and Yt^{3+} .

Tb^{3+} was shown to bind to the phosphate groups and bases of the DNA as demonstrated by T_m studies. This binding effect was found to be strongly pH dependent. However, using pH buffered solutions such as SSC buffer was found to be a problem: It was attempted to perform similar studies with Eu^{3+} , but the metal ion was found to interact with the citrate of the buffer and the addition of more Eu^{3+} salts led to precipitation without any major changes in T_m values of the oligonucleotide. This result was confirmed with proton NMR experiments where no amount of Eu^{3+} was sufficient to show phosphate binding or interference with the base pairing hydrogens of the oligonucleotide duplex. Without SSC buffer, it was however possible to observe strong interference of Eu^{3+} ions with the phosphates. HPLC studies of denatured oligonucleotide duplexes showed that the metal ions prevented duplexes from forming without breaking down the nucleotide chains. Fluorescence studies of double and single stranded nucleic acids showed that single stranded DNA complexes of Tb^{3+} were less fluorescent than double stranded, which contradicted previous literature.

CHAPTER 4: STOICHIOMETRIC CHARACTERISATION OF

LANTHANIDE ION/ DNA INTERACTION BY MALDI MASS SPECTROMETRY

4.1. Introduction

This chapter aims to provide complementary information to chapter 3, where lanthanide ions/ DNA interactions were studied using conventional methods.

The stoichiometry of the interaction of different lanthanide chloride salts (Yb^{3+} , Sm^{3+} , Eu^{3+} , Er^{3+} and Tb^{3+}) with different oligonucleotides was determined Matrix Assisted Laser Desorption Time of Flight (TOF) Mass Spectrometry. Although MALDI has been extensively used for the analysis of oligonucleotides (as described in the introduction), it is the first time it is used to study the interaction of oligonucleotides with lanthanide ions. Conventional techniques to estimate binding constants and the number of binding sites for metals on DNA include ultracentrifugation (Daune 1970) and potentiometry using ion selective electrodes (Clement *et al* 1973). MALDI MS has several important advantages over conventional nucleic acid analysis techniques: It allows rapid and accurate analysis of complex mixtures of oligonucleotides with great sensitivity, it is readily automatable and does not require extensive sample preparation or any kind of labeling.

In this chapter, the development of a method permitting the study of DNA/lanthanides adducts using MALDI-MS will be outlined. The choice of a suitable matrix was the first step of this investigation. Complexes of lanthanide chloride salts

with oligonucleotides were prepared using a range of lanthanide salt concentrations. These complexes were then analysed using MALDI MS with and without the use of internal standards. The reproducibility and accuracy of the MALDI TOF analysis method were also assessed.

4.2. Experimental set up

Oligonucleotides were synthesised on a Cruachem synthesiser using normal phosphoramidite chemistry. A 20 mer polydT and a 12 mer self complementary oligonucleotide of sequence 5'AAAAAATTTTTT 3' were used. The dry oligonucleotides were re-suspended in distilled water to obtain a concentration of 70 pmol/ μ L.

The MALDI mass spectrometer used was a computer driven Finnigan LaserMAT, fitted with a Nitrogen laser (337nm), with a power density of up to 10^8 W/cm² at the sample, installed with LaserMAT 2000 mass analyzer TOF (Time of Flight) version 1.3 software (Thermobioanalysis Ltd). Each analysis was performed in the negative ion mode with the minimum laser threshold power giving a suitable peak intensity. Samples were deposited on the mass spectrometer steel targets as 1 μ L aliquots followed by 1 μ L aliquots of chosen matrix. The mixture was allowed to dry at room temperature and then placed into the mass spectrometer. The position of the laser beam on the sample could be altered between 4 positions located on the dried spot.

Although the laser power used was varied from one sample to another, the lowest power possible was always chosen, as the resolution of the spectra is known to decrease with high laser powers. The power necessary to ionise the sample was observed to increase with the amount of metal present in the mixture. This could be due to the absorption of laser energy by the metal ions.

Selection of a matrix and a solvent:

The choice of matrix and solvent used to dissolve the sample DNA is of critical importance (Tang *et al* 1993). A number of matrices was investigated for use in this study. Hydroxypicolinic acid (HPA) is the most frequently cited matrix used for the analysis of nucleic acids by MALDI (Wu *et al* 1993). However, in our experiments, the spectra obtained were broad and the resolution was low, as can be seen in figure 4.1.

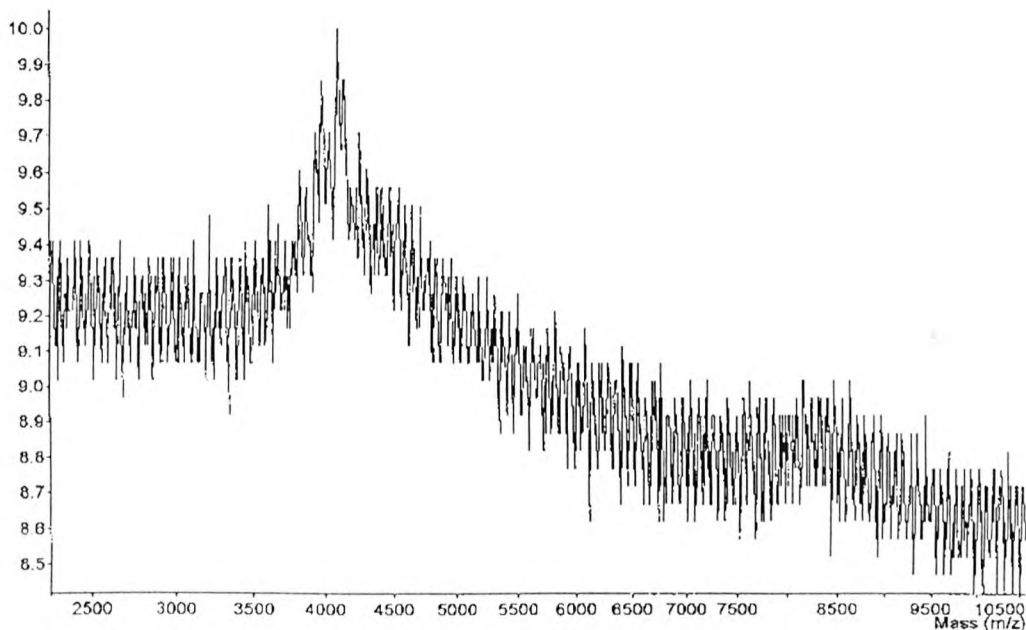


Figure 4.1. Spectrum of the analysis of 70pmol of 12 mer AT oligonucleotide using hydroxypicolinic acid (10 shots, laser aim 2, power 80%).

Thiothymine and hydroxyacetophenone (P.Lecchi 1995) were also tried and Hydroxyacetophenone (HAP) was chosen since it gave the best resolution. An example of the same 12 mer oligonucleotide is shown figure 4.2. Lower power laser was required to obtain a visible peak, as compared with hydroxypicolinic acid (55%,

figure 4.2 and 80% figure 4.1 respectively). Furthermore, it was found that the use of ammonium citrate and acetonitrile (50:50) improved the quality of the spectra when compared with other solvents mixtures such as acetonitrile/water 70:30 (Tang *et al* 1993). Other factors that affect the MALDI MS spectra include the presence of sodium ions in the sample mixture, which is known to affect the quality of the spectra obtained (Christian *et al* 1995). Ammonium citrate acts as a chelator for free sodium ions, thus reducing the number of sodium adducts.

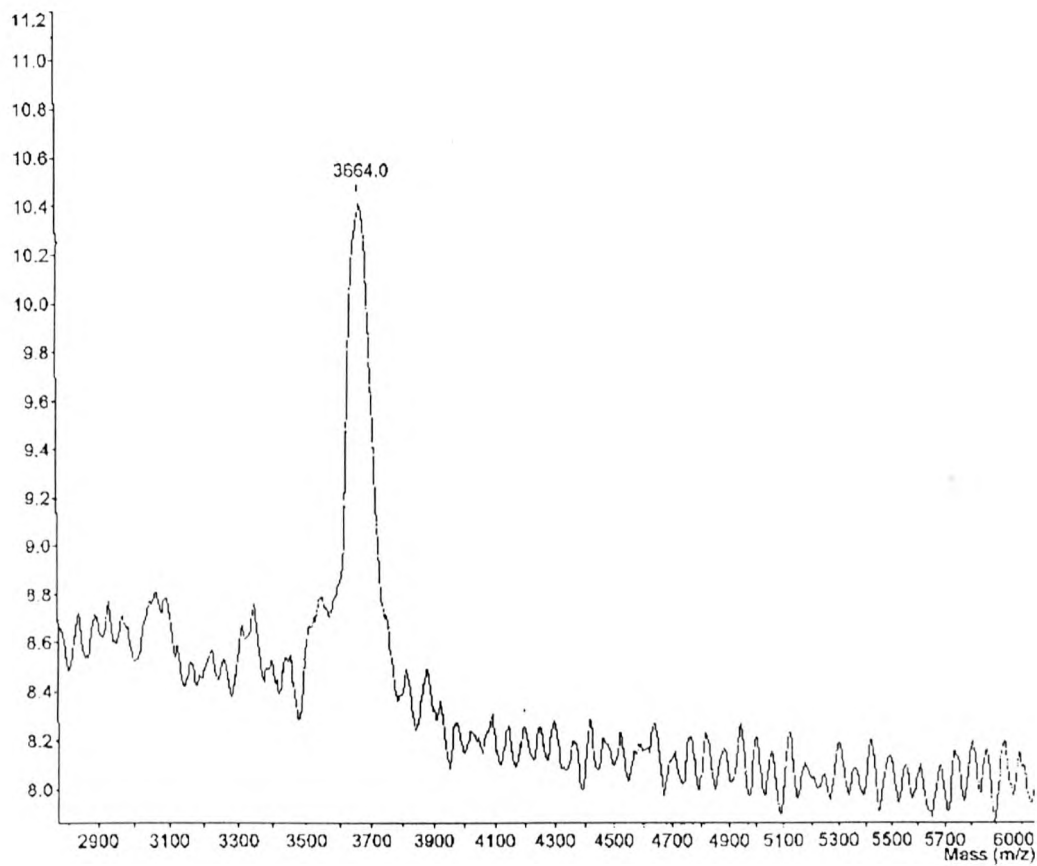


Figure 4.2. Analysis of 70 pmol of 12 mer oligonucleotide using HAP (3 shots, laser aim 3, power 55%)

4.3. Results

4.3.1. Study of the interaction of a 20 mer polydT oligonucleotide with lanthanide ions

The following series of experiments are aimed at studying mixtures of oligonucleotide/ lanthanide chloride containing increasing amounts of Ln^{3+} . Lanthanide chloride solutions (TbCl_3 , EuCl_3 , SmCl_3 , ErCl_3 , YbCl_3) were made up in distilled water, at a concentration of 0.03 M. A volume of 5 μl of oligonucleotide solution at 70 nmol/ μl was mixed with a different volume of lanthanide solution. A mass spectrum of the pure oligonucleotide was obtained for comparison purposes and is shown in figure 4.3 and it showed unique sharp peak can be observed at a mass of 6034.1 daltons. When this value is compared with the theoretical value for the oligonucleotide (6064 g/mol), the percentage accuracy was calculated as follows: $6034.1 \times 100 / 6064 = 99.50\%$.

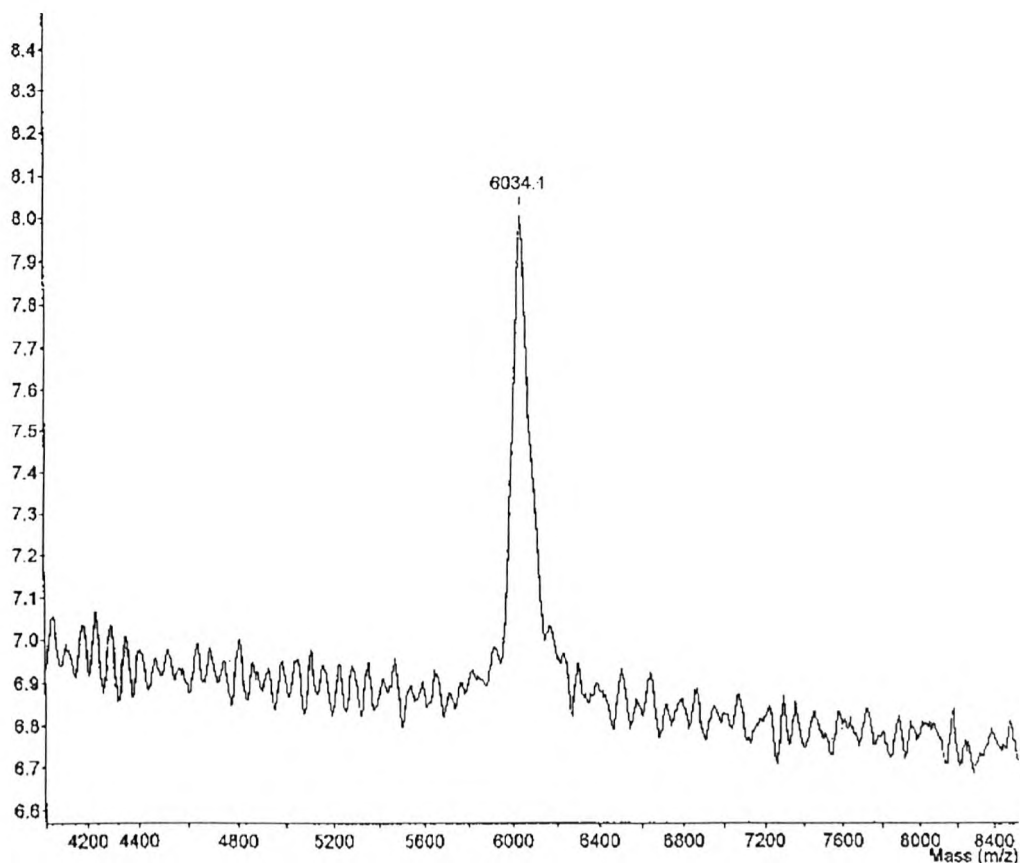


Figure 4. 3. Analysis of 350 pmol 20 mer polydT oligo in HAP (10 shots, laser aim 3, laser power 70%)

In subsequent experiments, aliquots of TbCl_3 solution were added to $5\mu\text{l}$ of $70\text{pmol}/\mu\text{l}$ of the oligonucleotide and the resulting mixtures analyzed by MALDI-MS. Table 4.1 shows the amount of TbCl_3 in nmoles added to the oligonucleotide sample and figure numbers relate to the corresponding mass spectra.

Amount of Tb^{3+} (nmol)	figure number
30	4.4
60	4.5
90	4.6
120	4.7
150	4.8

Table 4.1. Composition of Tb^{3+} -oligonucleotide samples and key to figures

When Tb^{3+} ions (30 nmol) were added to the oligonucleotide solution, no significant difference was observed in the MALDI spectrum (figure 4.4). When this spectrum was compared with the sample without metal ions (figure 4.3), only a minor band broadening was observed.

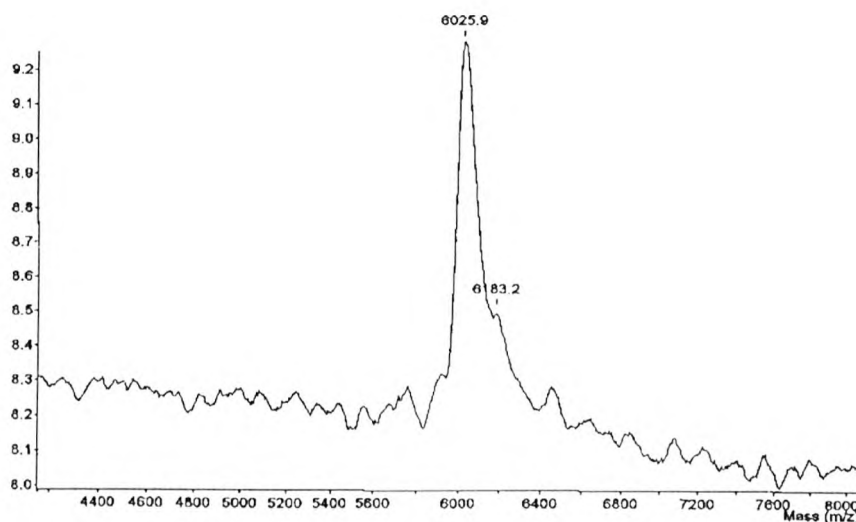


Figure 4.4. Analysis of 350pmol of 20 mer polydT oligo +30 nmol TbCl_3 using HAP (10 shots, laser aim 1, laser power 66%)

The addition of a larger amount of 60 nmol (figure 4.5) led to the appearance of several peaks, in addition to the one at 6054.2 daltons which was attributed to the oligonucleotide 20 mer polydT itself. The 3 other peaks were found at higher molecular weights (6203.0, 6357.1 and 6505.8 daltons).

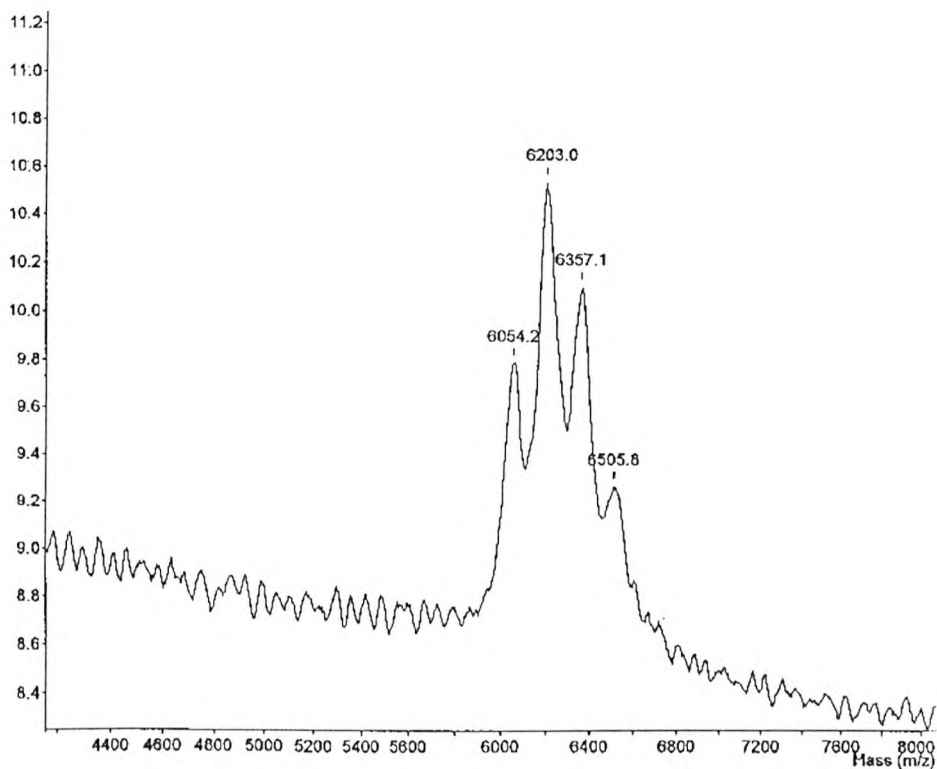


Figure 4.5. Analysis of 350pmol of 20 mer polydT oligo +60 nmol TbCl_3 using HAP (10 shots, laser aim 4, laser power 86%)

Upon adding more metal ion, 90 and 120 nmoles, the molecular weight of the different species was even higher, up to a maximum around 7300 daltons (figure 4.6, 4.7).

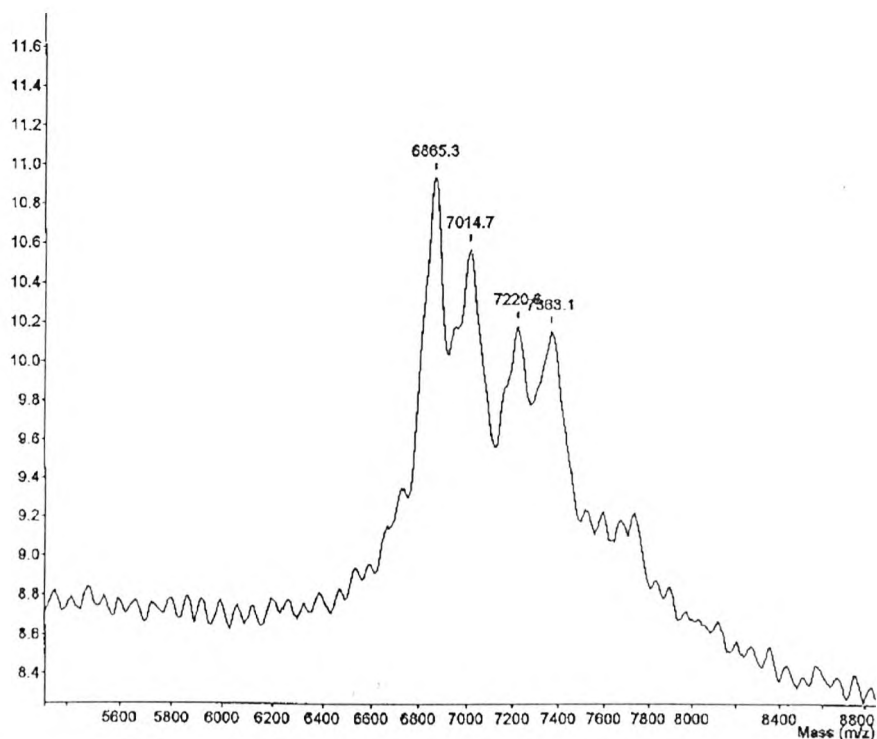


Figure 4.6. Analysis of 350pmol of 20 mer polydT oligo +90 nmol TbCl₃ using HAP (10 shots, laser aim 3, laser power 95%)

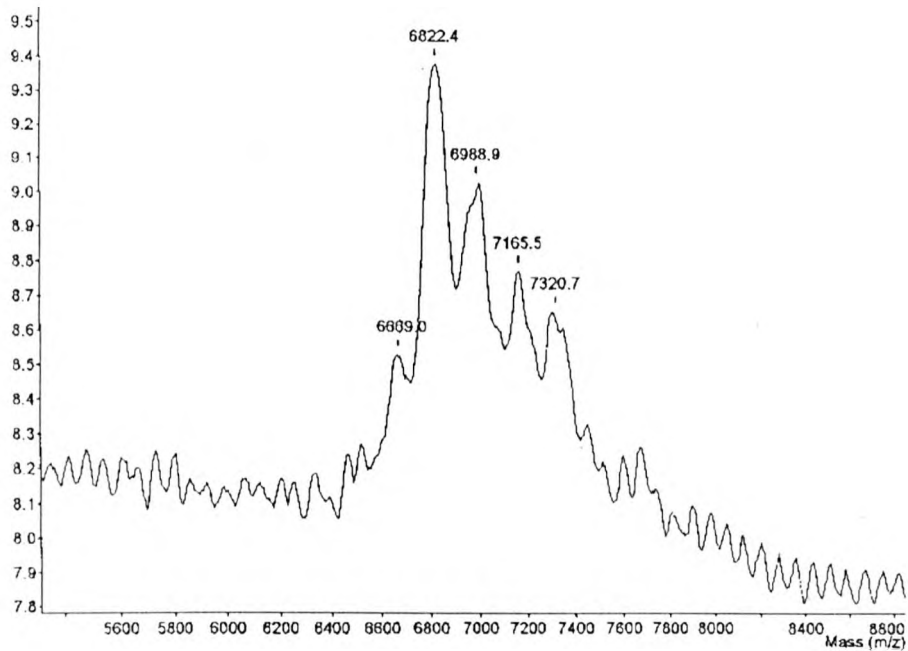


Figure 4.7. Analysis of 350pmol of 20 mer polydT oligo +120 nmol TbCl₃ using HAP (10 shots, laser aim 4, laser power 76%)

On addition of 150 nmol of Tb^{3+} to this same sample, complete breakdown of the oligonucleotide was observed (figure 4.8).

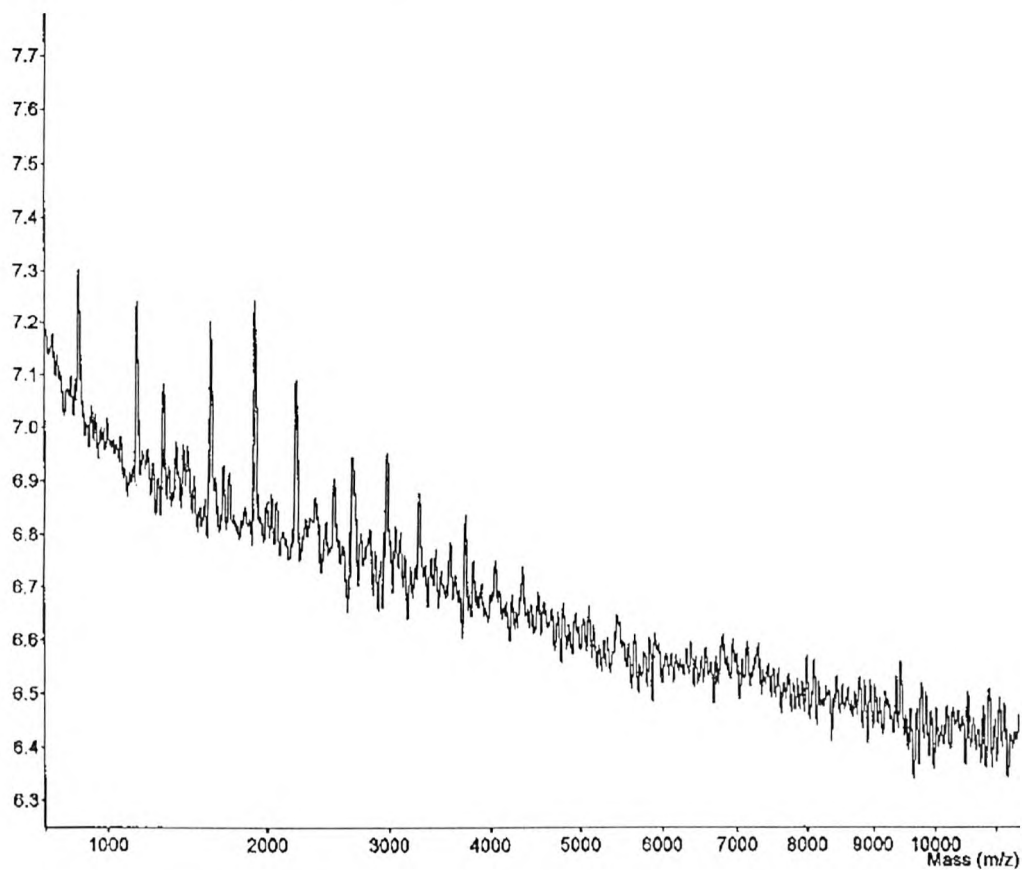


Figure 4.8. Analysis of 350pmol of 20 mer polydT oligo +150 nmol TbCl_3 using HAP (10 shots, laser aim 4, laser power 90%)

Table 4.2 summarises the values of the peaks obtained throughout this series of experiments.

Amount of Tb^{3+} Added /nmol	peaks /m/z							
0	6034.1							
30	6025.9							
60	6054.2	6203.0	6357.1	6505.8				
90					6865.3	7014.7	7220.6	7363.1
120					6822.4	6988.9	7165.5	7320.7

Table4. 2: Peaks obtained for 350 pmol of polydT oligonucleotide containing increasing amounts of Tb^{3+}

The difference in mass between a given peak and the consecutive peak was on average equal to 158.3. Since the relative ionic mass of Tb^{3+} was 158.27, the difference in mass between the peaks obtained from the analysis of each mixture can be attributed to the binding of Tb^{3+} ions to the oligonucleotide. For example, in the sample containing 60 nmol Tb^{3+} (figure 4.5), it is consistent with the data above to suggest that the first peak at 6054.2 was due to some pure oligonucleotide, the second peak at 6203.0 is due to the oligonucleotide with one Tb^{3+} ion, the third peak at 6357.1 to the oligonucleotide with 2 Tb^{3+} ions and the fourth peak at 6505.8 to the oligonucleotide with 3 Tb^{3+} ions. Assuming that the reason for the mass increase and the presence of different species in the sample was due to the binding of the Tb^{3+} ions to the DNA, the calculated accuracy of the identification of the metal was found to be 99.9%. The maximum number of Tb^{3+} ions that can bind to this particular oligonucleotide could be determined by observing the peak with the highest molecular weight. This highest peak was 7320.7 (figure 4.7), which was 1286.2 daltons higher than the sample analysed without metal ions. This difference amounts to 8.09 times the mass of Tb^{3+} . Thus the maximum number of Tb^{3+} ions which could bind to this 20 mer polydT oligonucleotide was 8.

A series of experiments using Eu^{3+} , Er^{3+} , Sm^{3+} and Yb^{3+} were performed, using the same methodology as above, i.e. analysis of complexes between oligonucleotide and increasing amounts of ions by MALDI MS. The results obtained are summarized in table 4.3.

ion	theoretical molecular weight/g/mol	average difference between peaks/m/z	accuracy of identification of the ion/ %	maximum number of ions per chain
Eu ³⁺	151.96	144	94.76	6
Sm ³⁺	150.36	150.71	99.76	8
Yb ³⁺	173.04	187.71	92.16	5
Er ³⁺	167.27	160	95.82	8

Table4.3. Summary of the key results of the interaction of some lanthanide ion with a 20 mer polydT oligonucleotide.

The maximum number of ions bound per oligonucleotide chain was observed to be 8 for Tb³⁺, Sm³⁺ and Er³⁺. It was lower for Eu³⁺ (6) and for Yb³⁺(5). It was also observed that the breakdown of the DNA was obtained at lower amounts of metal ions for Eu³⁺ and Yb³⁺ than for the other 3 lanthanides. This could be due to a higher catalytic reactivity of Eu³⁺ and Yb³⁺, or the conformation change of the oligonucleotide upon binding to Eu³⁺ and Yb³⁺ ions promotes breakdown. This catalytic effect was observed previously by others with another lanthanide ion, cerium³⁺ (Komiyama *et al* 1993).

4.3.2. Analysis of lanthanide adducts of a 12 mer dA₆T₆ oligonucleotide

The stoichiometry of the complexes of lanthanide ions with a 20 mer polydT have been observed to vary among a number of ions. It can also be suggested that this interaction will be different for oligos of different sequence. The following series of experiments aimed at studying a self complementary 12 mer dA₆T₆ oligo complexed with lanthanide ions. This study was performed in the same manner as with the 20 mer oligonucleotide as described above. A fixed amount of oligonucleotide (5µl at 70 pmol/µl) and a variable amount of the metal ion solution were used. The oligonucleotide was also analysed in its pure form as seen in figure 4.9.

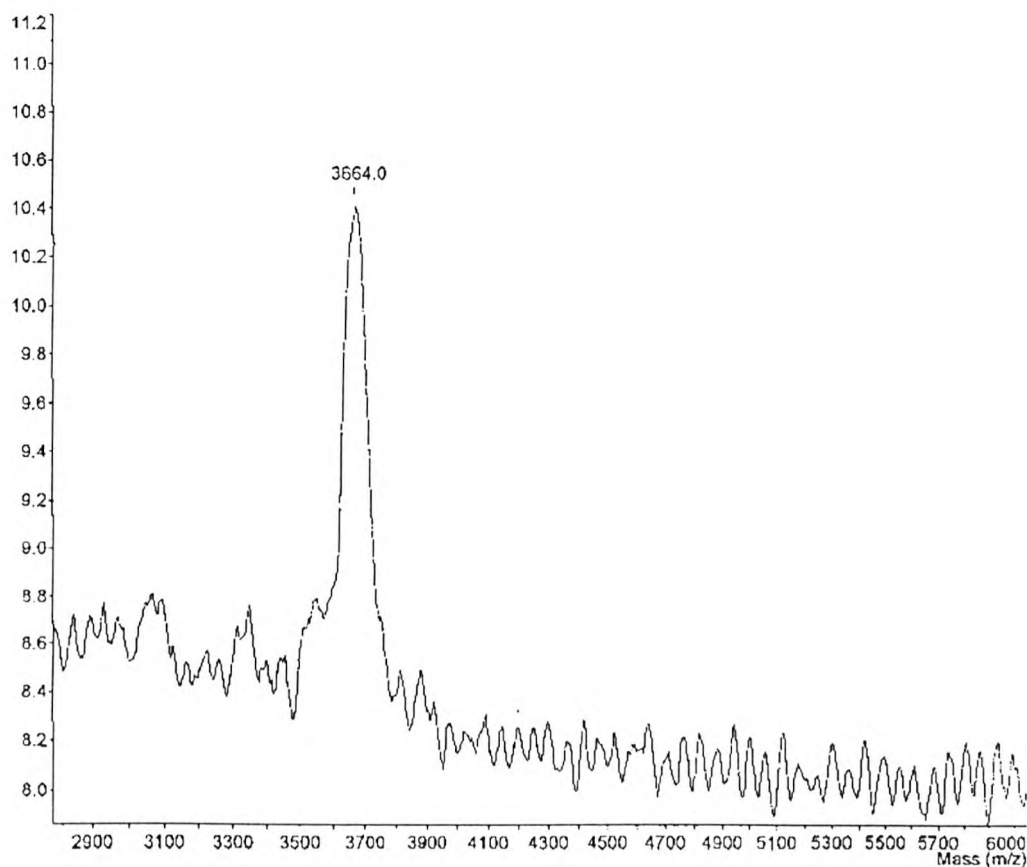


Figure 4.9. Analysis of 12 mer AT oligonucleotide in HAP (3 shots, laser aim 3, laser power 55%).

The observed mass of the pure oligo was found to be 3664.0 daltons, compared to 3692.4 daltons for its theoretical value, giving a very accurate molecular weight determination (99.23%).

Results for the interaction of 5 lanthanide ions with the 12 mer AT oligonucleotide are detailed in table 4.4.

ion	theoretical molecular weight/g/mol	average difference between peaks/m/z	accuracy of identification of the ion/ %	maximum number of ions per chain
Tb ³⁺	158.31	151.25	95.54	3
Eu ³⁺	151.96	135.66	89.2	3
Sm ³⁺	150.36	147.36	98	3
Yb ³⁺	173.04	147.16	85.04	3
Er ³⁺	167.27	140.01	83	2

Table 4.4. Summary of the study of the interaction of a 12 mer AT self-complementary oligonucleotide with Tb³⁺, Eu³⁺, Sm³⁺, Yb³⁺ and Er³⁺.

The observed accuracy for the identification of the metal ions is lower for the 12 mer oligonucleotide than for the 20 mer. This is probably due to the smaller size of the oligonucleotide. There are less sites for the metal ions to bind to and therefore the average difference in mass calculated between peaks is calculated on a smaller number of experimental values, hence a lower accuracy of measurement.

The difference between the values obtained in the analysis of the polyT oligonucleotide and the 12 mer AT oligonucleotide should also be noticed. The number of metal ions bound per base of the 12 mer (5'AAAAAATTTTTT3') is lower than for the 20 mer (20 polydT). A possible explanation might be that adenine has a lower affinity for the metals than thymine.

4.3.3. Improvement of the reproducibility of the MALDI MS analysis using internal standards

In order to improve the overall accuracy of the mass spectral measurements by the MALDI MS in this series of experiment, an internal standard was incorporated into the sample/matrix mixture. The peak obtained for the internal standard of known

mass provided a reference for the Peak Analysis software, enabling it to calibrate the m/z scale of each spectrum.

An internal standard for MALDI should have a similar structure and a mass of the same order to that of the sample to be analysed. An accuracy of 99.99% has been reported when using poly(dT) oligonucleotides as internal standards for the analysis of oligonucleotides (Wang and Blemann 1994). However, it is not possible to employ such a standard in the present application, as internal standard oligonucleotides would interact with the lanthanide ions in the sample and its molecular weight would thus be unpredictably affected. To overcome these limitations, insulin was employed as an internal standard. Insulin is detectable in negative mode and it desorbs well with the matrix used here (hydroxyacetophenone). A solution of insulin was prepared to a concentration of 0.6mg/ml in water/ methanol 1:1. The suitability of the protein as an internal standard was tested by monitoring the influence of the metal with the observed mass for the protein. The protein was analysed using hydroxyacetophenone (HAP), and the effect of Eu^{3+} on insulin was tested by mixing 1 μl of EuCl_3 0.03M, 1 μl of insulin solution and 1 μl of HAP matrix. The resulting spectra are shown in figures 4.10a and b. The data shows that the molecular weight of insulin was not shifted by the addition of Eu^{3+} in the mixture, indicating that no interaction between the protein and the metal ions is occurring. Insulin was therefore used as an internal standard in the subsequent experiments.

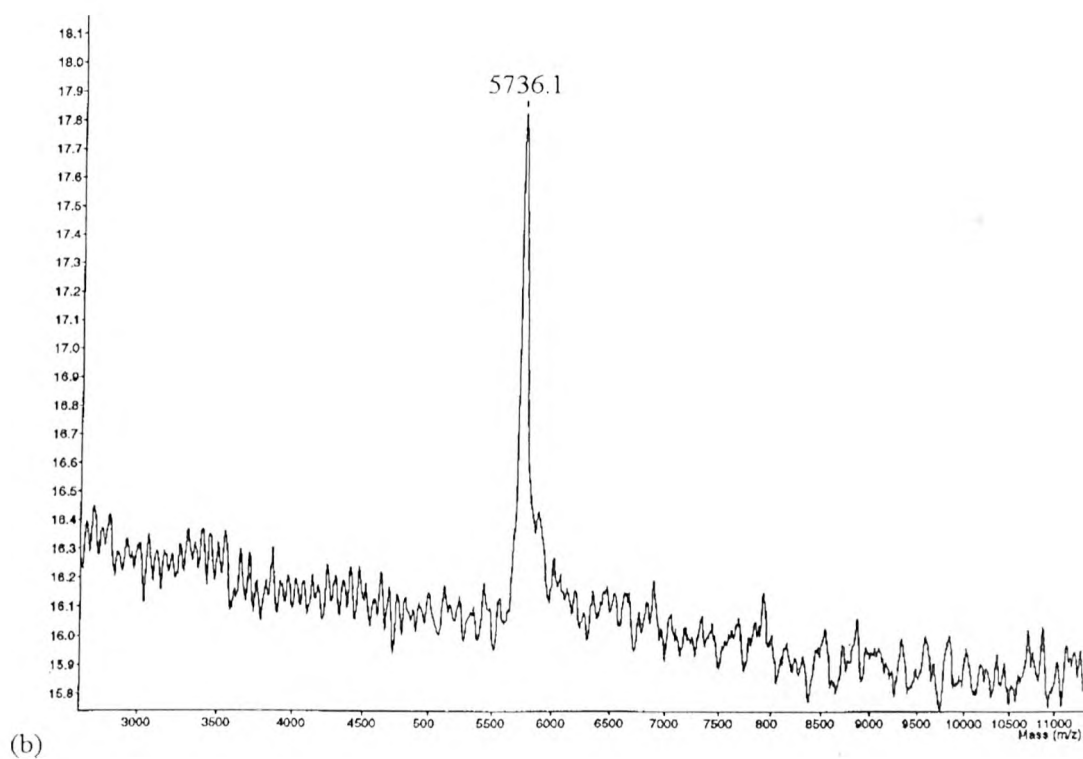
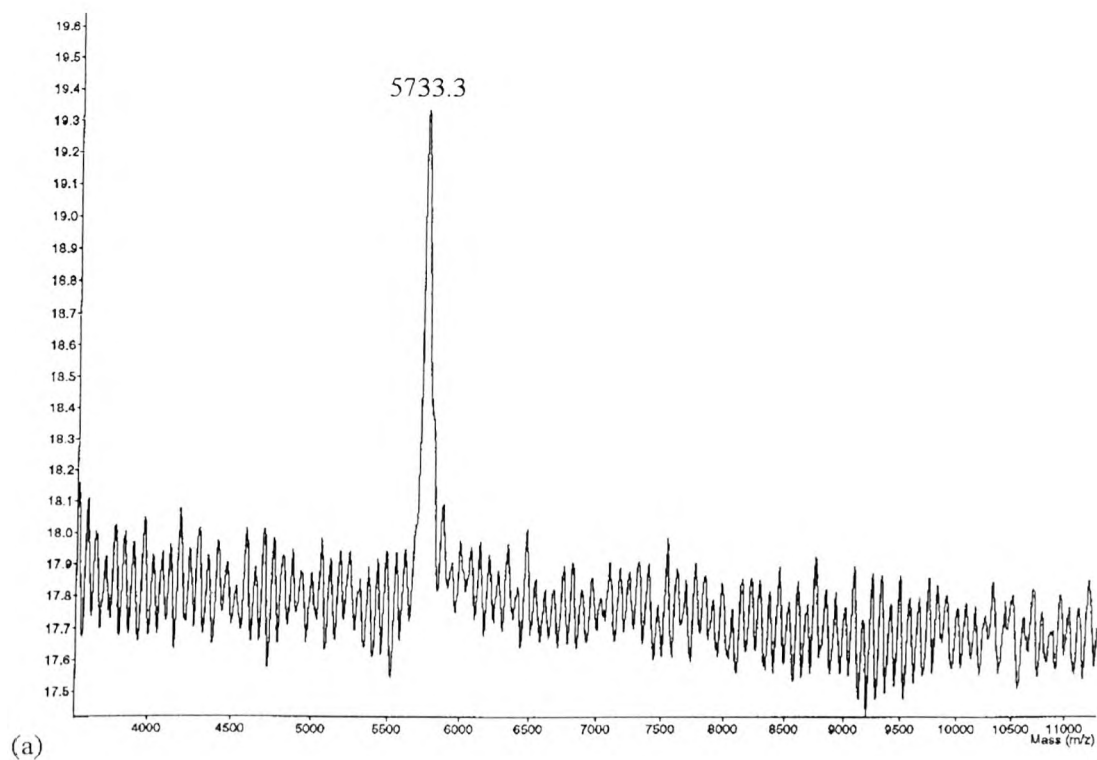


Figure 4.10. Above (a): spectrum obtained for insulin in HAP
below (b): spectrum of the analysis of insulin/ Eu^{3+} in HAP.

Lanthanide complexes of the oligos 12mer dA₆T₆ and poly dT used in the previous experiments were analysed a second time in presence of insulin in an attempt to improve the accuracy of their mass determination using MALDI.

Figure 4.11 shows a typical MALDI spectrum of the 12 mer 3'AAAAAATTTTTT5' using insulin as the internal standard for calibration of the software. The peak at 5733.4 daltons was due to insulin and the peak at 3674.9 daltons was due to the oligonucleotide. The theoretical value for the oligonucleotide is 3692.4 g/mol, giving an accuracy of 99.36%. The accuracy is slightly improved compared to the previous experiment performed without the internal standard (99.23%). It is however still low compared to other reported values (Fitzerald and Smith 1995).

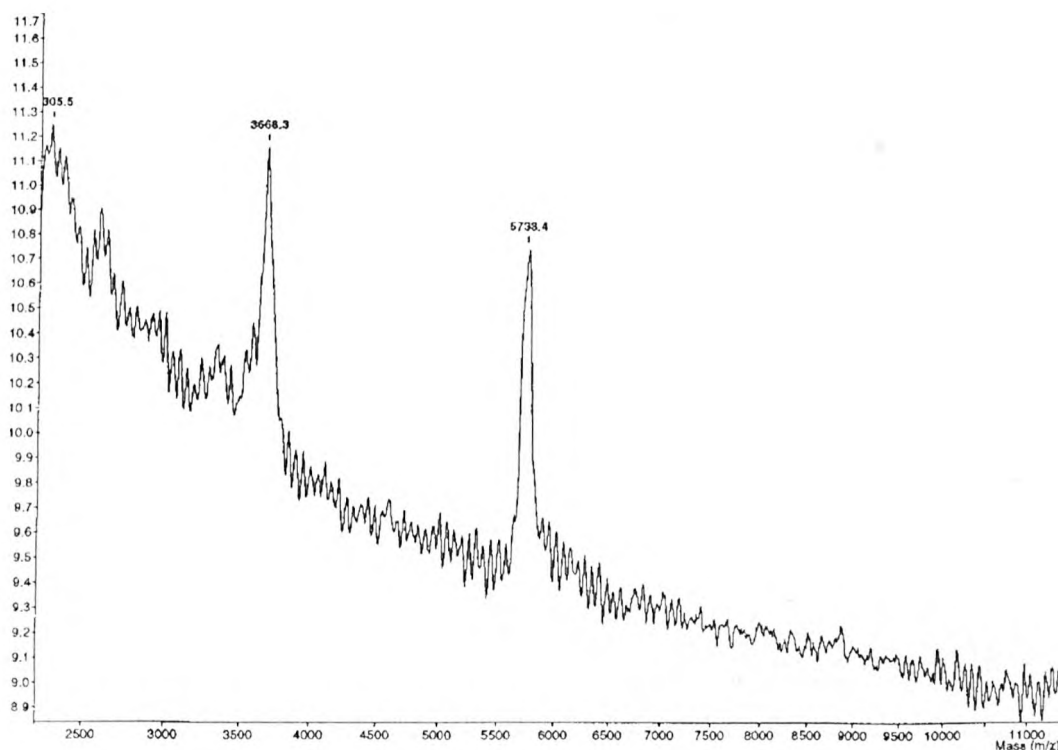


Figure 4.11. Spectrum of insulin and AT 12 mer in Hydroxyacetophenone (-5 shots, laser aim 4, laser power 95%)

The addition of EuCl_3 to the oligonucleotide was again observed to shift the molecular weight of the sample. A range of oligonucleotide solutions with increasing metal ion concentration was prepared and analysed on the MALDI. Breakdown of the oligo was observed at 90 nmols of Eu^{3+} . A sample of slightly lower metal ion concentration (60nmol) was used in a reproducibility study where the results of 10 consecutive identical measurements were compiled. From this data, the standard deviation was calculated, as well as the average molecular weight difference between peaks. This difference was assumed to be due to the presence of the Eu^{3+} ions and was used to calculate the accuracy of Eu^{3+} identification by comparison with the theoretical value. A typical spectrum obtained from that sample is shown figure 4.12. Table 4.5 shows the experimental data and calculated values of standard deviation, molecular weight shift and %determination accuracy.

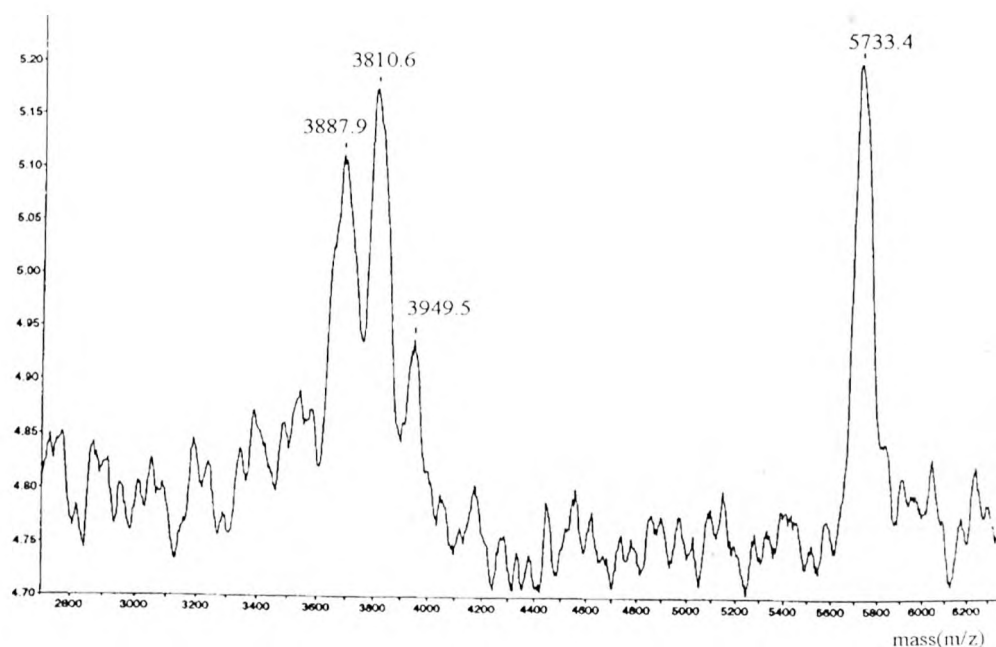


Figure 4.12. Spectrum of the 12 mer in the presence of Eu^{3+} (350pmol DNA were mixed with 60nmol EuCl_3 and 1 μ l insulin)

laser aim	peaks /m/z			
4	3692.4	3827.7	3965.7	4102.2
4	3692.4	3824.9	3958.5	4098.7
4	3692.4	3829	3963.9	4103.4
4	3692.4	3828.5	3963.3	4109.1
4	3692.4	3820.9	3958.4	4091.3
3	3692.4	3830	3965.5	
2	3692.4	3829.1	3988.7	4104.6
2	3692.4	3824.2	3968.9	4118.5
2	3692.4	3821.3	3954.9	4083.7
1	3692.4	3815.7	3954.4	4099.1
average	3692.4	3825.13	3964.22	4101.1
standard deviation	0	4.65261	9.86484	9.9625
molecular weight shift		123.3	138.7	144.7
accuracy of Eu^{3+} identification (%)		81.14	91.27	95.22

Table 4.5. Reproducibility study, using 12 mer oligonucleotide in presence of Eu^{3+}

It was found that the accuracy for the identification of Eu^{3+} values were low in this set of experiments (between 81.14% and 95.22%). However, when using results from laser aim 4 only, the standard deviation values were lower than when using all positions on the MALDI steel targets. This result highlighted a potential problem of homogeneity of the samples. The results for laser aim 4 are summarised in table 4.6.

	peaks/m/z			
average value of peak	3692.4	3826.2	3961.96	4100.94
std deviation	0	3.36006	3.32385	6.56071
molecular weight shift	133.8	135.76	138.98	
accuracy of identification of Eu^{3+} (%)	88.049	89.339	91.458	

Table 4.6: Reproducibility study using average values of peaks obtained on laser aim 4 only

A maximum of 3 ions per chain was observed for oligonucleotide 3'AAAAAATTTTTT 5'. It was not possible to use insulin with the oligonucleotide polydT₂₀ because strong signal suppression effects were observed. Insulin B chain was thus chosen as alternative internal standard for the analysis of the 20 mer. When analysed by MALDI MS in the same manner as insulin, the protein was unaffected by the presence of Eu³⁺. The mass determination for the 20 mer using MALDI with insulin B chain as the internal standard was performed. Figure 4.13 shows a typical MALDI spectrum. The peak at 3495.9 daltons is that due to insulin B chain and the peak at 6038.6 daltons is that due to the oligonucleotide. Its theoretical value is 6064 g/mol, giving an accuracy of 99.58%. This value is very similar to the one obtained when analysing without internal standard. A number of samples containing the 20 mer poly dT oligo and increasing metal ion (Eu³⁺) concentration was prepared and analysed on the MALDI. The sample giving the highest molecular shift was used for the calculation of the accuracy of Eu³⁺ identification. This sample is shown in Figure 4.14.

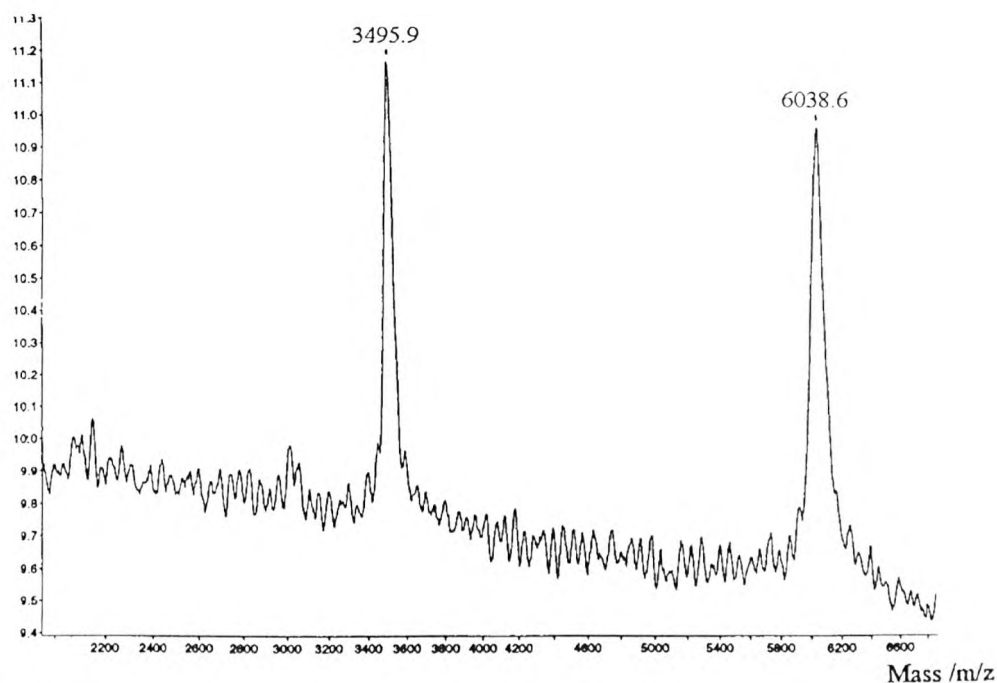


Figure 4.13. Spectrum of insulin chain B and 20 mer polyT in Hydroxyacetophenone

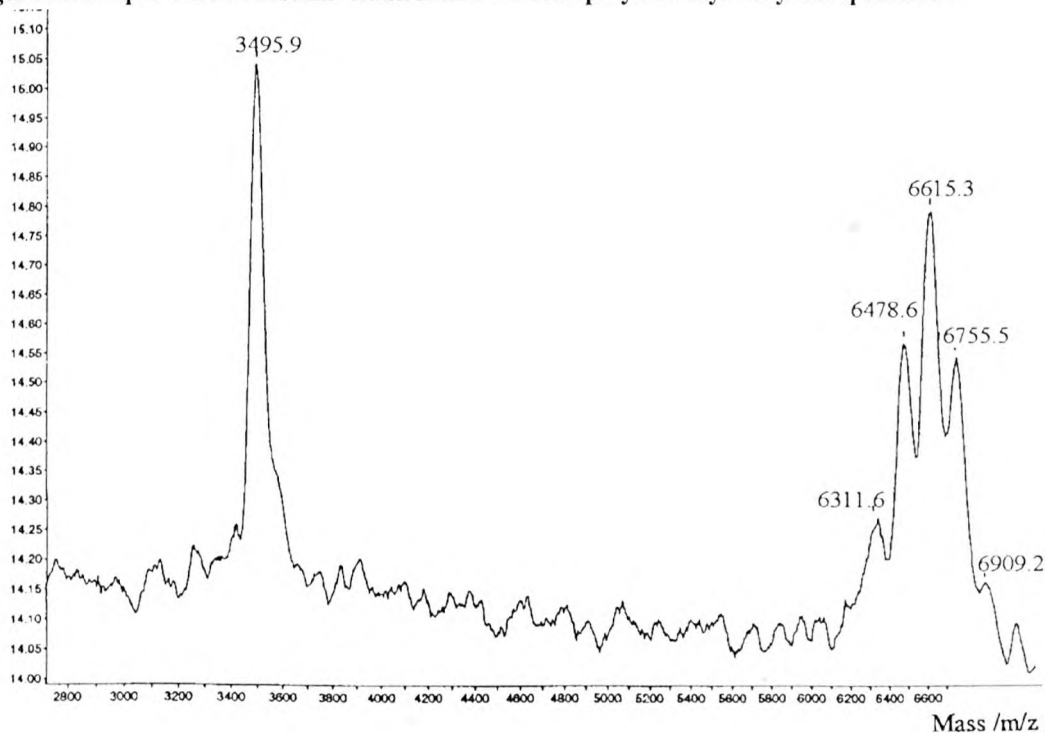


Figure 4. 14. Spectrum of insulin B chain and 20 mer polyT in Hydroxyacetophenone

In this set of experiments, the Eu^{3+} ions were identified with 91.06% to 95.95% accuracy. It can be concluded that using insulin and insulin chain B as internal

standards in the study of oligonucleotide/lanthanide ions complexes was inconclusive, in terms of improving the accuracy of the measurements.

4.4. Discussion and conclusions

The stoichiometry for the interaction with Sm^{3+} , Yt^{3+} , Eu^{3+} , Er^{3+} and Tb^{3+} was determined on 20 mer polydT oligonucleotide and 12 mer AT self complementary oligonucleotide. This was carried out using MALDI MS, which proved to be a sensitive, reliable and rapid method. MALDI allows the detection of the presence of any metal ions in a given oligonucleotide sample, and also the monitoring of the degradation of the DNA when saturation of the chain has occurred.

The study of the interaction of lanthanide ions with DNA using MALDI-MS was possible using A and T containing oligonucleotides and only the single stranded form was observable. An alternative analytical tool would have to be used to study this aspect of the interaction. Electronic ionisation mass spectrometry is a good candidate, as it allows the analysis of double stranded DNA as well as the study of non covalent interactions (Bayer *et al* 1994). It was found that for a 20 mer poly dT oligo, a maximum of 6 Eu^{3+} , 8 Sm^{3+} , 5 Yb^{3+} or 8 Er^{3+} ions could bind to each molecule without causing its breakdown. For the 12 mer self complementary dA_6T_6 , it was possible to bind a maximum of 3 ions for Tb^{3+} , Eu^{3+} , Sm^{3+} and Yb^{3+} were bound per molecule and 2 ions for Er^{3+} .

A limitation of the MALDI technique is its weakness when analyzing oligonucleotides containing C and G bases (Schneider *et al* 1994). This currently limits our understanding of lanthanide/DNA interaction to AT oligonucleotides. The presence of C and G bases in nucleic acids is not a problem when the $\text{C}+\text{G}/\text{A}+\text{T}$ is roughly equal to 1. A mixed base DNA /lanthanide adduct could therefore be analyzed, but this would complicate considerably the interpretation of the results.

This chapter ends the series of experiments aiming at understanding better the interaction of lanthanide ions with nucleic acids.

It was shown that lanthanide ions bind to DNA via their phosphate backbone primarily, as shown by ^{31}P NMR in chapter 3. The interpretation of the T_m studies with Tb^{3+} led to the conclusion that the ion was also interfering with the bases, although this could not be confirmed using proton NMR.

It was also found, using MALDI mass spectrometry, that the 5 ions studied bound with metal ion/ base ratios and that Eu^{3+} and Yb^{3+} showed stronger phosphodiester cleavage reactivity than Tb^{3+} , Sm^{3+} and Er^{3+} .

These observations could be exploited to design a new labeling strategy for the detection of surface bound oligonucleotide hybrids. An outline of this strategy is presented in chapter 7.

CHAPTER 5: THE APPLICATION OF SURFACE SECOND HARMONIC GENERATION TO THE DETECTION OF NUCLEIC ACIDS ON SURFACES

5.1. Introduction

Chapters 2, 3 and 4 of this thesis concerned mainly new labeling strategies for DNA analysis. As previously mentioned in chapter 1, although labelling is a common and well established procedure to achieve satisfactory sensitivity, there would be great advantage in using alternative detection methods that require no labeling (section 1.6.2. page 45). While surface plasmon resonance is dependent on the manufacture of highly homogenous metal coated surfaces, surface second harmonic generation offers the advantage of enabling the study of monolayers on any surface. SSHG has been described as a suitable detection method for biological assays and has already been shown to produce extremely sensitive results for immunoassays on plastic surfaces (Yang *et al* 1998). In this chapter it is proposed to study the second harmonic generation properties of DNA on surfaces that are commonly used for assays, such as glass and plastic. It is proposed to prepare coated surfaces of synthetic nucleic acids on glass and plastic surfaces and to measure the dependence of the second harmonic signal with the power of the laser and with the concentration of the oligonucleotide on the surface. The influence of the size of the oligonucleotide covering the studied surface on the second harmonic signal will be assessed, as will other parameters affecting the design of a DNA hybridisation protocol such as salt concentration. The results of these experiments will help assess the feasibility of designing a system using second harmonic to detect DNA hybrids on a surface.

5.2. Experimental set up

5.2.1. SSHG system

The first SSHG experimental set-up used to investigate the second harmonic signal properties on oligo coated surfaces in this work (as shown in figure 5.1) consisted of a Q-switched Nd:YAG laser (Spectron LS400), which provides an output at 1064 nm, (FWHM = 5 ns). In the experiments, the pulse energy was typically less than 1mJ. The output beam from the laser was firstly passed through a long pass colour glass filter (a_1) in order to remove any flash lamp light leaking from the cavity of the laser. It was then passed through a 1064nm interference filter (b, 10nm FWHM) a crystal polariser (c), an aperture (d) and finally a second colour glass filter (a_2). This final filter was necessary to remove any potential second harmonic signal generated from the intermediate surfaces, especially the aperture (d). The fundamental laser beam incident at a variable angle from the normal of the sample surface (e), resulted in second harmonic signals ($\lambda = 532$ nm) being generated at the surface. The SSHG generated was filtered using a monochromator followed by a 532nm interference filter (f, FWHM 10nm) to reject fundamental laser light and any fluorescence. The surface second-harmonic signals were detected using a photomultiplier tube (PMT) positioned at the output slit of the monochromator. The output from the PMT (Thorn EMI 9524A) was subsequently digitised by a digital storage oscilloscope (Tektronix TDS 620). The data obtained was transferred to a computer for data recording and analysis.

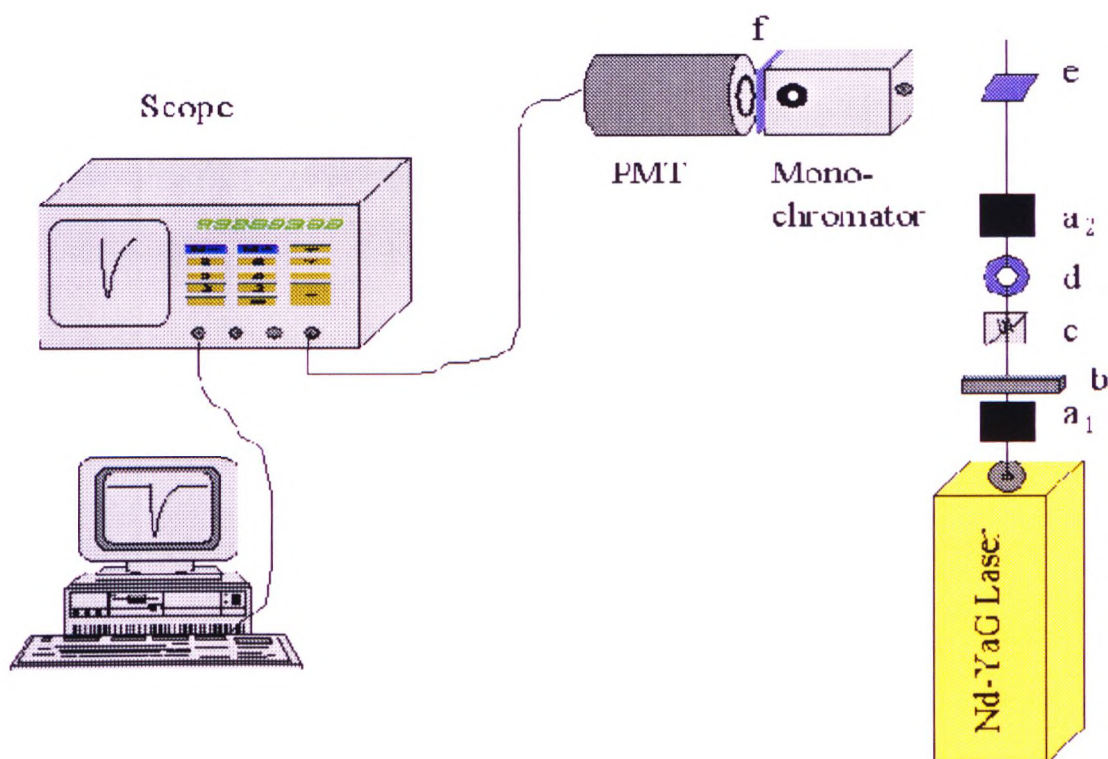


Figure 5.1. Diagram of the experimental set-up for surface second-harmonic generation studies of DNA. [(a) filter to cut the visible light, (b) half wave, (c) polarizer, (d) iris, (e) sample, (f) filter to cut the 1064 nm].

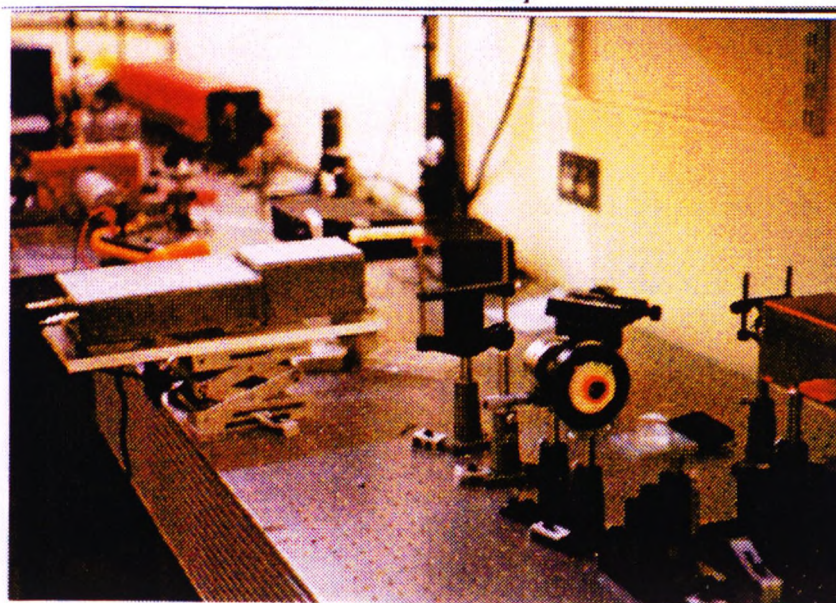


figure 5.2. Photograph of the SSHG system no 1.

The typical PMT output collected by the PMT at each pulse was very noisy. The signal was therefore smoothed by averaging typically 15 laser shots as shown in figure 5.3.

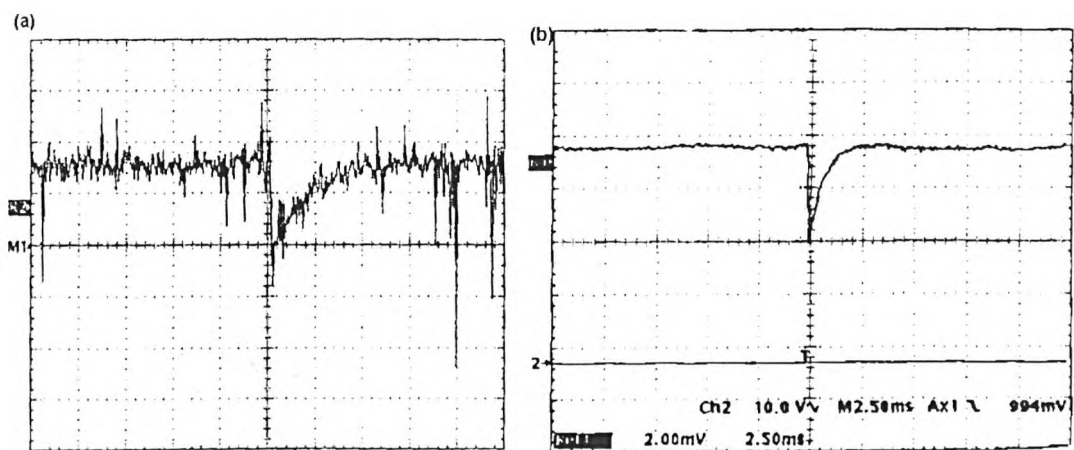


figure 5.3. Typical PMT output on the second harmonic system. (a). Single pulse. (b) average of 15 pulses.

5.2.2. Sample preparation

Because they are the material typically used in routine bioassays, glass and plastic were used as the solid support of the DNA samples in this set of experiments. As previously discussed, second harmonic generation signal is strongly affected by the nature of monolayers of molecules on surfaces. It is therefore desirable to create monolayers of nucleic acids on the surface of choice.

Several methods to produce DNA coated slides were tested. To assess their validity, a fluorescent oligonucleotide was used to coat the surfaces and the resulting surfaces were monitored with a scanning fluorescent microscope, as described below. A 488nm argon ion laser was used as a light source to excite the fluorescent molecules on the surface. It was spectrally filtered using a 488 nm interference filter (10 nm FWHM) and chopped using a rotating wheel. The beam was then directed onto a 50% beam splitter reflecting it at 90° through the lens onto the sample. The resulting fluorescence was collected by the microscope lens and passed through a spectral band pass filter centred on 520nm (20 nm FWHM) suitable for the detection of fluorescein and detected using a photomultiplier tube, whose output was connected to

a lock-in amplifier that took a frequency reference from the optical chopper. The sample was placed on a translation stage that could be used to move the sample under the fluorescent microscope using computer driven stepper motors. This system allowed 2D images of the fluorescence signal on this sample to be produced. The scanning fluorescence microscope is schematically represented in figure 5.5.

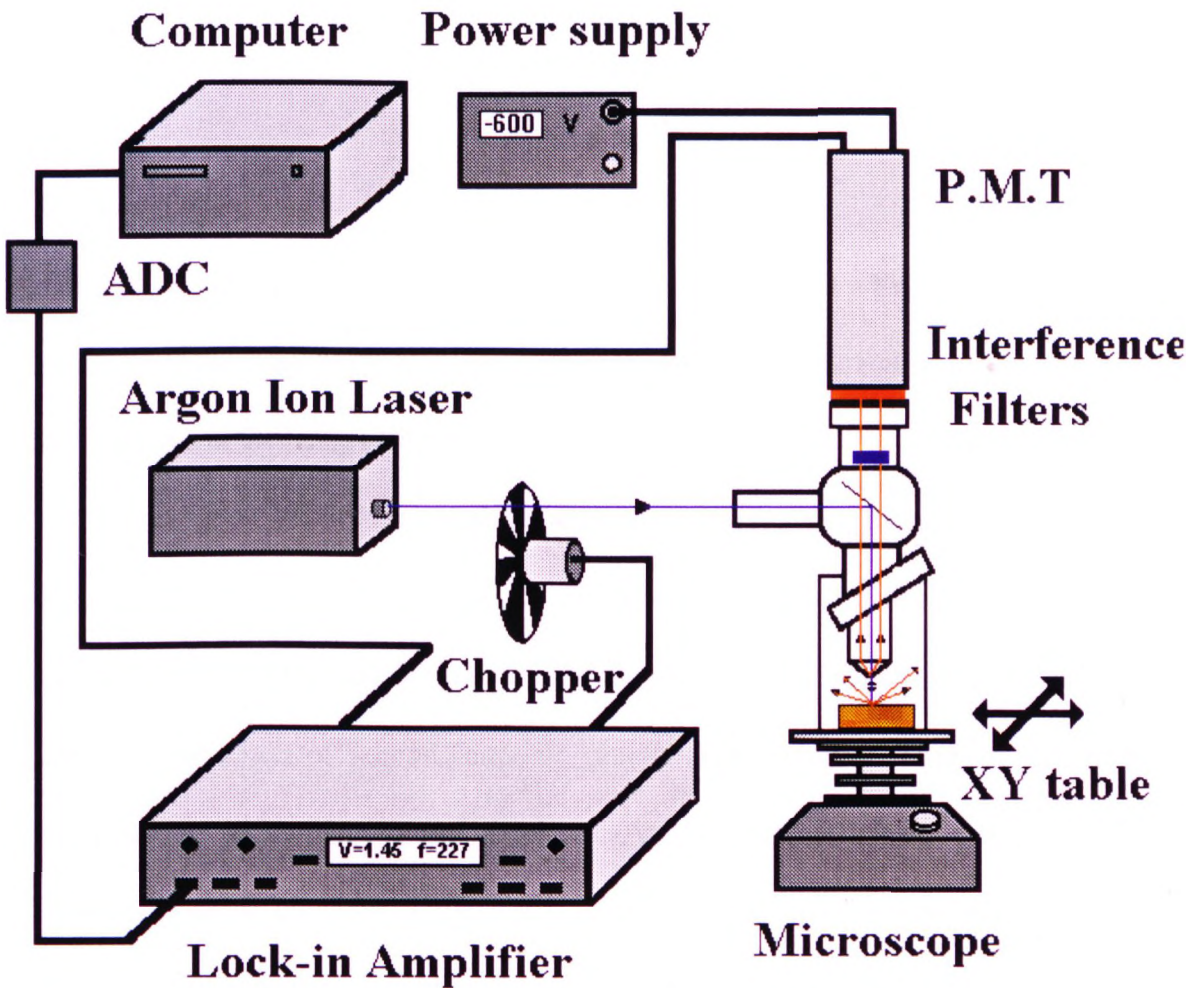


Figure 5.4. Schematic representation of the scanning fluorescence microscope used to monitor the coating of surfaces.

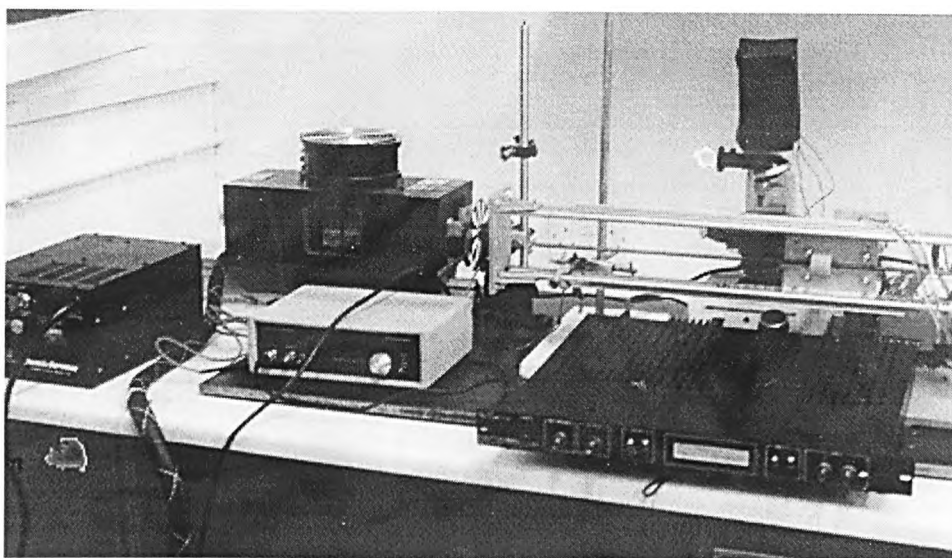


Figure 5.5. Photograph of the scanning fluorescence microscope used to monitor the coating of surfaces.

Glass surfaces:

Silanisation was used to coat glass slides, in order to create a hydrophobic surface, suitable for the adsorption of nucleic acids (hydrophobic interactions occur between the surface and the bases of the DNA).

1ml methacryloxypropyltrimethosilane (Sigma M6514) was diluted immediately prior to use in 200 ml ethanol. To this 6 ml of 1:10 glacial acetic acid :water was added. The glass (microscopy covering slips) was exposed for 1 hour, rinsed and dried. similar levels of Second harmonic generation signal were observed on treated and untreated slides (3mV signal, laser: 1050V, PMT: 1200V). This means that the silane coating of the slide is not likely to be a major source of interference when detecting DNA bound to silanised slides. A treated slide was dipped into diluted fluorescent oligonucleotide (1mM) and scanned using the fluorescence scanning system described above. An example of slides obtained with this method can be seen on figure 5.6.

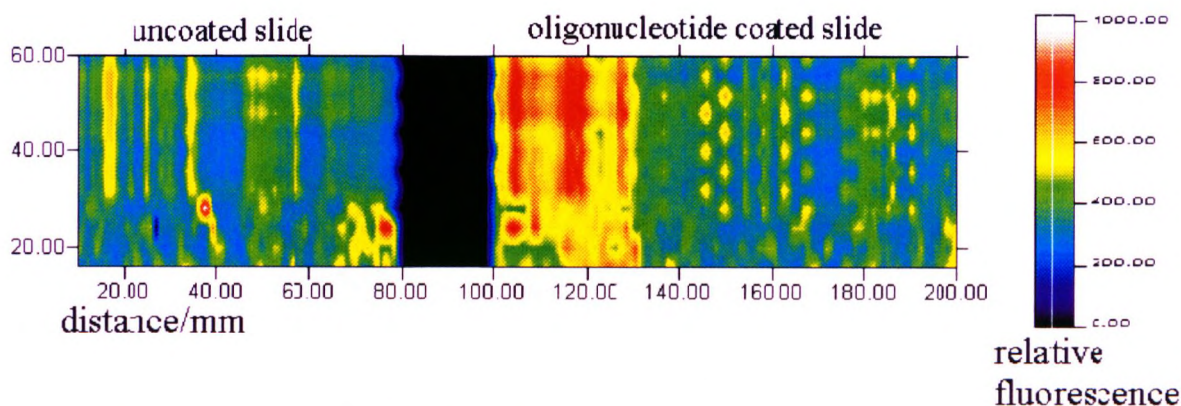


figure 5.6. Fluorescence scan of silanised slides. The slide on the left is not coated with the oligo. The slide on the right was silanised and subsequently dipped into a 1mM solution of fluorescein oligonucleotide. The dark area represents the gap between the two slides.

The overall fluorescent signal is higher on the coated slide (right slide, showing red areas, representative of a stronger fluorescence signal) than on the uncoated slide (left slide). However, the homogeneity of the coating is poor. Only a small portion of the surface is actually affected by the coating procedure. This could not be considered as a suitable technique to produce uniformly coated DNA surfaces.

Plastic surfaces:

Simple deposition of an aliquot of 200 μ l of fluorescent oligonucleotide (1mM) solutions into polystyrene plastic wells (2.5 cm diameter) and subsequent drying at 45°C in a ventilated oven was used to coat the plastic surfaces. The resulting surface was again scanned using the fluorescence scanner the 2D fluorescent map of two wells is shown on figure 5.7.

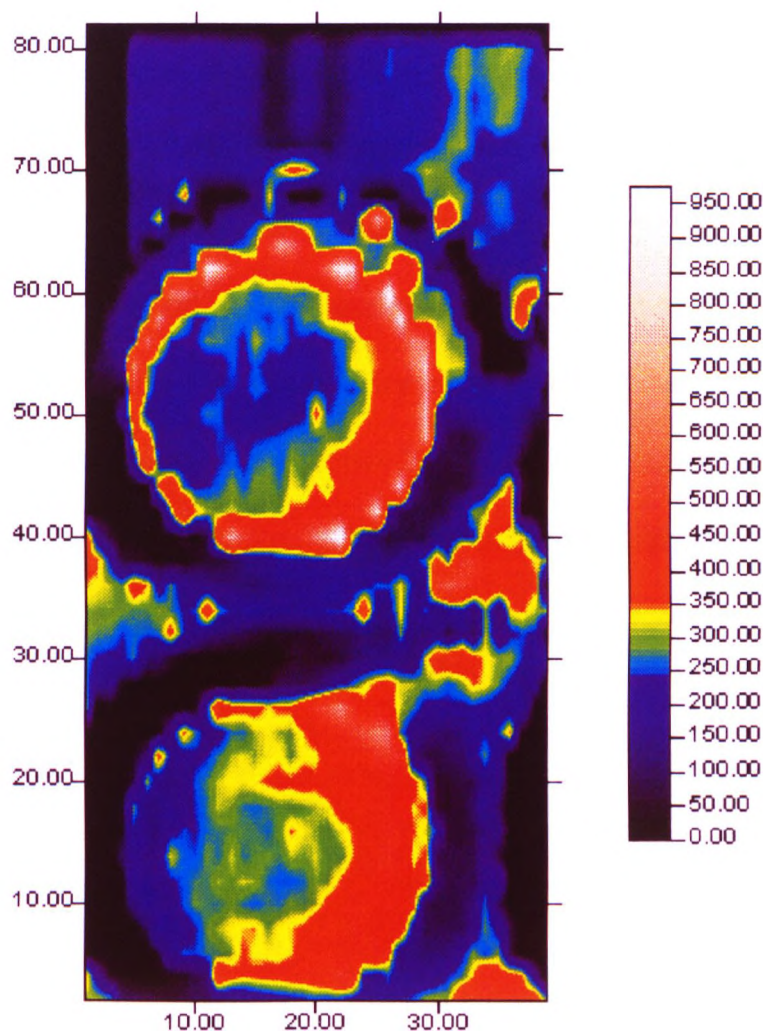


Figure 5.7. Fluorescent scan of plastic wells containing fluorescein labelled oligonucleotide

One can observe that the DNA molecules have been successfully deposited during the drying process. However, they are mainly in the external portion of the well. This type of drying effect has recently been studied in great detail and the cause of the ring formation has been identified to be capillary flows (Deegan *et al* 1997). Despite the apparent lack of homogeneity of the coating of glass and polystyrene as discussed above, it was decided to use the method described above because it was found by others (Nikiforov and Rogers 1995) that when evaluating different approaches to oligonucleotide immobilisation for hybridisation assays in 96 well polystyrene plates,

only the passive immobilisation in presence of salts met their performance criteria for their DNA genotyping tests.

It is important to create a DNA surface that will be measurable using SSHG, as well as a system where the DNA/solid surface interaction permit hybridisation in a optimum way. Therefore, although the quality of the DNA coating obtained using the passive drying methods described above may not give the optimum second harmonic signal output, the surfaces studied represent “real life” samples, typical of those that biologists would be able to prepare without any major investment in equipment to produce monolayers.

5.3.Results.

5.3.1. Variation of second harmonic signal with laser power

The dependence of the surface second harmonic (SSH) signal with incident laser power for surface layers of the 12-mer AAAAAATTTTTT oligonucleotide labelled with fluorescein deposited on glass slides was examined in a series of experiments. The fluorescein labelled oligonucleotide was initially employed to allow verification of the surface coating using a fluorescence microscope system (as shown in paragraph 5.2). Figure 5.8(a) shows the measured variation in SSH signal with laser pulse energy. The SSH is observed to vary nonlinearly with the laser energy. As can be seen from figure 5.8.(b) the SSH is, as expected for a second order process, linear with the square of the laser power. It is also interesting to note that over the laser pulse energy range used, no laser induced damage of the DNA was observed.

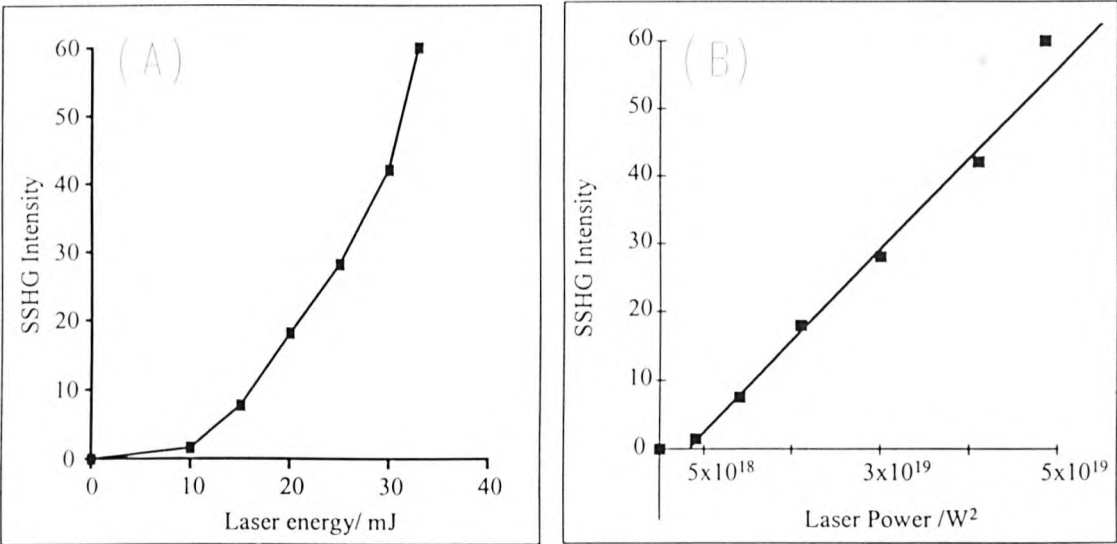


Figure 5.8. The surface second harmonic generated from a 12 mer oligonucleotide coated glass surface (a) at different incident laser energies and (b) plotted against the square of the laser power.

5.3.2. Variation of second harmonic signal with surface DNA density

The second harmonic signal given by a surface is affected by any changes in the structure of the molecules building that surface. As explained in the introduction (chapter 1 page 53), the SSHG signal should be concentration dependent and this experiment was aimed at verifying this.

A 12 mer AT oligonucleotide was diluted in 1M NaCl solution and these dilutions were deposited onto glass cover slips as 50 μ l aliquots. These slides were dried in an oven at 90°C and were then placed in the SSH system where the signal intensity for a fixed laser beam incident angle of 45° was recorded. The diameter of the resulting dried spots was found to be 5 mm. This was used to calculate the final DNA density on the cover slip which ranged from 3.74332×10^{-8} to 1.87166×10^{-6} moles/mm². The surface second harmonic results were plotted as shown in figure 5.9. as can be seen on the graph, the SSH signal was observed to decrease with the surface density of oligonucleotide.

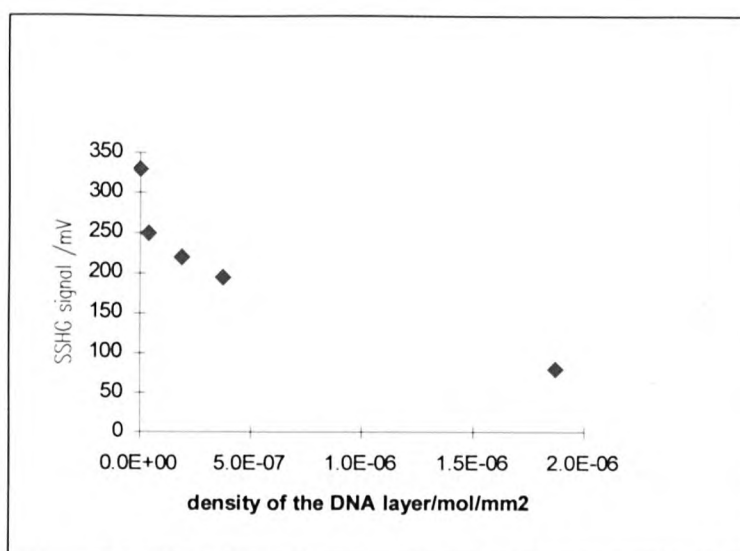


figure 5.9. SSHG signal of glass cover slips covered with DNA layers of different densities (data point at density=0 corresponds to the SSHG signal of a control surface without DNA)

A similar experiment consisted in preparing a multiwell plate by depositing a 50 μ l drop of the same oligonucleotide solution and covering it with 200 μ l distilled water to ensure even coverage of the whole well. The plate was then incubated at 50°C until dry.

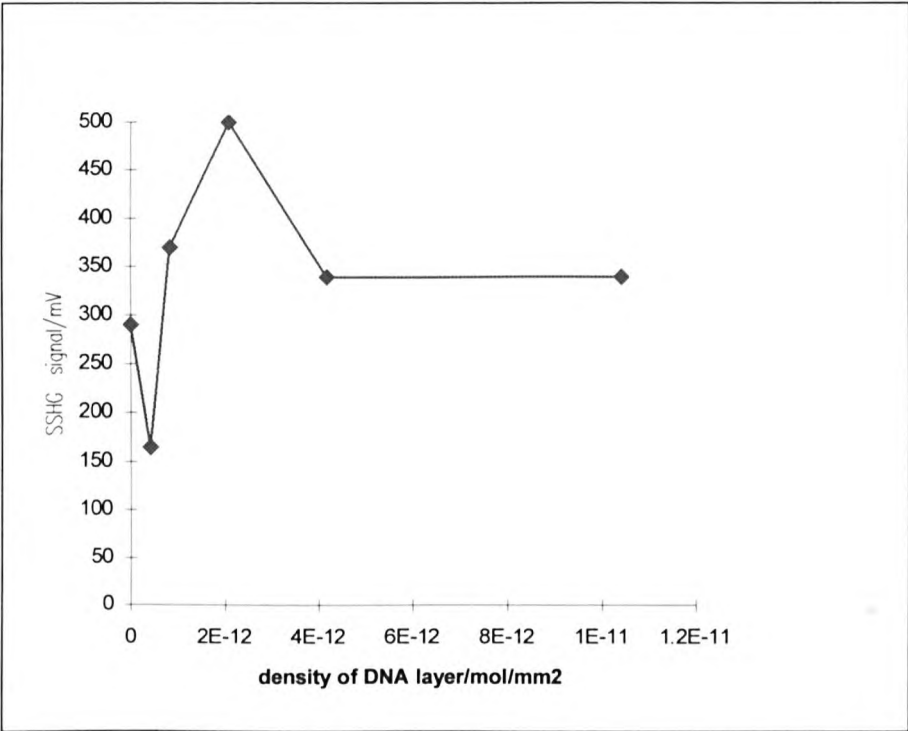


figure 5.10. SSHG signal of multiwell plate plastic wells covered with DNA layers of different densities

In this set of data, the second harmonic signal goes up and down in a manner that seems unrelated to the changes of DNA density at the surface. The following explanation may be possible: the DNA densities used in this experiment may have been too low to be detected by the present second harmonic system. It means that at such low concentrations of DNA, variations of the second harmonic signal being generated in a given detection system are extremely small. If this detection system is prone to experimental error, such as noise or laser intensity variations, then small

differences in the samples might be difficult to detect with this system, if possible at all.

5.3.3. Variation of second harmonic signal with the size of the oligonucleotide

The variation of the SSHG signal with the size of several oligonucleotides deposited at equal densities on a surface was investigated. Because $\chi^{(2)}$ is characteristic for the material coated on the probed surface, it is expected that oligos of different length will generate a different signal. Furthermore, it has been shown by others (Large *et al* 1996) that the length of the nucleic acids used affects their polarisability and therefore the way they arrange together on a surface coated with them. In this experiment, 3 oligonucleotides were used, containing the following sequence: 3'(AT)_n5', where n=6, 15 and 30, giving a total size of 12, 30 and 60 mer self complementary oligonucleotides. Spots of 5×10^{-7} mol/mm² of these oligonucleotides in 1M NaCl were prepared on glass cover slips. The resulting samples were therefore within the density range of figure 5.9, where second harmonic signal is correlated to DNA density. Therefore one is confident that the surface measurements are related to the DNA deposited and not to the glass surface.

The SSHG signal was measured using a 0.07W peak pulse power, 2mm diameter beam and 1000V PMT. The results of these measurements are summarised in figure 5.11.

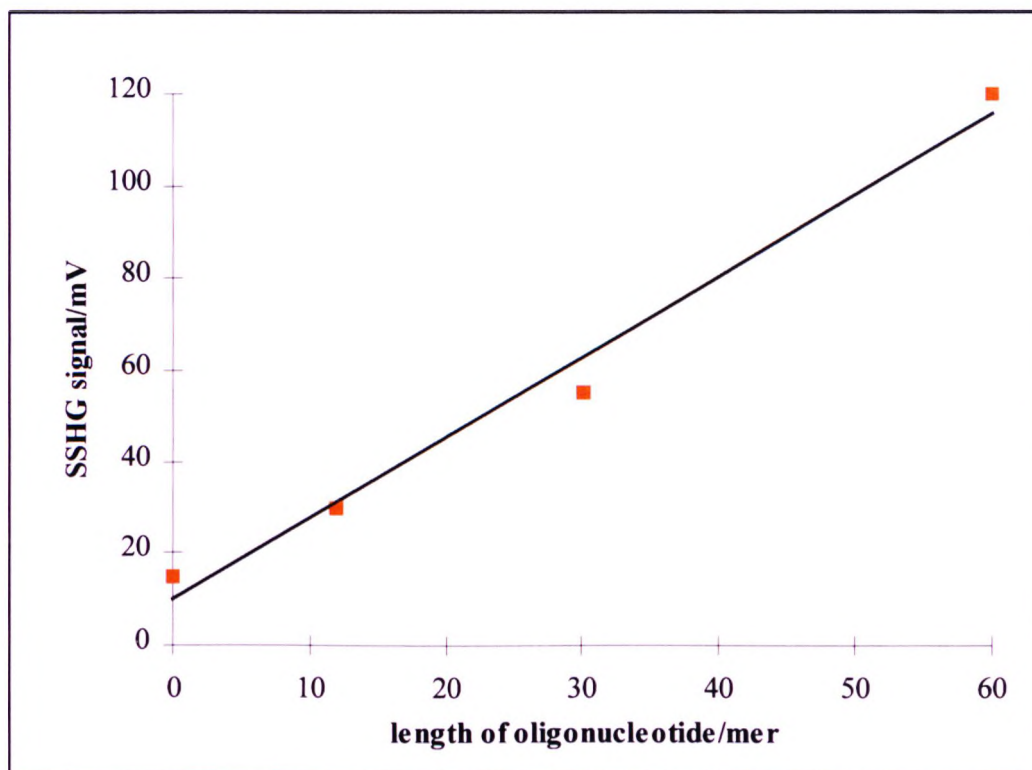


figure 5.11. SSHG signal for different sizes of AT containing oligonucleotides

The graph clearly shows that the size of the oligonucleotide present on the surface influences the intensity of the SH signal for AT containing sequences of oligonucleotides. It also shows that up to a length of 60 nucleotides, the SH signal increases linearly with the size of the oligonucleotide. This result shows that at equal surface densities, oligos of different sizes possess very different second harmonic properties, despite their composition being very similar (the three oligos studied here were composed of A and T only).

5.3.4. Effect of increased salt concentration on the SSHG signal

The effect of increasing salt concentration in the DNA solutions prepared was investigated. This is an important issue for several reasons: firstly, the size of the spot is greatly affected by the amount of salt present in the sample. Secondly, it is

essential to assess the effect of buffers that are required to perform the hybridisation, salt being a major component of these buffers, as it favours formation of double strands between complementary sequences.

A series of samples of 50µl of $1.47 \cdot 10^{-5}$ M 12 mer AT oligonucleotides were prepared in 0.01M NaCl and were deposited on glass coverslips.

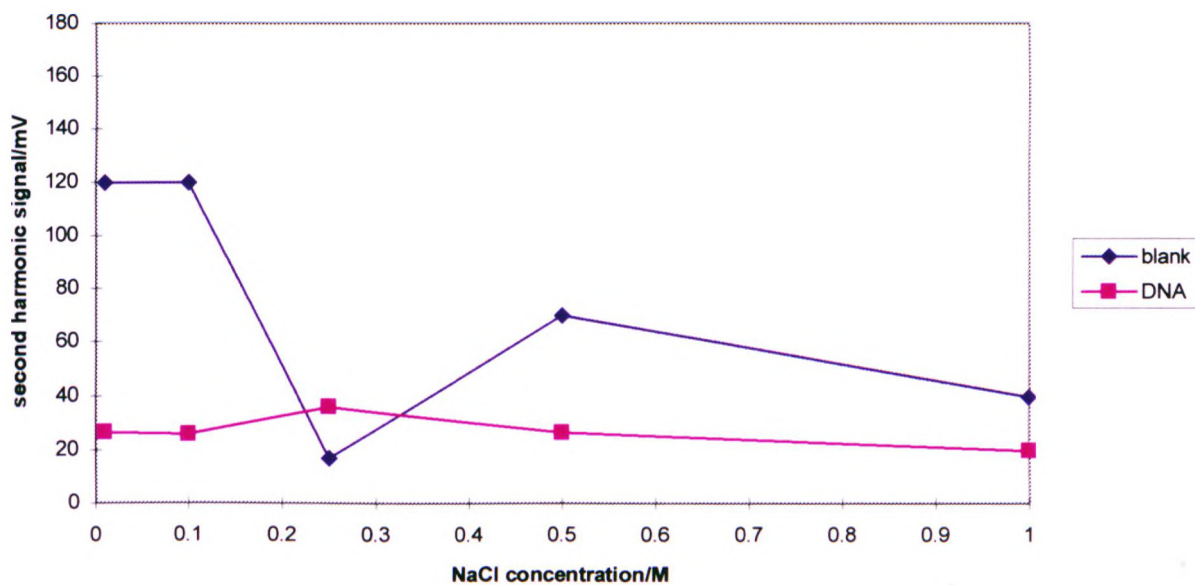


Figure 5.12. Influence of salt concentration on SSHG on a DNA sample of a fixed concentration.

It is known that drying salt solutions will form crystals, which themselves emit second harmonic signal. However, figure 5.12 shows that there is little effect on the surface second harmonic signal for different salt concentrations in a DNA sample. From 0 to 1 M NaCl, there is little or no variation in SH signal. On the contrary, blank samples containing no DNA show large variations of signal with varied salt concentrations. This might mean that the presence of DNA affects the way salt crystals form.

5.3.5. Variation of SSHG signal with the incident angle of the laser

The variation in the SSH with incident laser beam angle was investigated by mounting glass slides coated with oligonucleotides on a calibrated stage which allowed the sample to be rotated about a vertical axis, whilst ensuring that the laser beam was always incident on the same part of the sample. Two types of oligonucleotides were used: a 12 mer dA₆dT₆ and a 30 mer polydT. The results are shown in figure 5.13.

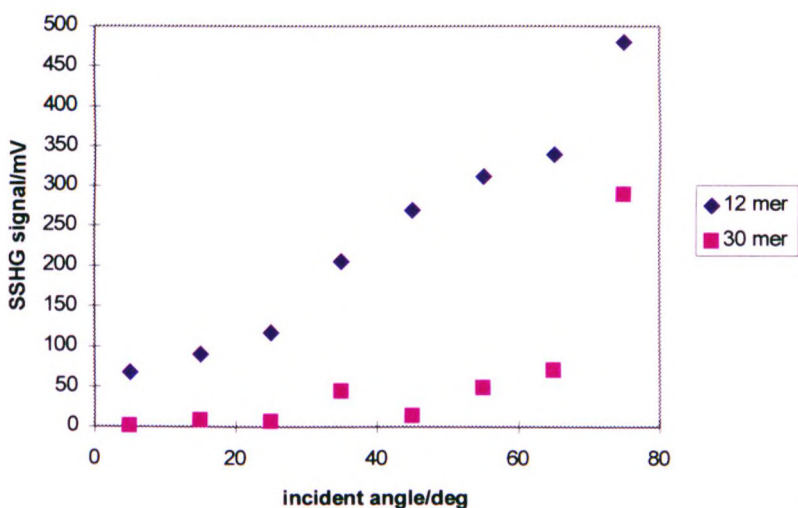


figure 5.13. Angle dependence of SSHG signal when using an incident laser beam

The measured SSH is observed to generally increase with increasing angle for both oligonucleotides. However, the patterns are very different for the 2 oligonucleotides, which could be accountable for their fundamentally different structures (one is single stranded and the other is double stranded). This result is important because it shows that the second harmonic detection method may be able to distinguish between single and double stranded samples, which is again, very useful when performing hybridisation assays, because the presence of single stranded DNA would be a negative result, whereas a double stranded DNA would be a positive result (ie the hybridisation has occurred). This result also shows that the second harmonic results

optimum sensitivity. Indeed, figure 5.13 shows that the signal is increased with angles between 60 and 80°.

5.3.6. Measurements using a detection system with reference

All experiments above were performed using the system described in figure 5.1. In the experiment described in section 5.3.2 where DNA at very low concentration was used (figure 5.10), no correlation between concentration and second harmonic signal could be detected. Strong background noise and poor reproducibility of measurements have been suspected to be the cause for this poor performance. It has been suggested that laser power fluctuations may have been the cause of these problems. In order to overcome the reproducibility and noise problems of the existing system, a reference arm was installed. This reference arm allowed to correct the output second harmonic signal by monitoring the laser output variations. The new system basically consisted of the same components as the one described above, with a reference arm added to it, used to correct the output signal when the intensity of the laser varied. This system is schematically represented in figure 5.14.

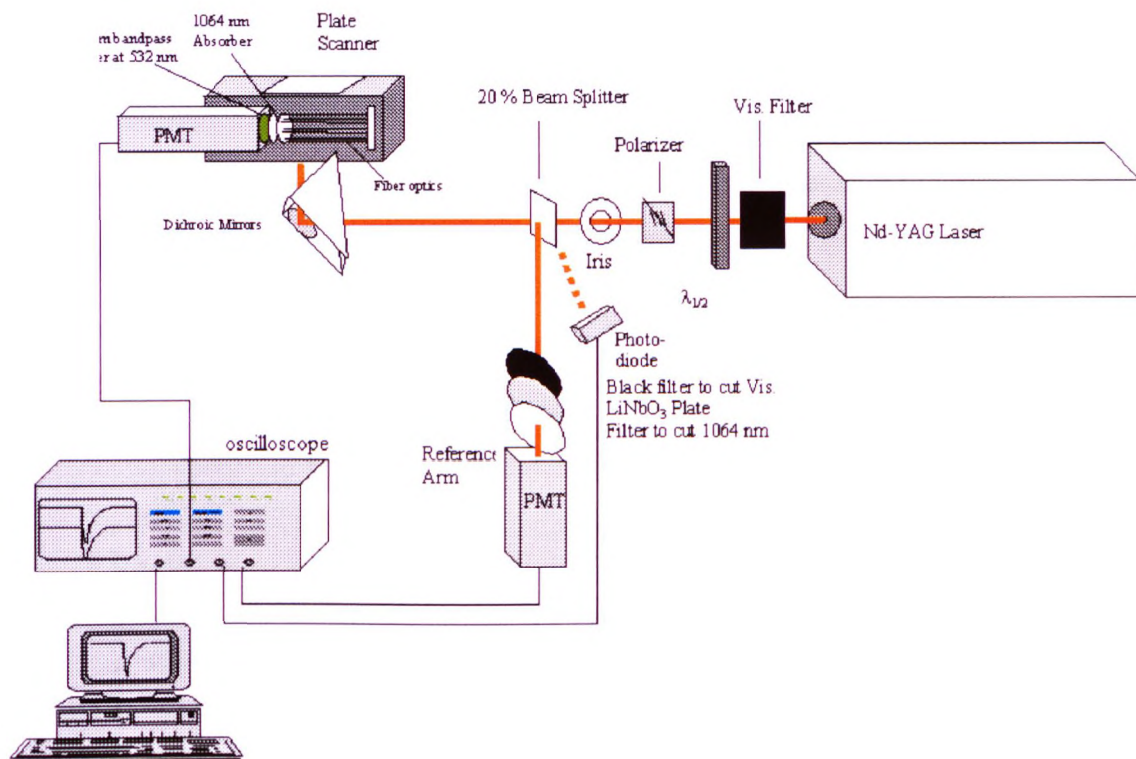


figure 5.14. Schematic representation of the surface second harmonic system with reference.

The reference arm represented on figure 5.14 comprised of a LiNbO₃ coated glass through which the laser beam passed and created a strong second harmonic signal. This was detected by a PMT and the signal was collected by the oscilloscope which used this reference signal to calculate the ratio of sample signal over reference signal. This ratio was then used as experimental values. This should allow to perform reproducible measurements by removing the error factor due to laser power fluctuation.

The effect of DNA density on surface second harmonic signal was again studied, this time over a large range going as low as 10^{-14} mol/mm² which is two orders of magnitude lower than the experiments of section 5.3.2, up to 10^{-9} mol/mm².

Three different oligos were used to coat the wells of a similar plate. The first one was a 5' end fluorescein labelled 5'AAAAAATTTTTT3' oligonucleotide. The other two were unlabelled polydAd₁₅T₁₅ and polydA₃₀dT₃₀. Dilutions of the 3 different oligos

were made, from 100pmol/ μ l to 1fmol/ μ l. 40 μ l of each dilution was placed in the wells of the plate, which was then placed in a ventilated oven at 45°C until total evaporation of the liquid had occurred. The bottom of the wells in the plate was then probed for second harmonic.

The signal obtained for the wells coated with the nucleic acids can be seen in figure 5.15.

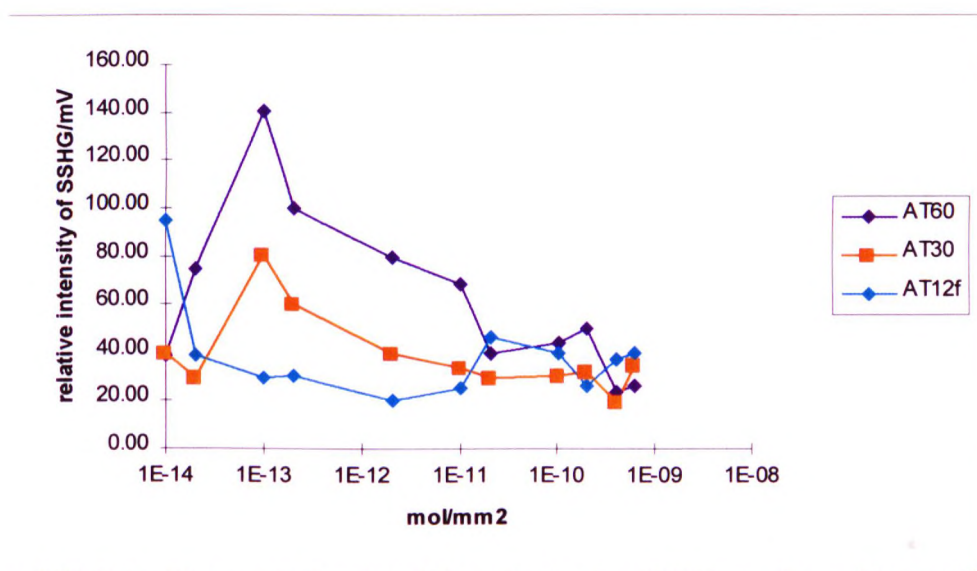


Figure 5.15. Second harmonic signal variation with density of DNA coating on Maxisorb™ wells.
Legend: AT12f: 12 mer 5' fluorescein labelled oligo. AT30: 30 mer dA₁₅dT₁₅. AT60: 60 mer dA₃₀dT₃₀.

The curves plotted on the graph of figure 5.15 for the oligos AT30 and AT60 possess common features: when the surface density is increased up to a certain point (10^{-13} mol/mm²), the signal increases. Then with further increases in surface concentration, the signal decreases slowly, as observed previously in section 5.3.2. These variations in signal could correspond to some important changes happening on the surface, thus affecting the second harmonic signal: between 10^{-14} and 10^{-13} mol/mm², the surface is only partially covered with DNA molecules, and the detection system is probing the plastic surface. At concentrations above 10^{-13} mols/mm², the surface is covered with a DNA monolayer and the plastic (the bulk

material) is not producing any contribution to the second harmonic signal. The density of the monolayer of DNA affects proportionally the $\chi^{(2)}$ value of the sample as described in chapter 1 (p 49), which results in this progressive decrease in signal.

The values obtained for the fluorescent oligo do not show any increase in second harmonic at low density, but the signal decreases steadily from 10^{-14} to 10^{-11} mol/mm² in a pattern similar to the other two oligos analysed here. Between 10^{-11} and 10^{-9} mol./mm², the values obtained for the three oligos go up and down in a way that appears random. This could be interpreted as being due to the surface being covered by multilayers of DNA.

This experiment shows that the sensitivity of the surface second harmonic system has been greatly improved over the previous one with the addition of a reference arm. One can say that surface densities as low as 10^{-13} mol/mm² can now be detected using the second harmonic system.

This set of data also confirms the previous observation that second harmonic signal increases with the size of an oligonucleotide (see section 5.3.3).

5.4. Discussion and conclusions

The second harmonic properties of surfaces coated with oligonucleotides were studied in this series of experiments. It was found that the signal was strongly dependent on the density of the DNA molecules deposited on the surface, and that the signal decreased when the density was increased. The sensitivity of the surface second harmonic generation system with reference arm allowed the detection of DNA densities as low as 10^{-13} mol/mm². It was also found that the size and the structure of the nucleic acids deposited affected the signal. This forms a set of data that validates some of the essential features that allow a detection technique to be used in a bioassay. Firstly, the concentration dependence of the oligonucleotide on the surface probed on the signal is of major importance, because a lot of bioassays require quantitative information. Secondly, the data set showing that the length of the oligonucleotide bound to the surface affects the second harmonic signal is of importance. This means that as well as being able to detect monolayers of oligos on a surface, the technique is capable of distinguishing between different samples of different structure but of same chemical composition.

CHAPTER 6: DISCUSSION AND CONCLUSIONS

6.1. New labelling methods for DNA sequencing

In chapter 2, the feasibility of using lanthanide chelates as labels for DNA sequencing was assessed. Two different chelates, BCPDA and DTAA-pAs were synthesised and complexed with several lanthanide ions, Eu^{3+} , Sm^{3+} , Yt^{3+} , Tb^{3+} and Er^{3+} . It was found that those two chelates were highly ion specific, because BCPDA was able to successfully form a fluorescent complex with only Eu^{3+} , and DTAA-pAs was forming fluorescent complexes only with Tb^{3+} . Therefore, the chelates studied here did not allow to use one chelate with four different ions as would have been ideally suited for the labelling strategy. Nevertheless, the labelling of sequencing reactions would still be possible by using four different chelates and four different lanthanide ions. As in the Applied Biosystems scheme, any eventual molecular mass distortion during electrophoresis separation of the fragments would probably require computer algorithms to perform correct base calling.

In this thesis, experiments were performed to assess the tolerance of a polymerase enzyme to the introduction of lanthanide ions and chelates in a chain extension reaction mixture. It was also intended to test for the incorporation of the modified bases into a chain extension catalysed by a polymerase enzyme, as it is known that such enzyme can be sensitive to any chemical modification of the bases. The PCR studies showed that the *Taq* enzyme is extremely sensitive to the presence of free lanthanide ions in solution, as well as free chelates and no incorporation of the

nucleotide analogue synthesised was shown. This means that to make the sequencing reaction possible using the lanthanide chemistry as outlined in this work, extensive purification of the free metal ions, purification of unreacted or unbound chelates and a possible addition of a linker arm on the 2' carbon of the thymidine derivative would be necessary. Furthermore, the type of polymerase enzyme used here may not have been the most suitable one for our purpose. Better alternatives to *Taq* polymerase are described in chapter 7.

6.2. The interaction of lanthanide ions with DNA: the basis of a novel DNA hybridisation bioassay?

Following the observation that lanthanide ions inhibited DNA polymerase enzymes in chapter 2, Chapter 3 and 4 attempted to determine the mode of binding of lanthanide ions to nucleic acids. It was found that the binding of Tb^{3+} , Eu^{3+} , Sm^{3+} , Er^{3+} and Yb^{3+} was base dependant. Tb^{3+} was shown to bind to the phosphate groups and bases of the DNA as demonstrated by T_m studies. This binding effect was found to be strongly pH dependent. HPLC studies of denatured oligonucleotide duplexes showed that the metal ions prevent duplexes from forming without breaking down the nucleotide chains. Phosphorus NMR was used to confirm the interaction of Europium ions with phosphate groups on the DNA. However, problems with the metal ions being chelated by the citrate present in the buffer prevented us from proving that the lanthanide ions were binding to the bases and thus preventing base pairing.

The stoichiometry for the interaction with Sm^{3+} , Yt^{3+} , Eu^{3+} , Er^{3+} and Tb^{3+} was determined on 20 mer polydT oligonucleotide and 12 mer AT self complementary oligonucleotide. This was carried out using MALDI MS. It was found that for a 20

mer poly dT oligonucleotide, a maximum of 6 Eu^{3+} , 8 Sm^{3+} , 5 Yb^{3+} or 8 Er^{3+} ions could bind to each molecule without causing its breakdown. For the 12 mer self complementary dA_6T_6 , it was possible to bind a maximum of 3 ions for Tb^{3+} , Eu^{3+} , Sm^{3+} and Yb^{3+} were bound per molecule and 2 ions for Er^{3+} . These differences in stoichiometry between the different lanthanide ions could be due to them possessing a different affinity for the nucleic acids.

A limitation of the MALDI technique is its weakness when analyzing oligonucleotides containing C and G bases (Schneider *et al* 1994). This currently limits our understanding of lanthanide/DNA interaction to AT oligonucleotides. The presence of C and G bases in nucleic acids is not a problem when the C+G/A+T is roughly equal to 1. A mixed base DNA /lanthanide adduct could therefore be analyzed, to broaden the existing knowledge of lanthanide ions/ nucleic acids interactions and stoichiometry with AT rich oligonucleotides to any sequence.

6.3. Applying SSHG detection to DNA hybridisation bioassays.

The second harmonic properties of surfaces coated with oligonucleotides were studied in the series of experiments presented in chapter 5. It was found that the signal was strongly dependent on the density of the DNA molecules deposited on the surface, and that the signal decreased when the density was increased. The sensitivity of the surface second harmonic generation system with reference arm allowed to detect DNA densities as low as 10^{-13}mol/mm^2 . It was also found that the size and the structure of the nucleic acids deposited affected the signal. Data showed that the length of the oligonucleotide bound to the surface affected the second harmonic. This

means that as well as being able to detect monolayers of oligos on a surface, the technique is capable of distinguishing between samples of different structure but of same chemical composition. Finally, the technique was shown to be applicable on surfaces such as glass and plastic, both of which are very commonly used in the bioassay laboratories.

6.4. Overall conclusions.

The overall conclusion of the DNA sequencing labelling work presented in this thesis is that the ideal chelate to be used in a sequencing labelling strategy (as described page 54) has not been identified. Many problems linked to the inhibition of the activity of the polymerase enzyme were also identified. This enzyme compatibility problem may be the most difficult one to solve in this labelling strategy. Extensive effort in time, labour and investment was necessary for Applied Biosystems to solve similar problems and to find the optimum linker length that would render the modified nucleotide acceptable by the enzyme (Parker *et al* 1995). The work presented in this thesis highlighted some possible interactions between lanthanide metals and DNA strands, which could be the reason of the failure of PCR. Therefore, a series of experiments aiming at identifying the interaction mechanisms between lanthanide ions and nucleic acids were performed. All these experiments have confirmed previous work by others, stating that lanthanide ions can bind nucleic acids in two different ways, namely on the phosphate backbone and on the bases. It was also shown that the stoichiometry of the interaction was ion-dependent, suggesting that although binding was occurring in a similar fashion for all ions studied here, the

affinity of the ions for nucleic acids was variable. Combined to the fluorescent properties of lanthanide ions, this difference in affinity could be exploited to label nucleic acids and displace ions with others as required. A possible labelling strategy following this is described for solid phase hybridisation applications in chapter 7.

Another scheme for solid phase hybridisation was also approached during this work. Surface second harmonic generation detection was used to characterise nucleic acid coated surfaces. It was found that the technique was directly applicable to the design of a DNA hybridisation scheme using second harmonic generation as a non labelling detection strategy. It would however be useful to put the surface second harmonic generation method in perspective with the general context of DNA analysis. The sensitivity achieved here was 10^{-13} mol/mm². In general, DNA sequencing, being the most powerful DNA analysis method, can be performed for samples as small as a picomole (10^{-12} mole). The SSHG system described here is capable of detecting DNA at only 1 order of magnitude lower, which may not seem enough for a hybridisation assay that provides far less information than sequencing. However, improvements of the current system may be possible to further increase its sensitivity and because it is a non labelling technique, this method may enable easier sample preparation, easier automation and higher throughput than standard fluorescent based assays. As laser technology is becoming cheaper and more reliable, the SSHG hybridisation assay described in chapter 7 may very well be a viable commercial option for the diagnostic industry in the future.

CHAPTER 7: FURTHER WORK.

7.1. Lanthanide chelates and DNA sequencing.

A 2' amino derivative of thymidine was synthesised during the investigation covered in chapter 2. The amino group was intended to serve as an attachment point for the chelate molecules. It was intended to test for the incorporation of these modified bases into a chain extension catalysed by a polymerase enzyme, as it is known that such enzyme can be sensitive to any chemical modification of the bases. However, the type of polymerase enzyme used here may not have been the most suitable one for our purpose:

The polymerase enzyme used for sequencing is slightly different in nature from *Taq*. It is a bacteriophage T7 polymerase (called SequenaseTM) that has been modified to remove its 3'→5' exonuclease activity either by incubating the enzyme in reducing agents (Tabor and Richardson 1987) or by genetic engineering. Its 5'→3' polymerase activity is not affected by this treatment, so that the resulting enzyme is highly processive and suitable for using the Sanger sequencing method on long tracts of DNA. Further details about the differences between *Taq* and Sequenase were published later (Reeve and Fuller 1995). It was found that the incorporation of ddNTPs by *Taq* polymerase was very inefficient (about 0.02 to 0.1 the rate of dNTPs), which in other terms, means that normal nucleotides get incorporated preferentially into the chain extension reaction. ThermosequenaseTM, the thermostable version of Sequenase, achieves much better ddNTP incorporations, about 20% of the rate of dNTPs. This is due to a mutation where tyrosine 526 of T7 DNA polymerase was replaced by a phenylalanine, reducing the discrimination against ddNTPs. This genetically engineered enzyme was also found to incorporate without any difficulty

dye labelled dideoxy nucleotides. Should this information have been available at the time of the experiments, Thermosequenase would have therefore been a very good choice to test for the incorporation of chelate labeled chain terminating nucleotides. The use of a *Taq* polymerase to test for the incorporation of the amino modified into a chain extension reaction produced, in the present work, results that could be judged as misleading. Using an enzyme such as Thermosequenase in our experiments would have given more significant results by reproducing the conditions met in a typical sequencing reaction.

In these polymerase tolerance studies, other experiments could be improved:

The use of 1% agarose gels stained by ethidium bromide to study the PCR reaction mixtures may have been inadequate, considering the low amounts of intermediate size products expected. Also, the resolution of such as gel is not great. It might have been more informative to use PAGE gels, which is the type used in sequencing and allows to discriminate differences of 1 base in length.

7.2. A novel hybridisation labelling format using lanthanide ions.

Further experiments would be required to strengthen the findings described in chapter 3 and 4. It would for example be of interest to analyse CG containing oligonucleotides and their complexes with lanthanide ions, as the literature states a major difference of behaviour between AT and CG containing DNA. This was not possible using MALDI mass spectrometry, but would be possible using ESI-MS.

The interaction of DNA and lanthanides and the properties of the resulting complexes could be the basis for a novel type of DNA hybridisation bioassay. In this assay, two different lanthanide ions would be required. For the purpose of the description, these ions will be named ion 1 and ion 2. Ion 1 would be made to interact with the surface bound oligonucleotides, that may or may not have hybridised to their complementary sequence. In both cases, the oligos will bind metal ion 1. The single stranded or double stranded DNA would then be made to lay close to the surface of the bulk material using appropriate physical or electrostatic methods. The bulk material would have been prepared with readily exchangeable metal ion 2 at its surface. The oligonucleotide strand lying close to the surface would exchange metal 1 for metal 2, but in case of a duplex, only 1 strand will be close enough to the surface to perform that exchange. The single stranded species would exchange completely. By detecting remaining ion 1 on the surface using an appropriate evanescent wave fluorescence detection method, one could easily identify matching sequences and reject mismatches that would not contain any of that ion. To be able to implement such a system, one would require to use 2 different lanthanide ions of very different emission wavelength and different affinity for DNA. Tb^{3+} and Eu^{3+} may have those

suitable properties, because they have shown to possess rather different affinities with citrate and probably DNA too. Their emission wavelength and fluorescence lifetimes are sufficiently far apart to allow easy discrimination. Figure 7.1 schematically represents the basic principles of this bioassay.

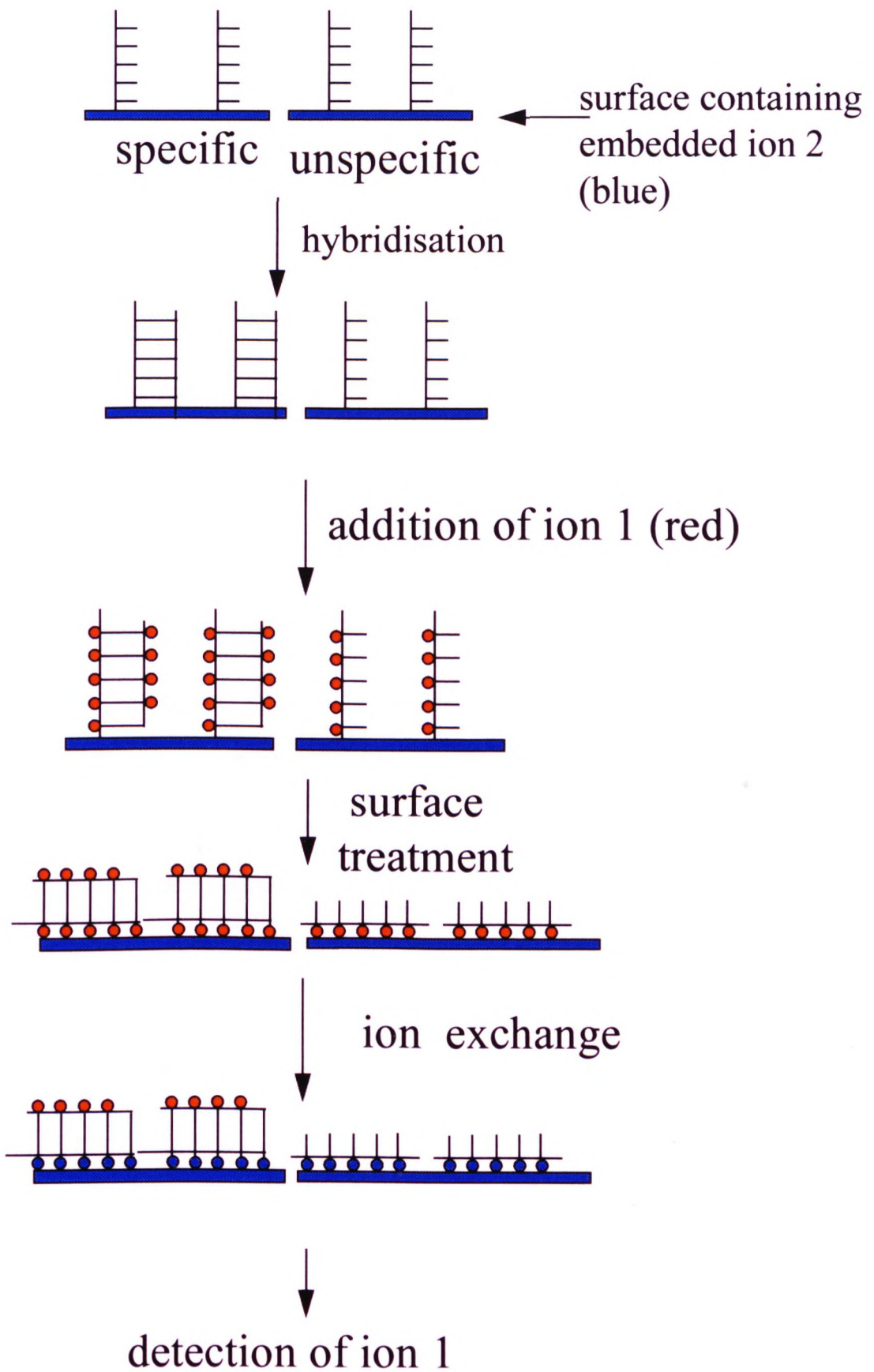


figure 7.1. Schematic representation of a surface based DNA bioassay using lanthanide ions as labels

7.3. A novel hybridisation labelling format using SSHG.

DNA bioassays (such as DNA hybridisation bioassays) aim at recognising the presence of a specific sequence of bases in a given sample using surface tethered nucleic acid targets containing the sequence complementary to the region of interest. In conventional techniques, the sample is labelled (using radioactive, chemiluminescent or fluorescent approaches). When using SSHG, no labelling of the molecule to be studied is necessary.

In this system, oligonucleotides or PCR products containing a sequence complementary to that of interest are linked to a glass or plastic surface, preferably in a monolayer, or by using other means of producing homogenous layers of DNA on a surface. The non linear optical characteristics of the DNA coated surface are measured. The sample is then hybridised to the surface bound probe using suitable conditions (salt concentration, temperature, time of reaction etc...). after stringency washing to remove unbound material, a new surface is produced, coated this time with the probe hybridised to the sample. New optical characteristics are measurable if hybridisation has occurred. If not, then characteristics similar to those obtained with the original surface should be measured, as all unbound/ unhybridised material should be washed off. The principles of an hybridisation assay are summarised in figure 7.2.

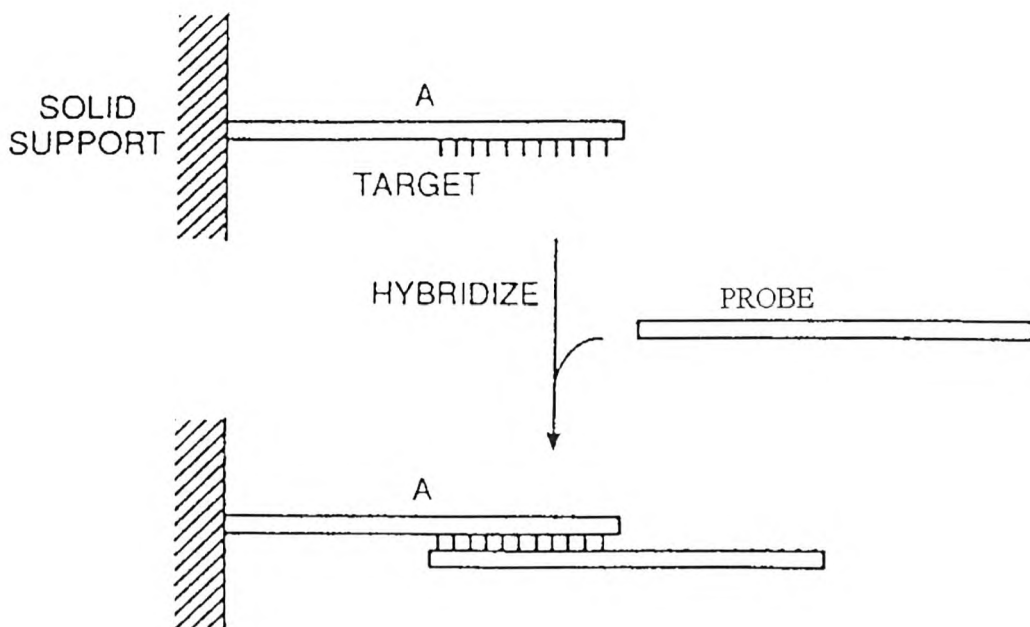


figure 7.2. Schematical representation of solid phase hybridisation.

Surface preparation considerations:

The second harmonic phenomenon measures only those molecules directly in contact with the surface of interest. If one requires the prepared surface to be representative of the composition of the original sample (in terms of concentration for example), this surface should be covered by a monolayer of the analyte to be examined. Any molecules added on top of this monolayer will not be measured by the technique. A standard technique to prepare DNA layers on glass surfaces is that of Langmuir Blodgett (LB) film formation. This is suitable for stretching DNA molecules onto surfaces (Michalet *et al* 1997) a useful approach for longer DNA fragments, because it makes the strands more available for hybridisation.

Other techniques have been described in the literature, involving the coating of amino silanised slides with λ DNA. These involve a preblocking step of some of the reactive groups on the surface with nucleotides, to allow suitable conditions for the sample DNA to stretch. (H Yokota *et al* 1997). The coating procedure is represented in figure 7.3.

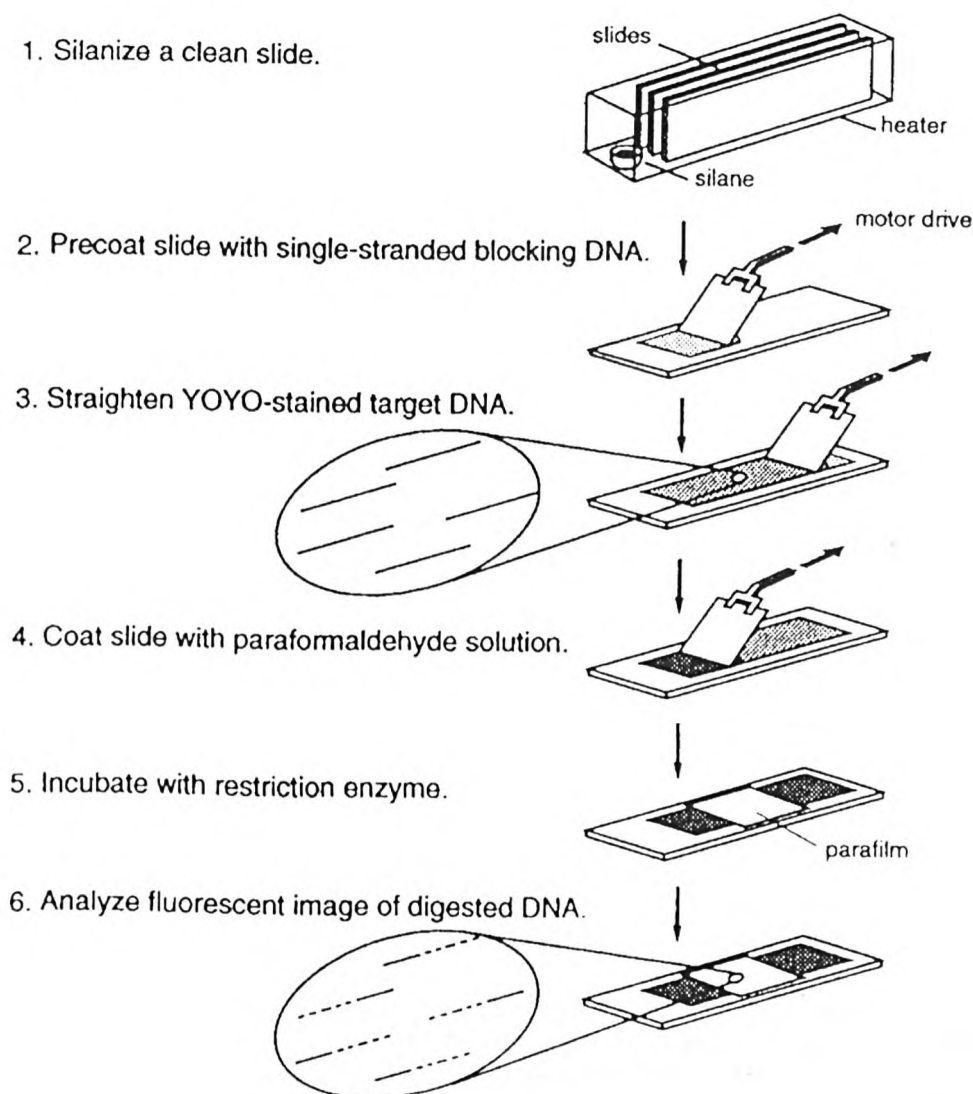


figure 7.3. Schematic diagram illustrating the procedure for straightening and optical mapping of single DNA molecules (reproduced from Yokota *et al* 1997)

Others have developed a technique to achieve the same result (stretched DNA molecules on a surface), where a droplet of the sample is evaporated between treated glass and a coverslip. This technique is illustrated in figure 7.4.

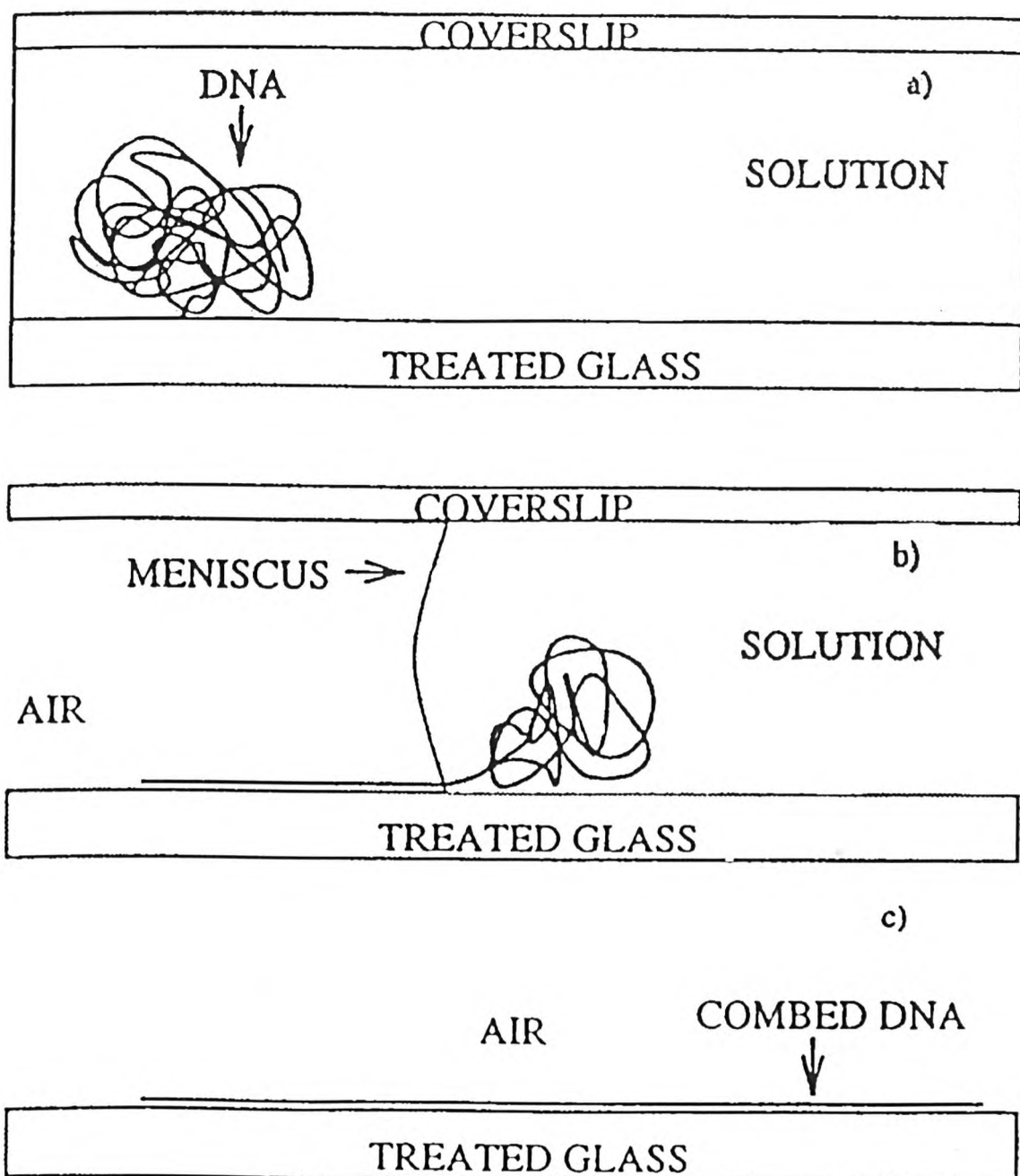


figure7.4. DNA incubated at the appropriate pH binds by one or 2 extremities onto a treated surface. As the interface moves, the DNA is stretched perpendicular to the receding meniscus. It is left linearised and dry behind the meniscus. (Allemand *et al* 1997)

One can also use wet spinning techniques to produce DNA coated surfaces, as described by Lee in 1994.

Coating techniques are often combined with suitable surface pretreatments. For example, when binding/ stretching of a large DNA molecule onto a surface is

required, various surfaces can be used successfully, such as vinyl silane, polystyrene, polymethylmethacrylate, clean glass, polylysine and amino silane. The success of the deposition depends strongly with the pH of the DNA solution, and the pH optimum value is variable according to the surface chosen (Allemand *et al* 1997). It is important to consider that although the stretching of DNA is desirable for SSHG because stretched DNA molecules are orientated all in the same direction, which optimises second harmonic signal output, a different deposition method maybe required to perform DNA hybridisation assays. Indeed, during solid phase hybridisation, the coated surface is covered with an aqueous solution containing the DNA probe as well as detergents and various salts. The hybridisation reaction is usually performed by incubation for several hours at a temperature 10°C lower than the melting temperature of the expected duplex, if this is known.

A common problem in solid phase hybridisation assays is the release of the attached DNA from its support during hybridisation. This seriously decreases the sensitivity of the assay as the free nucleic acids bind to the probe in solution. There is then no probe left to bind to the remaining attached nucleic acids. The duplexes are then washed away after the hybridisation, rendering their detection impossible. It might therefore be advisable to use covalent attachment to prevent this.

The type of application for the assay desired will also influence the mode of deposition of the nucleic acids used. For example, mutation analysis usually uses oligonucleotides, typically under a 25 bases in length, whereas expression analysis uses PCR products (around 1 kbp or more) as the target. Oligonucleotides are usually best attached using end covalent attachment, and PCR products are probably best attached throughout their length to avoid secondary structure effects.

To avoid complications with these extra chemistry steps, one could also perform the hybridisation in solution, subsequently preparing a surface with the target/probe mixture for SSHG analysis. After comparison of the second harmonic signal obtained with the target alone, one would be able to observe if the duplex has formed. This has the advantage of accelerating the hybridisation process which is much faster in solution than on a surface, but also has the disadvantage of not offering the possibility of washings after hybridisation to remove unbound or mismatched sequences.

Effect of DNA water content on Second harmonic signal:

A strong dependence of the SSHG signal on the water content of the DNA sample has been observed in previous work (Williamson *et al* 1993). Low water content samples (10 water molecules per base pair) are observed to give an order of magnitude lower signals than high water content samples (92%). Water content is a parameter that was not controlled for the current experiments, and this should be done in further work. Indeed, it is known that the degree of crystallisation is highly dependent on the RH (relative humidity): X ray diffraction patterns have been used to show that from 60% up to 92% of HR, wet spun films are crystalline and that above 92% they are semi-crystalline (Lindsay *et al* 1988). Also, the conformation of the DNA may be different depending on the humidity too. For example, the helical structure may change from A to B. Optical third harmonic generation studies of wet spun films of DNA have been reported (Szabo *et al* 1993). These studies might explain the phenomenon, where strong enhancement of the signal was also dependent on the RH. Enhancement is probably due to the increase in coherence length and to the fact that transition from A to B conformation occurs when increasing humidity

to 92% (Weidlich *et al* 1988). Indeed, it is well known that rehydration of DNA molecules provokes increase in mass loading, relaxational coupling to the hydration shell and softening of interatomic potentials. These mechanisms were observed using Raman spectroscopy (Lindsay *et al* 1988).

Crystal size is very dependent on the salt concentration of the sample deposited. It is therefore intriguing that no obvious changes were observed in this current study with the change of salt concentration.

Surface coating characterisation:

As said before, the nature of the nucleic acid coating is critical in second harmonic measurements, because the technique reliably probes monolayers only. Analytical tools for surface analysis could be useful in order to test different coating processes, such as silanisation or deposition of the DNA itself. Ellipsometry is an optical method capable of measuring layer thicknesses. It would also be useful to determine the conformation of the DNA sample once bound to the surface, and this could be done using atomic force microscopy, which can give subnanometer topographical information of surfaces.

Microarrays:

Because the current tendency of nucleic acid hybridisation methods is in favour of high throughput, achieved by using parallel analysis of large number of samples on small surfaces, it would be interesting to assess the feasibility of using SSHG measurements on surfaces arrayed with DNA. This would have to be done within the limits of the optical apparatus and would necessitate the reduction of the laser beam

down to the size of each DNA feature on the surface. The advantages would be numerous: all the nucleic acids would be bound and hybridised to the probe in a relatively homogenous manner and the reproducibility of the measurement between samples would be greatly improved, as compared to a system where each sample is analysed on a separate surface. The sample throughput would also be increased, reducing the cost and delay of analysis.

7.4. Conclusions.

The work carried out in this thesis required expertise in a large number of subject areas, such as analytical chemistry, organic chemistry, spectroscopy, surface chemistry. This is often the nature of work carried out to design methods and instruments for use in the bioanalytical lab. It is extremely challenging and requires a thorough understanding of the method and its applications, especially in the case of diagnostic methods, because non physicist/ chemists need to rely on the technology built by others to obtain suitable results.

REFERENCES:

- Allemand JF et al (1997)**, *Biophys J.* **73**(4):2064-70: pH-dependent specific binding and combing of DNA.
- Astbury W.T.(1947)**, *Symp.Sco.Exp.Biol. (Nucleic acids)* **1**, 66-76:X ray studies of nucleic acids.
- Atkinson T, Smith M (1984)**: Oligonucleotide synthesis : a practical approach, 35-81 (IRL press, Oxford)
- Badea M. and L. Brand (1979)**, In methods in Enzymology vol 61, pp378-425, ISBN 0-12-181961-2, Academic press.
- Barry J P et al(1995)**: *J. Mass. Spec.*, **30**, 993-1006
- Bauman et al (1984)**, Fluorescent hybridocytochemical procedures: DNA-RNA hybridisation in situ. In: Investigative microtechniques in medicine and biology, Ed. Chayen and Bitehsky.
- Bayer E. et al**, Analysis of double stranded oligonucleotides by electrospray mass spectrometry, *Anal. Chem.*, **66**, 3858-3853 (1994).
- Bailey M., B. Rocks, C. Riley (1984)**, *Analyst*, **109**, 1449-1450: Terbium chelate for use as a label in fluorescent immunoassays.
- Bilz H, Benedek G, Bussmann Holder A (1987)**, *Phys. Rev. B*, **35**,4840: Theory of ferroelectricity: the polarisability model.
- Calladine CR and Drew HR(1992)**: Understanding DNA, p27, Academic press ISBN 0-12-155086-9.
- Chan A., E. Diamantis, M. Kraiden (1993)**, *Anal. Chem.* , **65**, 158-163: Quantification of polymerase chain reaction products in agarose gels with a fluorescent Europium tag as label and time resolved fluorescence spectroscopy.
- Chan V, Graves D, McKenzie S (1995)**, *Biophysical journal*, **69**, 2243-2255: The biophysics of DNA hybridisation with immobilised oligonucleotide probes.
- Chang K. and K. Forcé(1993)**, *App. Spectr.* **47**, 24-29: Time resolved laser induced fluorescence study on dyes used in DNA sequencing.
- Chen C.H. et al (1995)**, SPIE proceedings vol 2386, paper 2386A-04: Laser desorption mass spectrometry for DNA sequencing.
- Chen RF, Knutson JR (1988)**, *Anal. Biochem.*, **172**,61: Mechanism of fluorescence concentration quenching of carboxyfluorescein in liposomes.

- Chien A, Edgar DB, Trela JM(1976)**, *J. Bacteriol.*, **127**, 1550: Deoxyribonucleic acid polymerase from the extreme thermophile *Thermus aquaticus*.
- Christian NP, Colby SM, Giver L, Houston CT, Arnold RJ, Ellington and Reilly JP (1995)**, *Rap. Comm. Mass Spec.*, **9**,1061-1066: High resolution matrix assisted laser desorption/ ionisation time of flight analysis of single stranded DNA of 27 to 68 nucleotides in length.
- Clement , Sturm, and Daune(1973)**, *Biopolymers*, **12**, 405-421: Interaction of metallic cations with DNA VI. Specific binding of Mg^{++} and Mn^{++} .
- Cohn WE, Bollum FJ (1961)**, *Biochim. Biophys. Acta*, **48**, 588.
- Collins ML and Hunsaker WR(1985)**, *Anal. Biochem.*, **151**, 211-224.
- Crick F.H.C and J.D. Watson(1954)**, *Proc. Roy. Soc. (London) Ser. A*, **223**, 80-96(1954)): the complementary structure of deoxyribonucleic acid.
- Dahlen P., J. Carlson, L. Liukkonen, H. Lija, H. Siitari, P. Hurskainen, A. Iit , Jeppsson J.O., T. L vgren (1993)**,*Clin. Chem.***39**, 1626-1631, Europium labelled oligonucleotides to detect point mutations: Applications to PI Z α_1 antitrypsin deficiency.
- Daune (1970)**, *Studia Biophys.*, **24/25**, 287-297: binding of divalent cations to DNA.
- Deegan. R , O. Bakajin, T. Dupont, G. Huber, S. Nagel and T. Witten (1997)**, *Nature*, **389**, 827: capillary flow as the cause of ring stains from dried liquid drops.
- Dekker C.R, Am M Michelson and A.R. Todd (1953)**, *Nucleotides, J. Chem . Soc.*,**19**, 947-951: pyrimidine deoxyribonucleoside diphosphates.
- Diamantis E.P.(1992) , Analyst**, **117**, 1879-1884: Europium and Terbium as candidate substrates for enzyme labelled time resolved fluorimetric immunoassays.
- Diamantis E P, T K. Christopoulos (1990)**, *Anal. Chem. ,* **62**, 1149A-1157A, Europium chelate labels in time resolved fluorescence immunoassays and DNA hybridisation assays.
- Dickson EF, Pollak A, Diamandis E (1995)**, *J Photochem Photobiol B*, **27(1)**, 3-19: Time-resolved detection of lanthanide luminescence for ultrasensitive bioanalytical assays.
- Duguid J, Bloomfield VA, Benevides J, Thomas G (1993)**, *Biophys. J. ,* **65**, 1916-1928: Raman spectroscopy of DNA metal complexes. 1. Interactions and conformational effects of the divalent cations: Mg, Ca, Sr, Ba, Mn, Co, Ni, Cu, Pd and Cd.
- Edelstein PH(1986)**, *J. Clin. Microbiol.*, **23**, 481-484.

Evangelista, A Pollak, B Allore, E F Templeton, R C Morton and E P Diamantis (1988),*Clin. Biochem.* , **21**, 173-178, A new Europium chelate for protein labelling and time resolved fluorometric applications.

Fitzerald M C(1993), The analysis of mock DNA sequencing reactions using matrix assisted laser desorption and ionisation mass spectrometry. *Rapid Commun. Mass Spec.*, **7**, 895-897.

Fitzerald, M C and Smith L.M. (1995): Mass spectrometry of nucleic acids: the promise of Matrix assisted laser desorption /ionisation (MALDI) mass spectrometry, *Annu.Rev.Biophys.Biomol. Struct.*, **24**, 117-140.

Fitzerald, M C, Parr GR, Smith LM(1993): Basic matrices for the Matrix assisted Laser Desorption /ionisation mass spectrometry of proteins and oligonucleotides, *Anal. Chem.*, **65**, 3204-3211

Franks F.(1975): The hydrophobic interaction, in “ *water, a comprehension treatise*” (F. franks ed.), pp1-94, Plenum press, New York. (1975).

Freeman and Crosby (1963), *J. Phys. Chem.*, **67**, 2717.

Furberg S.(1951), *Acta. Crystallogr.*, **3** , 325-331: the crystal structure of cytidine.

Glazer A. and H. Rye(1992), *Nature*, **359**, 859-861.

N Goddard, D. Pollard-Knight and C. Maule (1994): Real time biomolecular interaction using the resonant mirror sensor , *Analyst*, **119**, 583-588.

Gross D. and Simpkins H. (1981), *Journal Biol. Chem.*, **256**, 9593-9598: Evidence for two site binding in the Terbium(III)-nucleic acid interaction.

Gross DS, Simpkins H, Bubeinko E and Borer P (1982), *Arch. Biochem. Biophys.*, **2**, 401-410, Proton magnetic resonance analysis of Terbium ion - nucleic acid complexes: further evidence for 2 sites binding to polynucleotides.

Gulland. J M (1947), *Cold Spring Harbor Symp. Quant. Biol* , **12**, 95-103: the structure of nucleic acids.

Hanlon S.(1966), *Biochem. Biophys. Res. Comm.*, **23**, 861-867: the importance of London dispersion forces in the maintenance of the deoxyribonucleic acid helix.

Heidar Ali Tajmir -Riahi, Mancef Naoui and Rohana Ahmad (1993) article 1, J. Biomol. St. Dyn. , **10**, 865-877, Interaction of calf thymus DNA with trivalent La, Eu and Tb ions. Metal ion binding, DNA condensation and structural features.

Heidar Ali Tajmir -Riahi, Mancef Naoui and Rohana Ahmad (1993),article 2, *Biopolymers*, **33**, 1819-1827 : the effects of Cu^{2+} and Pb^{2+} on the solution structure of

calf Thymus DNA: DNA condensation and denaturation studie by Fourier Transform IR difference spectroscopy

Heller MJ and Morrisson LE, in : Rapid detection and identification of infectious agents, pp245-256, Academic press, New York(1985).

Helling et al(1974), *J. Virol*, **14**: 1235

Herskovits TT (1962), *Arch. Biochem and Biophys.*, **97**, 474.

Hettich and Buchanan(1991), *J. Am. Soc. Mass. Spectrom.*, **2**, 402(1991)

Holbrook SR, Sussman JL, Warrant RW, Church M and Sung Hou Kim (1977), *Nucl Ac.Res.*, **4**, 2811-2820: RNA -Ligand interactions: 1. Magnesium binding sites in yeast tRNA^{Phe}.

Hörer OL, Zaharia CN and Marcu (1977), *A Rev. Roum.Biochim.*, **14**, 175-179
Terbium fluorescence in aqueous solutions of nucleic acids.

Horn T, Chang CA, Urdea M (1997), *NAR*, **25**, 4842-4849: Chemical synthesis and characterisation of branched oligodeoxyribonucleotides (bDNA) for use as signal amplifiers in nucleic acid quantification assays.

Horowitz P and Windfield Hill(1989), *The art of electronics*, p 1032-1033, ISBN 0-521-37095-7

Huoponene, V. Juvonen, A. Iitiä, P. Dahlen, H. Siitari, P. Aula, E. Nikoskelainen, ML. Savontaus (1994), *Human mutation*, **3**, 29-36: Time resolved fluorometry in the diagnostic of leber hereditary optic neuroretinopathy.

Jeffreys.A.J(1979), *Cell*, **18**, 1-10.

Kafatos et al (1979), *Nucl. Ac. Res.*, **7**, 1541-1552.

Kessler C. (1994), *J. of Biotech*, **35**, 165-189.

Kirpekar F, Nordhoff E, Kristiansen K, Roepstorff P, Halner S, Hillenkamp F(1995), *Rapid Comm. Mass Spectrom.* ,**9**, 525-31: 7 Deaza purine base offer higher ion stability in the analysis of DNA by matrix assisted laser desorption/ionisation mass spectrometry.

Klakamp SL, Horrocks DeW(1992), *J. Inorg. Biochem.*, **46**, 185-193, Lanthanide ion luminscence as a probe of DNA structure. 1. Guanine containing oligomers and nucleotides.

Klakamp SL, Horrocks DeW (1992), *J. Inorg. Biochem.*, **46**, 193-205, Lanthanide ion luminescence as a probe of DNA structure. 2. Non guanine containing oligomers and nucleotides.

Komiyama M, Matsumoto Y, Hayashi N, Matsumura K, Tadeka N, Watanabe K (1993). *Polymer J.*, **25**, 1211-1214: hydrolysis of oligoDNAs by lanthanide metal (III) chloride.

Krumhansl JA, Wyman GM, Alexander DM, Garcia A, Lomdahl PS, Layne SP (1985): In: *Structure and motion: membranes, nucleic acids and proteins*. Adenine Press, 1985:407-415: Further theoretical studies of nonlinear conformational motions in double helix DNA.

Kwiatkowski M , Samiotaki M, Lamminmäki, Mukkala VM and Landegren U(1994), *Nucl. Ac. Res.* , **22**, 2604-2611: Solid phase synthesis of chelate labeled oligonucleotides: application in triple colour ligase mediated gene analysis.

Lallemand J-F, D. Bensimon, L. Jullien, A. Bensimon and V. Croquette(1997), *Biophys. J.*, **73**, 2064-2070: pH dependent specific binding and combing of DNA.

Large M., W. Blau, D. Croke, P. McWilliam and F. Kajzar (1996), *SPIE* vol **2852** paper 33: Molecular length dependent polarizability.

Lecchi P et al : 6 aza 2 thiothymine: a matrix for MALDI spectra of oligonucleotides, *Nucl. Ac. Res.* , **23**, 1276-1277 (1995).

Lee S.A(1994), final technical report for the grant no 01491-J-1457/ DTIC: synthesis of novel composite Platinum-DNA films via wet spinning.

Le Guerneve C, Seigneuret M (1996) *Biophys J* Nov;**71**(5): 2633-2644
High-resolution mono- and multidimensional magic angle spinning ¹H nuclear magnetic resonance of membrane peptides in nondeuterated lipid membranes and H₂O.

LePecq JB and Paoletti C(1971), *J. Mol. Biol.*, **59**, 43-62.

Li LC, He H, Nunnally BK, McGown LB (1997), *J Chromatogr B Biomed Appl*, **695**(1):85-92: On-the-fly fluorescence lifetime detection of labeled DNA primers.

Lindsay SM, Lee SA, Powell JW, Weidlich T, Demarco C, Lewen GD and Tao NJ (1988), *Biopolymers*, **27**, 1015-1043: The origin of the A to B transition in DNA fibers and films.

Litiä, L. Liukkonen, H. Siitari (1992), *Mol. Cell. Probes*, **6**, 505-512 : Simultaneous detection of two cystic fibrosis alleles using dual label time resolved fluorometry.

Lopez E., C. Chypre, B. Alpha, G. Mathis (1993), *Clin. Chem.* , **39**, 196-201, Europium (III) Trisbipyridine cryptate label for time resolved fluorescence detection of polymerase chain reaction products fixed on a solid support.

Luck and Zimmer (1972), *Eur. J. Biochem.* 29,528

Malvezzi AM, Liu JM, Bloembergen N(1984), *Appl. Phys. Lett.*, 45, 1019-1021: Second harmonic generation in reflection from crystalline GaAs under intense picosecond laser irradiation.

Mathies *et al*(1995), SPIE proceedings vol 2386, paper 2386A-10: New directions in high sensitivity fluorescence detection of DNA and capillary array electrophoresis.

Mathieson and Olayemi (1975),*Arch. Biochem. Biophys.* 169, 237.

Maxam AM and Gilbert W (1977), *Proc. Natl. Acad. Sci. USA*, 74, 560-564: a new method for sequencing DNA.

Mayer A. and S. Neuenhofer (1994), *Angew. Chem. Int. Ed. Engl.*, 33, 1044-1072.

McGall G, Labadie J, Brock P, Wallraff G, Nguyen T, Hinsberg W (1996), *Proc. Natl. Acad. Sci. USA*, 93, 13555-13560: Light directed synthesis of high density oligonucleotide arrays using semi conductor photoresists.

Michalet X, R.Ekong, F Fougereuse, S Rousseaux, C Shurra, S Povey, J S Beckmann, A Bensimon, N Hornigold, M van Slegtenhorst and J Wolfe 1997, *Science*: Dynamic molecular combing: stretching the whole human genome for high resolution studies(in press)

Mizrahi V, Stegeman GI (1989), *Phys. Rev. A*, 39, 3555-3562: microstructure of J band-forming cyanine dye monolayer probed by means of second harmonic generation.

Mutto V, Scott AC, Christiansen PL (1989), *Phys. Lett. A*, 136, 33: Thermally generated solitons in a Toda lattice model of DNA.

Nedderman Angus *et al* (1993), *J. Mol. Biol.* 230, 1068-1076.

Nguyen DC and RA Keller (1987), *Anal. Chem.*, 59, 2158

Nicholls P and Malcom A (1989), *J. Clin. Lab. Anal.* , 3, 122-135: Nucleic acid analysis by sandwich hybridisation.

Nikiforov TT and Rogers YH(1995), *Anal. Biochem.* 227, 201-209: the use of 96 well polystyrene plates for dna hybridisation based assays: an evaluation of different approaches to oligonucleotide immobilisation.

Nilsson, Persson B, Larsson A, Uhlen M, Nygren P (1997), *J. mol. Recognit.* , 10, 7-17: Detection of mutations in PCR products from clinical samples by surface plasmon resonance.

Nørgaard- Pedersen B., E. Høgdall, A. Iitiä, J. Arends, P. Dahlen, J. Vuust (1993) , *Screening*, **2**, 1-11: Immunoreactive trypsin and a comparison of two $\Delta F508$ mutation analyses in newborn screening for cystic fibrosis: an anonymous pilot study in Denmark.

Parker LT, Deng Q, Zakeri H, Carlson C, Nickerson DA, Kwok PY (1995) *Biotechniques*, **19**(1):116-121: Peak height variations in automated sequencing of PCR products using Taq dye-terminator chemistry.

Pezzano H and Podo F (1980), *Chem. Rev.*, **80**, 365-401, Structure of binary complexes of mono and polynucleotides with metal ions of the first transition group.

Pieles.U, Zürcher W, Star M and Moser H E(1993) *Nucl. Ac. Res.* **21**, 3191-3196, Matrix assisted laser desorption /ionisation time of flight mass spectrometry: a powerful tool for the mass and sequence analysis of natural and modified oligonucleotides.

Ploem J.S(1992): Fluorescence and luminescent probes for biological activity, chap1. Biological techniques series, Academic press.

Raymond Chang (1971), Basic principles of spectroscopy, Mc Graw-Hill book company, ISBN 07-010517-0

Reuben (1973), Paramagnetic lanthanide shift reagents in NMR spectroscopy, Pergamon Press, ISBN: 0 08 017144 3.

Richard H (1973), *Biopolymers*, **12**, 1-10: Interaction of metallic ions with DNA. V. Renaturation mechanism in the presence of Cu^{++} .

Ringer D, Howell B, Kizer D (1980), *Anal. Biochem.* , **103**, 337-342: use of terbium fluorescence as a new probe for assessing the single stranded content of DNA.

Roberts J and Thomson A (1979), *Prog Nucl. Acid Res. Mol. Biol.*, **22**, 71-129: The mechanism of action of antitumor Platinum compounds.

Rupprecht (1988), *Biopolymers*, **27**, 1015: A. The origin of the A to B transitions in DNA fibers and films.

Saavedra and E. Picozza (1989), *Analyst*, **114**, 835-838: Time resolved fluorimetric detection of Terbium labelled deoxyribonucleic acid separated by gel electrophoresis.

Saenger W(1984): Principles of nucleic acids structure, Springer-Verlag Ed, ISBN:0-387-90761-0.

Saha A.K., K. Kross, E. D. Kloszewski, D.A Upson, J. L. Toner, R. A Snow, C.D. Black, V.C Desai (1993), *J. Am. Chem. Soc.*, **115**, 11032-3, Time resolved fluorescence of a new Europium chelate complex: demonstration of highly sensitive detection of protein and DNA samples.

Saiki P, Gelfand DH, Stoffel S, Sharf SJ, Higushi R, Horn G, Mullis K, Erlich H (1988), *Science*, **230**, 1350: Enzymatic amplification of β globin genomic sequences and restriction site analysis for diagnostic of sickle cell anemia.

Sambrook, Fritsch, Maniatis(1989), Molecular cloning, vol 1 , ISBN 0-87969-309-6, CSH laboratory press.

Sambrook, Fritsch, Maniatis (1989), Molecular cloning, vol 2 , ISBN 0-87969-309-6, CSH laboratory press.

Samiotaki M, M. Kwiatkowski, N. Ylitalo, U. Kandegren (1997), *Anal. Biochem.*, **253**, 156-161: Seven color time resolved fluorescence hybridisation analysis of human papilloma virus types.

Sanders J K M and B K Hunter: modern NMR spectroscopy, ISBN:0 19 8555660, experimental considerations, p43.

Sanger F., Nicklen S and Coulson A(1977), *Proc. Natl. Acad. Sci. USA*, **74**, 5463-5467: DNA sequencing with chain terminating inhibitors.

Schecker J.A. et al (1995) , SPIE proceedings vol 2386, paper no 2386A-02.

Schneider, K, Chait, BT: Matrix Assisted Laser Desorption mass spectrometry of homopolymer oligodeoxyribonucleotides. Influence of base composition on the mass spectrometric response, *Org. Mass Spectrom.*, **28**, 1353-1361(1993)

Schuette, U Piele, S. Maleknia, S. Srivatsa, D. Cole, H. Moser, N. Afeyan (1995), *J. Pharm. Biomed. Anal.* **13**, 1195-1203: Sequence analysis of phosphorothioate oligonucleotides via matrix assisted laser desorption ionisation time of flight mass spectrometry.

Shchepinov, Case Green S,Southern E(1997), *NAR*, **25**, 1155-1161: Steric factors influencing hybridisation of nucleic acids to oligonucleotide arrays.

Shen YR(1989), *Nature*, **337**,519-524: Surface properties probed by second harmonic and sum-frequency generation.

Shoup R.R. Miles HT, Becker ED (1966): *Biochem. Biophys. Res. Comm.* **23**, 194: NMR evidence of specific base-pairing between purines and pyrimidines.

Sinanoglu O.(1968): Solvent effects on molecular associations, in “ *Molecular associations in biology*” (B Pullman, ed.), pp427-445, Academic press, new York.

S Silver and G Ji (1994), *Env.Health Persp.* , **102**, p107-113, Newer systems for bacterial resistances to toxic heavy metals.

- Sissoëff I , Grisvard J, Guillé E (1976),** *Prog. Biophys. Molec. Biol.*, **31**, 165-199, Studies on metal ions-DNA interactions: Specific behaviour of reiterative DNA sequences
- Siuzdak G(1994):** *Proc. Ntl.Acad.Sci.USA*, **91**, 11290-11297,The emergence of mass spectrometry in biomedical research.
- Slater GW, Mayer P, Grossman P (1995),** *Electrophoresis*, **16**, 75-83: Diffusion, Joule heating, and band broadening in capillary gel electrophoresis of DNA.
- Sloop F., G. Brown, R. Sachleben, M. Garrity, J. Elbert, K.Jacobson (1994),** *New. J. Chem*, **18**, 317-326 : Metalloorganic labels for DNA sequencing and labelling.
- Smith L, Sanders J, Kaiser R, Hughes P, Dodd C, Connell C, Heiner C, Kent S, Hood L(1986),** *Nature* **321**, 674-678: fluorescence detection in automated DNA sequence analysis.
- Soini E, Lövgren T(1987),** *CRC Crit. Rev. Anal. Chem*, **18**, 105-154.
- Soper A. et al(1995),** SPIE proceedings vol 2386, paper 2386A-12: Single lane, single fluor sequencing using dideoxy labelled heavy atom near IR fluorescent dyes.
- Southern E.M.(1975),** *J. Mol. Biol.* , **98**, 503-517: Detection of specific sequences among DNA fragments separated by gel electrophoresis.
- Srinivasan K. et al(1993),** *Appl. Theor. Electroph.*, **3**, 235-239: Enhanced detection of PCR products through use of TOTO and YOYO intercalating dyes with laser induced fluorescence--capillary electrophoresis.
- Stangret J and Savoie R (1993),** *J. Mol. Struc.*, **297**, 91-102: Raman spectroscopic study of the interaction of metal ions with pyridine and maleimide- models for nucleic acids
- Steinkopf S, Garoufis A, Nerdal W and Sletten E (1995),** *Acta Chem. Scand.* , **49**, 495-502, Sequence selective metal ion binding to DNA oligomers.
- Straughan BP and S. Walker (1976) (Ed),**Spectroscopy vol 3, ISBN 0-470-15033-5, Science paperbacks)
- Swerdlow H. et al(1991):** *Anal. Chem.* **63**, 2835-2841: Three DNA sequencing methods using capillary gel electrophoresis and laser-induced fluorescence.
- Syvanen A C., P. Tehen, M. Ranki, H. Soderlund (1986),** *Nuc. Ac. Res.* , **14**, 1017-28: Time resolved fluorometry: a sensitive method to quantify DNA hybrids.

Szabo A , Wang Y, Lee SA, Simon HJ, Rupprecht (1993), *Biophys. J*, **65**, 2656-2660: Optical third harmonic generation study of the hydration of DNA films.

Tabor S and Richardson CC (1987), *J. Biol. Chem.* ,**262** , 15330: Selective oxidation of the exonuclease domain of bacteriophage T7 DNA polymerase.

Tabor S. and C. Richardson (1990), *J. Biol . Chem.* **265**,8322-8329. DNA sequence analysis with a modified bacteriophage T7 DNA polymerase. Effect of pyrophosphorolysis and metal ions.

Tajmir-Riahi HA, Naoui M, Ahmad R (1993), *Biopolymers*, **33**, 1819-1827: The effects of Cu^{2+} and Pb^{2+} on the solution structure of calf thymus DNA: DNA condensation and denaturation studied by fourier transform IR difference spectroscopy.

Tang K, S. Allman, C. Chen, Rap. Comm. Mass. Spec. ,7, 943-948: matrix assisted laser desorption ionisation of oligonucleotides with various matrices.

Techera M, Daemen LL, prohofsky EW (1989), *Phys. Rev.A* , **40**, 6636 : Nonlinear model of the DNA molecule.

Tom HWK (1984): *Phys. Rev. Lett.*, **52**, 348-351: Surface studies by optical second harmonic generation: the adsorption of O_2 , CO and sodium on the Rh(111) surface.

Topal M, Fresco J (1980), *Biochemistry*, **19**, 5531-5537: Fluorescence of terbium ion-nucleic acid complexes: a sensitive specific probe for unpaired residues in nucleic acids.

Viale G, Dell'Orto P (1992) *Liver*, **12** :243-51: Non-radioactive nucleic acid probes: labelling and detection procedures.

Wang B H, Blemann K(1994). Matrix assisted laser desorption /ionisation time of flight mass spectrometry of chemically modified oligonucleotides. *Anal. Chem.*, **66**, 1918-1924

Watson J.D. and F.H.C Crick A structure for deoxyribonucleic acid, *Nature*, **171**, 737-738(1953)

Weidlich TS, M Lindsay and A Rupprecht (1988), *Phys. Rev. Lett*, **61**,1674-1677: Counterion effects on the structure and dynamics of solid DNA.

Weissman (1942), *J. Chem. Phys*, **10**, 214: Intramolecular energy transfer, Fluorescence of complexes of Europium.

Williams R. J. et al (1993), *Anal. Chem.*, **65**, 601-605.

Williamson W., Y. Wang, H. Simon and A. Rupprecht, *Spectr. Letters*, **26**, 849-858: Observation of optical second harmonic generation in wet spun films of Na-DNA.

Wood S.(1993), *Microchemical journal*, **47**, 330-337: DNA-DNA hybridisation in real time using BIAcore.

Wu K J, A. Steding, C. Becker (1993), *Rapid comm. Mass spec*, **7**, 142-146(1993),Matrix assisted laser desorption time of flight mass spectrometry of oligonucleotides using 3-hydroxypicolinic acid as an ultraviolet sensitive matrix.

Xiao XD, Shen YR(1993), SPIE vol 1857, *Lasers and optics for surface analysis: surface studies by non linear optics*.

Xu Y.Y, I. Hemmilä, T. Lövgren (1992), *Analyst*, **117**, 1061-1069 : Cofluorescence effect in time resolved fluoroimmunoassays, a review.

Yang L., D. McStay and PJ Quinn (1998): Surface second harmonic generation-A new scheme for immunoassays (to be submitted).

Yokota, F. Johnson, H. Lu, M. Robinson, A. Belu, M. Garrison, B. Ratner, Trask B. and D. Miller (1997), *NAR*, **25**, 1064-1070: A new method for straightening DNA molecules for optical restriction mapping.

Yonuschot G, Helman D, Mushrush G, Vande Woude G, Robey G (1978), *Bioinorg. Chem.* , **8**, 405-418, Terbium as a solid state probe for RNA.

Zamenhof S., G. Brawermann and E. Chargaff (1952), *biochim. Biophys. Acta*, **9**, 402-405: on the desoxypentose nucleic acids from several microorganisms.